
THE UNIVERSITY *of* EDINBURGH

# Role of Redox Regulated E3-ligase 1 in plant immunity at the cell surface

**Jibril Lubega**

**Doctor of Philosophy**

**Institute of Molecular Plant Sciences**

**The University *of* Edinburgh**

**March 2019**

## Abstract

S-nitrosylation, the addition of a nitric oxide moiety to a cysteine thiol to form an S-nitrosothiol (SNO) is emerging as a key redox-based post-translational modification in the control of plant immunity. *Redox Regulated E3 ligase 1* (*RRE1*) was initially identified following transcriptome analysis of pathogen challenged *Arabidopsis* S-nitrosylation and Salicylic acid induction deficient mutants. RRE1 has two conserved domains, an ankyrin repeat known to mediate protein-protein interaction and a RING finger motif driving E3 ligase activity. The expression of RRE1 correlated with expression level of *Arabidopsis thaliana* Penetration 1 protein (AtPEN1), a protein integral to surface level resistance against *Blumeria* pathogens. AtPEN1 recycling at the plasma membrane is a key feature of this immune response. Mutation in either *RRE1* or *AtPEN1* enhanced increased penetration rates of the non-adapted pathogen *Blumeria graminis* f. sp. *hordei* (*Bgh*). Previous data indicated that, XA21 binding protein *Hordeum vulgare* 35 (XBHV35) a barley homologue of RRE1 interacted with Candidate secreted effector protein 0443 (CSEP0443). CSEP0443 is highly expressed during early stages of fungal invasion likely aiding penetration and haustoria formation, thus promoting fungal aggressiveness. I investigated the functional relevance of RRE1 in pathogen-plant interaction with respect to AtPEN1 and CSEP0443.

Initially I investigated the contribution of CSEP0443 to *Bgh* pathogenicity in both host plant barley and non-host plant *Arabidopsis*. By applying BSMV-VIGS mediated HIGS to barley the expression levels of CSEP0443 was significantly reduced to 43%. The plants displayed low levels of *Bgh* susceptibility, reduced by 61% relative to wild-type. In non-host systems, expression of CSEP0443 enhanced *Bg*h penetration rates by 30% relative to wild-type. However, further growth of the pathogen was attenuated by cells undergoing programmed cell death.

The tight co-expression of RRE1 and AtPEN1 during *Bgh* challenge prompted to

investigate the possible interaction of the two proteins and the consequences of the interactions. My results displayed interactions of RRE1 and AtPEN1. RRE1 further, mediated the ubiquitination of AtPEN1, underpinning AtPEN1 as a substrate for RRE1. By mutating lysines 48 and 63 to arginine in ubiquitin, I revealed that AtPEN1 is sufficiently polyubiquitinated along the two ubiquitin sites. As the two types of polyubiquitinations target protein to different fates, I investigated the effect of these modifications. AtPEN1 conjugated with K48 linkages was degraded by 26S proteasome. AtPEN1 conjugated with K63 linkage was not targeted to vacuolar degradation, likely targeted for other functions like activation for relocalization. By applying mutagenesis to probable lysine residues in AtPEN1, lysine 103 and 281 were identified as the ubiquitination sites. My findings reveal the first syntaxin in plant systems whose ubiquitination sites have been disclosed.

Further, I investigated the possible interaction of RRE1 and CSEP0443. CSEP0443 exhibited an interaction with RRE1. Interaction was significantly observed with the RING domain likely aimed to compromise E3 ligase activity of RRE1. Indeed RRE1-RING-C340S, with the loss of E3 ligase activity due to disruption of zinc coordination, exhibited reduced interaction with CSEP0443. I investigated the consequences of the interaction by determining if RRE1 could ubiquitinate CSEP0443 or CSEP0443 could affect the ability of RRE1 to ubiquitinate AtPEN1. In my findings CSEP0443 was not ubiquitinated by RRE1 however, CSEP0443 compromised the ability of RRE1 to ubiquitinate AtPEN1. The results reveal RRE1 as a target for CSEP0443 in *Arabidopsis* adding to few effectors from *Bgh* proteome whose targets are disclosed. My findings support the hypothesis that RRE mediate the relocalizations of AtPEN1 to the site of attempted *Bgh* penetration by driving AtPEN1 polyubiquitination with K63 chain linkages. *Bgh* secrete CSEP0443 that hinder the E3 ligase ability of RRE1 hence curtailing the accumulation of AtPEN1 to fungal ingress sites.

## Lay Summary

The sessile nature of plants exposes them to a wide range of disease causing organisms (pathogens). To counteract pathogens, plants secrete an arsenal of defence proteins. Redox Regulated E3 ligase 1 (RRE1) is one of the defence proteins expressed following exposure to *Blumeria* pathogens. RRE1 belong to the family of proteins driving functional modification of proteins by adding ubiquitin to the selected substrate. The expression of RRE1 tightly harmonized with the expression of *Arabidopsis thaliana* Penetration 1 protein (AtPEN1), a surface membrane protein known to accumulate at attempted *Blumeria graminis* f. sp. *hordei* (*Bgh*) penetration sites to recruit anti-microbial agents. Loss of both *RRE1* and *AtPEN1* promote increased ability of *Bgh* to gain entrance in *Arabidopsis*, a non-host plant. The close relative of RRE1 in barley known as XA21 binding protein *Hordeum vulgare* 35 (XBHV35), interacts with Candidate secreted effector protein 0443 (CSEP0443), a protein secreted by *Bgh* into the host during early stages of infection to circumvent host defence. In this project I attempted to dissect the functional relevance of RRE1 following *Bgh* infection in non-host system. My findings revealed that RRE1 interacts with AtPEN1 and subsequently modifies it by polyubiquitination. The polyubiquitination presumed to activate AtPEN1 for re-localization to the site of *Bgh* ingress. I have established that RRE1 interacts with CSEP0443. The interactions are pronounced with the RING domain intended to compromise the E3 ligase activity. I displayed reduced RRE1 mediated ubiquitination of AtPEN1 in the presence of CSEP0443. I also demonstrated that the expression of CSEP0443 promotes the virulence of *Bgh* in both host and non-host systems. Taken together these findings imply that the assembly of AtPEN1 to the *Bgh* ingress sites are activated by RRE1 mediated polyubiquitination. The pathogen then secretes CSEP0443 to disrupt the ubiquitination ability of RRE1 diminishing AtPEN1 mobilization and pathogen gains ingress. Finally, the host attenuates the pathogen progression by inducing programmed cell death in the attacked cells.

## Declaration

I hereby declare that the work presented here is my own except where explicitly stated in the text* and has not been submitted in any form for any degree at this or other university.

Jibril Lubega

*Data of yeast two hybrid assay shown in **Figure 4-3 (A)** was conducted by Manda Yu and Loake Gary, permission has been granted for inclusion in this thesis.

## Acknowledgements

Many people contributed to the realisation of this thesis. Space does not permit me to list all of them individually. However, I am immensely thankful to all of them for the co-operation and advice extended to me.

My sincere thanks go to my Principal supervisor Prof Gary J. Loake for guiding the frame work of the study, reading the earlier drafts of the thesis, and the friendly culture he instituted in his laboratory. I am thankful to the academic committee members Prof Justin Goodrich, Dr Peter Hoebe and previously Dr Graham Mc Grann who contributed constructive ideas in meetings and whenever consulted.

I am thankful to my sponsors, Islamic development bank who supported me to study in one of the world's leading university may ALLAH rewards you abundantly.

I am thankful to Prof Pietro Spanu and Dr Francois Dussart who examined my thesis, provided useful comments for improvement and recommended me for the award of the degree.

I am thankful to Dr Manda Yu, who provided foundation from which this study was built on. I am thankful to all of you members of Loake laboratory for the support, you made my life easier to reach to this end.

I am thankful to my family members: Misses Farida for your support, daughters Mariam and Fartiha who took away my stresses whenever interacted with you. Misses Rashida for the interactive support, My mother Hajjat Mariam for your endless prayers and to my late farther Hajj Isa Ssagalabayomba who even though never went far in education levels, instilled a culture of education loving in me. May ALLAH rewards you with paradise.

Lastly, I am thankful to the almighty ALLAH who provided me with a gift of life, knowledge and guidance.

# Contents

## List of Figures

## List of Tables

## List of Abbreviations

| | |
|---|---|
| µg | microgram |
| µl | microlitre |
| 3AT | 3-amino-1,2,4-triazole |
| ADP | Adenosine diphosphate |
| AIP4 | Atrophin 1 interacting protein 4 |
| AMP | Adenosine monophosphate |
| ANOVA | Analysis of variance |
| APIP6 | AvrPiz-t Interacting Protein 6 |
| ARF-GEF | Adenosine diphosphate ribosylation factor, guanine nucleotide exchange factor |
| ARF-GEF protein | ADP ribosylation factor guanine nucleotide exchange factor |
| AtALIX | *Arabidopsis thaliana* Alix protein |
| atgsnor1-3 | *arabidopsis thaliana* S-nitrosoglutathione reductase |
| ATL9 | Arabidopsis toxicos en levadura 9 |
| AtNLA | *Arabidopsis thaliana* nitrogen limitation adaptation |
| ATP | Adenosine triphosphate |
| ATPase | Adenosine triphosphatase |
| AtPEN1 | *Arabidopsis thaliana* Penetration 1 |

| | |
|---|---|
| AtPEN2 | *Arabidopsis thaliana* Penetration 2 |
| AtPEN3 | *Arabidopsis thaliana* Penetration 3 |
| AtPHT1;1 | *Arabidopsis thaliana* phosphate transporter 1 |
| AtUBA | *Arabidopsis thaliana* Ubiquitin activating |
| AtUBC1 | *Arabidopsis thaliana* Ubiquitin conjugating enzyme 1 |
| AVR | Avirulence |
| AvrPiz-t | Avirulence effector Piz-t |
| AvrPtoB | Avirulence effector PtoB |
| BAG | Bcl-2-associated athanogene |
| BAK1 | BRI1-Associated receptor kinase1 |
| BARD1 | BRCA1-associated RING domain protein 1 |
| Bcl-2 | B-cell lymphoma 2 |
| BEC 3 | Blumeria Effector Candidate 3 |
| BEC 4 | Blumeria Effector Candidate 4 |
| BEC2 | Blumeria effector Candidate 2 |
| Bgh | Blumeria graminis f. sp. hordei |
| Bgt | Blumeria graminis f. sp. tritici |
| BOR1 | Borate transporter1 |

| | |
|---|---|
| BR | Brassinoteroid |
| BRCA1 | Breast cancer associated 1 |
| BRCT | C-terminal domain of a breast cancer susceptibility protein |
| BRI1 | Brassinosteroid insensitive1 |
| BSA | Bovine serum albumin |
| BSA | Bovine serum albumin |
| BSMV | Barley stripe mosaic virus |
| BTB | Broad complex/ tramtrack/bric -a-brac |
| C14 | Clan type peptidase 14 |
| CaMV | Cauliflower mosaic virus |
| CC-NB-LRR | Coiled Coil Nucleotide Binding domain and Leucine Rich Repeat |
| cDNA | Complementary deoxyribonucleic acid |
| CHIP | C-terminus of Hsc70-interacting protein |
| COP10 | Constitutive photomorphogenesis protein 10 |
| CPR1 | Constitutive expressor of *PR* genes 1 |
| CRN | Crinkler or crinkling- and necrosis-inducing protein |
| CSEP0055 | Candidate Secreted Effector Protein 0055 |
| CSEP0443 | Candidate Secreted Effector Protein 0443 |
| CTAB | Cetyl trimethyl ammonium bromide |

| | |
|---|---|
| CUL | Cullin |
| DAB | 3,3′-Diaminobenzidine |
| dATP | Deoxyadenosine triphosphate |
| DDBI | DNA damage binding protein 1 |
| ddH20 | Double distilled water |
| DEPC | Diethyl pyrocarbonate |
| DNA | Deoxyribonucleic acid |
| dNTP | Dinucleotide phosphate |
| DPI | Day post inoculation |
| DTT | Dithiothreitol |
| dTTP | Deoxythymidine triphosphate |
| E. coli | Escherichia coli |
| E6-AP | E6-associated protein |
| EBR1 | Enhanced blight and blast resistance 1 |
| eds1 | Enhanced disease susceptibility 1 |
| EDTA | Ethylenediaminetetraacetic acid |
| EFK | Effectors homologous to Avr k 1 and Avr a 10 |
| EGFP | Enhanced green fluorescent protein |
| Eg-R1 | Early Growth Response 1 |

| | |
|---|---|
| EKA | Effectors homologous to Avr k 1 and Avr *a* 10 |
| EMBL-EBI | European Molecular Biology Laboratory-European Bioinformatics Institute |
| ESCRT | Endosomal sorting complexes required for transport |
| ESCRT-0 | Endosomal sorting complexes required for transport-0 |
| ESCRT-1 | Endosomal sorting complexes required for transport-1 |
| EST | Expressed sequence tag |
| ETI | Effector triggered immunity |
| ETS | Effector triggered susceptibility |
| ExPASy | Expert Protein Analysis System |
| EYFP | Enhanced yellow fluorescent protein |
| flg22 | Flagellin 22 |
| FLS2 | Flagellin-sensing 2 |
| fmol | femtomoles |
| FREE1 | FYVE domain protein required for endosomal sorting 1 |
| FYVE | Phenylalanine Tyrosine Valine Glutamic acid |
| Gal4 | Galactose 4 transcription factor |
| GFP | Green fluorescent protein |
| GNOM | ARF guanine-nucleotide exchange factor GNOM |
| GoE2 | Golovinomyces orontii effector 2 |

| | |
|---|---|
| GSH | Glutathione Sepharose 4B |
| GSNO | S-Nitrosoglutathione |
| GSNOR1 | S-nitrosoglutathione reductase |
| GSSG | Glutathione disulphide |
| GST | Glutathione S-transferase |
| GTPase | Guanosine triphosphate hydrolases |
| HA | Hemagglutinin |
| HECT | Homologous to the E6-AP Carboxyl Terminus |
| HIGS | Host Induced Gene Silencing |
| Hip-2 | Huntingtin interacting protein-2 |
| His | Histidine |
| His-68 | Histidine-68 |
| HopAI1 | Hypersensitive response and pathogenicity (hrp) outer protein AI1 |
| HPI | Hour post inoculation |
| HR | Hypersensitive response |
| HRP | Horseradish peroxidase |
| Hrs | Hours |
| Hsc70 | Heat shock cognate 70 kDa protein |
| HsP70 | Heat shock protein 70 kDa |

| | |
|---|---|
| HvRACB | Hordeum vulgare RacB |
| IgG | Immunoglobulin G |
| IKK | Inhibitor of kappa B kinase |
| Ile-44 | Isoleucine-44 |
| IPTG | Isopropyl β-D-1-thiogalactopyranoside |
| IRT1 | Iron regulated transporter 1 |
| JA | Jasmosmic acid |
| JAMM | JAB1/MPN/Mov34 metalloenzyme |
| JAZ | Jasmonate Zim domain |
| JAZ1 | Jasmonate-zim-domain protein 1 |
| kDa | Kilo Dalton |
| KEG | KEEP ON GOING |
| LB | Lysogeny broth |
| Leu-8 | Leucine-8 |
| LIC | Ligation independent cloning |
| LHB1B1, LHCB1.4 | Light-harvesting chlorophyll-protein complex ii subunit B1 |
| LLVY-AMC | Leucine-Leucine-Valine-Tyrosine- 7-amino-4-methylcoumarin |
| LRP5/6 | Low Density Lipoprotein Receptor-Related Protein-5/6 |
| MAMPS | Microbe Associated Molecular Patterns |
| MAP3K7/TAK1 | Mitogen activated protein kinase kinase kinase 7 |

| | |
|---|---|
| MAPK | Mitogen activated protein kinases |
| MBP | Maltose binding protein |
| MEKK1 | Mitogen activated protein kinase kinase kinase 1 |
| MES | Methyl Ester Sulfonates |
| ml | millilitre |
| Mlo | Mildew locus O |
| mM | milimoles |
| MP3Ks | Mitogen-activated protein kinase kinase kinase kinase |
| MUSE2 | Mutant, Snc1-enhancing 2 |
| MVB | Multivesicular bodies |
| Myd88 | Myeloid differentiation primary response 88 |
| NADPH | Nicotinamide adenine dinucleotide phosphate |
| NBS-LRR | Nucleotide-binding site leucine-rich repeat |
| NCBI | National Center for Biotechnology Information |
| NEB | New England Biolabs |
| NEDD4 | Neural precursor cell expressed developmentally down-regulated protein 4 |
| NF-κb | Nuclear factor kappa-light-chain-enhancer of activated B cells |
| ng | nanogram |
| NIA1 | Nitrate reductase 1 |

| | |
|---|---|
| NIA2 | Nitrate reductase 2 |
| nM | nanomoles |
| NO | Nitric oxide |
| NOS | Nitric oxide synthase |
| NOSA | No spores A |
| NPR1 | Non-expressor of pathogenesis related protein 1 |
| NSF | N-ethylmaleimide-sensitive factor |
| $OD_{600}$ | Optical density at wavelength 600 nm |
| OsBAG4 | Oryza sativa BAG4 |
| OsIPA1 | Oryza sativa IDEAL PLANT ARCHITECTURE1 |
| OsIPI1 | Oryza sativa IPA1 INTERACTING PROTEIN1 |
| OsPUB44 | Oryza sativa plant U-box 44 |
| PAMP | Pathogen Associated Molecular Patterns |
| PBS | Phosphate-buffered saline |
| PBS-T | Phosphate buffered saline-tween 20 |
| PCD | Programmed cell death |
| PCR | Polymerase chain reaction |
| PDS | Phytoene desaturase |
| PEC6 | Puccinia striiformis effector candidate 6 |

| | |
|---|---|
| PEST sequence | Proline (P), Glutamic acid (E), Serine (S), Threonine (T) |
| PMSF | Phenylmethylsulfonyl fluoride |
| PR1 | Pathogenesis related protein 1 |
| PR5 | Pathogenesis related protein 5 |
| PRR | Pattern Recognition Receptors |
| Pst | Pseudomonas syringe pv. tomato |
| PSTha12J12 | P. striiformis f. sp. tritici gene expressed in haustoria |
| PSTha12J12 | Puccinia striiformis f. sp. tritici ha12J12 |
| PTI | PAMP triggered immunity |
| PUB | Plant U-box |
| qPCR | Quantitative polymerase chain reaction |
| R | Resistance |
| RB1 | Retinoblastoma protein |
| RBR | RING between RING |
| RING | Really Interesting New Gene |
| RISC | RNA-induced silencing complex |
| RNA | Ribonucleic acid |
| RNAi | RNA interference |
| RNF2 | RING domain of Ring finger protein 2 |

| | |
|---|---|
| ROPIP1 | ROP-interactive peptide 1 |
| ROR1 | Required for mlo Resistance 1 |
| ROR2 | Required for mlo Resistance 2 |
| ROS | Reactive oxygen species |
| RPM | Revolution per minute |
| Rpn11 | Regulatory particle non-ATPase 11 |
| Rpn13 | Regulatory particle non-ATPase 13 |
| Rpt | Regulatory particle |
| RRE1 | Redox Regulated E3 ligase 1 |
| RRE2 | Redox Regulated E3 ligase 2 |
| RT-PCR | Reverse transcription polymerase chain reaction |
| RuBisCO | Ribulose-1,5-bisphosphate carboxylase/oxygenase |
| SA | Salicylic Acid |
| SAG | SA O-3-glucoside |
| SDS PAGE | Sodium dodecyl sulfate |
| SDS PAGE | Sodium dodecyl sulfate- Polyacrylamide gel electrophoresis |
| *sid2* | salicylic acid induction deficient 2 |
| si-Fi | siRNA Finder |
| siRNA | Small interfering RNA |

| | |
|---|---|
| SNAP | Synaptosomal Associated Protein |
| SNAP33 | Synaptosomal Associated Protein 33 |
| SNARE | Soluble NSF Attachment Protein Receptor |
| SNC1 | Suppressor of NPR1, Constitutive 1 |
| SNO | S-nitrosothiols |
| SOC | Super Optimal Broth |
| Stx-3 | Syntaxin-3 |
| Stx-5 | Syntaxin-5 |
| Syp121 | Syntaxin 121 |
| SYP122 | Syntaxin 122 |
| TGN/EE | *trans*-Golgi network/early endosomes |
| Tir | Toll/interleukin-1 receptor |
| TIR-NB-LRR | TIR (toll interleukin 1 receptor)-nucleotide-binding-leucine-rich repeat |
| TLR | Toll-like receptors |
| TNF | Tumour necrosis factor receptor |
| TPL | TOPLESS |
| TRAF2 | TNF receptor-associated factor 2 |
| TRAF3 | TNF receptor-associated factor 3 |
| TRAF6 | TNF receptor-associated factor 6 |

| | |
|---|---|
| TRIF | TIR-domain-containing adapter-inducing interferon-β |
| UB10 | Ubiquitin promoter 10 |
| Ub13 | Ubiquitin conjugating enzyme 13 |
| UBA | Ubiquitin activating enzyme |
| UBC | Ubiquitin conjugating enzyme |
| UBIQ | Ubiquitin |
| UEV | Ubiquitin E2 variant |
| UFD | Ubiquitin Fusion Degradation |
| UPL1-7 | Ubiquitin protein ligase 1-7 |
| UPS | Ubiquitin proteasome system |
| USP14 | Ubiquitin Specific Peptidase 14 |
| UV | Ultra violet |
| Val-70 | Valine-70 |
| VAMP | Vesicle associated membrane protein |
| VAMP721/722 | Vesicle Associated Membrane Protein 721/722 |
| VIGS | Virus-induced gene silencing |
| VWA | von Willebrand factor (vWF) type A domain |
| WD40 | Tryptophan-aspartic acid- 40 domain |
| Wnt | Wingless/Integrated |

| | |
|---|---|
| WRKY53 | Tryptophan (W), Arginine (R), Lysine (K), Tyrosine (Y) |
| XB3 | XA21 binding protein |
| XBAT32, 34, 35 | XA21 binding protein *Arabidopsis thaliana* 32,34,35 |
| XBHV35 | XA21 binding protein *Hordeum vulgare* 35 |
| X-gal | X-galactose |
| Xoo | *Xanthomonas oryzae* pv. *oryzae* |
| XopPXoo | *Xanthomonas* outer protein P *Xanthomonas oryzae* pv. *oryzae* |
| Y/F/WxC | Tyrosine/Phenylalanine/Tryptophan x Cysteine |

# Chapter one

## 1.0 Introduction

### 1.1 The plant microbial pathogens

Plant pathogens devastate crops and natural ecosystems causing economic losses annually not only in terms of expected yields but also the huge investment in an attempt to curb them (Rahman *et al*, 2018). The challenges caused by microbial pathogens are considerable especially in less developed countries where access to control measures are limited (Savary *et al*, 2012). These great challenges are often associated with hunger/famine, ill health and poverty due to low food production (Anderson *et al*, 2010; Savary *et al*, 2012). Major pathogenic organisms include:

Bacteria. These are unicellular prokaryotic organisms (Vellai & Vida, 1999). They enter the plant through extracellular digestion of plant tissues, natural openings like hydathodes, lenticels, stomata, stigma nectathodes and wounds (Buonaurio, 2008; Kannan & Bastas, 2016). Bacteria can be spread by water, insects, infected soil, contaminated tools, on seed, and by wind-blown rain. Most bacterial plant pathogens survive as saprophytes living on crop debris and in soil (Tripathi, 2017). The top 10 bacterial pathogens have been identified based on their scientific/ economic importance with *Pseudomonas syringae* pathovars rated as the most pathogenic (Mansfield *et al*, 2012).

Mollicutes, which can be described as prokaryotes lacking cell walls with a miniature genome of 580 kb - 2200 kb (Xavier *et al*, 2014). They cause diseases in plants by living within the phloem cells from which they obtain their nutrients. Mollicutes are very effectively carried from plant to plant by insects in which they can also reproduce (Pollack *et al*, 1997; Razin, 2006). Mycoplasma is the most known genus in Mollicutes divided into Phytoplasma and Spiroplasmas. They are responsible for the group of plant diseases called yellow diseases

and are spread by insects such as leafhopper (Garnier *et al*, 2001).

Viruses and viroids. Most viruses consist of ribonucleic acid (RNA), surrounded by a protein coat (the capsid). A few plant pathogenic viruses contain deoxyribonucleic acid (DNA) rather than RNA. The viroids are subviral smallest replicons of about 250-400 nucleotides containing naked circular RNA genetic material (Flores *et al*, 2011; Hetal *et al*, 2015). All viruses and viroids are intracellular and are obligate parasites dependent on the plant cell for their reproduction (Hetal *et al*, 2015). The viruses and viroids that cause plant diseases are often disseminated by insects, and propagation of both infected vegetative materials and seeds (Flores *et al*, 2011). The viruses and viroids are the hardest pathogens to control due to their tendency to mutate rapidly (Sanjuán & Domingo-Calap, 2016). Effective best control strategy are best on complete destruction of the infected plant, since chemicals have proven inefficient. The symptoms of viral infection include yellowing, stunted growth in some parts of the plant and plant malformations like leaf rolls and uncharacteristically narrow leaf growth (Randles & Ogle, 1997; Serio *et al*, 2012).

Nematodes. These are small vermiform microorganisms that live in soil and feed on plant roots by piercing the cells with a needlelike structure called a stylet through which they suck up the cell contents (Mbega & Nzogela, 2012; Singh & Phulera, 2015). They lay eggs that hatch as larvae and go through four juvenile stages before becoming adults (Singh & Phulera, 2015). Nematodes have a 30-day life cycle, but they can remain in a dormant state for more than 30 years. Nematodes feed from outside or inside the root and cause enormous damage to roots, thus reducing nutrient and water uptake (Jones *et al*, 2013; Schmitt & Sipes, 2018). Root-knot nematodes the most damaging pathogens, stimulate division and expansion of root cells to create galls in which the female nematodes remain to feed and produce eggs (Jones *et al*, 2013).

Oomycetes, these are fungus-like eukaryotes, pathogenic to a large number of plants

and animals (Judelson & Blanco, 2005). They are distinct from fungus by possessing cellulose in the cell wall as opposed to chitin in fungus, being diploid during the vegetative stage of mycelia formation as opposed to haploid thalli formed in fungus. Morphologically they possess tubular cristae in their mitochondria and produce non-septate hyphae. Fungi produce flattened cristae and produce septate hyphae. Oomycetes are dispersed by both water and wind, and exhibit the biotrophic, nectrotrophic and hemibiotrophic feeding life styles. For example, *Hyaloperonospora parasitica*, *Plasmopara viticola*, as well as *Albugo candida*, which causes white rust are obligate biotrophs. *Phytophthora* species, are *Hemibiotrophs* having the ability to grow in axenic culture as do necrotrophs, such as *Pythium ultimum* (Fawke *et al*, 2015).

Fungi are eukaryotic, spore-bearing, heterotrophic organisms that produce extracellular enzymes to break down plant products to small molecules which they absorb as nutrients (González-Fernández *et al*, 2010). Fungi may grow as unicellular yeasts, but more commonly they grow as multicellular chains of elongated cells that form threadlike structures collectively called mycelium. About 80% of plant diseases can be traced to fungi, which have a great capacity to reproduce themselves both sexually and asexually (González-Fernández *et al*, 2010). Fungi can grow on living or dead plant tissue and can survive in a dormant stage until conditions become favorable for their proliferation. They can grow as ectophytes on plant surface or as endophytes in plant tissue. The fungal spores, which are the propagating material can be dispersed by wind, water, soil and animals to other plants. Successful fungal growth are favoured by the warm and humid conditions (Gladieux *et al*, 2017). While many fungi play useful roles in plant growth, especially by forming mycorrhizal associations with the plant's roots, others cause such common plant diseases as anthracnose, late blight, apple scab, club root, black spot, damping off, and powdery mildew. A number of plant pathogenic fungi have been ranked in the order of the most economic importance with *Blumeria*

*graminis* the causal agent of powdery mildews appear among the highly devastating pathogens (Dean *et al*, 2012).

### 1.1.1 Powdery mildew fungi pathogenesis

The powdery mildews belong to the Kingdom Fungi of phylum Ascomycota in the order of Erysiphales (Bindschedler *et al*, 2016). They have only one family, the Erysiphaceae subdivided into five tribes (Erysipheae, Golovinomycetinae, Cystotheceae, Phyllactinieae, Blumerieae) and further subtribes and more than 10 genera (Ale-agha *et al*, 2008). They form morphologically complex structures during asexual pathogenesis and produce fruiting bodies (chasmothecia), which develop after sexual reproduction (Spanu *et al*, 2010). They are obligate, biotrophic parasites symptomized by a white, powdery film on the leaves, stems, flowers and fruits of angiosperms (Takamatsu, 2013; Bindschedler *et al*, 2016). The powdery mildew fungi are wide spread causing significant economic loss in 129 temperate areas by infecting more than 9000 dicot and 650 monocot species including grape, tomato, barley and wheat favoured by high humidity (Hückelhoven, 2005; Glawe, 2008; Takamatsu, 2013).

Here we review the events of powdery mildew pathogenesis with respect to the barley powdery mildew, *Blumeria graminis* f. sp. *hordei* (*Bgh*). Once the mature spore lands on the epidermal tissue, physiological changes occur expeditiously within the conidium to initiate germination. Extracellular matrix containing esterase and cutinase enzymes are produced from the conidium within one minute. The matrix fastens the conidium on the waxy cuticle of the epidermal leaf surface resisting forces from blowing winds (Carver *et al*, 1999; Wright *et al*, 2002). Fixation is also supported by wart-like projections on the spore surface that get trapped into the leaf surface waxy materials (Zhang *et al*, 2005b). In a period of < 3 hours post inoculation the primary germ tube wall in contact with the epidermal surface develops a protrusion known as a cuticular peg. The cuticular peg penetrates the cuticle progressing up

to the cell wall. Apart from reinforcing the fastening of the spore, the cuticular peg also absorbs nutrients from the host cell to support further growth of spore (Edwards, 2002). The extracellular matrix, cuticular peg and material trafficking from the host cell into the spore enable the physiologically active conidium to sense the appropriate surface for further growth (Zhang *et al*, 2005b; Yamaoka *et al*, 2006). After recognizing the host surface mediated by signals sensed from both the cuticular peg and extracellular matrix, a septate appressorium germ tube emerges, elongates and differentiates into a hooked appressorium. The formation of appressorium happens within 9-10 hours post inoculation and is anchored on the leaf surface by hydrophobic materials in the extracellular matrix (Zhang *et al*, 2005b). To achieve penetration into the host cell, the appressorium forms a penetration peg at its tip by 12 hours that breach the cell wall by means of both enzymatic and mechanical force (Zhang *et al*, 2005b).

The penetration peg extends into the host cell and enlarges to form the multidigitate haustorium within 15-18 hours. During its extension in the cell, the haustoria invaginates the plasma membrane without causing puncture to form an extrahaustorial membrane enveloping it at the neck band (Micali *et al*, 2011; Spanu & Panstruga, 2017). The intracellular space between the extrahaustorial membrane and haustoria interface is occupied by a non-cytoplasmic, gel-like material, the extrahaustorial matrix keeping it from direct contact with the host cell cytoplasm and immune complexes (Li *et al*, 2005; Hückelhoven & Panstruga, 2011). The haustorium, extrahaustorial matrix, and host cell derived membrane are the sites of feeding, metabolism, molecular signaling events and delivery of fungal effector proteins (Panstruga & Dodds, 2009a; Zhang *et al*, 2012). The secondary hyphae emerge 24 hours after the primary haustoria has formed digitate structures at its terminal end. By 48 hours the secondary hyphae give rise to protrusions of appressoria hyphae, then a new generation of haustoria is produced. At maturity a single cell may contain up to 50 haustoria (Zhang *et al*,

2005b). By the completion of the cycle 72-96 hours, conidiophores develop from epiphytic hyphae and produce masses of conidia for further colonization. At the end of the host growth season, the fungus produces chasmothecia which act as resting structures to survive adverse conditions (Ale-agha *et al*, 2008) (Figure 1-1).

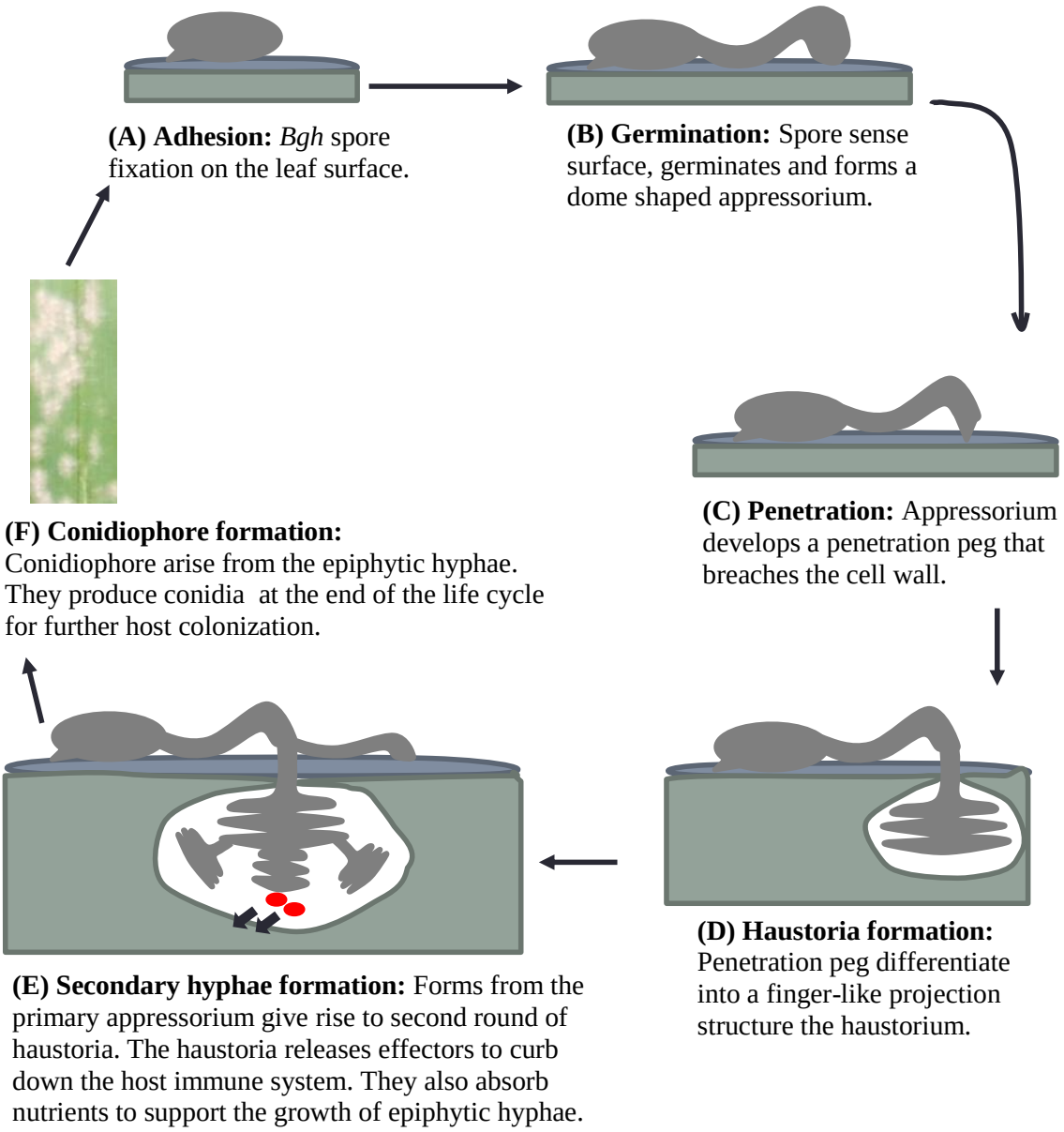


**Figure 1-1: Illustration of the infection cycle of *Bgh*.** (A) Once the viable spore lands on the leaf epidermal surface, its fixed by the extracellular matrix and the cuticular peg. (B) The secondary germ tube develops, elongates and forms an appressorium at the terminal end. (C) The appressorium forms a penetration peg which ruptures the cell wall aided by enzymes and mechanical force. (D) This structure then differentiates into

a haustorium, the feeding structure which invaginates the plasma membrane. (E) Secondary hyphae form from the terminal end of the initial appressorium and gives rise to a second generation of haustoria. (F) The epiphytic hyphae produce conidiophores bearing conidia that are released to the air for further host colonization.

### 1.1.2 Searches for putative *Bgh* effectors

Effectors are molecules which are synthesized by the pathogen to target host cellular processes and modify their function for successful plant colonization (Kamoun, 2007). Plant powdery mildew fungi secrete effector proteins to the plant cell from the haustoria to advance their virulence (Catanzariti *et al*, 2006; Kamoun, 2006; Panstruga & Dodds, 2009b; Thomma *et al*, 2011; Ahmed *et al*, 2015). A number of searches screenings have been conducted on the *Bgh* genome to reveal potential effectors.

Proteomic analysis of *Bgh* haustoria proteins identified nine proteins with signal peptides. The presence of a signal peptide implied a potential for secretion into the host (Bindschedler *et al*, 2009). Another search was aimed to identify *Avirulence* (*AVR*) genes from *Bgh* recognised by the corresponding *Resistance* (*R*) genes. By applying genetic delimitation, polymorphism and transcript analysis techniques, *AVRA10* and *AVRK1* were identified (Ridout *et al*, 2006). AVRA10 and AVRK1 are related proteins that belong to the large Effectors homologous *to* Avrk1 *and* Avra10 *(*EKA) family of at least 1000 paralogues in *Bgh* and are known to lack classical signal peptides required for transfer into the host cell (Ridout *et al*, 2006; Shen *et al*, 2007; Spanu *et al*, 2010).

Transcriptome analysis were conducted on epidermal cells of barley leaves inoculated with *Bgh* for 7 days. A total of 3200 unigenes were found to be upregulated in haustoria enriched leaf materials and corresponded to fungal genes. A large number of these genes encode small peptides with a signal peptide at the N-terminus. Most of these proteins had a conserved motif of "Y/F/WxC". The first amino acid of this motif can be any of the three aromatic residues, tyrosine (Y), phenylalanine (F) or tryptophan (W), and the last is always

cysteine (C) (Godfrey *et al*, 2010). Altogether a total of 107 effector proteins were identified, because of their haustoria expression and the presence of a signal peptide were referred to as *Bgh* Effector candidates (*Bgh*Efc). Cluster analysis of fungal Expressed sequence tag (EST) sequences revealed *BghEfc1* as the most prevalent EST, occurring 110 times. *BghEfc1* encodes a 109 amino acid residue peptide with a predicted signal peptide at the N-terminus. The mature protein is a truncated sequence of 88 amino acids lacking a signal peptide and has no homologues outside *Blumeria graminis* (Godfrey *et al*, 2010). *Bgh*Efc1 is synonym to Candidate Secreted Effector Protein 0443 (CSEP0443) (Pedersen *et al*, 2012). Expression level analysis of *BghEfc1/CSEP0443* revealed that this gene exhibited a progressive increase of expression reaching a maximum at day 4 post inoculation and then gradually declining. Thus, implying *BghEfc1/CSEP0443* might play a pivotal role in penetration and haustoria formation promoting fungal aggressiveness (Godfrey *et al*, 2010). Originally utilization of bioinformatics involving genome sequencing and assemblies identified 248 Candidate secreted effectors in the haploid *Blumeria* genome (Spanu *et al*, 2010; Spanu & Panstruga, 2012). Extensive genome wide analysis of *Bgh* isolate DH14 identified 491 Candidates for Secreted Effector Proteins (CSEPs) by searching for genes encoding secreted proteins without sequence similarity to proteins outside the powdery mildews (Pedersen *et al*, 2012). The 491 genes encoding CSEPs constitute over 7% of the pathogen's annotated genes and most were grouped into 72 families of up to 59 members. Among them were two major types of effector families: one comprising short proteins (100-150 amino acids) with a high relative expression level in haustoria compared with epiphytic fungal structures and one consisting of longer proteins (300-400 amino acids) with lower levels of differential expression (Pedersen *et al*, 2012). In addition to having characteristic signal peptides, most of the effector candidates are small, divergent proteins with no other targeting sequence or transmembrane domains (Saunders *et al*, 2012). Almost 307/491 CSEPs share a three-amino-acid motif,

called Tyrosine/Phenylalanine/Tryptophan x Cysteine ("Y/F/WxC"), in the N-terminus of the mature proteins (Pedersen *et al*, 2012). However, so far, there is no experimental evidence to indicate that this Y/F/WxC motif is required for translocation of the effector (Schmidt *et al*, 2014). Many of the CSEPs are predicted to have a similar structure to that of microbial ribonucleases (Pedersen *et al*, 2012; Kusch *et al*, 2014).

Experimental and proteogenomics based bioinformatics analysis of the proteome from sporulating hyphae and haustoria identified 71 peptides that were present exclusively in the haustoria. The proteins presented with canonical features of effector proteins such as being small on average ~235 amino acids, having an N-terminus signal peptide and absence of a transmembrane domain (Bindschedler *et al*, 2011). They had low sequence similarity to closely related fungi suggesting specificity within species interactions. The proteins were named as Blumeria Effector Candidates (BECs). A large proportion of these proteins were encoded by similar genes as CSEPs (Bindschedler *et al*, 2016).

### 1.1.3 Function role of *Bgh* effectors during infection

Filamentous pathogen effector proteins are typically produced in the endoplasmic reticulum (ER) and secreted through Golgi-derived vesicles by exocytosis. The effector proteins are transferred either to the apoplastic or cytoplasmic space of host cells (Hogenhout *et al*, 2009; Dodds & Rathjen, 2010; Jonge *et al*, 2011). *Bgh* effectors are probably secreted via the classical ER pathway similar to that identified in other phytopathogenic fungi. Once in touch with the host cell the effectors can behave in several ways to suppress plant defence (Godfrey *et al*, 2010; Spanu *et al*, 2010; Pedersen *et al*, 2012). To date only a few effectors have had their biological roles disclosed (Ahmed *et al*, 2016b). Host Induced Gene Silencing (HIGS) has typically been applied to reveal the functional contribution of a number of CSEPs, likely attributed to unreliable transformation procedures for *Bgh* (Nowara *et al*,

2010).

The CSEP0055/*Bgh*Efc3 is among the most highly expressed effector protein during the first 24 hours of *Bgh* infection, aiding fungal aggressiveness. Knock-down of CSEP0055 reduced fungal pathogenicity by~40%. The effector protein interacts with members of barley pathogenesis related (PR) proteins, PR1 and PR17. PR17c is required for penetration resistance locally accumulating at fungal penetration sites (Zhang *et al*, 2012). The Blumeria effector candidates BEC1005, BEC1011, BEC1016, BEC1018, BEC1019, BEC1038, BEC1054 and BEC1040 are expressed early during infection aiding haustoria formation thus promoting *Bgh* establishment. BEC1011 and BEC1054 are predicted to be similar to fungal ribonucleases and cause the greatest effect on disease emergence. Knocking down of either effector protein resulted in 60% to 70% reduction in disease development. BEC1011 specifically suppresses pathogen induced host cell death (Pliego *et al*, 2013; Spanu, 2017). BEC1054 target several host proteins including glutathione S-transferase, malate dehydrogenase and Pathogenesis related 5 protein isoforms thus compromising key players in defence responses (Pennington *et al*, 2016). CSEP0105 and CSEP0162 are expressed pre and post haustoria formation during *Bgh* infection. Both effectors target the heat shock proteins (Hsp) Hsp16.9 and Hsp17.5 compromising their chaperon activity (Ahmed *et al*, 2015a). The heat shock proteins are known to stabilize intracellular proteins involved in defence related signalling through their chaperon activity (Wang *et al*, 2004). The expression of CSEP0007, CSEP0025, CSEP0128, CSEP0211, CSEP0247, CSEP0345, CSEP0420 and CSEP0422 are elevated during the early stages of *Bgh*-plant interactions, likely required for fungal colonization. Other effectors, CSEP0139, CSEP0264 and CSEP0313 are strikingly upregulated in haustoria containing material suggesting a role during post penetration events (Aguilar *et al*, 2016). The nuclear and cytosolic localized effectors CSEP0081 and CSEP0254 are required during penetration and haustoria formation in *Bgh*. Silencing of the two CSEPs

markedly reduced penetration and haustoria formation rates (Ahmed *et al*, 2016b). The non-cognate effectors, $AVR_{A10}$ and $AVR_{K1}$ lacking a signal peptide has been described from the interaction between barley and *Bgh*. The absence of a signal peptide pre-supposes that they are delivered to the host cell via a different mechanism. Silencing of both effectors reduced the haustoria index in plants lacking cognate recognition genes indicating that they aid *Bgh* virulence (Ridout *et al*, 2006; Nowara *et al*, 2010).

### 1.2 Plant immunity against microbial pathogens

The immobile nature of plants subjects them to a wide range of biotic stresses (Møller *et al*, 2007; Macho & Zipfel, 2014). In order to counteract these effects plants have developed different layers of protection. The initial layer of defence involves conserved plant surface cell structures such as waxy materials, hairy surface, lignified cuticle and cell wall that make conditions unfavourable for the pathogen to penetrate. Significantly, plant cells also have transmembrane pattern recognition receptors (PRRs) that recognise conserved structures on intruding microbial pathogens known as pathogen associated molecular patterns (PAMPs) mediating PAMP-triggered immunity (PTI) (Zipfel and Felix, 2005; Macho and Zipfel, 2014; Furniss and Spoel, 2015; Nie *et al.*, 2017). PAMPs are generally possessed by all members of the same class and are required for pathogen viability. Flagellin on bacteria and chitin on fungi are among the PAMPs with well characterised PRRs (Kaku *et al*, 2006; Chinchilla *et al*, 2006; Miya *et al*, 2007). The defence responses involved during PTI are associated with mobilization of anti-microbial phytoalexins (Bednarek & Osbourn, 2009), biosynthesis of cell wall degrading enzymes (Mauch *et al*, 1988), signalling networks involving ion exchanges across the plasma membrane, Mitogen activated protein kinases (MAPK) signaling cascades, and reinforcement of the cell wall by deposition of callose in the forming papilla at the sites of microbial attack (Underwood & Somerville, 2008; Pitzschke *et al*, 2009; Ronald &

Beutler, 2010; Voigt, 2014).

The PTI layer of defence is superimposed upon 'gene-for-gene' protection, in which a dominant resistance (*R*) gene directly or indirectly recognises a pathogen effector protein encoded by an avirulence (*Avr*) gene (Jones & Dangl, 2006; Kadota *et al*, 2015). The recognition results in effector triggered immunity (ETI), associated with the programmed execution of host cells, restricting pathogen ingress (Jones & Dangl, 2006; Van Ooijen *et al*, 2010; Nie *et al*, 2017). *R* mediated resistance is based either on the surveillance of the cellular effector targets in the so called guard hypothesis or encodes the Nucleotide-binding site leucine-rich repeat (NBS-LRR) proteins. The NBS-LRRs recognise and bind directly the effectors or binds the effector-target complex. The R based -NBS-LRR are only effective against biotrophic and hemibiotrophic pathogens that can be attenuated by induced cell death at infection sites but not necrotrophic pathogens that promote cell death for successful colonization (Jones & Dangl, 2006; Voigt, 2014). The PTI-ETI plant immune system is summarised in a four phase zigzag model described by (Jones & Dangl, 2006).

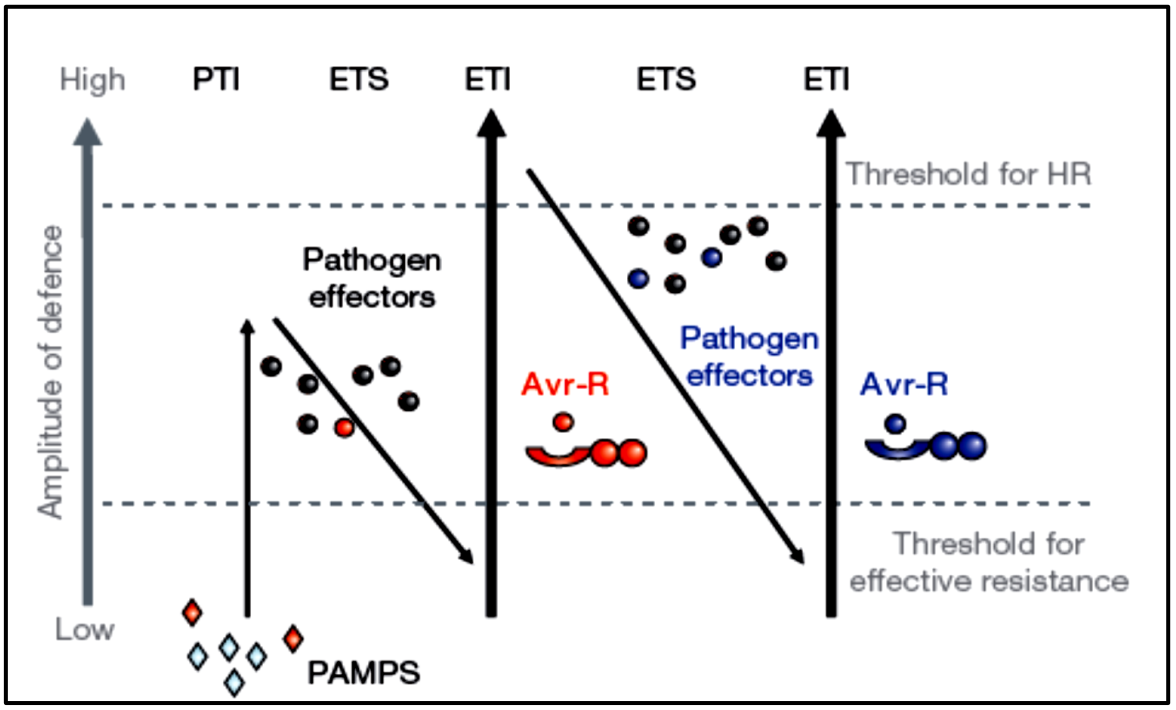

**Figure 1-2: In this scheme, the ultimate amplitude of disease resistance or susceptibility is proportional to (PTI–ETS1+ETI).** In phase 1, plants detect MAMPs/PAMPs, red diamonds) via PRRs to trigger PTI. In phase 2, successful pathogens secrete effectors to compromise PTI, or otherwise enable pathogen nutrition and dispersal, resulting in ETS. In phase 3, one effector (indicated in red) is recognized by an NBS-LRR protein, activating ETI, an amplified version of PTI that often passes a threshold for induction of hypersensitive response cell death. In phase 4, pathogen undergo natural selection, the emerged isolates have lost the red effector, and perhaps gained new effectors through horizontal gene flow (in blue), these can help pathogens to suppress ETI. Selection favours new plant NBS-LRR alleles that can recognize one of the newly acquired effectors, resulting again in ETI.

### 1.2.1 Role of S-nitrosylation in plant immunity

In mammalian systems the generation of nitric oxide (NO) is mediated by nitric oxide synthase (NOS), an enzyme existing in three isoforms, inducible (iNOS), endothelial (eNOS) and neuronal (nNOS) (Alderton *et al*, 2001; Guo, 2003). The Nicotinamide adenine dinucleotide phosphate (NADPH) dependant enzyme catalyses the conversion of L-arginine to citrulline and NO (Alderton *et al*, 2001; Yu *et al*, 2012, 2014). The generation of NO in plants is still under high controversy (Yu *et al*, 2012). Despite several completed genome projects the gene for the NOS has not been found (Malik *et al*, 2011; Yu *et al*, 2012; Jeandroz *et al*, 2016). Currently, a number of reports suggest that the generation of NO might be due to the reduction of nitrite by NADPH and pH dependant nitrate reductase (Bolwell & Daudi, 2009; Sanz *et al*, 2015). In *Arabidopsis*, nitrate reductase occurs commonly in the cytosol encoded by two structural genes as nitrate reductase 1 (*NIA1*) and nitrate reductase 2 (*NIA2*). *NIA2* exhibits the highest observed nitrate reductase activity (Wilkinson & Crawford, 1991). NO can also be directly generated from nitrates, though the reaction has a pronounced time lag in comparison to generation from nitrites (Rockel *et al*, 2002). The production of NO via these reactions has been demonstrated *in vivo* to be enhanced with increased oxygen supply and nitrite concentrations (Rockel *et al*, 2002).

Nitric oxide plays a vital role in regulating plant immunity often acting through S-

nitrosylation. S-nitrosylation is the reversible addition of a NO moiety to a reactive cysteine thiol residue of the target protein to form an S-nitrosothiol (SNO) altering protein stability and activity (Feechan *et al*, 2005; Martínez-Ruiz & Lamas, 2007). S-nitrosylation of glutathione tripeptide freely available in cytosol results into S-nitrosoglutathione (GSNO) a global reservoir and donor of NO. GSNO and SNO are regulated by GSNO reductase (GSNOR1) catalysing the reduction of GSNO to unstable intermediates which in the presence of glutathione are converted to the oxidised form, glutathione disulphide (GSSG) (Feechan *et al*, 2005; Malik *et al*, 2011; París *et al*, 2013). *atgsnor1-3* plants display distinct phenotypes such as delayed growth, loss of apical dominance, decline in fertility and disabled resistance to pathogens (Feechan *et al*, 2005). The increased susceptibility is attributed to elevated SNO levels upon pathogen infection suggesting that the excess SNO produced are not modulated due a loss of GSNOR1. Additionally, *atgsnor1-3* mutants are compromised in salicylic acid (SA) biosynthesis. The plants display a lowered expression of *PR1* a marker for SA dependant gene expressions after exposure to the avirulent pathogens *Pseudomonas syringe* pv. *tomato* DC3000 (*Pst*DC3000) (*avrB*) or *Blumeria graminis* f. sp. *tritici* (*Bgt*). Moreover, the accumulation of SA and its sugar derivative, SAG were reduced under *Pst*DC3000 (*avrB*) challenge and unchallenged conditions (Feechan *et al*, 2005). Furthermore, S-nitrosylation has been shown to regulate a number of other key immune regulators including NADPH oxidase (Yun *et al*, 2011, 2016), Non-expressor of PR1 (NPR1) (Spoel & Loake, 2011; Yu *et al*, 2012), *Arabidopsis thaliana* SA binding protein 3 (AtSABP3) (Wang *et al*, 2009; Yu *et al*, 2012), and peroxynitrite (Yun *et al*, 2012; Spoel & Loake, 2011).

S-nitrosylation has also been implicated in positive regulation of plant immunity, for example, by targeting effector proteins released by plant pathogens to circumvent host defence mechanisms (Ling *et al*, 2017). During the onset of hypersensitive response in *Arabidopsis* the bacterial effector protein, the hypersensitive response and pathogenicity (hrp)

outer protein AI1 (HopAI1) of *Pst*DC3000 is S-nitrosylated inhibiting the phosphothreonine lyase activity of the effector (Ling *et al*, 2017). HopAI1 enhances *Pst* strain 0288-9 virulence in tomato plants and the transgenic expression of HopAI1 in *Arabidopsis* increases susceptibility to *Pst*DC3000 by compromising PTI (Zhang *et al*, 2007a). HopAI1 targets and supresses mitogen activated protein kinases (MAPKs) activated by exposure to PAMPS (flg22) by removing a phosphate group from phosphothreonine required for HopAI1 activity (Zhang *et al*, 2007a). MAPKs are involved in signal transduction mediated by phosphorylation and de-phosphorylation of proteins leading to activation of defence genes that may orchestrate the development of a hypersensitive response (HR) (Taj *et al*, 2010). S-nitrosylation of HopAI1 occurs at a non-catalytic Cysteine 138 restoring MAPK signalling disarming this virulence strategy (Ling *et al*, 2017). In addition overexpression of a HopAI1$^{CS}$ S-nitrosylation insensitive mutant triggered autoimmunity and failed to promote the anticipated susceptibility to the pathogen in addition to the impairment of HR-cell death (Ling *et al*, 2017).

### 1.2.2 HIGS based RNA interference

RNA interference (RNAi) is a post transcription silencing mechanism based on sequence specific and homology of target gene. It is initiated when an RNAse III enzyme, termed dicer splices the long double stranded RNA or hairpin folded RNA into small interfering double stranded RNA (siRNA) of 20-25 bp with an extra 2 nucleotides at the 3' end. The siRNAs have the sense strand and the antisense strands referred to as the passenger and guide strands respectively. The passenger strand is degraded in the cytoplasm while the guide strand is incorporated into the argonaute-RISC (RNAi induced silencing complex). The guide strand binds the complementary sequences of the target gene which is degraded by argonaute enzymes at the central region (usually 10 - 11 nucleotides) attenuating expression

(Younis *et al*, 2014; Guo *et al*, 2016; Majumdar *et al*, 2017).

HIGS is an RNAi dependant mechanism involving the silencing of the targeted gene of a pathogen utilizing siRNA synthesized in the plant. The double stranded RNA can be stably made in the plant as a transgene or introduced into the plant by *Agrobacterium* or viral replication in the plant (Yin & Hulbert, 2015). HIGS has found a wide application in combatting a number of pathogens including nematodes (Banerjee *et al*, 2017), bacteria (Younis *et al*, 2014), and fungi (Yin & Hulbert, 2015; Majumdar *et al*, 2017). In barley and wheat the development of *Blumeria graminis* was reduced by silencing the *Avr10* effector aided by the HIGS (Nowara *et al*, 2010). The wheat rust fungi *Puccinia striiformis* f. sp. *tritici* (*PST*) or *Puccinia graminis* f. sp. *tritici* devastate wheat and other cereal crops by causing wheat stripe rust and stem rust disease respectively. Expression of the haustorially expressed *PSTha12J12* (PST gene expressed in haustoria *12J12*) in wheat using Barley Stripe Mosaic Virus-Virus Induced Gene Silencing (BSMV-VIGS) vectors mediated HIGS decreased the transcript levels of *PSTha12J12* and fungal virulence (Yin *et al*, 2011). HIGS is a powerful tool applicable in reverse genetics where stable transformations are of limited success. It has also been successfully applied to scrutinize candidate genes for fungal virulence in both rust and *Blumeria* pathogens (Yin *et al*, 2011; Aguilar *et al*, 2016).

### 1.2.3 Penetration resistance against fungal pathogens

Penetration resistance is part of nonhost resistance induced during PTI contributing to the arrest of non-adapted pathogens. Independent *Arabidopsis* mutant screens allowing increased penetration of *Bgh* identified *Arabidopsis thaliana PENETRATION* (*AtPEN1*) gene existing in three forms, *AtPEN1*, *AtPEN2* and *AtPEN3* (Collins *et al*, 2003; Stein *et al*, 2006).

*AtPEN2* (*At2g44490*) encodes a surface peroxisome localized myrosinase involved in catabolizing of indoglucosinates to toxic secondary metabolites (Lipka *et al*, 2005; Humphry

*et al*, 2010). The *AtPEN3* (*At1g59870*) encodes the Adenosine triphosphate (ATP)-Binding cassette transporter PLEIOTROPIC DRUG RESISTANCE8 (PDR8). It is postulated that the plasma membrane localized AtPEN3 is involved in the transport and efflux of toxic products from indoglucosinate metabolism into the apoplast at attempted penetration sites (Stein *et al*, 2006; Humphry *et al*, 2010). Under pathogen challenge, AtPEN3 accumulates strongly at the sites of pathogen attack corresponding at sites of papilla formation (Stein et al, 2006; Underwood & Somerville, 2008). For its recruitment and focal accumulation at sites of attempted penetration, AtPEN3 requires delivery by functional actin filaments but not microtubules (Underwood & Somerville, 2008). Mutations in AtPEN3 supported increased invasion of the non-adapted powdery mildew (*Erysiphe pisi*), Oomycetes (*Phytophthora infestans*) and necrotrophic fungi (*Plectosphaerella cucumerina*) while surprisingly led to elevated resistance to the adapted pathogen *Golovinomyces orontii* in an SA-dependant mechanism (Stein *et al*, 2006).

*AtPEN1* (*At3g11820*) encodes a membrane anchored Syntaxin 121 (Syp121) (Collins *et al*, 2003; Assaad *et al*, 2004). The Syntaxins are a group of Soluble NSF (N-ethylmaleimide-sensitive factor) Attachment Protein Receptor (SNARE) machinery involved in the transport and excretion of cargo materials at the plasma membrane (Jahn & Scheller, 2006). AtPEN1 interacts with Vesicle associated membrane protein, VAMP721 (At1g04750) and VAMP722 (At2g33120) known to play a role in limiting nonhost powdery mildews. AtPEN1 preferentially interacts with VAMP721/722 and Synaptosomal associated protein 33 (SNAP33) (At5g61210) to form a ternary SNARE complex (Kwon *et al*, 2008a). VAMP722 has been demonstrated to localize on the endomembrane compartments, while the SNAP33 pathogen inducible counterpart assembles at the peripheral plasma membrane (Kwon *et al*, 2008a; Humphry *et al*, 2010). Homozygous mutants of both *vamp721/722* and *snap33* are lethal indicating that secretory system is essential for cell viability. The tertiary focal

accumulation of AtPEN1, VAMP722 and SNAP33 at the pathogen penetration sites suggests that they are required for timely fusion of vesicle containing toxic materials with the plasma membrane during attempted pathogen ingress (Assaad *et al*, 2004; Bhat *et al*, 2005; Kwon *et al*, 2008a). Indeed the SNARE together with an adenosine diphosphate (ADP) ribosylation factor (ARF) Guanosine triphosphate hydrolases (GTPase) and the GTP exchange factor GNOM (ARF guanine-nucleotide exchange factor) mediate secretion of exosomes to form the papilla (Nielsen & Thordal-Christensen, 2012). AtPEN1 also has orthologues elsewhere. For-example in barley, Required for mlo Resistance 1 (ROR1) and ROR2 are required for the *mlo* enhanced penetration resistance but also contribute to the basal level resistance. Like AtPEN1, ROR2 shows surface plasma membrane localization. The protein has close resemblance to AtPEN1 compared to other *Arabidopsis* syntaxins with 62% identity and 77% similarity in the cytosolic region (Collins *et al*, 2003).

Loss of functions mutations in *AtPEN1* lead to four genotypes with increased *Bgh* penetration success. *atpen1-1*, *atpen1-2* and *atpen1-4*, have a stop codon early in the open reading frame, the encoded truncated peptides are either non-translated or un stable *in vivo*. *atpen1-3* encodes a non-dysfunctional AtPEN1 with an amino acid residue substitution un-able to impart penetration resistance (Collins *et al*, 2003; Assaad *et al*, 2004). Although the mutants displayed increased *Bgh* invasion, further growth of the fungus was abolished by the induced HR-like cell death response implying AtPEN1 mutation alone can not support pathogen colonization (Collins *et al*, 2003). In addition, loss of AtPEN1 and its close relative syntaxin 122 a non-translocatable syntaxin are linked to an induction of salicylic acid dependent resistance to host fungal pathogens (Kobae *et al*, 2006; Stein *et al*, 2006; Zhang *et al*, 2007b, 2008).

AtPEN proteins are not only required for cell wall based resistance but also play a role in ETI. Loss of function mutations in AtPEN1, AtPEN2 and AtPEN3 are associated with

a weakened HR response following activation of both coiled coil nucleotide binding domain and leucine rich repeat (CC-NB-LRR) and toll interleukin 1 receptor-nucleotide-binding-leucine-rich repeat (TIR-NB-LRR) R-proteins as well as unregulated cell death in response to non-host mildew pathogens (Johansson *et al*, 2014).

### 1.3 Redox Regulated E3 ligase 1 (RRE1)

*RRE1* (*At4g14365*) was initially identified following transcriptome analysis of pathogen challenged *Arabidopsis gsnor1-3* and salicylic acid induction deficient 2 (*sid2*) mutants. Previous data suggests that transcription of *RRE1* is exquisitely sensitive to changes in NO levels following attempted pathogen infection (Yu, 2012). RRE1 protein has two conserved domains, the ankyrin repeats in the N-terminus and a really interesting new gene (RING) finger motif in the C-terminus (Mosavi *et al*, 2004; Noel *et al*, 2014).

Ankyrin repeat motifs are among the most common protein domains composed of 30-34 amino acid residues. These molecules are known to function exclusively in protein-protein interactions (Li *et al*, 2006; Parra *et al*, 2015). They are usually described as composed of a helix-turn-helix conformation and strings of tandem repeats packed in a linear array to form helix-loop-helix-$\beta$-hairpin/loop fold. The complex fold of the ankyrin repeat are linked together by the intra and inter specific hydrophobic and hydrogen bonds (Guo, 2009). The unique features of these motifs in protein interactions specificity, stability, folding and unfolding are provided by their elongated and repetitive nature supporting bond formations (Li *et al*, 2006).

The RING domain consists of eight conserved cysteine and histidine residues co-ordinately binding two zinc ions in a cross-brace structure (Kosarev *et al*, 2002; Stone *et al*, 2005). Metal ligand pairs are typically characterized by the presence of cysteine and histidine residues essential for catalytic activity of the protein (Prasad *et al*, 2010). The RING domain

proteins are classified as a sub-class of ubiquitin ligase or E3 ligases for specific recognition of target proteins causing the attachment of ubiquitin to a lysine residue on a selected substrate leading to a multitude of consequences. The presence of E3 ligase activity in RRE1 suggests a potential role in protein ubiquitination dependant plant immunity (Yu, 2012). RRE1 proteins accumulated during infection with *Arabidopsis* powdery mildew (*Golovinomyces orontii*) and loss of *RRE1* led to enhanced susceptibility to *Pst*DC3000 and *Arabidopsis* powdery mildew (Yu, 2012).

RRE1 is homologous to XA21 binding protein *Arabidopsis thaliana* 34 (XBAT34) based on protein sequence identity. XBAT34 is described as a RING-Hca proteins (Stone *et al*, 2005). The six XBAT family proteins are related to rice XA21 binding protein (XB3) in sequence structure and domain organization (Nodzon *et al*, 2004; Carvalho *et al*, 2012). XB3 is an E3 ligase that binds XA21 a receptor like kinase involved in race specific resistance to the bacterial blight pathogen (*Xanthomonas oryzae pv.oryzae*) (Wang *et al*, 2006b). XB3 is necessary for the full accumulation of XA21 protein and for its mediated resistance. In *Arabidopsis* the role of XBAT32 and XBAT35 has begun to be elucidated. XBAT32 is involved in lateral root development, while XBAT35 plays a novel role in ethylene signalling, negatively regulating apical curvature (Nodzon *et al*, 2004; Carvalho *et al*, 2012).

Other RING E3 ligases have been demonstrated to function in plant immunity. *Arabidopsis* toxicos en levadura 9 (ATL9) is an *Arabidopsis* C3-H2-C3 RING finger E3 ligase with a proline (P), glutamic acid (E), serine (S), and threonine (T) (PEST) sequence required for proteolytic signal recognition by ubiquitin proteasome system (UPS) during self-regulation. Its expression is induced by chitin and it manifests resistance to the adapted pathogen *Golovinomyces orontii* in a mechanism that still remains to be elucidated (Berrocal-Lobo *et al*, 2010; Deng *et al*, 2017). The rice enhanced blight and blast resistance 1 (*EBR1*) encodes a RING E3 ligase that interacts with BAG (Bcl-2-associated athanogene) family

protein *Oryza sativa* BAG4 (OsBAG4) (You *et al*, 2016). BAG has been shown to be involved in apopstosis, autoimmunity, and tumorigenesis in mammals and cytoprotection in plants (Kabbage & Dickman, 2008). OsBAG4 has elevated accumulation in *ebr1* and mediates increased spontaneous programmed cell death (PCD), stunted growth and autoimmunity. These BAG proteins cause enhanced resistance to bacteria pathogens (*Xanthomonas oryzae pv. oryzae*) and fungal pathogens (*Magnaporthe oryzae*) likely by activating PTI. EBR1 ubiquitinates OsBAG4 for degradation, thereby regulating PCD and autoimmunity (You *et al*, 2016). The list of E3 ligases implicated in plant immunity is increasing over time, however, the challenge still remains to uncover their potential targets and the associated molecular pathways leading to immunity (You *et al*, 2016).

## 1.4 The ubiquitination system

### 1.4.1 Components of the ubiquitination system

#### 1.4.1.1 Ubiquitin

Ubiquitin is a small polypeptide of, 8.5 kDa and 76 amino acid residues highly conserved in eukaryotes. The differences between animal, plant and fungal ubiquitins are only two or three amino acid residues and this suggests that ubiquitin from different species may function interchangeably (Callis, 2014). Ubiquitin possess a compact secondary structure made of a core of 16-17 hydrophobic residues interlinked by intra molecular hydrogen bonding conferring the protein stability and heat labile properties. Prominent features of the structure consists of 3.5 turns of an amphipathic α-helix and a short $3_{10}$-helix packed with five-strands of β-sheets reversing in seven turns (Vijay-Kumar & Charles 1987). The surface of ubiquitin is highly complex with diverse functionalities attributed to high amino acid conservation. The initial surface loop mainly contains leucine-8, and is able to adopt different conformations for interaction with distinct ubiquitin binding proteins (Lange

*et al*, 2008). Another region, containing isoleucine-44, leucine-8, valine-70 and histidine-68, called the isoleucine-44 hydrophobic patch, interacts with the proteasome and other ubiquitin binding proteins (Callis, 2014). In terms of localization, ubiquitin is found to act in the nucleus, cytoplasm and plasma membrane principally functioning in protein modifications (Vijay-Kumar *et al*, 1985, 1987).

#### 1.4.1.2 Ubiquitin activating enzyme, UBA or (E1)

Ubiquitin activating enzyme or E1 is the first enzyme of the ubiquitin conjugation cascade. It was also the first characterized elution from the ubiquitin binding column hence the term E1 (Callis, 2014). In *Arabidopsis* two genes *UBA1*, (*At2g30110*) and *UBA2* (*At5g06460*) encode the E1 proteins. The proteins are about 123 kDa and are closely related with 81% identity in amino acid sequence and virtually 44-75% identity to other E1 in other organisms (Hatfield *et al*, 1997). The N- termini of the UBA are highly divergent with only ~47% similarity achieved in the first ~70 amino acids when indels introduced to maximize sequence alignment (Callis, 2014). Like other E1s the AtUBAs have an active conserved cysteine for formation of intermediate thio-ester bond with ubiquitin during the conjugation process. Both UBAs activate ubiquitin with equal affinities in an ATP dependent manner (Hatfield *et al*, 1997). In animal cells, E1 localize both in the nucleus and cytoplasm and therefore it's likely that ubiquitination occur in both of these cellular compartments (Bachmair *et al*, 2001).

#### 1.4.1.3 Ubiquitin conjugating enzyme, UBC or (E2)

The E2 is a second enzyme in the ubiquitination pathway and it is predicted to be over 37 E2s in the *Arabidopsis* genome (Kraft *et al*, 2005a). They contain a ~150 residue UBC domain which acts as a site for thioester formation (Stewart *et al*, 2016). The UBC enzymes

have a compressed structure consisting of four α-helices, a short $3_{10}$ helix near the catalytic cysteine and a four-stranded antiparallel β-sheet (Wenzel *et al*, 2011; Stewart *et al*, 2016). The N-terminal helix or helix 1 (H1) part of the UBC domain provides a packing interface for E1 binding. Both E1 and E3 bind to the same site on E2, indicating that they are mutually exclusive and therefore the activated E2 must dislodge E1 in order to reload E3 (Eletr *et al*, 2005). The interaction site for E2/E3 is comprised of residues in the H1 and in loop 4 and 7, though some E2-E3 interactions are maintained by salt bridges (Wenzel *et al*, 2011). Almost all E2s have a conserved histidine-proline-asparagine sequence in their UBC domain about 10 residues upstream the catalytic cysteine residue. The asparagine in the peptide is critical for E2 catalysis, mediating E2-E3 isopeptide bond formation by stabilizing the oxyanion intermediate formation during the lysine residue attack (Wu *et al*, 2003). The histidine and proline upstream the asparagine are dispensable in E2 catalysis however they play a structural role and maintaining a tight turn of these residues (Wu *et al*, 2003; Callis, 2014). E2 tend to demonstrate diversity of working with E3s from a narrow range to broad specificity towards E3s (Criqui *et al*, 2002; Kraft *et al*, 2005). A certain class of enzymes possessing UBC domain lack the catalytic active cystine referred to as Ubiquitin conjugating Enzyme Variants (UEV). In *Arabidopsis* the Constitutive photomorphogenesis protein 10 (COP10) (At3g13550) is the best characterized UEV identified from a screen of plants grown in dark conditions but displaying light grown attributes. COP10 enhance the activity of several E2s in *Arabidopsis* by stimulating ubiquitin-E2 thioester bond formation. *In vitro*, the catalytically inactive E2 interacts with both E2s and E3s subunit protein DNA damage binding protein 1 (DDB1). The interactions suggests that COP10 may regulate the ability of E2 to form E2-E3 specific complexes (Yanagawa *et al*, 2004; Lau & Deng, 2009).

#### 1.4.1.4 Ubiquitin ligases or (E3)

The E3 ligase comes in the third position in the ubiquitination cascade and it facilitates the transfer of ubiquitin to the substrate. There are over 1500 predicted E3 ligases in the *Arabidopsis* genome (Stone *et al*, 2005; Hua & Vierstra, 2011), such varied and numerous occurrences make protein modification possible in the ubiquitination pathway (Stone, 2014a). The plant ubiquitin ligases are classified into four categories; the Homologous to the E6-AP Carboxyl Terminus (HECT), U-box, RING, and RING between RING (RBR) based on the ability to mediate substrate ubiquitination (Stone, 2014a; Callis, 2014).

The HECT E3s derive their name from a conserved HECT domain present in human HECT the first enzyme of the group analysed (Callis, 2014). The ~350 amino acid residue C terminal domain is involved in accepting ubiquitin from UBCs and transferring it to the selected substrates for ubiquitination (Marín, 2013; Lorenz, 2018). The *Arabidopsis* genome is known to contain seven *HECT* encoding proteins referred to as ubiquitin protein ligases (UPL1-UPL7) (Chen & Hellmann, 2013). The proteins are grouped into four families based on HECT sequence similarity and protein structure (Marín, 2013; Lan *et al*, 2018). Only UPL1, UPL3 and UPL5 have annotated functions. UPL1 mediate autoubiquitination *in vitro* in an assay requiring the positionally conserved cysteine in HECT domain, E1 and UBC8 of *Arabidopsis* (Bates & Vierstra, 1999; Chen & Hellmann, 2013). UPL3 is involved in ubiquitination of the activators of trichome branching and endoreplication. The *upl3* mutants have increased trichome branching, increased endoreplication resulting in enlarged nuclei and are hypersensitive to gibberellic acid, consistent with the role of gibberellic acid in trichome development (Downes *et al*, 2003). The UPL5 negatively regulates senescence by targeting the tryptophan (W), arginine (R), lysine (K), tyrosine (Y) 53 (WRKY53) transcription factors to proteasome degradation. WRKY53 overexpression accelerates senescence, therefore UPL5

is required to ensure that ageing manifests in an appropriate time frame (Miao & Zentgraf, 2010).

U-box proteins are also referred to as plant U-box (PUB) (Callis, 2014; Trujillo, 2018). They are a modification of RING E3 ligases forming a scaffold structure similar to the RING domain (Lyzenga & Stone, 2012; Byun *et al*, 2017). The cysteine and histidine residues that chelate the two zinc ions are replaced by a network of hydrogen bonds from cysteine, serine and glutamate side chains (Aravind & Koonin, 2000; Callis, 2014). In addition to hydrogen bonds, the tertiary structure is also stabilized by hydrophobic cores and salt bridges necessary for the activity of the U-box (Ohi *et al*, 2003; Andersen *et al*, 2004). The plant genome encodes an enormous number of U-box E3 ligases. For-example, *Arabidopsis* encodes 64 compared to two in *Saccharomyces cerevisiae* and nine in humans (Li *et al*, 2008; Yee & Goring, 2009). The 64 PUB family can be divided into 13 groups based on the inclusion of other domains (Yee & Goring, 2009). About 64% contain armadillo repeats involved in protein-protein interaction which is fewer than the RING-containing ligases with ankyrin repeats, von Willebrand factor (vWF) type A domain (VWA), tryptophan-aspartic acid- 40 domain (WD40) and C-terminal domain of a breast cancer susceptibility protein (BRCT) (Mudgil *et al*, 2004; Stone *et al*, 2005). The U boxes tend to have more kinase domains (23%) compared to one in RING proteins (Trujillo, 2018). Like RING E3 ligases, the U-box has a ~70 amino acid conserved motif which forms a docking site with both the E2 and the substrate. Subsequently, the E2 completes ubiquitin transfer to the selected substrate (Yee & Goring, 2009; Trujillo, 2018). The interactions of E2 and PUB are mediated by hydrophobic surfaces (Zhang *et al*, 2005a; Trujillo, 2018).

The RING type E3 ligases are characterized by the RING domain, a ~40-60 amino acid residue region containing an octet of spatially conserved cysteine and histidine residues chelating two zinc atoms to form a cross brace structure (Callis, 2014). The spacing between

the cysteine and histidine are well conserved differentiating them from other RING containing proteins such as transcription factors. It is also essential for E3 ligase activity and binding with the Ubcs (Stone *et al*, 2005; Callis, 2014). Bioinformatic analysis combined with manual curation of the *Arabidopsis* genome identified 490 RING containing proteins (Stone *et al*, 2005; Callis, 2014). Although a large number are of canonical C3H2C3 and C3HC4 structure, eleven percent are RING domain variants. However, they still retained the ability to mediate E3 ligase activity (Stone *et al*, 2005). The RING finger proteins may contain additional domains such as ankyrin repeats, transmembrane, kinase and DNA-RNA binding domains (Stone *et al*, 2005).

The RING finger motif plays a critical role in ubiquitin ligation to substrates or to RING finger proteins themselves (Hegde, 2004; Deshaies & Joazeiro, 2009; Hegde, 2010). In their mechanism of action the RING finger ligases do not form a thioester intermediate with ubiquitin, instead the conserved RING domain of these E3 ligases binds both the substrate and the E2 to mediate the transfer of ubiquitin from the E2 to the substrate (Stone *et al*, 2005). Although the majority of RING ligases functions in a monomeric fashion, there are multi-subunit RING based E3 ligases referred to as Cullin (CUL)-RING ligases (CRLs). In plants, three CRLs have been identified as CUL1, CUL3a/b and CUL4. Cullin acts as a scaffold where RING domain containing E2-ubiquitin binding and substrate-recruiting sub-units assemble (Hotton & Callis, 2008; Hua & Vierstra, 2011; Stone, 2014b). The substrate recruiting subunit may bind directly to the CUL or bind through an adaptor protein. The CUL1 employs S-Phase Kinase-associated Protein (SCF) or *Arabidopsis* SKP-like (ASK) based F-box to recruit target substrates (Lechner *et al*, 2006). The DWD proteins in *Arabidopsis* directly interact with DDB1 and thus may serve as substrate receptors for the DDB1–CUL4 machinery (Lee *et al*, 2008). The CUL3a/b binds directly with substrate proteins, retinoblastoma (RB1) protein and broad complex/ tramtrack/bric -a-brac (BTB).

Mutations in CUL3a/b is embryo lethal indicating that BTB-CUL3 is essential for plant development (Gingerich *et al*, 2005).

RBR E3 ligases are intermediate between the RING and HECT ligases. Structurally the RBR proteins contain three cysteine/histidine rich regions at the N-terminus, in the middle and at the C-terminal end. The latter is less conserved and generally described as a RING-like domain. In the mechanism of action, the E2-ubiquitin temporary complex is non-covalently bound to the first RING of RBR ligase. The ubiquitin is transferred to a conserved cysteine in the second RING domain at C-terminal end like in HECT. The RBR completes the ubiquitin transfer to the selected substrate (Spratt *et al*, 2014; Callis, 2014). The *Arabidopsis* genome contains 42 RBR proteins subdivided into four groups. The Aldriane (ARI) E3 ligases are the most pronounced group with 16 expressed genes and two pseudogenes, however, their functions are largely unknown (Mladek *et al*, 2003; Marín, 2010). Only ARI14 has been implicated in positive regulation of pollen formation, fertilization and seed set (Ron *et al*, 2010).

#### 1.4.1.5 E4 ubiquitin ligases

Efficient recognition and engagement of the proteasome is based on long multiubiquitination chains conjugated on target substrates. The E4 is a novel ubiquitination factor that ensures long chains are obtained, in its absence only few ubiquitin moieties are ligated that may be insufficient to promote proteasomal degradation *in vivo* (Koegl *et al*, 1999). Initially E1, E2 and E3 drive substrate ubiquitination, the E4 binds on ligated ubiquitin conjugates prompting further addition of ubiquitin yielding long chains (Koegl *et al*, 1999). Generally, E4 are characterized by a conserved C-terminal U-box of 70 amino acid residues that structurally resemble the RING domain of RING finger E3 ligases. E4 has been predominantly demonstrated in organisms other than plants. For-example, Ubiquitin fusion

degradation 2 (UFD2) in yeast regulating stress tolerance, no spores A (NOSA) from *Dictyostelium* regulating developmental processes and C-terminus of Hsc70-interacting protein (CHIP) from humans negatively regulating Hsp70 ATPase activity (Hoppe, 2005). However, in *Arabidopsis* mutant, Snc1-enhancing 2 (MUSE2) an E4 ligase together with constitutive expressor of *PR1* (CPR1) an E3 ligase has been shown to negatively regulate immune receptors controlling spatial and temporal manifestation of immunity (Huang *et al*, 2014).

#### 1.4.1.6 The proteasome compartment

The 26S proteasome involved in the turnover of ubiquitinated proteins is made up of two components, the 19S (subunit) regulatory particle and the 20S core particle highly conserved from archaea to eukaryotes. The regulatory particles are two components at either side of the cylindrical core particle (Hegde, 2010). They contain receptors for recognition and unfolding of ubiquitinated proteins allowing access into the core particle (Marques *et al*, 2009). Unfolding is aided by ATPases located at the base of the regulatory particles (Rpt). Six ATPases regulatory particle (Rpt) 1-6 and four non ATPases regulatory particles (Rpn) 1, 2, 10 and 13 are located at the base of the regulatory particle. The other regulatory particle, also known as the lid, contains only non ATPase "Rpn3, 5, 6-9, 11, 12 and 15" (Hegde, 2010). Rpn11 and 13 function as deubiquitinases for the substrates allowed into the core particle, while Rpn1 reversibly associates with another deubiquitinase, ubiquitin specific peptidase 14 (Usp14) to stimulate substrate degradation through deubiquitination (Hegde, 2010). The core particle is made of two main subunits α and β, each subdivided into two units. The two α subunits at either side of the regulatory particle contain seven units (α1-α7). They function as a gate allowing only the unfolded substrates to progress inside through the tiny opening of 13 Å in diameter in the middle of outer α rings referred to as α annulus

(Cheng, 2009). Such a restricted opening ensures that only unfolded proteins can progress inside (Cheng, 2009). The two β subunits form the catalytic or proteolytic site of the proteasome. Each is made of seven units (β1-β7) gated by the α subunits. The proteolytic activity is performed by β1, β2 and β5 of each unit. The catalytic sites of these subunits are located on the N-termini inside the chamber. This proteolysis results in short 3-32 amino acid-long peptides (Marques *et al*, 2009; Hegde, 2010). These can undergo further proteolysis by other proteases and amino peptidases to yield amino acid residues. The ubiquitin chains are not proteolyzed, rather they are disassociated from the substrates by the deubiquitinases for recycling. The deubiquitinases are of two groups; the low molecular weight deubiquitinases also known as, C-terminal hydrolase, and high molecular weight deubiquitinases also known as ubiquitin specific proteases, all with preference choice for substrates (Hegde, 2010).

### 1.4.2 The ubiquitination pathway

The ubiquitination system involves modification of membrane, cytoplasmic and nuclear localized proteins by decorating them with ubiquitin conjugates (Callis, 2014). The process involves a cascade of enzymatically controlled steps that ultimately add ubiquitin to a substrate (Stone *et al*, 2006; Li *et al*, 2014). It is initiated when E1 activates the ubiquitin at its C- terminus in an ATP dependant process (Haas & Rose, 1982; Koegl *et al*, 1999). The ubiquitin forms a thioester linkage with the E1 at the conserved cysteine residue leading to the formation of an E1-ubiquitin intermediate. The E1 then transfers ubiquitin to an E2 at the conserved cysteine forming E2-ubiquitin intermediate linked by thioester linkage (Hegde, 2010). Finally, the E3 can bind the E2-ubiquitin complex and the substrate at its conserved cysteine. In this context the E2 can transfer the ubiquitin to the selected substrate on ε-$NH_2$ lysine residue or the ubiquitin can be conjugated to E3 and E3 completes the final transfer to

the substrate resulting in isopeptide bond formation (Prasad *et al*, 2010; Lyzenga & Stone, 2012). Ubiquitin ligation may also be made to an α-$NH_2$ group of serine, threonine or cysteine residue of a substrate as described in mammalian cells (Callis, 2014) (Figure 1-3).

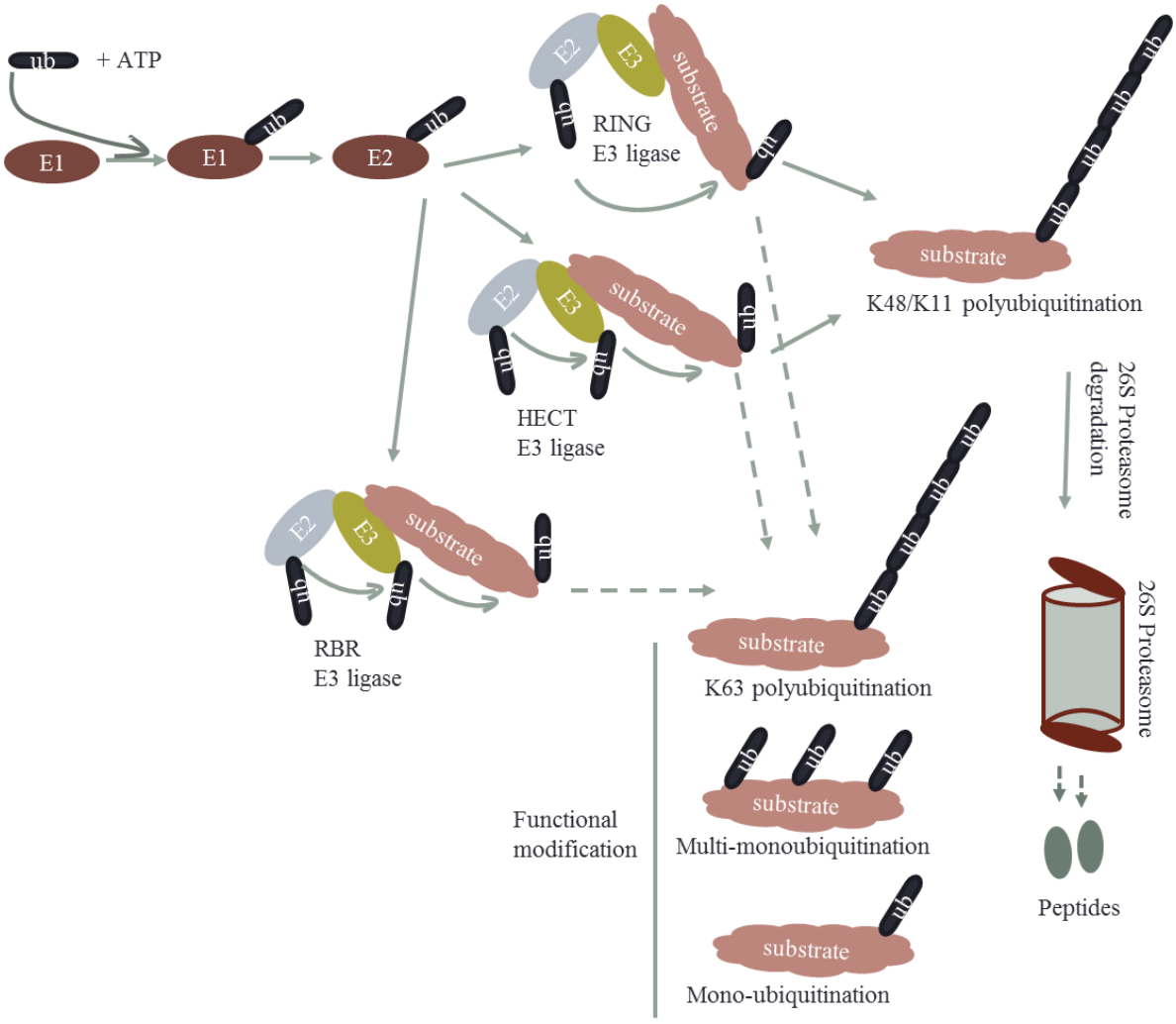


**Figure 1-3: The mechanism of ubiquitination.** The process is initiated when E1 binds ubiquitin in an ATP dependent manner. The conjugated ubiquitin is transferred to an E2. Transferring ubiquitin to the substrate is dependent on the nature of the E3. In the RING type E3, the E3 binds with the E2 and the E2 completes the transfer of ubiquitin to the selected substrate. In the HECT type of E3, the E3 binds with the E2 and ubiquitin is transferred to the E3 which then completes the transfer to the substrate. In the RBR E3 ligase, the N-terminal RING domain binds the E2 and the ubiquitin is transferred to the second RING domain at the C-terminus which completes the transfer to the substrate. Ubiquitin conjugated on the substrate may lead to proteasomal degradation or may functionally modify the target protein for non-proteolytic events, depending on the type of ubiquitination.

### 1.4.3 Different modes of substrate ubiquitination

The versatility of ubiquitin in regulating different cellular processes is attributed to the ability to be linked to proteins in different forms (Sadowski *et al*, 2012). Mono-ubiquitination involves the addition of ubiquitin monomer to a single site on the substrate. Multi-mono-ubiquitination involves repetitive addition of ubiquitin on the same substrate at different sites. Polyubiquitination involves the linkage of ubiquitin chains to the substrate. The first added ubiquitin serves as the acceptor of the additional ubiquitins in repeated cycles (Behrends & Harper, 2011). The linkage chains mostly occur in a linear fashion (homotypic), being diverse in length but may also form branched chains (heterotypic) where ubiquitin moiety are self-ubiquitinated at two or more sites (Sadowski *et al*, 2012). Ubiquitin linkages in the cell can be formed through all the seven lysines (K) within ubiquitin (K6, K11, K27, K29, K33, K48 and K63) (Peng et al, 2003a). Polyubiquitin chains can also be generated through the α-amino group of N-terminal methionine (M1) (Sadowski *et al*, 2012; Tanno & Komada, 2013). The generation of different chains provides structural diversity allowing proteins with specific ubiquitin recognition domains, to recognize them for different fates (Sadowski *et al*, 2012). Proteome analysis of yeast, *Arabidopsis* and mammalian cells revealed linkages via K48 and K63 as the most abundant polyubiquitin chains followed by K11, K33 and K29/K6 (Callis, 2014; Tanno & Komada, 2013; Kim *et al*, 2013; Paez Valencia *et al*, 2016).

Variable protein outcomes can occur depending on the number of ubiquitins attached (Weissman, 2001; Li *et al,* 2014). Mono-ubiquitination, multi-monoubiquitination and K63 polyubiquitination generally acts as a signal for non-proteolytic functions including regulation of DNA repair, signal transduction, endocytosis, protein activation, vesicle sorting, chromatin organization and the control of other basic cellular processes (Xu *et al*, 2009; Kim *et al*, 2013; Hegde, 2010; Callis, 2014). The K48 and K11 linkages of at least 4 ubiquitins are associated with regulation of nuclear, cytosolic and endoplasmic reticulum membrane

proteins by targeting them to 26S proteasome degradation (Glickman & Ciechanover, 2002; Sadowski *et al*, 2012; Satija *et al*, 2013).

Polyubiquitination at K6, K27, K29 and K33 are less intensively investigated though information related to their roles are now emerging. K6 poly-ubiquitin chains built by the Breast cancer associated 1 (BRCA1)-BRCA1-associated RING domain protein 1 ligase, a cancer suppressor protein might be involved in DNA repair (Nishikawa *et al*, 2004). The K6 chain linkages are involved in mitochondrial quality control and increase response to ultra violet (UV) and ionizing radiations implying a DNA damage response role (Ordureau *et al*, 2014; Elia *et al*, 2016). K27 polyubiquitination is implicated in DNA damage responses and host immune responses triggered by microbial DNA (Akutsu *et al*, 2016). K29 linkages are involved in attenuating wingless/integrated (Wnt) signalling by modifying Axin, a protein involved in the pathway leading to the activation of Wnt. The ubiquitination of Axin disrupts the interactions with Wnt coreceptors low density lipoprotein receptor-related protein-5/6 (LRP5/6), which subsequently attenuates Wnt-stimulated LRP6 phosphorylation and represses Wnt/β-catenin signalling. The Wnt/β-catenin signalling pathway is required for embryo formation and its abolition is associated with tumorigenesis and other human diseases (Fei *et al*, 2013; Akutsu *et al*, 2016). K33 chains are demonstrated to negatively regulate both the T-cell antigen receptor and adenosine monophosphate (AMP) activated protein kinases related kinase. K33 chains are also shown to mediate post Golgi trafficking, a role that is mostly performed by K63 polyubiquitins (Huang *et al*, 2010; Yuan *et al*, 2014; Akutsu *et al*, 2016). The ubiquitin N-terminal methionine residue polyubiquitination on the nuclear factor kappa-light-chain-enhancer of activated B cells (NF-κB) modulator, is known to activate the NF-κB transcription factor (Sadowski *et al*, 2012). Branched poly-chains along K6, K27 and K48 are demostrated in auto-ubiquitination of the polycomb E3 ligase RING 1B histone H2A likely to be necessary in gene silencing (Ben-Saadon *et al*, 2006) (Figure 1-4).

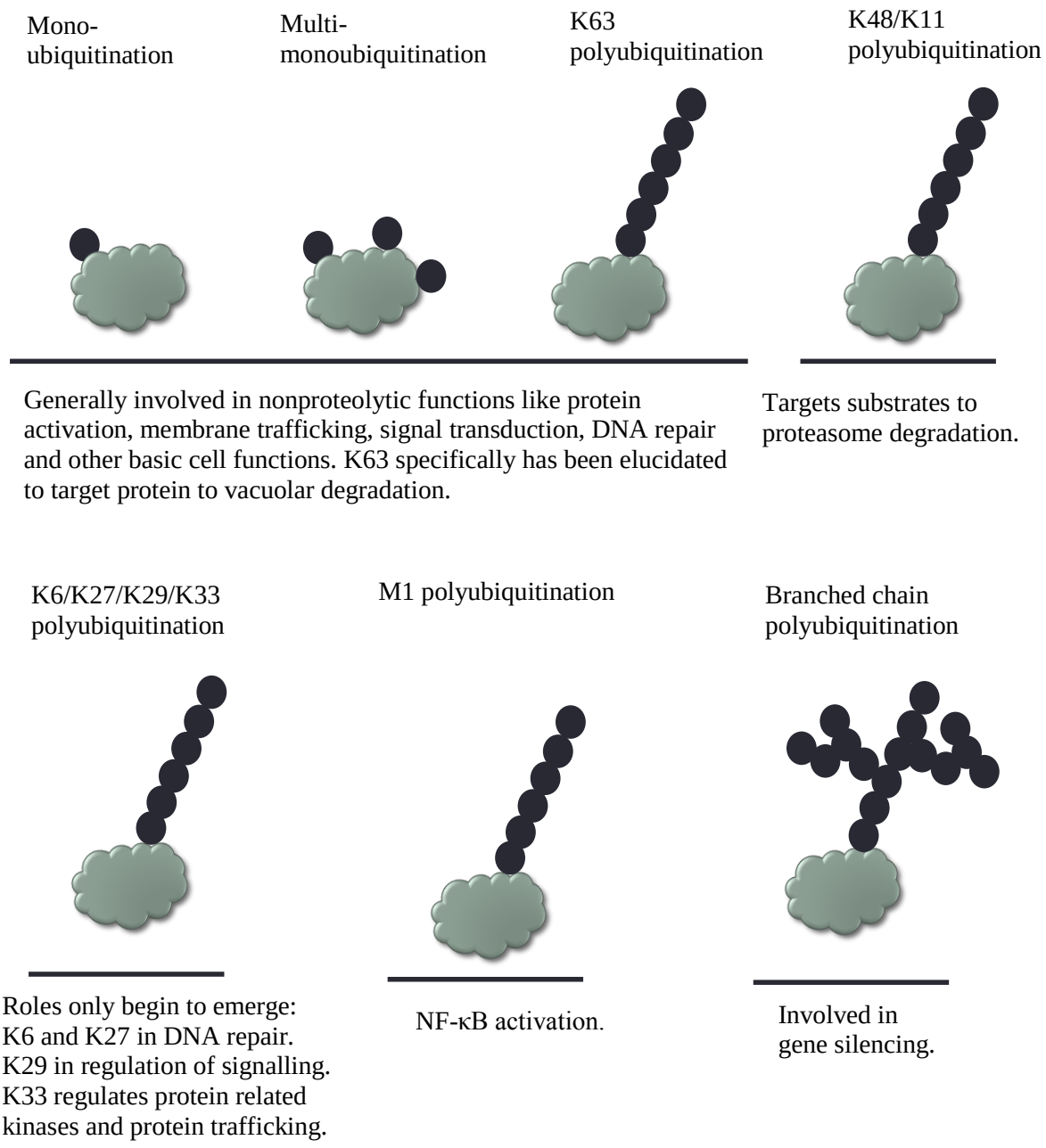


**Figure 1-4: Different modes of substrate ubiquitination lead to a range of fates.** Mono-ubiquitination, multi-monoubiquitination and K63 polyubiquitination generally modifies the substrate to drive non-proteolytic functions. K48 and K11 polyubiquitination are associated with 26S proteasome mediated degradation. K6, K27, K29 and K33 polyubiquitination are not widely investigated and their roles have only just begun to emerge. For example in DNA repair, regulation of signalling and protein related kinases. Methionine 1 polyubiquitination has been linked to transcription factor activation. Branched chain polyubiquitination has been linked to gene silencing.

### 1.4.4 The role of ubiquitination in protein trafficking

Protein modification by mono-ubiquitination or K63 polyubiquitination is linked to substrate trafficking for non-proteasome proteolytic events (Xu *et al*, 2009; Tian & Xie, 2013). In plants there is limited information related to trafficking or recycling driven by ubiquitination. However, endocytosis of membrane proteins have been described (Johnson & Vert, 2016; Romero-Barrios & Vert, 2018). The phytohormone auxin, required for root gravitropism, is transported by the plant plasma membrane auxin carrier transporter PIN2 in *Arabidopsis*. The auxin exporter protein can be modified via K63-linked ubiquitin chains. This modification regulates the endocytosis and targeting of the proteins for vacuolar sorting (Leitner *et al*, 2012a). Mutation of multiple lysine residues in PIN2 (pin2KR) prevents trafficking of the plasma membrane exporter. Except for degradation, its internalization can be triggered by the in-frame fusion of a single ubiquitin to the pin2KR mutant, reinstating the involvement of ubiquitin K63 chains at later steps of the endocytic cycle (Leitner *et al*, 2012b, 2012a; Erpapazoglou *et al*, 2014). The plant polyhydroxylated steroid hormone BRASSINOSTEROID (BR) is required for several aspects of plant growth and development such as seed germination, photomorphogenesis, fertility, elongation, stomatal development and flowering. The hormone is recognized by a localized plasma membrane bound receptor complex composed of the BRASSINOSTEROID INSENSITIVE 1 (BRI1) receptor kinase and BRI1-ASSOCIATED RECEPTOR KINASE 1 (BAK1) (She *et al*, 2011; Hothorn *et al*, 2012). The post translational modification of BRI1 receptor kinase by a K63 linked polyubiquitin chain results in recognition at the *trans*-Golgi network/early endosomes (TGN/EE) and subsequent targeting to the vacuole (Martins *et al*, 2015). This ubiquitination negatively regulates BRI1 activity and results in BR hypersensitivity (Martins *et al*, 2015). The *Arabidopsis* pattern-recognition receptor FLAGELLIN-SENSING 2 (FLS2) for bacterial flagellin is required to activate innate immunity against bacterial pathogens.

Polyubiquitination of FLS2 by the U-box E3 ubiquitin ligases PUB12 and PUB13 leads to degradation and attenuation of immune signaling. The *pub12* and *pub13* mutants display increased immune responses to flagellin applications (Lu *et al*, 2011). FLS2 is likely to be modified by K63 linked polyubiquitin chains (Romero-Barrios & Vert, 2018).

The IRON REGULATED TRANSPORTER 1 (IRT1) transports iron across the plasma membrane to the inside of the plant cell. Overexpression of IRT1 results in iron overload and oxidative stress implying it has to be tightly regulated for plant survival. IRT1 cycles between the plasma membrane and the early endosome/*trans*-Golgi network. Mono-ubiquitination of IRT1 leads to its internalization and targeting for vacuolar degradation, maintaining optimal iron levels (Barberon *et al*, 2011; Zelazny & Vert, 2015). Borate transporter 1 (BOR1) is required for boron influx into the cell. BOR1 localizes at the plasma membrane and is continuously translocated to the early endosomes. BOR1 levels are tightly regulated to avoid boron toxicity. Mono-ubiquitination at K586 promotes internalization in the multivesicular bodies (MVB) and targeting to the vacuolar for turnover (Kasai *et al*, 2011; Dubeaux & Vert, 2017). The *Arabidopsis thaliana* phosphate transporter 1 (AtPHT1;1) is required for entry of phosphate across the plasma membrane. AtPHT1;1 undergoes K63 polyubiquitination driven by the *Arabidopsis thaliana* nitrogen limitation adaptation (AtNLA) RING E3 ligase and *Arabidopsis thaliana* Alix (AtALIX) protein (Cardona-López *et al*, 2015; Johnson & Vert, 2016). The ubiquitination targets the protein to MVB and leads to vacuole degradation when sufficient levels of phosphate are obtained. Other cell surface proteins including syntaxin 122 (SYP122) have been shown to be modified by K63 linked ubiquitin chains *in vivo*, while others like AtPEN3 are postulated to be modified by K63 polyubiquitination. However, the exact mechanism and subsequent fate remains to be discovered (Johnson & Vert, 2016).

Protein modifications driven by mono-ubiquitinations and K63 linked polyubiquitin

chains are not only associated with endocytosis for vacuolar degradation but are also associated with the activation of proteins for immune responses. In humans, K63 polyubiquitination drives MAPKs activation and NFκB signalling that controls innate and acquired immunity (Wu & Karin, 2015). MAPKs control fundamental processes such as cell differentiation, proliferation, stress responses, cell survival and motility through direct phosphorylation and subsequent activation of cognate transcription factors. The regulation of MAPK activation by Ubc13 is controlled by K63 based polyubiquitination of TNF (Tumour necrosis factor receptor) receptor-associated factor 2 (TRAF2) and TRAF6 which are involved in activation Mitogen-activated protein kinase kinase kinase kinase (MP3Ks), Mitogen activated protein kinase kinase kinase 7 (MAP3K7/TAK1) and Mitogen activated protein kinase kinase kinase 1 (MEKK1) involved in MAPK pathways (Matsuzawa *et al*, 2008; Karin & Gallagher, 2009). The NFκB transcription factor is a key regulator of innate immunity, lymphoid cell survival and inflammation (Hayden & Ghosh, 2008; Wu & Karin, 2015). Ub13 and TRAF6 RING E3 ligases mediate the synthesis of K63 polyubiquitin chains that are conjugated to the inhibitor of kappa B kinase (IKK) complex. The activation of IKK by ubiquitination drives NFκB signalling (Deng *et al*, 2000; Hacker & Karin, 2006).

### 1.5 Project aim

Our interest in RRE1 was aroused by the observation that *RRE1* showed SA-independent upregulation upon avirulent pathogen challenge. Mutations in *RRE1* compromised resistance against host adapted and non-adapted barley powdery mildew pathogens. In addition, *RRE1* was co-expressed with the SNARE encoding gene, *AtPEN1*, during *Bgh* challenge (Yu, 2012). AtPEN1 is required for full penetration resistance in *Arabidopsis* against the non-host barley powdery mildew fungus (Collins *et al*, 2003; Stein *et al*, 2006). *AtPEN1*/*SYP121* together with its close relative *SYP122* negatively regulates

salicylic acid (SA) defence pathways and SA levels in the syntaxin double mutant, *syp121–1 syp122–1*, is drastically elevated (Zhang *et al*, 2007b). AtPEN1 is central to the involvement of the SNARE-complex-mediated exocytosis and/or homotypic vesicle fusion events at attempted pathogen penetration sites to impart penetration resistance (Collins *et al*, 2003). Indeed AtPEN1 continuously recycles to endosomes and to the plasma membrane to ensure deposition of material in papilla in order to confer efficient penetration resistance (Nielsen & Thordal-Christensen, 2012). Intriguingly, CSEP0443 a *Bgh* effector protein was found to interact with XA21 binding protein *Hordeum vulgare* 35 (XBHV35) a barley homologue of RRE1 (Zhang, 2012; Aguilar, 2015).

Taken together I aimed to investigate the possible interaction of RRE1 with AtPEN1 in mediating cell wall based defence. I investigated whether RRE1 could ubiquitinate AtPEN1 to promote recycling or trafficking. In that context, RRE1 might regulate the timely release of vesicles to sites of attempted pathogen penetration via ubiquitination events. I finally aimed to investigate the potential functional consequences of the interaction of RRE1 and CSEP0443 during cell surface resistance against *Bgh* mediated by AtPEN1.

# Chapter two

## 2.0 General materials and methods

### 2.1 Experimental materials and growth conditions

#### 2.1.1 Plant growth

The *Arabidopsis thaliana* (*Arabidopsis*) ecotype Columbia (Col-0), *35S::EGFP-AtPEN1-pen1-1*, *35S::EGFP-AtPEN1-pen1-1-rre1, pen1-1, rre1* plants are available from the Loake Laboratory. Transgenics for the project were generated by *Agrobacterium* mediated transformation in these backgrounds depending on the objective investigated. For growth, the seeds were vernalised at 4ºC for 3 days. The seeds were placed on potting medium consisting of peat moss, vermiculite and sand (4:1:1) in pots of 5 x 5 cm. The plant cultures were transferred in a growth room and grown under a 16 hours light/8 hours dark regime, light intensity 110 $\mu molm^{-2}s^{-1}$ at 20ºC with relative humidity 60 - 65%.

The barley *Hordeum vulgare* (cv. Golden Promise) and *Nicotiana benthamiana* seeds were soaked in water for 5 minutes and transferred to soil in pots containing the above components. The seeds were exposed to the above regime of dark and light intensity for germination and continued growth.

#### 2.1.3 Growth and inoculation of powdery mildews

The Barley powdery mildew *Blumeria graminis* f. sp. *hordei* DH14 (*Bgh*) isolate was maintained on barley plants in a growth chamber as described by Adam & Somerville (1996). Briefly for infection, green infected leaves from 3 to 4 weeks-old plants were cut and spores collected by a cotton bud, the spores were transferred on to 2 weeks-old grown plants when they had true healthy leaves via rubbing the cotton bud. The inoculated plants were maintained in the growth cabinet at 22ºC day, 18ºC night, light intensity 110 $\mu molm^{-2}s^{-1}$

under a 16 hours light/8 hours dark regime and 60% humidity. The fungus was occasionally subcultured on to new barley plants.

For experimental investigations, inoculation was done as described by Luc & Somerville, (1996). High density inoculations (20 - 50 conidia $mm^{-2}$) were done by collecting spores from individual colonies on the infected leaves. Collected spores were dusted evenly along the adaxial leaf surfaces from the cotton ball. Inoculated *Arabidopsis* plants were incubated for 72 hours except for electrolyte determination where incubation was done for 24, 48, 72 and 96 hours. Inoculation of barley plants for Host Induced Gene Silencing (HIGS) was done in a similar manner on the fifth and sixth leaves and the plants incubated for 1 to 6 days.

**2.2 Genotyping of plant materials**

To confirm whether *35S::EGFP-AtPEN1-pen1-1*, *35S::EGFP-AtPEN1-pen1-1-rre1, pen1-1, rre1* plants are true to type, genotyping was undertaken. Genomic Deoxyribonucleic acid (DNA) was extracted from 100 mg of *Arabidopsis* leaves by homogenizing in 300 µl of 1x CTAB buffer (10 g/l of CTAB**,** 40.91 g/l of NaCl, 50 ml/l of 1 M Tris base pH 8.0**,** 20 ml of 0.5 M EDTA pH 8.0) in a 1.5 ml Eppendorf tube. Tissue homogenization was done using tissue lyser mediated beads for 1 minute at 30 seconds frequency and incubated at 65$^{o}$C for 20 minutes. The plant extracts were mixed with 300 µl of chloroform by vortexing vigorously and centrifuged at 21,000*g* for 5 minutes. The upper aqueous layer was transferred to a new Eppendorf and 300 µl of isopropanol added, incubated at 4$^{o}$C for 5 minutes followed by centrifugation at 21,000*g* for 5 minutes. The supernatant was removed and the pellet washed with 1 ml of 70% ethanol by centrifugation at 21,000*g* for 5 minutes. The ethanol was removed and the pellet air-dried for 30 minutes, suspended in 50 µl of autoclaved double distilled water (dd$H_2$0) and incubated at 4$^{o}$C overnight for complete dissolution of DNA.

Genotyping polymerase chain reaction (PCR) was carried out using gene specific primers listed in (Table 1) with the following conditions; 2 µl genomic DNA, dNTP mix (200 µM) (Thermo Scientific), forward and reverse primer (0.2 µM each), 1x Crimson *Taq* reaction buffer, Crimson *Taq* DNA polymerase (1.25 units/50 µl reaction) New England biolabs (NEB) at initial denaturation of 95ºC for 3 minutes, cycle 95ºC (1 minute), 52 - 55ºC (30 seconds) and 72ºC (1 - 2 minutes) for 35 cycles and final extension of 72ºC for 3 minutes. Conditions varied according to the gene amplified as indicated in (Table 1). Reaction products (20 µl) were analysed by 1% agarose gel electrophoresis using GeneRuler 1 kb plus ladder (Thermo Scientific), run in 1x TAE buffer (40 mM Tris base, 1mM disodium EDTA, 20 mM glacial acetic Acid) at 80 V for 1 hour.

**Table 1: List of primers for genotyping plant materials**

| Gene | Sequence | Amplicon (bp) |
|---|---|---|
| *35S::EGFP-AtPEN1-pen1-1*<br>*35S::EGFP-AtPEN1-pen1-1-rre1* | F: atggtgagcaagggcgaggagctgttca<br>R: cttgtacagctcgtccatgccgagagtgat | 717 bp |
| *RRE1* | F: gtatcaaatcacttcaccatgaag<br>R: cattggctgtggaactccttt | 1555 bp |
| *ACTIN1* | F: catcaggaaggacttgtacgg<br>R: gatggacctgactcgtcatac | 350 bp |
| *rre1* | F: gccttttagaaggataaaagcctgctcc<br>R: catggactttggacttctggagtcatcaataat | 1200 bp |
| *pen1-1* | F: atgaacgatttgttttccagctcattctctcg<br>R: tcaacgcaatagacgccttgcctga | 1039 bp |

**2.3 Bacterial growth and plasmid isolation**

Plasmid was isolated using the QIAGEN plasmid mini prep kit QIAGEN, 2015. Single bacteria colonies were picked and cultured in 5 ml of lysogeny broth (LB) medium with appropriate selective antibiotics (kanamycin 50 µg/ml, carbenicillin or ampicillin 100

µg/ml for *Escherichia coli*) or (rifampicin 100 µg/ml, gentamycin 25 µg/ml in addition to kanamycin for *Agrobacterium tumefaciens* (*Agrobacterium*). Cultures were incubated at 37°C for *Escherichia* (*E. coli*) or at 28°C for *Agrobacterium* with shaking at 200 rpm overnight. Plasmid purification was done with the QIAprep Spin mini prep kit as per accompanying manual. Five milliliters of cultures were centrifuged at 2,800*g* for 5 minutes and the supernatant discarded. The pelleted bacterial cells were resuspended in 250 µl of P1 buffer and transferred to a 1.5 ml Eppendorf tube. The lysis reaction was initiated by the addition of 250 µl of P2 solution. After gentle inverting the tube 4 - 6 times and incubating for 5 minutes at room temperature, proteins and polysaccharides were precipitated by the addition of 350 µl of neutralization buffer N3. This was followed by centrifugation at 17,900*g* for 10 minutes, after plasmid DNA in supernatant was loaded into QIAprep spin column followed by centrifugation for 1 minute at 17,900*g*. The column was washed twice with PE (750 µl) by centrifugation at 17,900*g* each time for 1 minute to remove possible contaminants. An extra centrifugation at 15,800*g* for 2 minute to remove residual wash buffer was done. The column was placed into a 1.5 ml microcentrifuge tube and 50 µl of double distilled autoclaved water (dd$H_20$) was added. This was left to stand for 1 minute, and centrifuged at 17,900*g* for 1 minute to elute the plasmid DNA. To check the integrity of the eluted plasmid DNA, 5 µl of the DNA was subjected to electrophoresis in 1% agarose gel, 1x TAE buffer and visualized under ultraviolet light. The isolated DNA was stored at -20°C for future use.

### 2.4 DNA purification

#### 2.4.1 DNA gel purification

DNA was purified using the QIAGEN gel extraction kit QIAGEN, 2015. The DNA fragment was excised from the agarose gel with a clean sharp scalpel and dissolved in 3 volumes of Buffer QG to 1 volume of gel (100 mg ~ 100 µl) in 1.5 ml Eppendorf tube. The

tube was incubated at 50°C for 10 minutes with gentle inverting every 2 minutes until the gel slice completely dissolved. Isopropanol was added in the ratio of 100 mg agarose slice to 100 µl of isopropanol to increase the yield. To bind DNA, the dissolved solution was transferred in QIAquick spin column and centrifuged for 1 minute at 15,800*g* and flow-through discarded. To wash the column, the Buffer PE (0.75 ml) was added and centrifuged for 1 minute at 15,800*g*. This step was done twice to ensure clean DNA obtained. Flow-through was discarded and centrifuged for an additional 1 minute at 15,800*g* to completely remove the residual ethanol. DNA was eluted by placing the QIAquick column into a clean 1.5 ml microcentrifuge tube. Forty microliters of $ddH_2O$ was added to the centre of the QIAquick membrane, stood for 1 minute and centrifuged for 1 minute at 15,800*g*. The DNA was stored at -20°C for future use.

### 2.4.2 PCR DNA product purification

PCR product purification was done using the QIAGEN kit following manufacturer's protocol QIAGEN, 2008. The DNA product was mixed with buffer PB in a ratio of 1:5. The mixture was then transferred into a QIAquick spin column for DNA binding and spun at 15,800*g* for 1 minute in a table centrifuge at room temperature. Flow-through was discarded followed by washing the column twice by adding 0.75 ml of buffer PE each time centrifuging for 1 minute at 15,800*g*. After the last wash the column was centrifuged for additional 2 minutes to remove the residual ethanol and placed in a clean 1.5 ml Eppendorf tube. Elution was done by adding autoclaved $ddH_2O$ to centre of the membrane, left to stand for 1 minute at room temperature and centrifuged for 1 minute at 15,800*g*. The collected DNA was kept at -20$^{o}$C for future use.

## 2.5 Plasmid construction for protein expression in *E. coli*

Plasmid constructs *pGEX-4T-1-GST-RRE1*, *pGEX-4T-1-GST-RRE1-RING*, *pGEX-4T-1-GST-RRE1*-C340S and *pETG-MBP-AtPEN1* were already available in the Loake Laboratory. Only *pET40A-MBP-CSEP0443*, *pGEX-4T-1-GST-RRE1-Ankyrin repeat* and *pGEX-4T-1-GST-20S* proteasome (α7) subunit have been designed in this study.

### 2.5.1 Plasmid construction for *in vitro* expression of MBP-CSEP0443

To express fusion proteins with the maltose-binding protein (MBP), plasmid *pETG-40A* (European Molecular Biology Laboratory) was utilized. The *CSEP0443* gene encoding a mature 99 amino acid residues protein was amplified by PCR. The reactions involved the use of Phire Hot Start II DNA polymerase using *att*B gene sequence attached to gene specific primers (Table 2), in the following conditions; 1 µl *CSEP0443* template, dNTP mix (200 µM), forward and reverse primer (0.5 µM each), 1x Phire buffer (Thermo Scientific), Phire hot start DNA polymerase (1 unit) (Thermo Scientific). The PCR conditions involved an initial denaturation of 98ºC for 30 seconds, denaturation of 98ºC for 5 seconds, annealing of 60ºC for 5 seconds and extension of 72ºC for 10 seconds for 40 cycles followed by a final extension at 72ºC for 1 minute. Reaction product (50 µl) was resolved in 1% agarose gel in 1x TAE buffer at 90 V for 55 minutes. The resulting PCR product was cut out, cleaned and cloned via the Gateway method following the manufacturer's protocol (Invitrogen, 2003).

Briefly, for the BP recombination reaction, 3 µl of *att*B *CSEP0443* purified PCR product (50 ng/µl), 1 µl of pDONR$^{TM}$ 221 vector (Invitrogen) supercoiled (150 ng/µl), and 1 µl of 5x BP clonase$^{TM}$ enzyme were mixed in a 1.5 ml Eppendorf tube. For the LR recombination reaction, 1 µl of entry clone (75 ng/µl), 1 µl of *pETG-40A* destination vector (75 ng/µl), 1 µl of LR clonase and 2 µl of autoclaved dd$H_2O$ were mixed in 1.5 ml Eppendorf tube. In both cases the reaction components were incubated for 1 hour at 25ºC and later 2 µl

of proteinase K solution (2 µg/µl) was added to stop the reaction and incubated at 37ºC for 10 minutes. The DNA ligates were then used in the transformation of *E. coli* cells of DH5α$^{TM}$ and later plasmid DNA isolated from DH5α$^{TM}$ used in the transformation of *E. coli* BL21. For both BP and LR reactions the resulting transformants were verified by genotyping PCR and Sanger sequencing before transformation into the final expression strain BL21. The genotyping PCR was carried out using gene specific and vector primer in the following conditions; template 1 µl, dNTP mix (200 µM), forward and reverse primer (0.2 µM each) (Table 2), 1x Crimson *Taq* reaction buffer (New England Biolabs), Crimson *Taq* polymerase (1 unit) (New England Biolabs), at initial denaturation of 95ºC for 5 minutes, denaturation of 95ºC for 1 minute, annealing of 55ºC for 30 seconds and extension of 72ºC for 1 minute for 35 cycles and final extension of 72ºC for 2 minutes.

### 2.5.2 Plasmid construction for *in vitro* expression of GST-RRE1-Ankyrin repeat protein

For the recombinant expression of the Glutathione S-transferase (GST)-RRE1-Ankyrin repeat, the *RRE1-Ankyrin repeat* cDNA was amplified and cloned into the *pGEX-4T-1* vector. Phusion High-Fidelity PCR was used following manufacturer's protocol to introduce the *Bam*HI and *Xho*I restriction sites on the fragment. The reaction contained the following components; 1x High-Fidelity Phusion buffer, 200 µM dNTP's mixture, 0.5 µM of each of the forward and reverse primers (Table 2), 1.0 units/50 µl PCR reaction and 1 µl of template. For the PCR condition, the initial denaturation of DNA was performed at 98°C for 3 minutes, followed by 35 cycles of amplification with denaturing at 98°C for 1 minute, annealing at 65°C for 30 seconds and extension at 72°C for 1 minute. The final extension was performed at 72°C for 5 minutes. The PCR products were visualized by electrophoresis on a 1% agarose gel with ethidium bromide staining and purified using a gel purification kit. The

purified fragment was cloned into the multiple cloning site of the *pGEX-4T-1* vector. Cloning was done separately by digesting the purified PCR product and *pGEX-4T-1* vector with *Bam*HI and *Xho*I restriction enzymes. The total 50 µl reaction mixture contained 1x NEB2 buffer, 2.5 µl *Bam*HI 20,000 U/ml (NEB), 2.5 µl *Xho*I 20,000 U/ml (NEB) and either 30 ng/µl PCR product or 84 ng/µl of vector and made to total volume with autoclave dd$H_2O$. The reactions were incubated at 37°C for 8 hours and inactivated by incubating at 75°C for 5 minutes. This followed the protocol for the purification of PCR products in section 2.4.2. Ligation of the insert in the vector was done in a 10 µl reaction by mixing 6 µl of insert, 3 µl of plasmid, 1 µl of T4 DNA ligase 400,000 U/ml (NEB), 1 µl of ligation buffer (NEB) and autoclaved dd$H_2O$. Ligation reaction was incubated for 16 hours at room temperature followed by transformation of *E. coli* DH5α. Positive transformants were confirmed by genotyping PCR and verified by sequencing for in-frame fusion with N-terminal GST tag embedded in the vector before transformation of the expression strain *E. coli* BL21. The primers used for plasmid construction and genotyping are listed in (Table 2).

### 2.5.3 Plasmid construction for *in vitro* expression of the GST-20S proteasome (α7) protein

The full coding sequence of *20S proteasome* (*α7*) subunit was PCR-amplified from *Arabidopsis* ecotype Col-0 cDNA, using specifically designed primers as described by Book *et al*, (2010). The Phusion High-Fidelity PCR conditions and reaction mixture was generally as described in section 2.5.2. The amplified fragment and *pGEX-4T-1* vector were digested with the enzymes *Eco*RI 20,000 U/ml (NEB) and *Not*I 20,000 U/ml (NEB). The setup for the digestion, ligation and later transformation into *E. coli* DH5α and BL21 were generally the same as described in section 2.5.2. Primers used are listed in (Table 2).

**Table 2: Primers used to make constructs for protein expression**

| Gene and primer sequences | Amplicon (bp) |
|---|---|
| ***CSEP0443*** | 318 bp |
| *CSEP0443* F: atgaaaaacctaagctttgtttcgcttgc | |
| *CSEP0443* R: tcatttacaatccacagatacgttatcccgagtagctgttatccct | |
| *ATTB1-CSEP0443* F: gggacaagtttgtacaaaaaagcaggcatgaaaaacctaagctttgtttcgcttgc | |
| *ATTB2-CESP0443* R: ggggaccactttgtacaagaaagctgggtctcatttacaatccacagatacgttatcccgagtagctgttatccct | |
| ***RRE1-Ankyrin repeat*** | 348 bp |
| *RRE1-ANK* F: atggtgagtaacaacaacgtcgaaggt | |
| *RRE1-ANK* R: ctagattgcgcgtacgacattactgtaac | |
| *Bam*H1-*RRE1-ANK* F: aaaaggatccatggtgagtaacaacaacgtcgaaggt | |
| *Xho*1-*RRE1-ANK* R: aaaaactcgagctagattgcgcgtacgacattactgtaac | |
| ***20S proteasome (α7) subunit*** | 750 bp |
| *20S* F: atgagtagcattggaactgggtacg | |
| *20S* R: ttagtcagcatccatctcctcgagcg | |
| *Eco*RI-*20S* F: aaaaagaattcatgagtagcattggaactgggtacg | |
| *Not*I-*20S* R: aaaaagcggccgcctattagtcagcatccatctcctcgagcg | |

## 2.6 Preparation of competent bacterial cells

The preparation of *E. coli* competent cells was performed as described by Chang (*et al*, 2017). A single colony was inoculated in 5 ml of LB medium and grown overnight at 37°C with moderate shaking at 7*g*. From the overnight culture, 1 ml of the culture was inoculated in 100 ml of fresh LB media in a half litter flask and grown at 37$^{o}$C with shaking at 7*g* until the $O.D_{600nm}$ reached 0.4. The culture was incubated at 4$^{o}$C for 30 minutes and later divided into 50 ml equal volumes in sterile polypropylene tubes before centrifugation at 3,000*g* for 5 minutes. The supernatant was discarded and the pellets suspended in 25 ml of

ice cold 0.1 M $CaCl_2$ and incubated on ice for 15 minutes before centrifugation at 3,000*g* for 5 minutes. The supernatant was discarded and the cells from one tube was poured into the other tube and gently mixed up together. The cells finally were suspended in 2 ml of ice cold 0.1 M $CaCl_2$ supplemented with 20% glycerol and divided into aliquots of 50 µl and 100 µl cells in 1.5 ml pre-cooled Eppendorf, immediately frozen in liquid nitrogen and stored at -80$^oC$ for future use.

For *Agrobacterium* the competent cells was prepared as described by Wang, (2006). A single colony of disarmed *Agrobacterium* strain GV3101 was inoculated in 5 ml LB medium supplemented with gentamycin (25 µg/ml) and rifampicin (100 µg/ml), and grown over night at 28°C with gentle shaking at 200 rpm. Five hundred microliters of the overnight culture (1/100 volume) was inoculated in 50 ml LB media and grown till $OD_{600\ nm}$ reached 0.5 - 0.7. The culture was cooled on ice for 10 minutes and centrifuged at 4,000*g*, for 5 minutes at 4$^oC$. The supernatant was discarded and the cells suspended in 10 ml of ice-cold distilled water and centrifuged for 5 minutes at 4,000*g* at 4°C and the supernatant discarded. This step was repeated twice to completely remove the antibiotics and later re-suspended in 10 ml 0.15 M $CaCl_2$ and spanned at 4,000*g* for 5 minutes. The supernatant was discarded and the pellet was suspended in 1 ml ice-cold 20 mM $CaCl_2$. These were aliquoted into 100 µl aliquots in 1.5 ml tubes, immersed in liquid nitrogen and later stored at -80$^oC$.

### 2.7 Transformation of bacteria cells

#### 2.7.1 Transformation of *E. coli* cells

The transformation of *E. coli* bacteria was based on heat shock described by Froger & Hall, (2007). A 50 µl aliquot of competent *E. coli* (DH5α or BL21) was thawed on ice for 7 minutes and 2 µl - 4 µl of either plasmid DNA (10 ng) or ligation mixture was added. The tube was gently swirled and tapped for thorough mixing. After 30 minutes of incubation on

ice, the tubes were placed in 42ºC water bath for exactly 42 seconds without shaking. Immediately after incubation, the tubes were placed on ice for 5 minutes. Then, either 450 µl of LB or Super Optimal broth with Catabolite repression (SOC) medium was added to the transformation mixture. The bacterial cells were incubated for 1 hour at 37ºC with shaking at 200 rpm to allow recovery from the heat shock and start expression of the selectable marker gene. After 1 hour of incubation, the culture was centrifuged for 2 minutes at 2,800*g*, supernatant was discarded and suspended in 100 µl of fresh LB or SOC media. The culture was plated on selective pre-warmed LB agar medium containing appropriate antibiotics and incubated overnight at 37ºC. Single colonies were then picked to initiate cultures for genotyping, plasmid purification and making glycerol stocks for long term storage.

### 2.7.2 Transformation of *Agrobacterium tumefaciens*

The 100 µl aliquot of competent *Agrobacterium* strain GV 3101 was thawed on ice for 7 minutes prior to addition of 10 µl of plasmid DNA (120 ng/µl). The tube was gently swirled and tapped for thorough mixing and incubated on ice for 30 minutes. The tube was then frozen in liquid nitrogen for 5 minutes, thawed at 37ºC for 5 minutes and then placed on ice for 5 minutes. Then, 1 ml of SOC medium was added to the transformation mixture and the bacterial cells incubated for 4 hours at 28ºC with shaking at 200 rpm to allow recovery from the heat shock and start expression of the selectable marker gene. After 4 hours of incubation, the bacterial mixture was centrifuged for 5 minutes, room temperature, at 2,800*g* and supernatant discarded. The pellet was suspended in 200 µl of SOC medium followed by plating on selective pre-warmed LB agar medium. The plates were incubated at 28ºC for 2 - 3 days. Single colonies were then picked for genotyping PCR, to initiate cultures for plant transformation and to make glycerol stocks for long-term storage.

**2.8 Fusion protein expression and purification**

A single colony was inoculated into 5 ml LB media supplemented with ampicillin (50 µg/ml) and 1% glucose (except for *MBP* tagged constructs where glucose was not added) and grown overnight at 37°C shaken at 200 rpm. A 1 ml culture was drawn off and used to inoculate 100 ml of fresh LB containing ampicillin (50 µg/ml) supplemented with 0.2% glucose for the case of MBP tagged protein expression. The cultures were incubated for 2 - 3 hour at 37°C shaken at 200 rpm until $O.D_{600\ nm}$ reached 0.5 - 0.6 for GST tagged proteins and 0.7 - 0.8 for MBP tagged proteins. The cultures were cooled on ice and protein expression was induced by adding 0.1 mM isopropyl b-D-1-thiogalactopyranoside (IPTG) for the GST tagged proteins except for the *pGEX-4T-1*-GST-20S proteasome (α7) subunit where 0.6 mM IPTG was added. For the MBP tagged proteins, the induction was initiated by the addition of 1 mM IPTG. The cultures were then incubated at room temperature shaken at 200 rpm. For the expression of GST tagged proteins, incubation was done for 6 hours except for *pGEX-4T-1*-GST-20S proteasome (α7) subunit that was done for 3 hours and for the *pGEX-4T-1*-GST-RRE1Ankyrin repeat that was done for 1 hour at 15$^{o}$C. For the expression of MBP tagged proteins, incubation was done for 3 hours at room temperature.

For protein purification cells were harvested by centrifugation at 4$^{o}$C for 15 minutes at 4,000*g*. Cell pellets were resuspended in 1 ml lysis buffer containing; 25 mM Tris-HCl pH 7.5, 100 mM NaCl, 0.1% Triton, 1 mg/ml lysozyme, 1x proteinase inhibitor cocktail (Sigma-Aldrich), 0.5 µl/1000 µl benzonase nuclease and incubated on ice for 30 minutes. The lysates were centrifuged at 15,800*g* for 30 minutes at 4°C. For the GST tagged proteins, the soluble fraction of proteins were loaded into a gravity column containing pre-washed 150 µl glutathione Sepharose® 4B (GE Healthcare). Pre-washing of the glutathione Sepharose beads was performed with column buffer containing; ice cold 1x Phosphate Buffered Saline (PBS) (0.137 M NaCl, 0.0027 M KCl, 0.01 M $Na_2HPO_4$, 0.0018 M $KH_2PO_4$), 140 mM NaCl and

2.7 mM KCl. Washing was done three times at room temperature, each time adding 1 ml of the column buffer and standing the gravity column tube until all the buffer had flowed through. The protein lysates and glutathione Sepharose beads were incubated for 1 hour on a roller at 4$^{o}$C. Later the column was washed three times with ice cold 1x PBS at 4$^{o}$C and the protein incubated with an elution buffer containing 50 mM NaCl and 20 mM reduced glutathione (prepared by dissolving glutathione powder in 2 M Tris-HCl pH 7.5) for 1 hour at 4$^{o}$C on a roller. For the MBP recombinant proteins, 1 ml of Amylose resin (NEB) was loaded into the gravity column and washed five times with 5 ml of column buffer containing 20 mM Tris-HCl pH 7.4, 0.2 M NaCl, 1 mM EDTA pH 7.4, and 1 mM DTT (dithiothreitol) each time adding 1 ml performed at room temperature. Protein lysates were added to the washed resin and incubated for 1 hour on a roller at 4$^{o}$C. Proteins were eluted in six fractions of 0.5 ml by adding at once 3 ml of elution solution made of 10 mM maltose.

### 2.9 *In vitro* pull-down assay for protein interactions

To characterize the protein-protein interactions between GST-RRE1, GST-RRE1-RING, GST-RRE1-Ankyrin repeat, GST-RRE1-C340S, MBP-AtPEN1 and MBP-CSEP0443, *in vitro* pull down assay of GSTs and co-immunoprecipitation of MBP were carried out (Nguyen & Goodrich, 2006). Initially the glutathione Sepharose beads used to trap GST tagged proteins were washed 3 times in ice cold 1x PBS by centrifugation at 4°C, 800*g*, for 30 seconds followed by discarding the supernatants. After washing, the resin was suspended in 1x ice cold PBS, 3 volumes of the resin. The purified proteins were thawed completely on ice and adjusted to 4.3 ng/µl for GST tagged proteins as bait proteins and 0.88 ng/µl for MBP tagged proteins as the prey protein. For a 120 µl reaction, 40 µl of glutathione Sepharose resin slurry were transferred into 1.5 ml micro-centrifuge tubes on ice followed by 40 µl of GST tagged proteins. The lid was tightly closed and mixed gently so that the beads are

dispersed in the protein solution and did not settle at the bottom of the tube. They were then incubated for $2^1/_2$ hours at 4°C on a rotary roller. Then 40 µl of MBP tagged were added and again incubated for $2^1/_2$ hours at 4°C on a rotary roller. After incubation the tubes were centrifuged at 800*g* at 4°C for 2 minutes and the unbound proteins were removed by aspiration for analysis as loading controls. The residual proteins were continuously washed four times, each time with 100 µl of ice-cold 1x PBS followed by centrifugation at 800*g*, at 4°C for 2 minutes and the supernatants were discarded. Finally, the residual proteins were suspended in 20 µl of autoclaved dd$H_2O$ followed by 1x SDS loading buffer and boiled at 98°C for 5 minutes. The denatured proteins were spanned for 30 seconds in a micro-centrifuge and the supernatant loaded for analysis. Generally, the SDS PAGE and western blot analysis were carried out as in section 2.16 with the use of conjugated HRP anti-MBP and anti-GST antibodies (Table 3).

**Table 3: List of antibodies used**

| **Primary antibody** | **Dilution** |
|---|---|
| Anti-flag (BIORAD) | 1:3000 |
| Anti-Ubiquitinylated proteins Clone FK2 (Merk Millipore Corporation) | 1:3000 |
| Anti-Myc | 1:3000 |
| mAb to HA tag (Abcam) | 1:3000 |
| Mono Anti-polyHis HRP conjugated (Alpha diagnostic) | 1:5000 |
| Anti-MBP monoclonal HRP conjugated (NEB) | 1:15000 |
| Anti-GFP HRP conjugated (Miltenyi Biotech) | 1:1000 |
| Anti-GST HRP conjugated (RPN 1236V) | 1:20000 |
| **Secondary antibody** | |
| Anti-mouse IgG HRP linked antibody (Cell Signalling) | 1:4000 |

### 2.10 RRE1 ligase mediated activity on AtPEN1 *in vitro*

The ubiquitination assays were generally performed as described by Sato *et al*, (2009). To assess the ubiquitination of AtPEN1, a 30 µl reaction was carried out. The reaction contained 10 ng/µl E1 (Human ab125733, abcam), 3 ng/µl of purified E2 (AtUBC1), 3 ng/µl of purified GST-RRE1 as E3 ligase enzyme, 0.099 ng/µl AtPEN1, reaction buffer 1x (0.5 M TrisHCl pH7.5, 0.1 M $MgCl_2$, 0.2 mM $ZnSO_4$), 6.7 mM ATP, 66 ng/µl histidine tagged ubiquitin (human, Enzo Life Sciences) and autoclaved dd$H_2O$. Mixing was done by pipetting up and down followed by a brief spin in a micro centrifuge and then incubated at 30$^o$C for 2 hours. Reactions were stopped by adding 1x SDS loading sample buffer, and 4 mM DTT followed by separation in SDS PAGE and later analysis on a western blot as in section 2.16.

For the determination of K48 or K63 ubiquitin sites mediated ubiquitination, mutated ubiquitins were used. The assay was set up as described above but in addition Histidine 6 ubiquitin K48 only and K63 only (Human Boston Biochem) were used.

To determine the ability of purified 20S proteasome subunit α7 to bind the ubiquitinated AtPEN1, the reactions were performed as described by McKeon *et al*, (2015). MBP-AtPEN1 was initially incubated with 3 µl of amylose resin prewashed three times in 1x PBS. After incubation for $1^1/_2$ hours at 4$^o$C, the protein conjugated on the beads was subjected to ubiquitination assay as described above incubated for 3 hours. The AtPEN1 ubiquitinated with either ubiquitin K48 only or K63 only was incubated with either 100 nM GST-20S proteasome α7 subunit, or GST alone for 1 hour at 4°C on a roller. At the end of the incubation the proteins were washed 5 times in 1x PBS and the bound proteins were analysed by SDS PAGE and immunoblotting with anti-GST antibody.

For the assessment of the ability of the impurified 26S proteasome in cell extracts to bind the polyubiquitinated AtPEN1 the set up was made as described by Peth *et al*, (2011).

Proteins were extracted from *Arabidopsis* Col-0 previously infected with *Bgh* for 24 hours. The extraction buffer contained, 50 mM Tris-HCl (pH 7.5), 100 mM NaCl, 10 mM $MgCl_2$, 5 mM DTT, 5 mM ATP, and 1x protease inhibitor cocktail (ROCHE). Initially MBP-AtPEN1 was conjugated on amylose beads and subjected to ubiquitination as described above. After the ubiquitination activity, the reactions were washed 5 times with washing buffer (50 mM Tris HCl pH 7.5, 100 mM NaCl, 10% glycerol and 1 mM DTT) each time centrifuging at 500*g* for 5 minutes at 4$^{o}$C. The washed polyubiquitinated protein 20 µl was incubated with 30 µl of (22.8 ng/µl) 26S proteasome in protein lysates in 150 µl of binding buffer (25 mM Hepes-KOH pH 8, 125 mM Potassium acetate, 1 mM DTT, 2.5 mM $MgCl_2$, 0.1 mg/ml BSA, 0.05% Triton x-100 and 1 mM ATP). After incubation for 30 minutes at 4$^{o}$C on a roller, the un bound proteasome was washed with 400 µl of binding buffer lacking BSA and then with 1 ml of 50 mM Tris HCl pH 7.5, 10 mM $MgCl_2$, 1 mM DTT and 1 mM ATP. The activity of the bound 26S proteasome was measured by incubating with 50 µM of the fluorogenic substrate LLVY-amc in 50 mM Tris HCl pH 7.5, 10 mM $MgCl_2$, 40 mM NaCl, 1 mM DTT and 1 mM ATP. Cleavage of the LLVY-amc peptide was monitored at excitation of 380 nm and emission of 460 nm after incubation for 40 minutes at 30$^{o}$C and expressed as U/minute.

To assess the ability of the of the 26S proteasome to degrade the polyubiquitinated AtPEN1 an assay was set up following the protocol described by García-Cano *et al*, (2014). The ubiquitination of AtPEN1 with ubiquitin mutants was set up as described above. Protein cell lysates from plants treated as described above was extracted in a buffer made of (50 mM Tris-HCl (pH 7.5), 100 mM NaCl, 10 mM $MgCl_2$, 5 mM DTT, 5 mM ATP, and 1x protease inhibitor cocktail). The ubiquitinated AtPEN1 was again incubated with 20 µl of the protein extracts for 30 minutes at room temperature. In addition, control reactions were set up containing 50 µM MG132 26S proteasome inhibitor. After the reaction, the protein was subjected to western blot analysis with anti-MBP antibody.

To assess the influence of CSEP0443 on ubiquitination of RRE1 against AtPEN1, the reactions were setup as described above, in addition 3 ng/µl of either MBP-CSEP0443 or MBP was introduced into the reaction mixture.

To assess if CSEP0443 is ubiquitinated by RRE1, the reaction was set up as described above excluding AtPEN1, containing 3 ng/µl of either MBP-CSEP0443 or MBP. Additionally, 3 ng/µl of Bovine serum albumin (BSA) was set up as a positive control.

### 2.11 Genetic constructs for *in vivo* investigations

*In vivo* experiments in *N. benthamiana* and *Arabidopsis* were made by generating genetic constructs using either Golden Gate modular cloning (MoClo) (Weber *et al*, 2011; Engler *et al*, 2014), or site directed mutagenesis (Agilent Technologies, 2015). For Golden Gate MoClo, vectors *pAGM1287* for level 0 acceptor, *pICH47742*, *pICH47751*, *pICH47761*, for level 1 positions 2, 3, 4 and *pAGM4723* for level 2 acceptor were utilized. *pICH41744* endlinker 2, *pICH41766* endlinker 3, *pICH41780* endlinker 4 for level 2 positions 2, 3 and 4 constructions, *pICSL11024* for kanamycin resistance already in position 1 level 1, modules *pICSL50007* for Flag tag, *pICSL50010* for Myc tag, *pICSL50009* for HA tag, *pICSL12015* for Ubiquitin promoter, *UBIQ5* for ubiquitin terminator, *pICH45214* for *LHB1B1* promoter, *pICH77901* for mannopine synthase terminator, *pICH41414* for *CaMV 35S* terminator were kindly obtained from Alistair McCormick group, at the University of Edinburgh. The *CaMV 35S* promoter was amplified from pEarly Gateway vector (*pEG*)-*202*, *EYFP* was amplified from *pEG-101*, *CSEP0443* was amplified from *pET-40A* while other gene fragments, the *AtPEN1*, the *UBIQ* and its mutants *K48R*, *K63R*, *K48R-K63R*, and *RRE1* were amplified from Col-0 cDNA using primers sets in (Table 4). Underlined sequences in the table indicate point of mutations in the sequence. The PCR reactions and conditions were set up as in section 2.5.1. After visualizing the gel, the fragments were cut and cleaned using a PCR kit as

in section 2.4.1. All gene sequences with *Bpi*I/*Bsa*I sites were mutated to codons coding the same amino acid by making base substitutions and selected based on the codon usage in *Arabidopsis*. For all constructions the vectors were normalized to 10 fmol and the inserts to 20 fmol. For level 0 construction, in addition to the vector and insert, the reaction mixture contained *Bpi*I enzyme 0.5 U/µl (Thermo Scientific), T4 DNA ligase enzyme 400 U/µl (Thermo Scientific), T4 DNA ligase reaction buffer 1x (Thermo Scientific), and BSA 1x (NEB) to a final volume of 10 µl. The reactions were incubated at 37ºC for 10 minutes followed by 25 cycles of 37ºC for 1 minute: 30 seconds and 16ºC for 3 minutes, followed by incubation at 16ºC for 10 minutes, 50ºC for 10 minutes and final inactivation at 85ºC for 5 minutes preceded by transforming DH5α. Blue/white selection were done on plates containing 100 µg/ml of spectinomycin, 0.5 mM IPTG and 40 µg/ml X-gal (X-galactose). Level 1 constructions were done as in level 0 except *Bsa*I 0.5 U/µl (Thermo Scientific) was used as a digesting enzyme and carbenicillin 50 µg/ml was used as a selection antibiotic in addition to IPTG and X-gal. Level 2 constructions were done as in level 0 except that kanamycin 50 µg/ml was used as a selection antibiotic and both IPTG and X-gal were excluded in the plates. In all cases transformants were screened by genotyping PCR using vector primers for level 0, level 1, and level 2 combined with gene specific primers (Table 4). The presence of the right size of the inserts were also verified by *Bsa*I digestion for level 0 and *Bpi*I digestion for level 1, and in all levels the plasmids were sent for sequencing using respective level vector primers.

Site directed mutagenesis was used to generate the *AtPEN1-K103R*, *AtPEN1-K103R-K281R* and *AtPEN1-K103R-K281R-K285R-K307R* genetic constructs. The reaction mixture composed of 2.5 µl of 10x ultra-high reaction buffer, 7.8 ng/µl of template, 1 µl of 10 µM of each forward and reverse primer (Table 4), 2.5 µl of 2.5 mM dNTP mix (Newmarket scientific), 1.5 µl of Quick Solution and autoclaved dd$H_2O$ to a total volume of 25 µl. Then

followed by addition of 0.5 µl of *PfuUltra* HF DNA polymerase (2.5 U/µl). The reaction mixture was subjected to PCR: Initial denaturation at 95$^{o}$C for 1 minute, then 18 cycles of denaturation 95$^{o}$C for 50 seconds, annealing 60$^{o}$C for 50 seconds and extension 68$^{o}$C for 10 minutes: 30 seconds (1 minute per kilo base); followed by a final extension at 68$^{o}$C for 7 minutes. After the completion of the cycling process, the reaction mixture was placed on ice for 2 minutes. After cooling 1 µl of *Dpn*I restriction enzyme (10 U/µl) was added and mixed thoroughly by pipetting up and down followed by incubation at 37$^{o}$C for 1 hour to digest the parental plasmid. Then 4 µl of *Dpn*I treated mixture was transformed in 100 µl of *E. coli* DH5α. Positive colonies were confirmed by both genotyping PCR and Sanger sequencing to check for the mutation.

**Table 4: Primers used to make constructs for *in vivo* protein expressions**

| **Golden gate cloning method** | |
|---|---|
| **Gene** | **Primer sequences** |
| ***AtPEN1*** | |
| | *AtPEN1* F: atgaacgatttgttttccagctcattctctcg |
| | *AtPEN1* R: tcaacgcaatagacgccttgcctga |
| | *AtPEN1 GG* F: tgaagacataatgaacgatttgttttccagctcattctctcg |
| | *AtPEN1 GG* R: tgaagacatcgaacgcaatagacgccttgcctga |
| | *AtPEN1 Mut Bsa*I F: tgaagacatgtttcaggaagaaattgatggactctatggat |
| | *AtPEN1 Mut Bsa*I R: tgaagacataaaccattgaggacagaggtcctggttcgatcg |
| ***AtPEN1-K281R*** | |
| | *AtPEN1-K281R* F: tgaagacataggaacacgcgaaaatggacatgtattgcca |
| | *AtPEN1-K281R* R: tgaagacattcctctggtaaacccgagcggtttgtagct |
| ***AtPEN1-K285R*** | |
| | *AtPEN1-K285R* F: tgaagacatagatggacatgtattgccattattattctcatcatcatca |
| | *AtPEN1-K285R* R: tgaagacatatcttcgcgtgttcttctggtaaacccga |
| ***AtPEN1-K307R*** | |

*AtPEN1-K307R* F: tgaagacatagaccgtggaacaacagcagtggc

*AtPEN1-K307R* R: tgaagacatgtcttaaaacagcaagaaccacaacagttatgatgat

***AtPEN1-K281R-285R***

*AtPEN1-K281R-285R* F: tgaagacataggaacacgcgaagatggacatgtattgcca

*AtPEN1 GG* R: tgaagacatcgaacgcaatagacgccttgcctga

***AtPEN1-K281R-285R-K103R***

*AtPEN1-K281R-285R* F: tgaagacataggaacacgcgaagatggacatgtattgcca

*AtPEN1-K307R* R: tgaagacatgtcttaaaacagcaagaaccacaacagttatgatgat

***RRE1***

*RRE1* F: atggggcaacaacaatcacagtccaagga

*RRE1* R: tcaaacatgatatagcttaatgacctgatcaatgttggcgc

*RRE1 GG* F: tgaagacataatggggcaacaacaatcacagtccaagga

*RRE1 GG* R: tgaagacatcgaaacatgatatagcttaatgacctgatcaatgttggcgc

*RRE1 Mut Bsa*I F: tgaagacatgtttcgtacacacggttaagttacttctgtctcacg

*RRE1 Mut Bsa*I R: tgaagacataaacctctttttgcagcatggtgcagagga

***UBIQUITIN***

*Ubiq* F: atgcagatctttgttaagactctcaccgga

*Ubiq* R: accaccacggagcctgagaaccaagt

*Ubiq GG Mod* F: tgaagacataatgcagatctttgttaagactctcaccgga

*Ubiq GG Mod* R: tgaagacatcgaaccaccacggagcctgagaaccaagtgga

*Ubiq-K48 GG* F: tgaagacatcgtcagctagaggatggccgtacgttggct

*Ubiq-K48R GG* R: tgaagacatgacgtccggcgaaaataagcctctgctgatccgga

*Ubiq-K63R GG* R:

tgaagacatcgaaccaccacggagcctgagaaccaagtggagggtggattcctctgga

***CAMV 35S PROMOTER***

*CaMV 35S* F: tgagacttttcaacaaagggtaatatcggga

*CaMV 35S* R: gtcctctccaaatgaaatgaacttcct

*CaMV 35S GG* F: tgaagacatggagtgagacttttcaacaaagggtaatatcggga

*CaMV 35S GG* R: tgaagacatcattgtcctctccaaatgaaatgaacttcct

*CaMV 35S GG Mut part2* F: tgaagacattacgttccaaccacgtattcaaagca

*CaMV 35S GG Mut part1* R: tgaagacatcgtattcttttttccacgatgctcctcgtgggt

***CSEP0443***

*CSEP GG* F: tgaagacataatggctaaatattatacatgtggcggtgtcct

*CSEP GG* R: tgaagacatcgaacctttacaatccacagatacgttatcccgagtagctgttatccct

***FULL LENGTH AND***

***TRUNCATED CSEP0443-EYFP-FLAG***

*FULLCSEPEYFP GG* F: tgaagacataatgaaaaacctaagctttgtttcgcttgcgct

*TRUCCSEPEYFP GG* F: tgaagacataatggctaaatattatacatgtggcggtgtcct

*CSEP GG* R: tgaagacatcgaacctttacaatccacagatacgttatcccgagtagctgttatccct

*CSEP-EYFP GG* F: tgaagacatgtgagcaagggcgaggagctgttcaccggggt

*CSEP-EYFP GG* R: tgaagacattcactttacaatccacagatacgttatcccgagtagctgttatccct

***EYFP***

*YFP GG* F: tgaagacataatggtgagcaagggcgaggagctgttcaccggggt

*YFP GG* R: tgaagacatcgaattgtacagctcgtccatgccgagagtgat

Level 0

F (0015): cgttatcccctgattctgtggataac
R (0016):gtctcatgagcggatacatatttgaatg

Level 1

F (0229): gaaccctgtggttggcatgcacatac
R (0230): ctggtggcaggatatattgtggtg

Level 2

F (0231): gtggtgtaaacaaattgacgc
R (0232): ggataaacctttcacgccc

**Site directed mutagenesis**

***AtPEN1-K103R,***

***AtPEN1-K103R-K281R* and**

***AtPEN1-K103R-K281R-K285R-K307R***

*AtPEN1-K103R* (*QCSMUT*) F: cgcgttgaagaaggcgaggatgattaaagttaaactcg

*AtPEN1-K103R* (*QCSMUT*) R: cgagtttaactttaatcatcctcgccttcttcaacgcg

### 2.12 Transformation of *Arabidopsis* and selection of transformants

The procedure for *Arabidopsis* transformation and selection was performed following a protocol described by Zhang *et al*, (2006). The *Agrobacterium* colony of GV3101 strain was inoculated into a 5 ml LB liquid media supplemented with kanamycin (50 µg/ml), rifampicin (100 µg/ml) and gentamycin (100 µg/ml). The cultures were grown for 2 days at 28$^{o}$C with shaking at 200 rpm. The 5 ml culture was diluted in 500 ml LB media supplemented with the above antibiotics and grown again for an overnight in the above conditions. The bacteria were harvested by centrifuging at 25$^{o}$C, 4,000*g* for 10 minutes. The bacteria pellet was suspended in 500 ml solution of 5% sucrose containing 0.01% Silwet L-77. For transformation, floral dipping was done by submerging the flowers and buds of the *Arabidopsis* plants in bacteria suspension for 10 - 15 seconds. The plants were briefly drained and kept lying flat on tray covered with a transparent cover to preserve humidity and placed under low light intensity in the growth chamber for 24 hours. The plants were then appropriately tied on support sticks and continued growth until seed harvesting.

For selection of transformants (T) on media, the harvested seeds were either immediately vernalized for 3 days at 4$^{o}$C immersed in 200 µl of water before sterilization or were initially surface sterilized and later vernalized before plating. The seeds were surface sterilized by treating them with 70% ethanol for 1 minute and then in 50% bleach supplemented with 0.05% Tween 20 for 10 minutes. During treatment with bleach the suspension was vortexed vigorously every 2 minutes. The seeds were washed 3 - 4 times with clean autoclaved dd$H_2O$ until all bleach was removed. The sterilised seeds were plated on full strength MS media supplemented with either kanamycin (50 µg/ml) and carbenicillin (50 µg/ml) for T1 selection or kanamycin (50 µg/ml) alone for T2 and T3 selections. The plated seeds were kept under light for 5 days and the selected transformants were transferred to soil for further growth. Selections were continued until homozygous plants were obtained.

### 2.13 Transient assay in *N. benthamiana*

The procedure was performed as described by Liu *et al*, (2016). Single colonies of respective *Agrobacterium* constructs were grown overnight in 5 ml LB supplemented with kanamycin (50 µg/ml), rifampicin (100 µg/ml) and gentamycin (100 µg/ml). Bacteria were harvested by centrifuging at 5,000*g* for 5 minutes in a table top centrifuge. The pellet was washed once in infiltration media containing MES 10 mM pH 5.2, $MgCl_2$ 10 mM and acetosyringone 0.2 µM to remove residual antibiotics. The pellet was suspended in 0.5 ml infiltration media and $O.D_{600\ nm}$ adjusted to 0.2 – 1 depending on the assay before infiltration in the leaves of 3 weeks-old *N. benthamiana* plants that have been previously kept under light for 2 hours before infiltration. The plants were further grown for 2 days before protein extraction.

### 2.14 RNA extraction, RT-PCR and qPCR

For the RNA extraction, 100 mg of either *Arabidopsis* or barley leaves, either non-infected or *Bgh* infected at indicated time points were collected and immediately frozen in liquid nitrogen. The leaves were finely ground in liquid nitrogen using mortar and pestle previously sterilized by autoclaving. The finely ground frozen tissues were suspended in 1 ml TRIzol® Reagent (Life technologies) and incubated for 10 minutes at room temperature. The homogenized tissues were centrifuged at 12,000*g* for 10 minutes at 4$^{o}$C. The supernatant was mixed with 0.2 ml chloroform and incubated for 3 minutes at room temperature before being centrifuged again at 12,000*g* for 5 minutes. About 80% of the aqueous phase were collected and mixed with 0.5 ml isopropyl alcohol mixed briefly for 3 seconds and centrifuged for 5 minutes at 12,000*g*. The pellet was washed once in 70% ethanol (prepared in Diethyl pyrocarbonate (DEPC) treated water) by centrifuging at 7,500*g* for 5 minutes at 4$^{o}$C. The pellet was air dried for 20 minutes and suspended in 50 µl of RNAse free water. The

suspended pellet was then incubated at 60$^{o}$C for 10 minutes for complete solubilization followed by agarose gel electrophoresis to check RNA integrity. Then followed by concentration determination using a nanodrop.

For Reverse transcription (RT)-PCR, 1.5 µg of RNA was used for cDNA synthesis prior to RT-PCR. The 20 µl reaction mixture contained: 2 µl of 100 µM dNTP mix, 5 µl of 5x reaction buffer, 2 µl of 10 µM oligo (dT) primer (Table 5), 1 µl of reverse transcriptase enzyme and 1 µl of RNAse inhibitor. The PCR set up for cDNA synthesis involved 25$^{o}$C for 10 minutes, 37$^{o}$C for 2 hours, 85$^{o}$C for 5 minutes and 4$^{o}$C forever. For RT-PCR reactions, the synthesised cDNA was either diluted 1:10 or undiluted followed by a PCR reaction mixture of 1x reaction buffer, 200 µM of dNTPs, 0.2 µM of primers (Table 5), 0.2 U/µl of Maximo *Taq* DNA polymerase (Thistle Scientific Ltd) and 1 µl of the template. The reaction mixture was amplified in a PCR set up of 94$^{o}$C for 3 minutes, 94$^{o}$C for 1 minute, 54$^{o}$C for 30 seconds, 72$^{o}$C for 40 seconds for 27 cycles and a final extension of 72$^{o}$C for 2 minutes before storage at 4$^{o}$C. The PCR products were resolved in 1% agarose gel in 1x TAE buffer and visualised under ultraviolet light.

The quantitative (q)PCR was performed as described by Godfrey *et al*, (2010) with modifications. Quantification was performed on a Light Cycler 480 real-time PCR detection system using the Light Cycler 480 SYBR Green I master (Roche) in 10 µl reaction. The assays were performed in two biological replications. Each sample loaded in three technical replicates. The transcripts levels of *CSEP0443* in both the control and test samples were normalized to the *Bghβ-tubulin* transcript level. Primers listed in (Table 5).

**Table 5: Primers used for RT-PCR and quantitative PCR**

| **RT-PCR** | | |
|---|---|---|
| **Gene** | **Primer sequence** | **Size (bp)** |
| ***CSEP0443*** | F: atgaaaaacctaagctttgtttcgcttgc<br>R: tttacaatccacagatacgttatcccgagtagctgttatccct | 318 |
| ***CSEP0443-FLAG*** | F: gctaaatattatacatgtggcggtgtcct<br>R: tttacaatccacagatacgttatcccgagtagctgttatccct | 255 |
| ***UBIQUITIN-FLAG*** | F: atgcagatctttgttaagactctcaccgga<br>R: tcacttatcgtcatcgtccttataatcagct | 315 |
| ***AtPEN1-MYC*** | F: gtttaccagaagaacacgcgaaaatggaca<br>R: caaatcctcctctgagataagcttctgctca | 300 |
| ***RRE1-HA*** | F: ccaatgttcctgcactaagtgatgatgct<br>R: gtcaggaacatcgtatgggtacgaaacatgatatag | 269 |
| ***EYFP-FLAG*** | F: tccgccacaacatcgaggacggca<br>R: tcacttatcgtcatcgtccttataatcagct | 302 |
| ***CSEP0443-EYFP-FLAG*** | F: ttttaacgttgaccagccaccggaaggaagt<br>R: agggtgggccagggcacgggca | 300 |
| ***ACTIN*** | F: aggttctgttccagccatc<br>R: ttagaagcatttcctgtgaac | 350 |
| ***Bghβ-tubulin*** | F: cagcagatgtttgatccgaa<br>R: agaacatagggcagtttga | 240 |
| **Oligo (dT)** | R: ttttttttttttttttttt | |
| **qPCR** | | |
| ***CSEP0443*** | F: gcttttcttaagccatttgatgcctgtactggct<br>R: ttcgtttcaacctctacttcgatcctacttccag | |
| ***Bghβ-tubulin*** | F: atcgtatccgctacttcaga<br>R: ctgaggccgagtctaatatg | |

### 2.15 Protein extraction from plants and co-immunoprecipitation assays

Proteins were extracted from 4 g leaves of 3 weeks-old *Arabidopsis* plants and from 2 g of Agro-infiltrated *N. benthamiana* leaves. The leaves were harvested and immediately frozen in liquid nitrogen. Depending on the purpose of the experiment, *Arabidopsis* plants were initially inoculated with *Bgh* spores and incubated for 3 days before harvesting. The leaves were then finely ground in liquid nitrogen before further crushed in extraction buffer described by Li et al, (2015). The buffer composed of: Tris-HCl 50 mM pH 7.5, NaCl 150 mM, EDTA 5 mM, 0.1% Triton x-100, Nonidet P-40 0.2%, PMSF 0.5 mM, and protein inhibitor cocktail 1x. For protein extractions intended for ubiquitination assessment depending on the objective MG132 50 µM or concanamycin A 0.5 µM were either added in the buffer or infiltrated in leaves after 1 day of incubation before harvesting. The tissue lysates were centrifuged at 15,800*g* for 15 minutes at 4ºC and the protein suspensions were collected.

For co-immunoprecipitation assays, the protein suspensions were filtered through 0.4 µM millipore filters and protein concentrations determined using the Bradford reagent (Bio-Rad). The proteins were adjusted to 200 - 350 µg depending on the assay using the extraction buffer. The diluted proteins were incubated appropriately with 2 µg of the anti-flag, anti-Myc, anti-HA antibodies conjugated on agarose beads over night at 4ºC on a roller. The proteins were then washed three times with 1 ml of ice cold 1x PBS each time centrifuging at 2,800*g* for 30 seconds before discarding the supernatant. The washed proteins were boiled in 1x SDS loading dye (10 mM Tris-HCl pH 6.8, 2% SDS, 0.025% bromophenol blue and 8% glycerol) containing either 100 mM DTT or 10% β-Mercaptoethanol at 95ºC for 5 minutes. The proteins were then centrifuged briefly for 30 seconds in a micro-centrifuge and 10 - 20 µl of the supernatant loaded in SDS gel for western blot analysis.

### 2.16 SDS PAGE and western blot analysis

Generally SDS PAGE and western blot analysis were carried out as described by Sambrook *et al*, (2012). Proteins were separated in SDS PAGE (0.375 M Tris-HCl pH 8.8, 0.05 % (w/v) SDS, 7% or 10% or 15% Acrylamide/Bis-acrylamide, 0.05% w/v ammonium persulphate and 0.066% TEMED) in 1.5 mm glass chambers (Bio-Rad) depending on the expected size of the target protein using colour prestained protein standard (P7712S NEB). Electrophoresis was conducted in a running buffer (25 mM Tris-base, 0.2 M Glycine and 0.1% SDS) initially at 80 V and after traversing the stacking gel (0.3075 M Tris-HCl, pH 8.8, 0.1% (w/v) SDS, 4.02% Acrylamide/Bis-acrylamide, 0.05% w/v ammonium persulphate and 0.099% TEMED) the voltage was increased to 120 – 150 V.

After protein separation, the gel was covered with a nitrocellulose membrane, stacks of filter papers and western blotting was carried out in the Mini Trans-Blot cell (Bio-Rad) in 1x transfer buffer ( 14.4 g/l glycine, 3.02 g/l Tris-base, and 20% methanol) at 20 V, 0.03 A, 4$^{o}$C for overnight. The membrane was blocked with 5% (w/v) of skimmed-milk powder in 1x PBS and 0.1% Tween 20 (PBS-T) for 1 hour. The membrane was incubated with respective antibodies (Table 2) for 1 hour and followed by 3 times washing with PBS-T at 10 minutes interval. The membrane was incubated with equal volumes (500 µl) of chemiluminescence solution A and solution B for 1 minute. The luminescence signal was detected by exposure of the blot to an X-ray film.

Protein gels for analysis of proteins purified from bacteria were stained in coomassie blue staining (50% methanol, 10% glacial acetic acid and 0.1% Coomassie brilliant blue stain) for 1 hour at room temperature with gentle shaking. The stain was decanted off and replaced with a destaining solution (40% methanol, 10% glacial acetic acid). Destaining was continued with 3 - 4 changes until when the gel was clear and photographed.

### 2.16.1 Relative protein and DNA quantification

ImageJ software, a Java-based image processing programme was used to measure the relative quantity of proteins and DNA in the gels. Gel image was opened in ImageJ software. The image was either left in the coloured version or converted to grey scale by selecting 8-bit under the analyse menu depending on the clarity. Using the selection rectangular tool, individual bands were selected by dragging the rectangular tool from one band to another. Then followed by navigating the analyse menu to find select the first lane, second lane under the gel sub menu. Again, under the gel sub menu, the plot lanes option allowed each band to be plotted. By using the straight line under the tool menu, the area under the peak corresponding to individual bands was marked. By using the wand (tracing) tool each band peak area was selected generating numerical values. Selecting label peaks option under the gel sub menu converted the values into percentages. The values were then transferred in spreadsheets for analysis.

## 2.17 Host Induced Gene Silencing constructions

The Barley Stripe Mosaic Virus vectors (BSMV) *pCaBS-α, pCaBS-β, pCaBS-γ* and *pCa-γb:PDS* (*Phytoene desaturase*) used for Host Induced Gene Silencing (HIGS) were kindly obtained from Attila Molnar laboratory at the University of Edinburgh. The vectors and the procedure for cloning in the fragments were previously described by Yuan *et al*, (2011); Lee *et al*, (2015). The siRNA Finder (Si-Fi) software (http://labtools.ipk-gatersleben.de/) and Small interfering RNA (siRNA) scan software were used to predict the off target gene for RNAi *CSEP0443* in *Bgh* and barley transcriptome (Aguilar *et al*, 2016; Ahmed *et al*, 2016b). *CSEP0443* was checked against the entire *Bgh* coding sequence and barley genome. Full length *CSEP0443* fragment was amplified with gene specific primers

flanked by 5'-AAGGAAGTTTAA-3'on forward primer and 5'-AACCACCACCACCGT-3' on reverse primer (Table 6). The PCR set up and reactions were performed as in section 2.5.1. The PCR products were separated in 1% agarose gel and visualized under ultraviolet light before cutting out the band with a clean scalpel and cleaned with a PCR kit as in section 2.4.1. The plasmid *pCa-γbLIC* with a ligation independent cloning (LIC) site for cloning in *CSEP0443* was linearized in a reaction mixture containing; 1x reaction buffer (Thermo Scientific), 1 µl fast digest *Apa*I (Thermo Scientific), plasmid DNA 1 µg in a total reaction of 20 µl. The components were mixed, centrifuged briefly, incubated at 37$^{o}$C for 2 hours before inactivating the enzyme at 65$^{o}$C for 5 minutes. To generate sticky ends on both the plasmid and insert, 500 ng of linearized plasmid in 50 µl reaction volume or PCR product 200 ng in a 10 µl reaction volume were mixed with 1x T4 buffer and T4 DNA polymerase 0.6 U for the PCR product and 6 U for the plasmid DNA. For the plasmid reaction 5 mM of dTTP was added and for the PCR product reaction 5 mM of dATP was added and in each case reactions were made to the required volumes with nuclease free water. The components were mixed, centrifuged briefly and incubated at 20$^{o}$C for 30 minutes before stopping the reaction by incubating at 75$^{o}$C for 10 minutes. To ligate the insert into the vector, 10 µl of the insert reactions were mixed with 2 µl of the vector reactions, incubated at 66$^{o}$C for 2 minutes, cooled to 25$^{o}$C and incubated for 10 minutes to allow annealing of the complementally ends. For transformation 2 µl of the ligates were used to transform 100 µl DH5α competent cells. Successful transformants were confirmed by genotyping PCR using LIC primers (Table 6), PCR reactions and conditions as set up in section 2.5.1 annealed at 54$^{o}$C and extended at 72$^{o}$C for 45 minutes. Further the sequences were verified by Sanger sequencing. The verified plasmids and other plasmids the *pCaBS-α*, *pCaBS-β*, *pCaBS-γ* and *pCa-γb:PDS* were individually transformed in *Agrobacterium* strain GV3101.

For the inoculation of the virus on the susceptible barley plants, initially the virus was

multiplied in three weeks-old *N. benthamiana* plants. Briefly the *Agrobacterium* of individual vectors were grown for an overnight in 5 ml LB media supplemented with (50 µg/ml) kanamycin, rifampicin (100 µg/ml) and gentamycin (100 µg/ml). The bacteria were harvested, processed in the infiltration media as in section 2.13 with modification of acetosyringone (150 µM) and $O.D_{600\ nm}$ adjusted to 1.7. The bacteria suspensions were kept at room temperature for 3 hours before infiltrating two leaves of individual plants. Prior infiltration the bacteria suspensions were mixed in three equal proportion of ratio 1:1:1 having *pCaBS-α*, *pCaBS-β* and one of either *pCa-γb* or *pCa-γb:PDS* or *pCa-γb:CSEP0443*. The infiltrated plants were incubated in growth conditions described in section 2.1.1 for 10 days. After incubation the infiltrated leaves were removed and ground initially in liquid nitrogen using the pestle and mortar and then in the phosphate buffer made of 20 mM sodium phosphate ($Na_3PO_4.12H_2O$) and 1% celrite (Acros Organics). The ground tissues were immediately mechanically rubbed on the third and fourth leaves of 10 day-old barley plants and the plants returned to the growth conditions described in section 2.1.1 for 12 - 14 days.

The leaves were then inoculated with *Bgh* spores after observing viral symptoms indicated by photo bleaching in *pCa-γb:PDS*, mild mosaic and mild chlorosis in other transformants. The plants were incubated in the growth cabinet set for six days. During incubation the leaf samples were collected each day for RT-PCR as described in section 2.14 and final imaging taken on the sixth day. Leaves for staining against fungal structures were also collected on the sixth day and preceded as in section 2.18.1.

**Table 6: Primers used in HIGS constructions**

| Gene | Primer sequences |
|---|---|
| *CSEP0443* | F: aaggaagtttaaatgaaaaacctaagctttgtttcgcttgc<br>R: aaccaccaccaccgttttacaatccacagatacgttatcccgagtagctgttatccct |
| *LIC* | F: gatcaactgccaatcgtgagtaggt<br>R: ccaattcaggcatcgttttcaagttcg |

### 2.18 *Bgh* pathogenicity assays

The assays conducted related to aniline blue staining, trypan blue staining and 3,3′-Diaminobenzidine (DAB) staining were performed based on protocols described by Koch & Slusarenko, (1990); Song *et al*, (2015); Liu *et al*, (2016). The electrolyte leakage determination was based on the procedure described by (Campos *et al*, 2003; Kneeshaw *et al*, 2017).

#### 2.18.1 Aniline blue staining for callose deposition and fungal structures

Initially the selected *Arabidopsis* plants were inoculated with *Bgh* spores and incubated in growth cabinet for 72 hours. The inoculated leaves were removed and immediately transferred to lactophenol clearing solution containing lactic acid, phenol, glycerol, ethanol and water in a ratio of 1:1:1:1:2 for 24 hours to completely remove the chlorophyll. For visualizing callose deposition, the cleared leaves were rinsed in 50% ethanol and finally rinsed in water. The leaves were then stained in 0.01% aniline solution dissolved in 150 mM $K_2HPO_4$ (pH 9.5) for 3 hours at room temperature, mounted on the microscope slides and observed under epifluorescence microscope with the excitation of 365 nm and emission of 420 nm. Relative quantification of callose deposition in the images taken was done using ImageJ software as described in section 2.16.1 and was expressed in percentages

of total area. For visualizing the fungal structures, the cleared leaves were stained in 0.06% aniline blue for 24 hours at room temperature dissolved in lactophenol solution and observed under differential contrast microscopy.

### 2.18.2 Trypan blue staining

The *Arabidopsis* leaves previously inoculated with *Bgh* for 72 hours were submerged in lactophenol solution (10 g phenol, 10 ml glycerol, 10 ml lactic acid, 10 ml water and 10 mg trypan blue). The leaves were boiled for 2 minutes at 100$^{o}$C in a water bath and left for an overnight. The leaves were then destained in chloral hydrate solution 2.5 g/ml until cleared usually changing the destaining solution after every 24 hours. The cleared leaves were rinsed in water and visualised under bright field microscopy. Relative quantification of cell death in the images taken was done using ImageJ software as described in section 2.16.1 and was expressed in percentages of the total area.

### 2.18.3 Reactive oxygen species staining

The *Arabidopsis* leaves incubated with *Bgh* spores for 72 hours were immediately submerged in DAB solution prepared by dissolving 1 mg/ml of DAB powder in water pH 3.8 and vacuum infiltrated for 20 minutes. The leaves were then incubated in DAB solution for 24 hours in dark. The stained leaves were cleared in 95% ethanol for 20 minutes and then transferred in 50% ethanol. The cleared leaves were mounted on microscope slides and images taken by bright field microscopy. Relative quantification of reactive species production in the images taken was done using ImageJ software as described in section 2.16.1 and was expressed in percentages of the total area.

### 2.18.4 Electrolyte leakage determination

The *Arabidopsis* plants were inoculated with *Bgh* spores for 24, 48, 72 and 96 hours and incubated in the growth cabinet. Ten leaf discs of 7 mm diameter were cut out from the respective sets of infected plants using a cork borer. The leaf discs were washed thoroughly in de-ionised water three times and after incubated in 10 ml of de-ionised water at room temperature exposed to light. Electrolyte leakage was measured immediately < 10 minutes or 0 hour, at 6, and 14 hours using the conductivity meter. Total electrolyte leakage was measured after keeping the leaf discs at 72$^{o}$C for $2^{1}/_{2}$ hours and left to cool for an overnight before the conductivity meter was used to obtain the measurements.

## 2.19 Confocal and Differential interference contrast (DIC) microscopy

The Leica SP5 and Zeiss LSM880 Airyscan confocal microscopes were employed to visualize the localization of AtPEN1 and CSEP0443 respectively while DIC microscope was used to visualise *Bgh* infection. For confocal microscopy the freshly harvested leaves were immersed in 0.85 M sodium chloride for 10 minutes to induce plasmolysis before examination. The Excitation of Enhanced green fluorescent protein (EGFP), Enhanced yellow fluorescent protein (EYFP) and chlorophyll was done at 488, 519, 470 nm, respectively. Fluorescence emission was detected at 535 nm (EGFP), 555 nm (EYFP) and 680 nm (Chlorophyll). The Zeiss LSM880 Airyscan has an option for linear unmixing allowing separation of EYFP and EGFP emissions. For DIC microscopy the leaves were immersed in 20% glycerol and examined under 62x oil immersion objective.

# Chapter three

## 3.0 The impact of CSEP0443 on *Bgh* virulence in both host and non-host plants

### 3.1 Introduction

*Blumeria graminis* f. sp. *hordei* (*Bgh*) secrete a number of effector proteins to circumvent the host defence system (Ahmed *et al*, 2016a). The effectors are known to be released at different stages of fungal growth and to act in different areas of plant cells. In a screen to uncover the effectors released during early stages of *Bgh* invasion, *Bgh* Effector Candidate 1 (*Bgh*Efc1)/ Candidate Secreted Effector Protein 0443 (CSEP0443) was found to be highly expressed (Godfrey *et al*, 2010; Pedersen *et al*, 2012). *CSEP0443* encodes a 109 amino acid protein with an N-terminal signal peptide and a conserved tyrosine/phenylalanine/tryptophan x cysteine (Y/F/WxC) motif sequence (Godfrey *et al*, 2010). The presence of the signal peptide implies that CSEP0443 is directed in the fungal secretory route and released in the cytosol of the host. The secreted 88 amino acid residue mature protein lacks a signal peptide and has no homologues outside *B. graminis* (Godfrey *et al*, 2010). The effector expression reached a maximum within 4 - 5 days corresponding to the time of maximum haustorial formation.

To dissect the possible function of CSEP0443 in aiding *Bgh* virulence in host plants, Barley Stripe Mosaic Virus vectors for Virus Induced Gene Silencing (BSMV-VIGS) were used (Holzberg *et al*, 2002; Yuan *et al*, 2011; Lee *et al*, 2015). The vectors were previously shown to be applicable in Host Induced Gene Silencing (HIGS) to demonstrate the potential influence of fungal genes in virulence (Liu *et al*, 2016). These vectors are based on the ribonucleic acid (RNA) interference (RNAi) concept where the hairpin construct targeting fungal transcripts are expressed inside the host. The silencing of *CSEP0443* by a mechanism

of RNAi could reveal the importance of the effector in *Bgh* pathogenicity.

To understand the influence of CSEP0443 in promoting the virulence of *Bgh* in the non-host plant *Arabidopsis*, *CSEP0443* was stably transformed into *Arabidopsis*. The stable transgenic plants were inoculated with *Bgh* spores and the penetration rates were assessed by successful haustoria formation (Collins *et al*, 2003). My investigation would reveal whether the expression of CSEP0443 in *Arabidopsis* promotes *Bgh* pathogenicity in this ordinarily non-host and the influence on callose deposition, reactive oxygen species (ROS) production, electrolyte leakage and cell death.

## 3.2 Materials and methods

### 3.2.1 HIGS constructions

The BSMV vectors *pCaBS-α*, *pCaBS-β*, *pCaBS-γ* and *pCa-γb:PDS* (*Phytoene desaturase*) used for HIGS were kindly obtained from Attila Molnar laboratory at the University of Edinburgh. The vectors and the procedure for cloning in the fragments were previously described by Yuan *et al*, (2011); Lee *et al*, (2015). The siRNA Finder (Si-Fi) software (http://labtools.ipk-gatersleben.de/) and small interfering RNA (siRNA) scan software were used to predict the off target gene for RNAi *CSEP0443* in *Bgh* and barley transcriptome (Aguilar *et al*, 2016; Ahmed *et al*, 2016b). *CSEP0443* was checked against the entire *Bgh* coding sequence and barley genome. Full length *CSEP0443* fragment was amplified with gene specific primers flanked by 5'-AAGGAAGTTTAA-3'on forward primer and 5'-AACCACCACCACCGT-3' on reverse primer (Table 6). The Polymerase chain reaction (PCR) set up and reactions were performed as in section 2.5.1. The PCR products were separated in 1% agarose gel and visualized under ultraviolet light before cutting out the band with a clean scalpel and cleaned with a PCR kit as in section 2.4.1. Further steps that followed including the cloning of CSEP0443 in *pCa-γbLIC* plasmid, the transformation of *Escherichia coli*, *Agrobacterium tumefaciens*, multiplication of virus in *Nicotiana*

*benthamiana*, and inoculation of barley plants with virus are exactly as described in section 2.17.

### 3.2.2 RNA extraction, RT-PCR and qPCR

Prior RNA extraction on barley, plant leaves expressing empty *pCa-γb* and *pCa-γb:CSEP0443* genes were inoculated with *Bgh* spores after observing viral symptoms indicated by photo bleaching in *pCa-γb:PDS*, mild mosaic and mild chlorosis in *pCa-γb* and *pCa-γb:CSEP0443* lines. The plants were incubated in the growth cabinet for six days. During incubation the leaf samples were collected each day, frozen in liquid nitrogen and later stored at -80$^{o}$C until processed. For assessing *Bgh* virulence on lines expressing either *pCa-γb* or *pCa-γb:CSEP0443*, number of colonies formed were counted at day six. Leaves for staining against fungal structures were also collected at day six and preceded as in section 2.18.1. During RNA extraction, 100 mg of *Arabidopsis* or barley leaves were finely ground in liquid nitrogen using mortar and pestle. The tissues were then suspended in 1 ml TRIzol® Reagent (Life technologies) and incubated for 10 minutes at room temperature. All other steps that followed are exactly as described in 2.14. For Reverse transcription (RT)-PCR, the extracted RNA was adjusted to 1.5 µg final concentration followed by cDNA synthesis. All other steps that followed including quantitative (q)PCR experimental set up are exactly as described in section 2.14. Primers used are listed in (Table 5).

### 3.2.3 Genetic construct for *in vivo* expression of CSEP0443 in *Arabidopsis*

*In vivo* expression of CSEP0443 in *Arabidopsis* was made by generating genetic construct using Golden Gate modular cloning (MoClo) (Weber *et al*, 2011; Engler *et al*, 2014). Vectors *pAGM1287*, *pICH47742*, *pAGM4723* were utilized. *pICH41744* endlinker 2,

*pICSL11024* for kanamycin resistance, *pICSL50007* for Flag tag, *pICSL12015* for Ubiquitin promoter, *UBIQ5* for ubiquitin terminator modules were additionally used. *CSEP0443* fragment amplified using primer sets in Table 4 and PCR conditions in section 2.5.1 was cut and cleaned using a PCR kit as in section 2.4.1. *CSEP0443* fragment was cloned in level 0 vector *pAGM1287* and then transferred in level 1 vector *pICH47742* ligated with ubiquitin promoter, ubiquitin terminator and a carboxyl (C) terminal flag. Finally, the two full transcription units of kanamycin resistance, *CSEP0443* and endlinker 2 were ligated in level 2 vector *pAGM4723*. The enzymes used and general steps involved in cloning are described in section 2.11.

### 3.2.4 Protein extraction from *Arabidopsis* and immunoprecipitation assay

The leaves (4 g) were harvested from 3 week-old homozygous *Arabidopsis* plant transformed with *UB10::CSEP0443-FLAG*. Leaf samples were immediately frozen in liquid nitrogen, later finely ground in liquid nitrogen before further crushed in extraction buffer described by Li *et al*, (2015) section 2.15. The tissue lysates were centrifuged at 15,800*g* for 15 minutes at 4$^{o}$C and the protein suspensions were collected.

For immunoprecipitation assay, the protein suspensions were filtered through 0.4 µM millipore filters and protein concentrations determined using the Bradford reagent (Bio-Rad). The proteins were adjusted to 350 µg final concentration using the extraction buffer. The diluted proteins were incubated appropriately with 2 µg of anti-flag antibody conjugated on agarose beads over night at 4$^{o}$C on a roller. The proteins were then washed three times with 1 ml of ice cold 1x phosphate buffered saline (PBS) each time centrifuging at 2,800*g* for 30 seconds before discarding the supernatant. The washed proteins were boiled in 1x Sodium dodecyl sulfate (SDS) loading dye containing 10% β-Mercaptoethanol at 95$^{o}$C for 5 minutes.

The proteins were then centrifuged briefly for 30 seconds in a micro-centrifuge and 20 µl of the supernatant loaded in SDS gel for western blot analysis.

### 3.2.5 SDS PAGE and western blot analysis

Sodium dodecyl sulfate-Polyacrylamide gel electrophoresis (SDS PAGE) and western blot analysis were carried out as described by Sambrook *et al*, (2012). Proteins were separated in 15% SDS PAGE in 1.5 mm glass chambers (Bio-Rad) superimposed with a stacking gel. The rest of steps are as described in section 2.16. The membrane was incubated with anti-flag antibody (1:3000) for 1 hour, followed by 3 times washing with PBS-Tween 20 (PBS-T) at 10 minutes interval, and again incubation with anti-mouse IgG HRP antibody (1:4000) for 1 hour (Table 3). The membrane was again washed 3 times in PBS-T at 10 minutes interval. Finally, the membrane was incubated with chemiluminescence solution A and solution B as in section 2.16.

### 3.2.6 *Bgh* pathogenicity assays

The assays conducted related to aniline blue staining, trypan blue staining and 3,3′-Diaminobenzidine staining were performed based on protocols described by Koch & Slusarenko, (1990); Song *et al*, (2015); Liu *et al*, (2016). The electrolyte leakage determination was based on the procedure described by Campos *et al*, (2003); Kneeshaw *et al*, (2017). The steps performed in this chapter are exactly as described in the subsections of 2.18.

### 3.2.7 Bright field and Differential interference contrast (DIC) microscopy

Visualization of *Bgh* fungal structures in barley was done by using both the bright

field and DIC microscopy. Leaf samples were covered with 20% glycerol and examined under 20x objective for bright field microscopy and 62x oil immersion objective for DIC.

### 3.2.8 Statistical analysis

For comparison of means, data was analyzed using Microsoft Excel student *t*-Test assuming unequal variances. Statistical significance was reported at either $P < 0.05$ or $P < 0.01$.

## 3.3 Results

### 3.3.1 The impact of CSEP0443 on *Bgh* virulence in the host plant barley

#### 3.3.1.1 *Bgh CSEP0443* cloned into BSMV mediated vectors and transiently transformed into barley

The BSMV vectors *pCaBS-α*, *pCaBS-β* and *pCa-γb* used were previously described by Yuan *et al*, (2011). Off-target analysis with si-Fi predicted possible silencing of *CSEP0220*. However, the prediction showed only two efficient siRNA hits compared to 28 hits for *CSEP0443*. The effector analysis conducted previously indicated that *CSEP0220*/*BghEfc*67 is expressed late during *Bgh* infection and was not detected in the haustoria at 6 day post inoculation (dpi) (Pedersen *et al*, 2012). Therefore, at early times following attempted infection only *CSEP0443* will be silenced. No possible silencing was detected in barley transcriptome using siRNA scan software. Full length *CSEP0443* was cloned into the ligation independent cloning site of the *pCa-γb* vector and transformants were confirmed by genotyping PCR and Sanger sequencing. All the vectors were individually transformed into *Agrobacterium* strain GV3101 preceded by infiltration in the abaxial leaf surface of *N. benthamiana* plants. Successfully multiplication of the virus in *N. benthamiana* was shown by mosaic like symptoms in the systemic leaves after growing the plants for a further 10 days (Figure 3-1 B-D). Non infiltrated plants remained healthy (Figure 3-1A).

**(A)** Non-infected **(B)** *pCa-γb* **(C)** *pCa-γb:PDS* **(D)** *pCa-γb:CSEP0443*

**Figure 3-1: *N. benthamiana* plants transiently transformed with BSMV-VIGS-HIGS vectors.** Prior infiltration, *Agrobacteria* carrying BSMV vectors, *pCaBS-α* and *pCaBS-β* were mixed in equal ratios with either *pCa-γb* or *pCa-γb:PDS* or *pCa-γb:CSEP0443* and infiltrated in the abaxial leaf surface. The infiltrated plants were incubated for 10 days in the *N. bethamiana* growth conditions to allow multiplication of virus. (A) Plants not infiltrated with any genetic construct. (B) Plants infiltrated with *Agrobacterium* carrying an empty vector. (C) Plants infiltrated with *Agrobacterium* carrying vector for *PDS*. (D) Plants infiltrated with *Agrobacterium* carrying a vector for *CSEP0443*. Plants are representative of six independent *N. benthamiana Agrobacterium* infiltrations. Scale bars represent 1 centimetre.

To infect the barley plants with BSMV, extracts from previously infiltrated *N. benthamiana* leaves were rubbed on the barley plants and the plants mantained in appropliate growth conditions. Growth of the virus in the inoculated barley leaves were indicated by a photobleaching phenotype and mosaic symptoms in the positive control experiments, as silencing the *PDS* prevents carotenoid synthesis (Figure 3-2 C). The empty vector *pCa-γb* and *pCa-γb*:*CSEP0443* displayed mild mosaic symptoms and mild leaf yellowing all indicative of successful viral colonisation (Figure 3-2 B and D), while the non-inoculated leaves remained with a green phenotype and healthy (Figure 3-2 A). Futher the presence of the viral particles were confirmed by RT-PCR using primers that bind the ligation independent cloning site of the γ particles (Figure 3-2 lower panel).

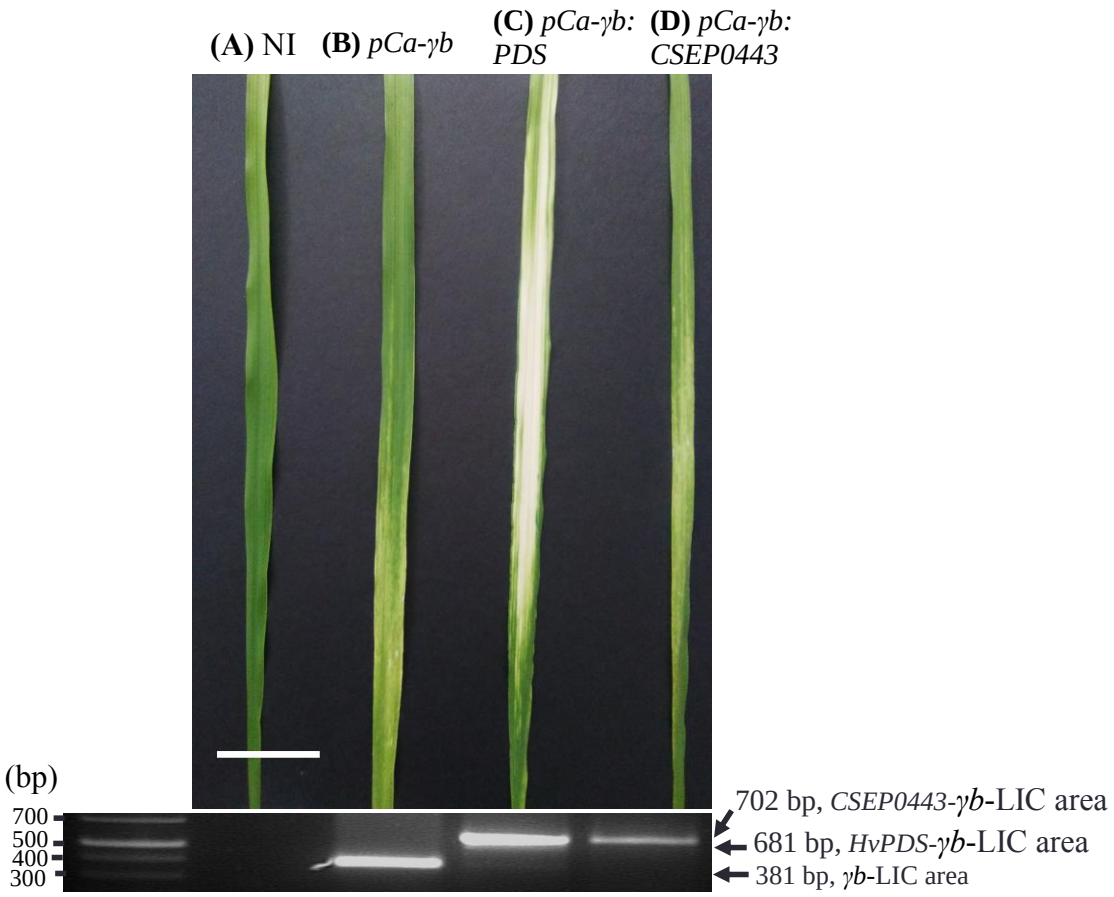


**Figure 3-2: BSMV vectors inoculated on barley leaves.** Inoculated barley leaves manifest symptoms of viral infection indicating successful viral colonisation of leaf tissues. Inoculation of the barley leaves with the virus was done by surface rubbing the 3rd and 4th leaves with leaf tissue extracts from *N. benthamiana* previously infected with BSMV. The plants were incubated in barley growth conditions for 12-14 days. (A) Barley non-infected (NI) with virus maintain a green and healthy phenotype. (B) Barley infected with virus carrying empty vector display yellow and mosaic like appearance. (C) Barley leaf infected with virus carrying *PDS* display photobleaching. (D) Barley leaf infected with virus carrying *CSEP0443* display yellow and mosaic like appearance. Scale bar represent 1 centimetre. NI refers to non infected. The presence of viral particles are further confirmed by RT-PCR in the lower panel.

### 3.3.1.2 *BghCSEP0443* transcript abundance reduced in barley plants transiently expressing *pCa-γb:CSEP0443*

The barley leaves inoculated with BSMV vectors *pCa-γb* (control) or *pCa-γb:CSEP0443* (test) were inoculated with *Bgh* spores and incubated for 1, 2, 3, 4, 5 and 6 days. Leaf samples were collected each day post fungal inoculation. RNA was extracted

followed by complementary deoxyribonucleic acid (cDNA) synthesis and subjected to RT-PCR. The expression levels of *CSEP0443* were completely undetectable between day 1 and 2. The transcripts were mildly detectable on day 3, increased gradually through day 4 and 5 and declined again on day 6 (Figure 3-3 A). In comparison to the plants expressing only the *pCaγ-b* viral particles, the *CSEP0443* transcripts were detectable from day 1 increased gradually through day 2, 3, and reached maximum on day 4. Transcript level started declining from day 5 through day 6 (Figure 3-3 A). By using ImageJ software the relative quantity of *CSEP0443* transcript levels was determined and expressed as percentanges (Figure 3-3 C).

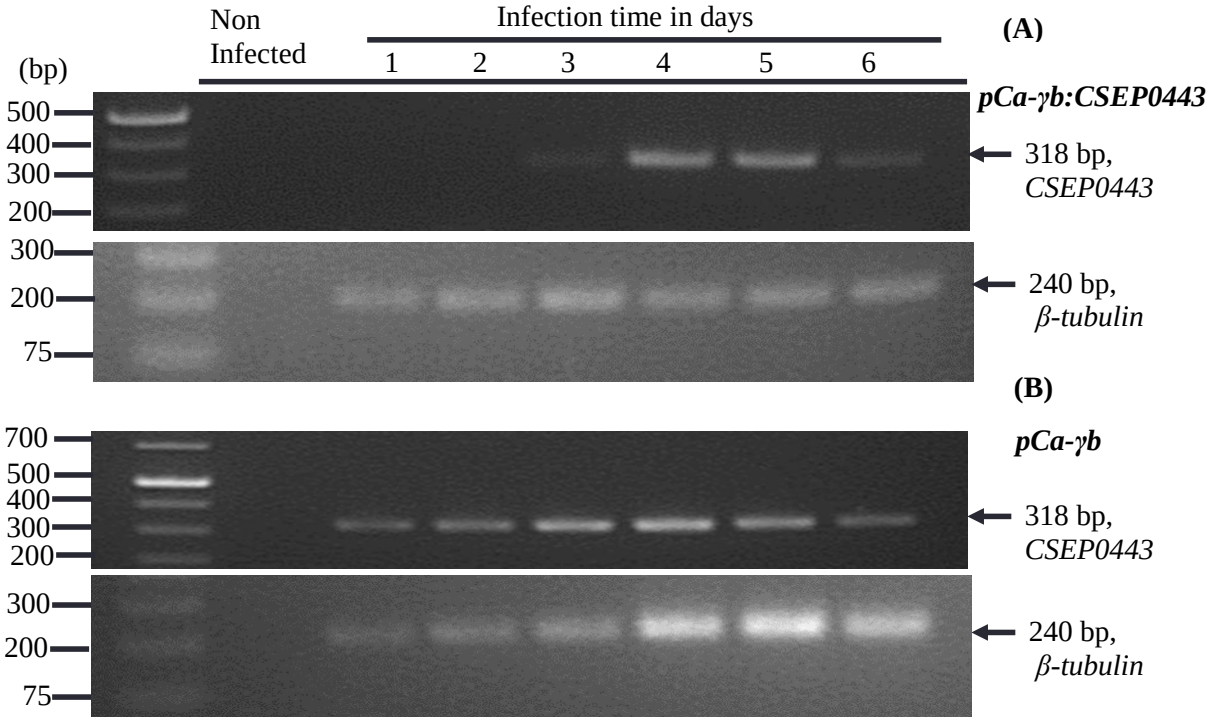

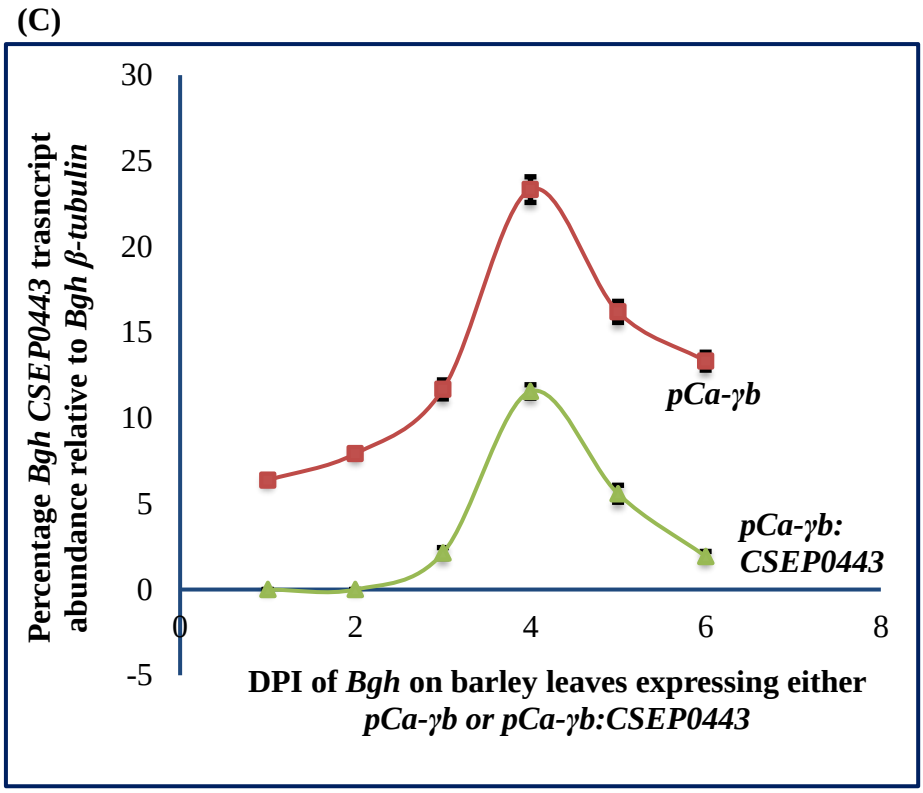


**Figure 3-3: Reduction in transcript levels of *CSEP0443* in barley plants transiently expressing *CSEP0443*.** Barley plants previouly infected with BSMV were inoculated with *Bgh* spores on the 5th and 6th leaves and the plants incubated for 1-6 days. RNA was extracted from leaf samples collected each day post *Bgh* inoculation and subjected to RT-PCR relative expression analysis. (A) RT-PCR analysis of *CSEP0443* expression in plant lines of *CSEP0443* silencing. Decline in *CSEP0443* expression detected. *Bgh β-tubulin* used as a reference. (B) RT-PCR analysis of *CSEP0443* expression in lines having no *CSEP0443* silencing. *CSEP0443* increased gradually from day 1 to day 4, then started to decline. *Bgh β-tubulin* used as a reference. (C) The line graphs indicate the relative quantification of the *CSEP0443* expression in both silencing and non silencing conditions, determine by ImageJ software on the gel bands. Error bars represent mean ± standard error. *n* = three biological replicates of independent experiments set up and conducted at the same time. DPI refers to day post inoculation.

Further the synthesised cDNA from *pCa-γb* control or *pCa-γb*:*CSEP0443 Bgh* infected plants was analysed by qPCR. Transcript quantification was accomplished with SYBR Green I master. The transcript abundance in *CSEP0443* knock-down plants was considerably lower across all the 6 days. At day 4 where *CSEP0443* is expected to have the

highest expression level, the transcript was down-regulated by 43% compared to the plants having no *CSEP0443* silencing effect (Figure 3-4).

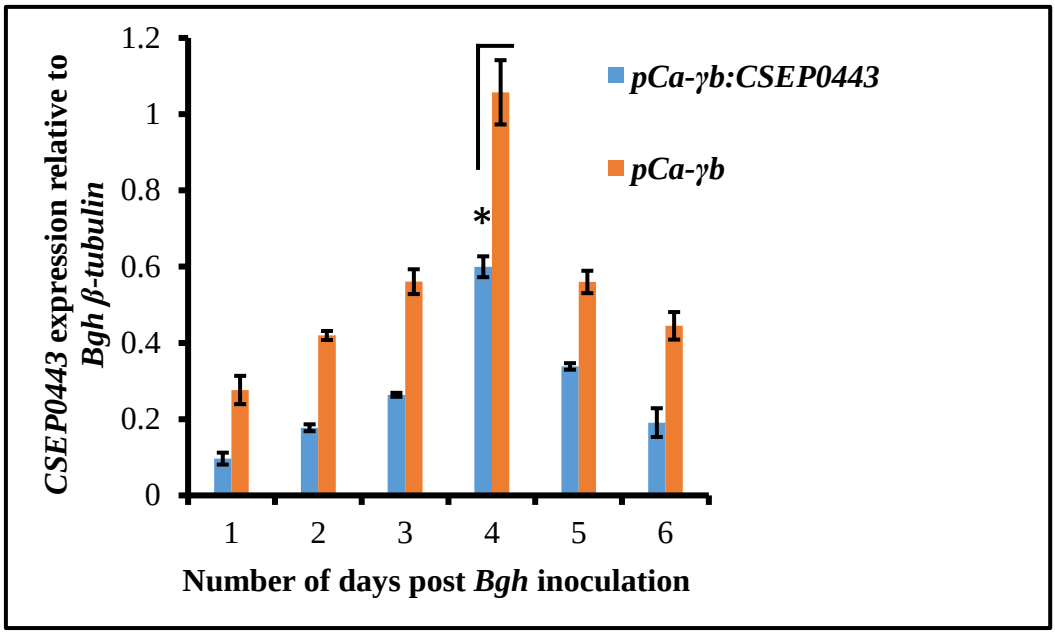


**Figure 3-4: qPCR of the transcript abundance of *CSEP0443* after knock-down.** Barley plants previously infected with BSMV carrying empty vector and *CSEP0443* target were inoculated with *Bgh* spores on the 5th and 6th leaves. The plants were incubated for 1-6 dpi and samples collected each day. cDNA was synthesized from RNA extracted from infected leaves and subjected to qPCR analysis. *CSEP0443* expression was normalised relative to *Bgh β-tubulin*. Low transcript levels of *CSEP0443* was detected in plants where knock-down constructs are delivered (green bars). Transcript level of *CSEP0443* increased gradually from day 1 to day 4 in plant lines where *CSEP0443* is not targeted (orange bar). The results are from two biological replicates of independent experiments set up and conducted at the same time. Error bars represent mean ± standard error. Asterisks indicate significant differences when *pCa-γb*:*CSEP0443* and *pCa-γb* are compared. *t*-test, $P < 0.05$. DPI refers to day post inoculation.

### 3.3.1.3 Knock-down of *CSEP0443* reduced *Bgh* virulence

Barley plants expressing either *pCa-γb* or *pCa-γb*:*CSEP0443* were analysed for *Bgh* growth at the sixth day of incubation. The pustule numbers of *Bgh* in *CSEP0443* silenced lines were reduced by 61% compared to the lines carrying no silencing effect (empty vector *pCa-γb*) (Figure 3-5 A and B). Plant lines expressing *pCa-γb*:*PDS* for silencing *PDS* gene

were included as positive control. The plants show photo-bleaching effect but were not inoculated with *Bgh* (Figure 3-5 A). Further the leaves from *pCa-γb* and *pCa-γb*:*CSEP0443* lines were stained to detect internal fungal structures using aniline blue in lactophenol solution. The plants transientlly expressing *pCa-γb*:*CSEP0443* for *CSEP0443* silencing effect had low number of haustoria (Figure 3-5 D and E), reduced by 33% as compared to the plants expressing empty vector *pCa-γb* not possessing *CSEP0443* silencing effect (Figure 3-5 C and E).

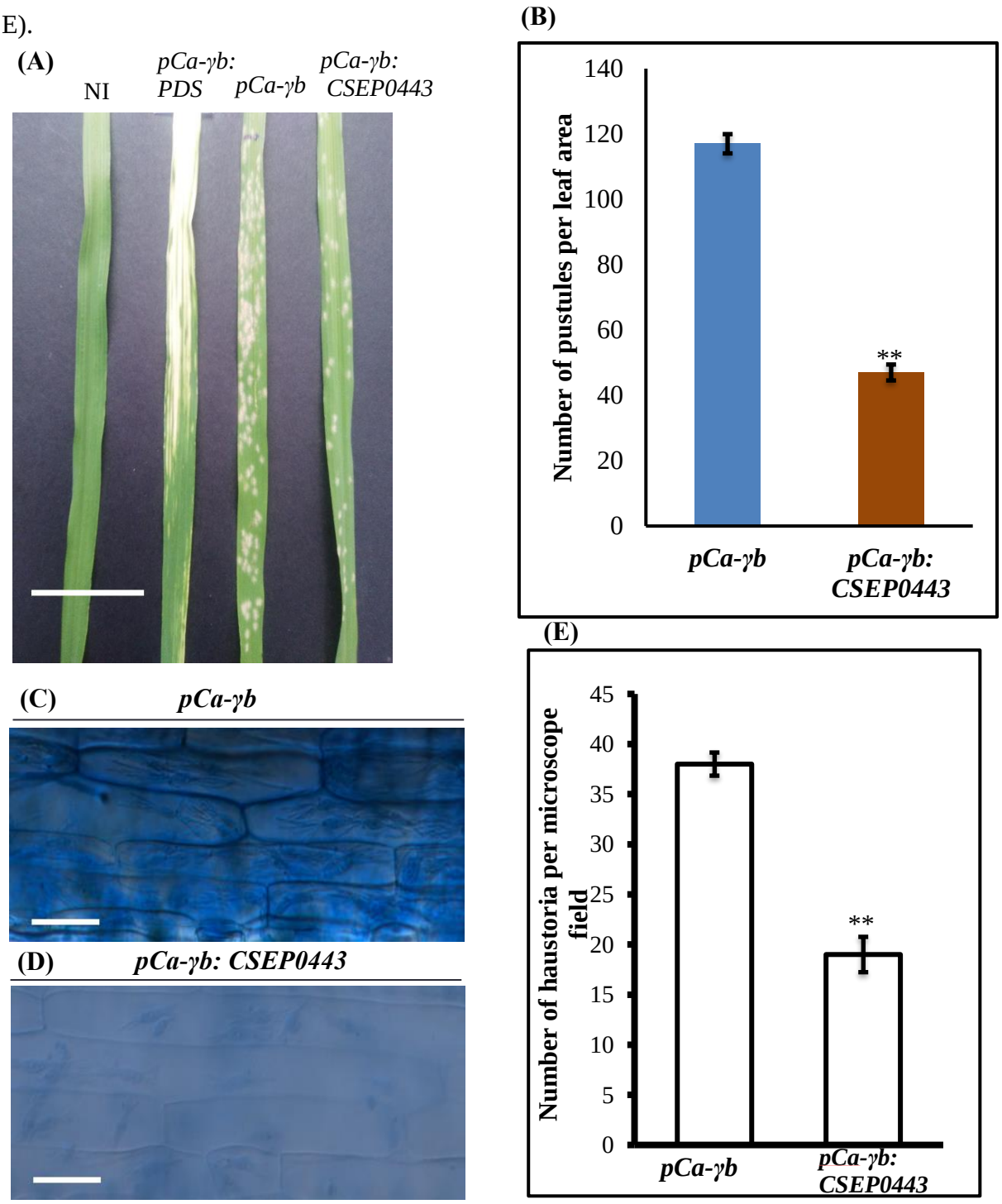

**Figure 3-5: Barley plants transiently expressing *pCa-γb:CSEP0443* show reduction in *Bgh* fungal growth.** Barley plants previously infected with BSMV carrying empty plasmid and *CSEP0443* targeted silencing were infected with *Bgh* spores on the 5th and 6th leaves. The plants were incubated for 6 days and *Bgh* virulence assessed by counting the number of colonies that formed. Barley plants with targeted *PDS* silencing were included as positive control for viral multiplication and translocation. (A) Lane 1 present non *Bgh* infected barley plant leaf. Lane 2 present barley plant leaf showing *PDS* silencing but not inoculated with *Bgh*. Lane 3 present barley plant leaf expressing empty vector and inoculated with *Bgh*. It shows increased number of pustules. Lane 4 present barley plant leaf with targetd *CSEP0443* silencing inoculated with *Bgh*. It shows low pustle numbers. Scale bar represent 1 centimetre. NI refers to non infected. (B) Histogram generated from the quantification of *Bgh* colonies in *CSEP0443* non silenced and silenced plant lines. Error bars represent average number of pustules from 9 leaves at day 6 post *Bgh* inoculation for each vector ± standard error, *t*-test **, $P < 0.01$. (C and D) Barley leaves stained for fungal structures. Initially the 5th and 6th leaves of barley plants carrying empty vector and targeted *CSEP0443* were infected with *Bgh*. The plants were incubated for 6 days. Leaf samples were collected and cleared in lactophenol before stained with lactophenol-aniline blue solution and examined on the miscroscope. (C) The leaves from barley plants carrying empty vector show more haustoria formation. (D) The leaves from barley plants with targeted *CSEP0443* silencing show low haustoria formation. Scale bars represent 175 μm. (E) Histogram for quantification of the haustoria from 45 microscopic fieds, 5 fields from each of the 9 leaves. Error bars represent mean ± standard error, *t*-test **, $P < 0.01$. *n* = two biological replicates.

### 3.3.2 The impact of CSEP0443 on *Bgh* virulence in the non-host plant *Arabidopsis*

#### 3.3.2.1 Expression of CSEP0443 in *Arabidopsis*

The mature *CSEP0443* lacking the signal peptide was cloned with a C- terminal *FLAG* tag into plant expression vectors using Golden Gate Modular cloning. To test whether the construct generated was able to express CSEP0443, the construct was initially transiently transformed in 3 weeks-old *N. benthamiana*. After incubation of the plants for 2 days the proteins were extracted and subjected to immunoprecipitation with anti-flag antibody conjugated on beads. Immunoblotting with anti-flag antibody detected CSEP0443. Proteins immunoprecipitated from *N. benthamiana* transformed with empty vector were used as negative control (Figure 3-6).

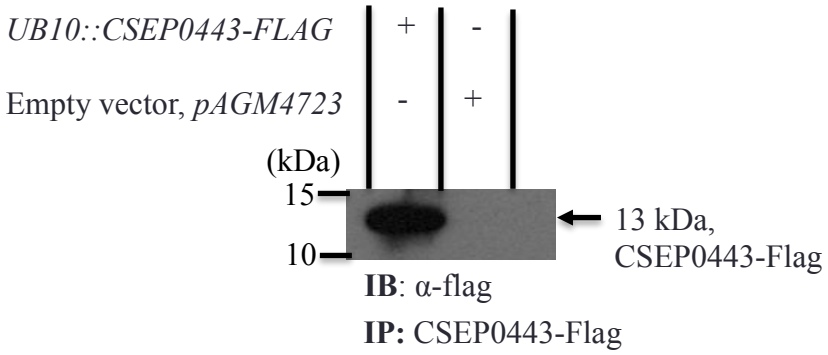


**Figure 3-6: Transient expression of CSEP0443 detected in *N. benthamiana*.** The *N. benthamiana* leaves were infiltrated with *Agrobacterium* carrying a vector for the expression of *UB10::CSEP0443-FLAG* and incubated for 2 days. Protein was extracted from infiltrated leaves and immunoprecipitated with anti-flag antibody. Then followed by immunoblotting with anti-flag antibody. *N. benthamiana* transformed with empty vector used as a negative control.

After confirming the ability of the construct to express CSEP0443, the construct was transformed into *Arabidopsis* Col-0 to generate stable lines. Transformation was accomplished by the floral dipping using *Agrobacterium* GV3101 strain. Following three levels of selection, homozygous *Arabidopsis* lines constitutively expressing the *CSEP0443* under the *UBIQ* promoter were regenerated. The plants displayed a typical wild-type Col-0 growth phenotype at all stages of development (Figure 3-7).

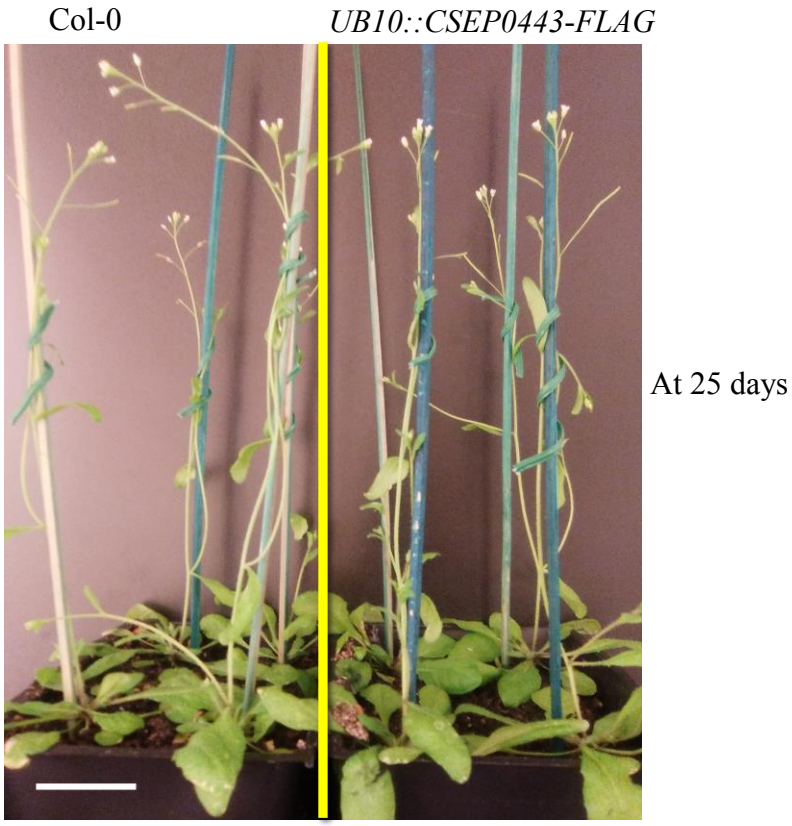


**Figure 3-7: *Arabidopsis* lines constitutively expressing *CSEP0443*.** The *UB10::CSEP0443-FLAG* was transformed in *Arabidopsis* Col-0 by floral dipping in *Agrobacterium* suspension to generate stable homozygous transgenic plants**.** Plants display wild-type Col-0 growth morphology. The image is a representative of four independent lines. Scale bar represent 3 centimetres.

To test whether the stable transformants were expressing CSEP0443, initially RNA was extracted from 3 weeks-old plants. cDNA was synthesised and subjected to RT-PCR. Four out of six homozygous lines progressed had the *CSEP0443* transcript detected (Figure 3-8 A). Following transcript detection total protein was extracted from all the plant lines in non-denaturing buffer and subjected to immunoprecipitation with anti-flag antibody conjugated on agarose beads. Detection of the protein was accomplished by immunoblotting with anti-flag antibody and CSEP0443 was detected in all the four lines at the same levels (Figure 3-8 B).

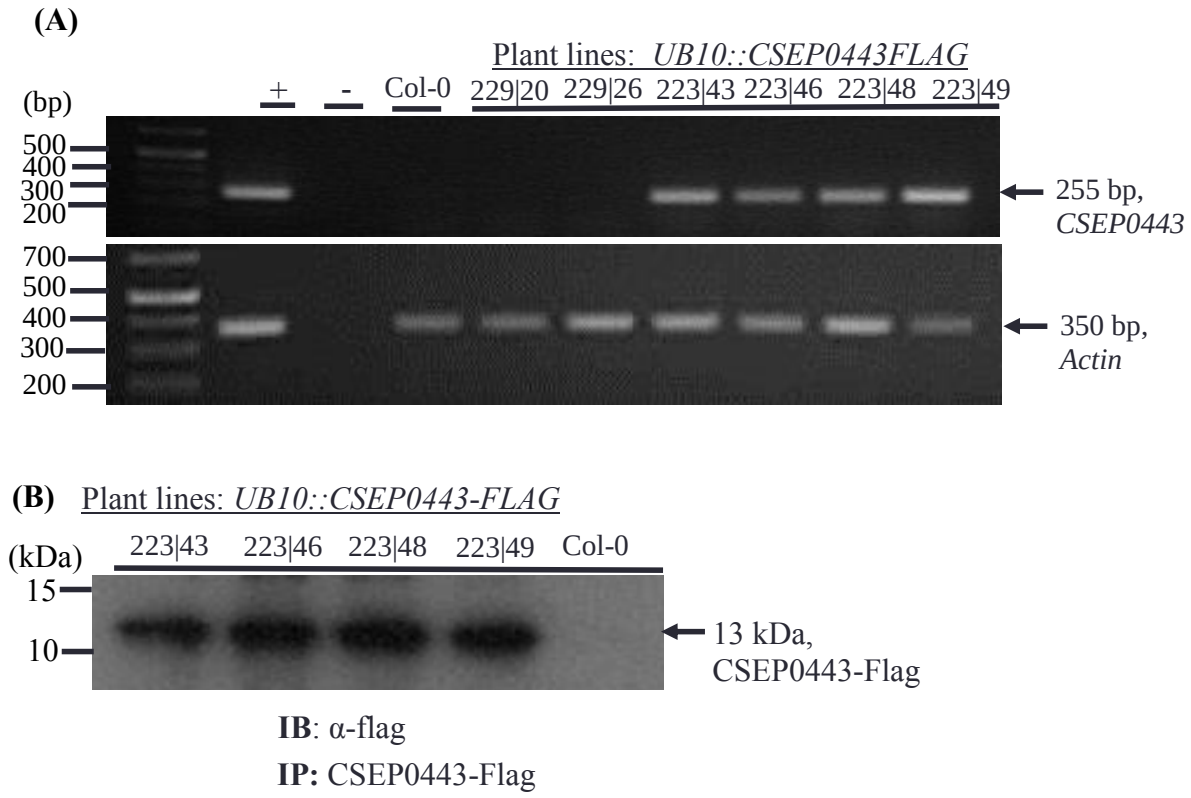


**Figure 3-8: Expression of CSEP0443 detected in *Arabidopsis*.** (A) RT-PCR gel image for the relative *CSEP0443* expression level in *Arabiposis* Col-0. RNA was extracted using TRIzol reagent from the generated homozygous lines followed by cDNA sythesis. *CSEP0443* transcript was detected in all the four lines. *Arabidopsis Actin* used as a reference gene. (B) Proteins were extracted in a non-homozygous buffer from homozygous lines and immunoprecipitated with anti-flag antibody. Detection of the 13 kDa, CSEP0443-Flag was perfomed by immunoblotting with anti-flag antibody. Col-0 used as a negative control.

### 3.3.2.2 The expression of CSEP0443 in *Arabidopsis* enhances the virulence of *Bgh*

To determine the consequence of CSEP0443 expression in *Arabidopsis*, plant lines already confirmed to be expressing this fungal protein and wild-type Col-0 were challenged with *Bgh*. Plants were incubated for 3 days and later inoculated leaves stained for fungal structures using aniline blue in lactophenol solution. The leaves were analysed by employing bright field and DIC microscopy. Successful penetrations were measured by counting the number of spores that successfully formed atleast primary haustorium and expressed as percentages (Figure 3-9 A). Plants expressing CSEP0443 had increased *Bgh* penetration

events (69%) (Figure 3-9 B), however few were able to form surface hyphae (data not shown).

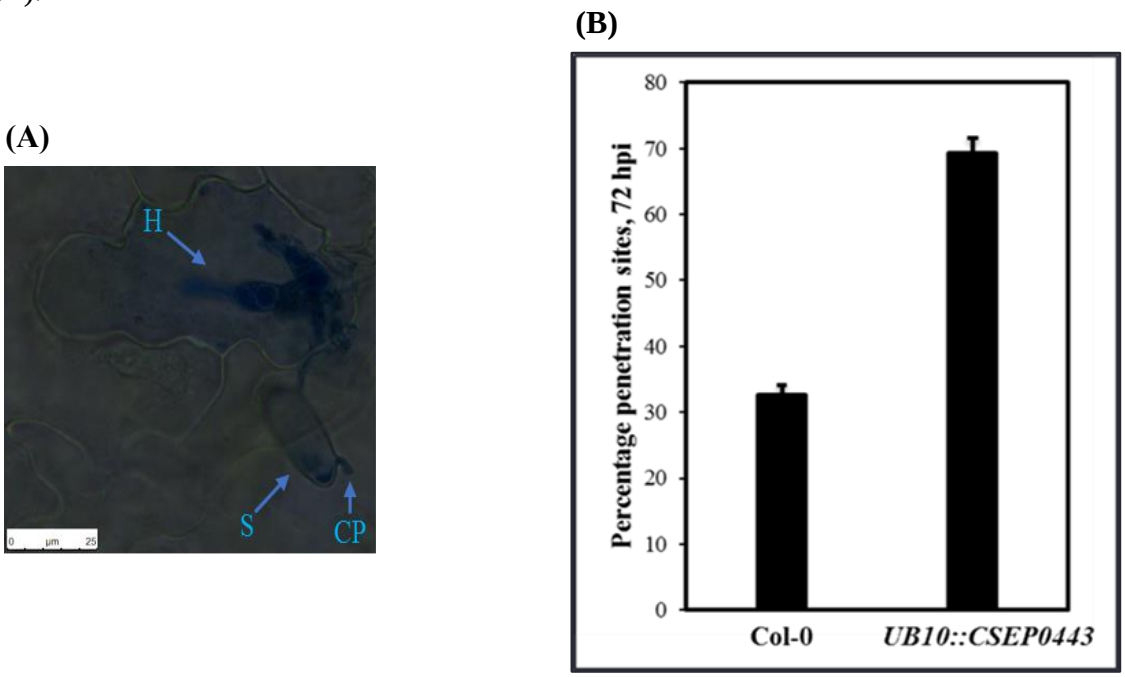


**Figure 3-9: The expression of CSEP0443 in *Arabidopsis* increases the vilurence of *Bgh***. Wlid type Col-0 and *UB10::CSEP0443* in Col-0 background were inoculated with *Bgh* and incubated for 3 days. Infected leaves were cleared in lactophenol solution and stained with lactophenol-aniline blue solution followed by examination for fungal structures on the microscope. *Bgh* penetration rates was scored by counting the number of conidia that formed the haustoria. (A) Image display a conidum with formed haustora inside the cell, S refers to spore, CP refers to cuticular peg, H refers to haustoria. (D) Histogram shows the quantification of *Bgh* peneration rates on both the wild-type and Col-0 expressing *CSEP0443*. Error bars represent mean ± standard errors. The means are obtained after three indipendent biological replications. Asterisks indicate significant difference from Col-0, *t*- test, $P < 0.01$.

### 3.3.2.3 Expression of CSEP0443 compromises callose deposition upon *Bgh* infection in *Arabidopsis*

*Arabidopsis* plants constitutively expressing CSEP0443 and wild-type Col-0 were challenged with *Bgh*. The plants were incubated for 3 days and the leaves cleared in lactophenol solution followed by staining with aniline blue. Examination under the epifluorescence microscope detected callose deposition shown by blue fluorescence (Figure 3-10 B and D), that was later relatively quantified using ImageJ software and expressed as

percentages. Plants expressing CSEP0443 show a (23%) decline in callose deposition (Figure 3-10 D and E purple bar), as compared to the wild-type (77%) (Figure 3-10 B and E green bar).

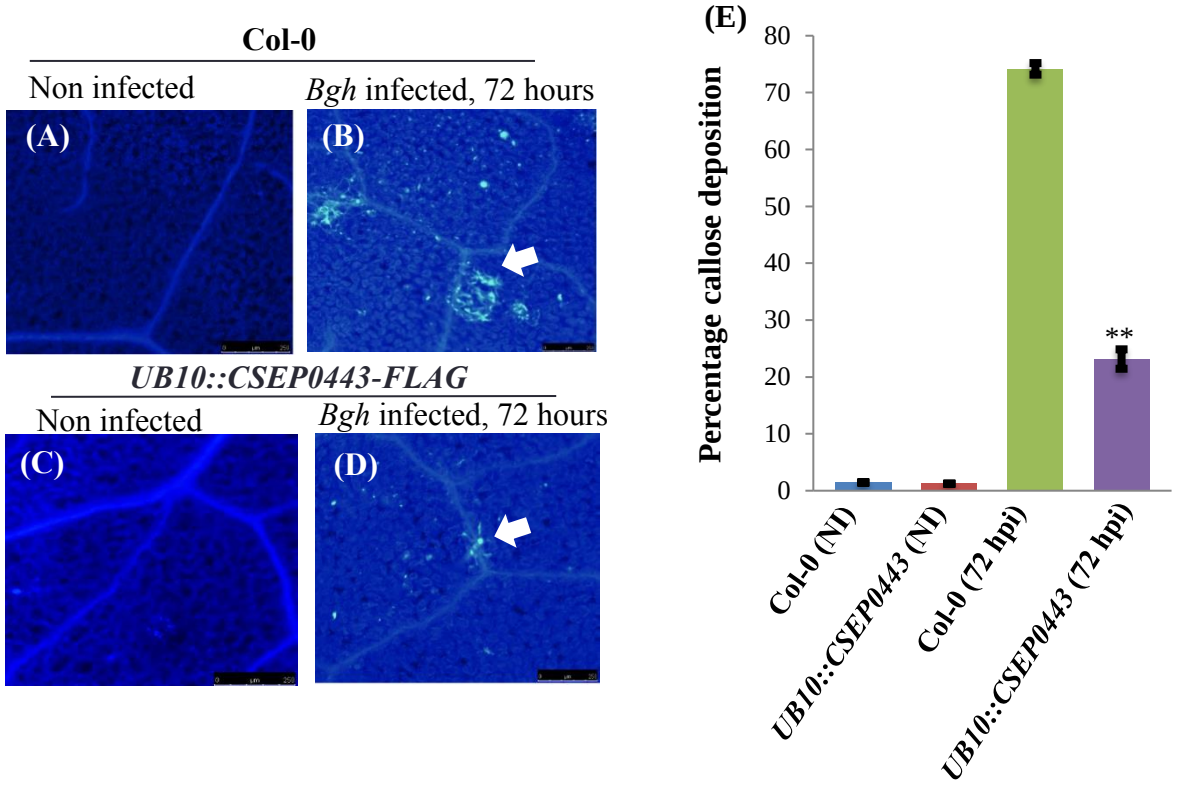


**Figure 3-10: Reduced callose deposition in plants expressing CSEP0443.** Wild-type Col-0 and Col-0 expressing *UB10::CSEP0443-FLAG* were infected with *Bgh* and incubated for 3 days. Infected leaves were collected, cleared in lactophenol solution and stained with aniline blue dissolved in di-potassium hydrogen phosphate solution. The leaves were examined for callose deposition by observing for blue fluorescence using epifluorescence microscope set at 365 nm and 420 nm for excitation and emission respectively. (A) Wild-type Col-0, not inoculated with *Bgh*. (B) Wild-type Col-0, inoculated with *Bgh*. (C) Col-0 expressing CSEP0443, not inoculated with *Bgh*. (D) Col-0 expressing CSEP0443 inoculated with *Bgh*. (E) Histogram shows the relative quantification of callose using ImageJ software. Error bars represent mean ± standard error. Asterisks indicate significant difference in terms of callose deposition from Col-0, *t*-test $P < 0.01$. NI refers to non infected, hpi refers to hours post inoculation. Arrows show callose deposition.

### 3.3.2.4 *Arabidopsis* expressing CSEP0443 have increased ROS production upon *Bgh* infection

To investigate whether the expression of CSEP0443 provokes the production of reactive oxygen species (ROS) after *Bgh* challenge, plants expressing CSEP0443 were utilized. *Arabidopsis* plants expressing CSEP0443 and wild-type Col-0 were inoculated with *Bgh* spores. The plants were further maintained for 3 days in the growth cabinet. The inoculated leaves were collected, stained in DAB stain and cleared in ethanol. The leaves were then observed under lower power fields. ROS production was detected shown as brown precipitate, later relatively quantified using ImageJ software and expressed in percentages. Plants expressing CSEP0443 display increased ROS production to (65%) upon *Bgh* challenge compared to wild-type (Figure 3-11 B, D and E). The production of ROS was induced by *Bgh* exposure as low ROS detected in absence of *Bgh* (Figure 3-11 A, C and E).

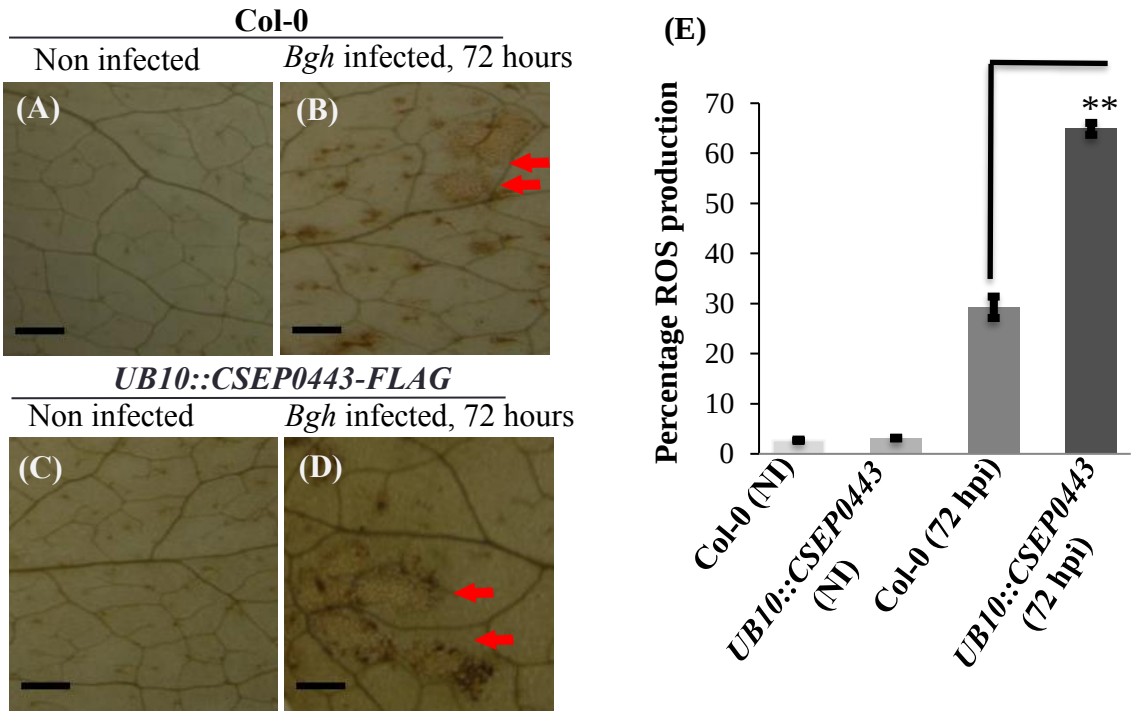


**Figure 3-11: The expression of CSEP0443 is associated with increased ROS upon *Bgh* challenge.** Plants, wild-type Col-0 and Col-0 expressing *UB10::CSEP0443-FLAG* were inoculated with *Bgh* and incubated for 72 hours. Infected leaves were collected and submerged in DAB solution, vacuum infiltrated and then incubated in dark for an

overnight. The leaves were cleared in ethanol and examined under the bright field microscope. ROS production was assessed by examining the leaves for brown precipitate deposition formed by the reaction of DAB with ROS. (A) Col-0 non infected with *Bgh*. (B) Col-0 infected with *Bgh*. (C) Col-0 expressing CSEP0443, but not infected with *Bgh*. (D) Col-0 expressing CSEP0443 infected with *Bgh*. Scale bars represent 160 µm. (E) Histogram showing the relative quantification of ROS using ImageJ software. Error bars represent mean ± standard errors. Means obtained after three independent biological replications. Asterisks indicate significant differences in terms of ROS production when compared to Col-0, *t*-test $P < 0.01$. Arrows show brown precipitate of DAB staining. NI refers to non infected, hpi refers to hour post inoculation.

#### 3.3.2.5 The expression of CSEP0443 increases cell death upon *Bgh* infection in *Arabidopsis*

Previous studies have revealed that despite increased *Bgh* penetration rates in *pen1-1* mutants, successful growth of the fungus was inhibited by the cells undergoing PCD (Collins *et al*, 2003). To unveil whether plants expressing CSEP0443 have increased cell death upon *Bgh* challenge, *Arabidopsis* lines having CSEP0443 expression were utilized. The plants were surface inoculated with *Bgh* spores and incubated for 72 hours. The infected leaves were collected and boiled in lactophenol-trypan blue. Stained leaves were cleared in chloral hydrate solution and examined under low power objective. Cell death shown by blue precipitate deposits was detected (Figure 3-12 B and D), later relatively quantified using ImageJ software and expressed in percentages. Plants expressing CSEP0443 display increased cell death to (76%) upon *Bgh* infection as compared to the wild-type (Figure 3-12 B, D and E). The induction of cell death seems to be induced by *Bgh* challenge as low cell death detected (<2%) in non *Bgh* challenged plants (Figure 3-12 A, C and E).

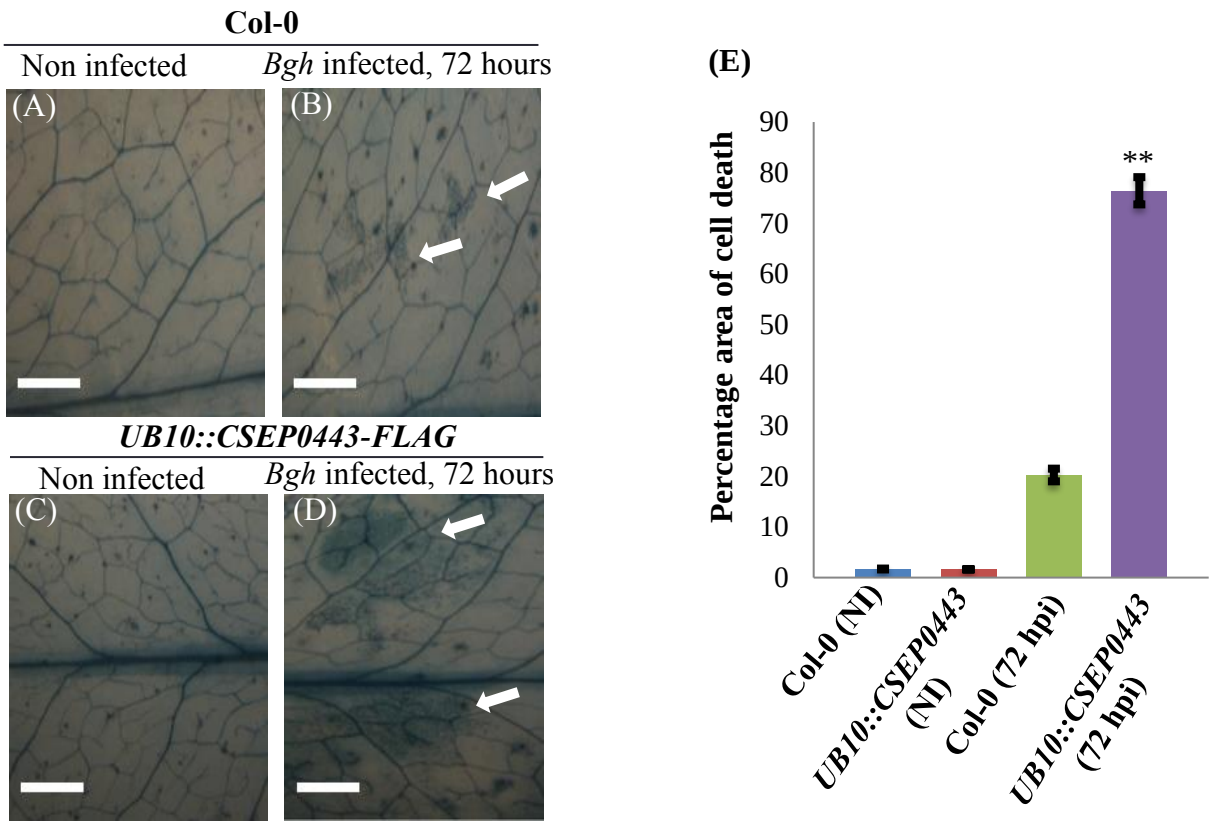


**Figure 3-12: *Arabidopsis* expressing CSEP0443 display increased cell death upon *Bgh* infection.** Plants wild-type Col-0 and Col-0 expressing *UB10::CSEP0443-FLAG* were inoculated with *Bgh* and incubated for 72 hours. Infected leaves were collected, submerged in lactophenol solution containing trypan blue stain and boiled for 2 minutes at $95^0$C. The leaves were then cleared in several changes of chloral hydrate solution and examined by bright field microscopy. Cell death examined by assessing the formation of blue precipitate. (A) Wild-type Col-0, non infected with *Bgh*. (B) Wild-type Col-0 infected with *Bgh*. (C) Plants expressing CSEP0443 non infected with *Bgh*. (D) Plants expressing CSEP0443 infected with *Bgh*. Scale bars represent 200 µm. (E) Histogram showing the relative quantification of cell death using ImageJ software. Error bars represent mean ± standard error. Means obtained after three independent biological replications. Asterisks indicate significance difference with respect to Col-0. *t*-test, $P < 0.01$. Arrows show blue precipitate staining of trypan blue staining. NI refers to non infected, hpi refers to hour post inoculation.

### 3.3.2.6 High electrolyte leakage detected upon *Bgh* infection in *Arabidopsis* expressing CSEP0443

As electrolyte leakage is one of the events associated with cell death, I investigated if plants expressing CSEP0443 showed changes in the extent of this immune response. Three week old *Arabidopsis* plants were inoculated with *Bgh* spores and incubated for either 1, 2, 3

or 4 days. Leaf discs were collected from the inoculated leaves and thoroughly rinsed in water. The leaf discs were then incubated in water and measurements were taken using the conductivity meter at 0, 6, and 14 hours. Finally, percentage electrolyte leakage was obtained by reference to the total leakage (see materials and methods). Plants expressing CSEP0443 manifested increased electrolyte leakage compared to wild-type. The electrolyte leakage in both the wild-type and the CSEP0443 expressing transgenics increased with the increase in the number of days of infection (Figure 3-13).

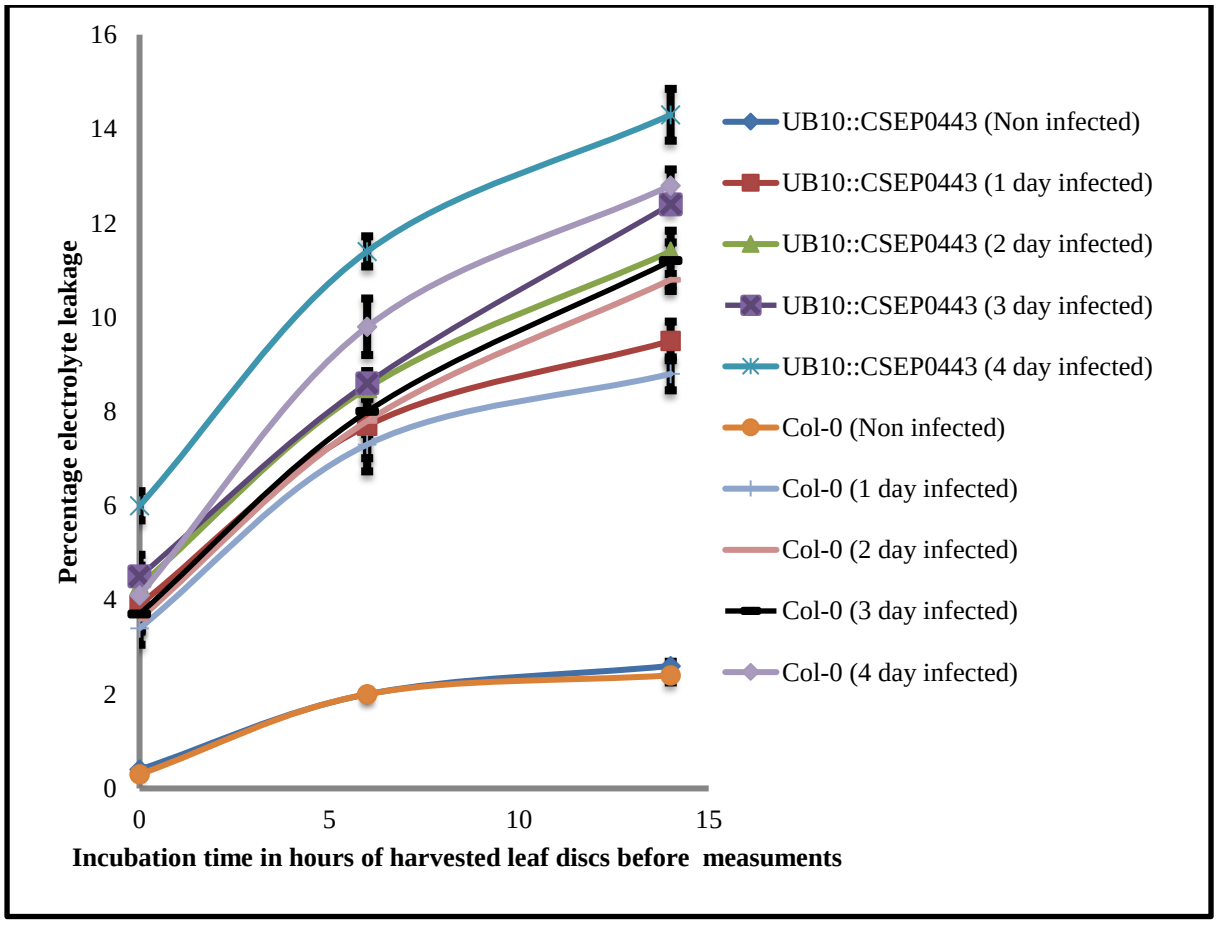


**Figure 3-13: High electrolyte leakage detected in plants expressing CSEP0443.** Plants, wild-type Col-0 and Col-0 expressing *UB10::CSEP0443-FLAG* were inoculated with *Bgh* and incubated for 1 to 6 days. Ten leaf discs were punctured from leaves corresponding to each day post inoculation and rinsed in water. In parallel leaf discs were also punctured out from non infected plants. The leaf discs were floated on water and kept under light. Measurements were conducted immediately, after 6 hours and after 14 hours respectively using a conductivity meter. Total electrolyte leakage was then obtained by boiling the leaves and then measurements taken. Electrolyte leakage

was expressed as a percentage of the total. *n* = three biological replicates. Error bars represent mean ± standard error.

### 3.4 Discussion

The *Bgh* genome currently is predicted to encode over 700 Candidates for secreted effector proteins (CSEPs) based on the presence of a signal peptide at the N-terminus of the protein, the absence of a transmembrane domain and their presence being limited to the Erysiphales (Spanu *et al*, 2010; Pedersen *et al*, 2012; Frantzeskakis *et al*, 2018). Many of these CSEPs are secreted from haustoria during the pathogen-host interactions and some are thought to overcome the host pathogen associated molecular patterns (PAMP) and Resistance (*R)*-mediated resistance or reprogramme host cells enabling pathogenesis (Pedersen *et al*, 2012; Chaudhari *et al*, 2014). To date relatively few effectors have been investigated to determine their possible mechanism of action and their consequential targets (Schmidt *et al*, 2014; Aguilar *et al*, 2016; Ahmed *et al*, 2015b, 2015a). The slow progress in uncovering the function of effectors from *Bgh* has been attributed to the difficulty of *Bgh* transformation, and also the recalcitrant of *Bgh* to grow on selective media (Nowara *et al*, 2010; Spanu & Panstruga, 2012; Ahmed *et al*, 2015). HIGS based on the mechanism of Ribonucleic acid interference (RNAi) where the barley plant is transiently transformed by constructs carrying target pathogen genes is becoming the easiest and most rapid alternative to study *Bgh* effectors (Yin *et al*, 2011; Knip *et al*, 2014).

*Bgh*Efc1/CSEP0443 is expressed during the early stages of fungal infection suggesting a pivotal role in aiding pathogenesis (Godfrey *et al*, 2010). In barley, my data indicates that knockdown of *CSEP0443* reduced *Bgh* abundance by 61%. Additionally, the number of haustoria were reduced to 33% of that in *CSEP0443* silenced plants. The findings imply that CSEP0443 is important in *Bgh* virulence. However, the potential target(s) remain to be disclosed, like most effectors CSEP0443 lacks conserved domains which makes it

difficult to postulate the likely mechanism of action. How the silencing of only one CSEP could reduce haustoria abundance by that magnitude is a matter of debate (Thordal-Christensen *et al*, 2018), but many effectors have been shown to compromise haustorial development by 30-70% (Zhang *et al*, 2012; Pliego *et al*, 2013; Ahmed *et al*, 2015a; Aguilar *et al*, 2016; Ahmed *et al*, 2016b). The small heat shock proteins (Hsp) are involved in stabilizing host defence proteins through their chaperone activity. Silencing of *CSEP0105* and *CSEP016* reduced haustoria formation by 40%, these effectors are known to interact with barley small heat shock proteins Hsp16.9 and Hsp17.5 (Ahmed *et al*, 2015a). Further silencing of *CSEP0055* also down-regulated haustoria formation by 40%. The effector interacts with Pathogenesis related protein (PR)1 and PR17 host defence proteins. It is postulated that these proteases may digest the pathogen surface proteins likely including directly the secreted effectors and pathogen responds by producing CSEP0055 to inhibit their activity. By inhibiting the proteases, CSEP0055 paves a way for the action of other effectors secreted sequentially that would otherwise be targeted and degraded (Zhang *et al*, 2012). The importance of CSEP0443 to *Bgh* virulence suggests it may function in a conceptually similar fashion, albeit targeting different host proteins. My data suggests CSEP0443 joins a list of over 48 *Bgh* effectors that has been shown by HIGS to be vital in *Bgh* aggressiveness (Zhang *et al*, 2012; Pliego *et al*, 2013; Schmidt *et al*, 2014; Ahmed *et al*, 2015a; Aguilar *et al*, 2016).

Having elucidated the relevance of CSEP0443 in *Bgh* virulence in the host plants, I investigated its possible role in the non-host plant, *Arabidopsis*. CSEP0443 was constitutively expressed in *Arabidopsis* Col-0 ecotype. The plants exhibited a phenotype similar to the wild-type without any cell death like symptoms (Terpe, 2003; Kim *et al*, 2016). The stable constitutive expression of the Oomycete pathogen *Phytophthora sojae* Crinkler or crinkling- and necrosis-inducing protein (CRN) effector (PsCRN 108) in *Arabidopsis* also did not induce aberrant growth effects (Song *et al*, 2015). The inoculation of *Bgh* on plants

expressing CSEP0443 increased host epidermal penetration rates.

To get further insight I checked the callose deposition, callose is a polysaccharide in the form of β-1,3-glucan deposited at the site of attempted fungal penetration. The deposited callose reinforces the plant cell wall at sites of attempted penetration, contributing to papilla formation (Chen & Kim, 2009). Callose deposition was greatly reduced in plants expressing CSEP0443 as compared to the wild-type. The decline in strength of the wall at the penetration site could favour enhanced penetration rates. Indeed, the expression of effectors including Puccinia striiformis effector candidate 6 (PEC6) and PsCRN108 also compromised callose deposition and promoted pathogen virulence (Song *et al*, 2015; Liu *et al*, 2016). Therefore, my data suggests that CSEP0443 might target enzyme function related to callose deposition or regulatory circuits that control the expression of these enzymes.

Further plants expressing CSEP0443 were assessed for reactive oxygen species (ROS) production following *Bgh* infection. Plants expressing CSEP0443 have increased ROS when compared to the wild-type, following attempted *Bgh* infection. The production of ROS in plants has been associated with redox signalling mechanisms for plant physiology, plant development and plant immunity involving orchestrating events leading to programmed cell death (PCD) (Yu *et al*, 2012; Corcoran & Cotter, 2013; Couturier *et al*, 2013). As the expression of CSEP0443 promotes *Bgh* penetration rates, the increase in ROS production could be related to the ability of the plant attempting to terminate further pathogen growth. In that instance, ROS likely activate downstream defence genes rather than strengthening the cell wall by crosslinking the papillae components. Effectors like PEC6 were shown to act by compromising ROS production (Liu *et al*, 2016). My results indicate that CSEP0443 does not suppress the ROS pathway due to increased ROS after *Bgh* challenge in plants expressing the protein. Earlier studies indicate that when papillae is ineffective during the primary level of defence ROS production is completely abolished (Huckelhoven *et al*, 1999; Vanacker *et al*,

2000). The increase in ROS in my case implies that CSEP0443 can-not compromise overall papillae formation.

The plants expressing CSEP0443 were evaluated for cell death events after *Bgh* infection. The plants displayed increased cell death when compared to the wild-type. Plants normally execute cell death after the first layer of defence is breached by the biotrophic pathogen (Coll *et al*, 2011). The increased cell death in plants expressing CSEP0443 when infected with *Bgh* could be attributed to their ability to enhance *Bgh* penetration. The manifestation of cell death intends to attenuate any further growth of the biotrophic pathogen. This is line with few sporelings observed to form surface hyphae despite increased penetration rates in plants expressing CSEP0443 (data not shown). Previously Collins *et al*, (2003) also reported increased PCD in *pen1-1* mutants despite enhancing penetration rates of *Bgh*. My results imply that individual expression of CSEP0443 is not sufficient to completely break non-host resistance in *Arabidopsis*, as *Bgh* penetrated cells continue undergo self-execution.

To further investigate the occurrence of cell death, plants expressing CSEP0443 were assessed for the level of electrolyte leakage after *Bgh* challenge. Electrolyte leakage is mainly related to $K^+$ efflux mediated by increased plasma membrane conductance. Induced electrolyte leakage is often accompanied by accumulation ROS leading to PCD (Demidchik *et al*, 2014). Plants expressing CSEP0443 displayed increased electrolyte leakage when compared to the wild-type following attempted *Bgh* infection. The elevated levels of electrolyte leakage reinforced the observed increased cell death in plant lines expressing CSEP0443. Likely due to the host plant recognizing *Bgh* effectors following enhanced *Bgh* penetration in CSEP0443 expressing plants relative to wild-type.

# Chapter four

## 4.0 RRE1-AtPEN1 interactions and ubiquitination events

### 4.1 Introduction

Redox regulated E3 ligase 1 (RRE1) was identified following global expression analysis of genes upregulated in *arabidopsis thaliana s-nitrosoglutathione reductase 1-3* (*atgsnor1-3*) and *salicylic acid induction deficient 2* (*sid2*) mutants following challenge with *Pseudomonas syringae* pv. tomato DC3000 *avirulence B* (*Pst*DC3000(*avrB*) (Yu, 2012). RRE1 was also found to be upregulated with *Blumeria graminis* f. sp. *hordei* (*Bgh*) challenge (Yu and Loake unpublished). *atgsnor1-3* plants have loss of S-nitrosoglutathione reductase 1 (GSNOR1) function, an enzyme that controls the cellular levels of S-nitrosylation, a post-translational modification involving the addition of nitic oxide (NO) to free cysteine thiols to form S-nitrosothiols. In addition, the mutant has impaired salicylic acid (SA) accumulation and is defective in SA signalling (Feechan *et al*, 2005). The *sid2* mutant also does not accumulate SA and has decreased expression of SA responsive genes (Nawrath, 1999). Both mutants have compromised resistance to both virulent and avirulent microbial pathogens (Nawrath, 1999; Feechan *et al*, 2005). The high expression of pathogen triggered *RRE1* in such backgrounds suggested its expression was independent of SA but probably transcriptionally regulated by NO. NO has been shown to be elevated upon infection with powdery mildew pathogens (Schlicht & Kombrink, 2013). RRE1 was characterized and found to have two conserved domains: an ankyrin repeat at the amino terminus (N) that mediates protein-protein interactions and a Really Interesting New Gene (RING) domain at the carboxy (C) terminus that mediates E3 ligase activity (Yu, 2012).

*Arabidopsis thaliana PENETRATION 1* (*AtPEN1*) encodes syntaxin 121 (Syp121) that localise at the plasma membrane. AtPEN1 was revealed from a genetic screen intended to investigate penetration resistance against the non-host pathogen *Bgh* in *Arabidopsis*

(Collins *et al*, 2003). Mutation in *AtPEN1* led to one of the mutants *pen1-1* known to have a pre-mature stop codon in the reading frame with complete loss of protein (Collins *et al*, 2003; Zhang *et al*, 2007b). AtPEN1 mediates the recruitment of vesicles containing anti-microbial agents at the papilla (Collins *et al*, 2003; Nielsen & Thordal-Christensen, 2013). AtPEN1 is also part of the Soluble NSF (N-ethylmaleimide-sensitive factor) Attachment Protein Receptor (SNARE) complex controlling vesicle trafficking and bulk transport of cargo in the cell (Bock *et al*, 2001). Structural analysis of AtPEN1 using Expert Protein Analysis System (ExPASy) bioinformatics tools reveals that it has 20 lysines in the sequence and 17/20 are surface exposed. These exposed lysines could be sites for regulation of functional activities of AtPEN1 by RRE1 mediated E3 ligase activities.

Mutants *rre1* and *pen1-1* both have increased susceptibility to *Bgh* pathogens (Collins *et al*, 2003; Yu, 2012). Like *RRE1*, *AtPEN1* is an SA independent NO responsive gene (Zhang *et al*, 2007b; Yu, 2012). The AtPEN1 and its non-recycling homologue Syntaxin 122 (Syp122) negatively regulate salicylic acid, ethylene, jasmonic pathways and programmed cell death (Zhang *et al*, 2007b). Due to the co-expression of RRE1 and AtPEN1 during *Bgh* infection and under other conditions, I investigated whether the two proteins interact both *in vitro* and *in vivo*. I also investigated the consequences of the possible interaction by determining whether AtPEN1 could be a possible substrate for RRE1.

## 4.2 Materials and methods

### 4.2.1 Genotyping of plant lines utilized in transformations

Plant lines *pen1-1*, *rre1, 35S::EGFP-AtPEN1-pen1-1* and *35S::EGFP-AtPEN1-pen1-1-rre1* were utilized in transformation. Genomic deoxyribonucleic acid (DNA) was extracted from leaves (100 mg) of the above *Arabidopsis* lines by homogenizing in 300 µl of cetyltrimethyl ammonium bromide (CTAB) buffer as described in section 2.2. Genotyping

polymerase chain reaction (PCR) was carried out using gene specific primers listed in (Table 1), with the reaction and PCR conditions carried out as described in section 2.2. PCR products were separated as described in section 2.2.

### 4.2.2 *In vitro* pull-down assay for the interaction of RRE1, RRE-Ankyrin with AtPEN1

The expression and purification of glutathione S-transferase (GST)-RRE1, GST-RRE1-Ankyrin, Maltose binding protein (MBP)-AtPEN1 are as described in section 2.8. To characterize the protein-protein interactions between GST-RRE1, GST-RRE1-Ankyrin repeat and MBP-AtPEN1 an *in vitro* pull down assay of GST tagged proteins and co-immunoprecipitation of MBP-AtPEN1 was carried out (Nguyen & Goodrich, 2006). Initially glutathione Sepharose beads were washed 3 times in ice cold 1x PBS by centrifugation at 4°C, 800*g*, for 30 seconds followed by discarding the supernatants. After washing, the resin was suspended in 1x ice cold PBS, 3 volumes of the resin. The purified proteins were thawed completely on ice and adjusted to: 4.3 ng/µl for GST-RRE1, 4.3 ng/µl for GST-RRE1-Ankyrin and 0.88 ng/µl for MBP-AtPEN1. For a 120 µl reaction, 40 µl of glutathione Sepharose resin slurry were transferred into 1.5 ml micro-centrifuge tubes on ice followed by 40 µl of GST-RRE1, GST-RRE1-Ankyrin proteins. The proteins were then incubated for $2^1/_2$ hours at 4°C on a rotary roller, followed by addition of 40 µl of MBP-AtPEN1 and again re-incubated for another $2^1/_2$ hours at 4°C. The rest of steps are as described in section 2.9.

### 4.2.3 RRE1 mediate the ubiquitination of AtPEN1 *in vitro*

The ubiquitination assay was performed as described by Sato *et al*, (2009). The assay was carried out in a 30 µl reaction containing 10 ng/µl E1, 3 ng/µl of purified E2, 3 ng/µl of purified GST-RRE1, 0.099 ng/µl AtPEN1, 1x reaction buffer, 6.7 mM adenosine triphosphate (ATP), 66 ng/µl histidine-ubiquitin and autoclaved double distilled water ($ddH_2O$). The rest of steps are as described in section 2.10.

### 4.2.4 Genetic constructs for *in vivo* investigations of RRE1 and AtPEN1

Investigations of RRE1 and AtPEN1 in *N. benthamiana* and *Arabidopsis* were made by generating genetic constructs using Golden Gate modular cloning (MoClo) (Weber *et al*, 2011; Engler *et al*, 2014), and site directed mutagenesis (Agilent Technologies, 2015).

For investigating the interactions of AtPEN1 and RRE1, amplified fragments of *AtPEN1* and *RRE1* respectively were cloned in *pAGM1287* for level 0 acceptor. The fragments were transferred in level 1 vectors. *AtPEN1* was cloned in level 1 position 2 with *35S* Cauliflower mosaic promoter (*CaMV 35S*) and *CaMV 35 S* terminator, and a C-terminal *MYC* tag. *RRE1* was cloned in level 1 position 3 with a light-harvesting chlorophyll-protein complex ii subunit B1 (*LHB1B1*) promoter, mannopine synthase (*MAS*) terminator and a C-terminal *HA* tag. Finally, the two full transcription units of *AtPEN1* and *RRE1* together with *Kanamycin* resistance cassette already in level 1 position 1 and endlinker 3 were cloned in level 2 vector (*pAGM4723*).

For investigation of the ubiquitination of AtPEN1, cloning was done as described above except that *RRE1* was excluded, and *AtPEN1* was cloned in level 1 position 3 and *Ubiquitin* initially first cloned in level 0 vector was transferred to level 1 position 2 with a Ubiquitin 10 (*UB10*) promoter, Ubiquitin 5 terminator (*UB5*) and a C-terminal *FLAG*. The three full transcription units of *Kanamycin* cassette, *AtPEN1* and *Ubiquitin*, and endlinker 3 were finally ligated in level 2 vector.

For investigating the dependency of AtPEN1 on RRE1 for ubiquitination, the cloning was done as described above, additionally *RRE1* was cloned in level 1 position 4 and finally the four transcription units and endlinker 4 were ligated in level 2 vector. Details of the PCR set up for amplifications, vectors and modules involved, cloning reactions and selections are as described in section 2.11.

For the identification of ubiquitination sites in AtPEN1, candidate lysines selected as

described in section 4.7 were mutated to arginine. Muted full transcription units of *AtPEN1* variants were combined with *Ubiquitin* full transcription unit, *Kanamycin* resistance cassette and endlinker 3 as described above and finally ligated in level 2 vector. Primer used are listed in (Table 4). PCR amplifications, cloning reactions and selections are described in section 2.11. Site directed mutagenesis was used to generate the *AtPEN1-K103R*, *AtPEN1-K103R-K281R* and *AtPEN1-K103R-K281R-K285R-K307R* genetic constructs on the previously Golden Gate MoClo made constructs. Primers used are listed in (Table 4). All proceeded steps are as described in section 2.11.

### 4.2.5 Transient protein expression in *N. benthamiana*

The procedure was performed as described by Liu *et al*, (2016). The initial steps of bacterial growth and harvest are as described in section 2.13. The harvested pellet was washed once in infiltration media containing MES 10 mM pH 5.2, $MgCl_2$ 10 mM and acetosyringone 0.2 µM to remove residual antibiotics. The pellet was suspended in 0.5 ml infiltration media and $O.D_{600\ nm}$ adjusted to 0.2 for assays involving ubiquitination site determination and 1 for the ubiquitination of AtPEN1. Further steps are described in section 2.13.

### 4.2.6 RNA extraction and RT-PCR

For the RNA extraction, 100 mg of *Arabidopsis* leaves, were collected and immediately frozen in liquid nitrogen. The leaves were finely ground in liquid nitrogen using mortar and pestle previously sterilized by autoclaving. The finely ground frozen tissues were suspended in 1 ml TRIzol® Reagent (Life technologies). The rest of steps were as described in section 2.14. For RT-PCR, the extracted RNA was adjusted to 1.5 µg final concentration followed by cDNA synthesis as described in section 2.14. Synthesized cDNA was subjected

to PCR amplification in conditions and set up as described in section 2.14 using primers listed in (Table 5).

### 4.2.7 Protein extraction and co-immunoprecipitation assays

Proteins were extracted from 4 g of 3 weeks-old *Arabidopsis* leaves and from 2 g of Agro-infiltrated *N. benthamiana* leaves. The leaves were harvested and immediately frozen in liquid nitrogen. For ubiquitination and interaction assays proteins were extracted from both non infected and *Bgh* infected *Arabidopsis* plants, that had been previously incubated for 3 days. The leaves were then finely ground in liquid nitrogen before further crushed in extraction buffer described by Li *et al*, (2015). Buffer components are as described in section 2.15. MG132 50 µM was additionally included in the buffer. The rest of steps are as described in section 2.15.

For co-immunoprecipitation assays, the protein suspensions were filtered through 0.4 µM millipore filters and protein concentrations determined using the Bradford reagent. The proteins were adjusted to 200 µg for the investigation of ubiquitination sites and 350 µg for protein detections, interactions and ubiquitinations. The diluted proteins were incubated with 2 µg of anti-HA antibody for RRE1 detection, anti-flag for ubiquitin detection, and anti-Myc antibody for AtPEN1 detection and ubiquitination assays. All antibodies were conjugated on agarose beads. The rest of steps are as described in section 2.15. Finally, proteins were boiled in 1x SDS (Sodium dodecyl sulfate) loading dye containing 10% β-Mercaptoethanol at 95$^{o}$C for 5 minutes and further preceded as in section 2.15.

### 4.2.8 SDS PAGE and western blot analysis

Sodium dodecyl sulfate-Polyacrylamide gel electrophoresis (SDS PAGE) and western blot analysis were carried out as described by Sambrook *et al*, (2012). Proteins were separated in 10% (for the other investigations), or 15% (for detection of ubiquitin expression)

SDS PAGE in 1.5 mm glass chambers (Bio-Rad) superimposed with stacking gel. The preceded steps were as described in section 2.16. Finally, the membrane was incubated with primary antibodies horseradish peroxidase (HRP) or non HRP conjugated (Table 2), for 1 hour and followed by 3 times washing with phosphate buffered saline-tween 20 (PBS-T) at 10 minutes interval. In case of non HRP conjugated antibodies further incubation for 1 hour with anti-mouse IgG HRP antibody followed. After incubation the membrane was washed again 3 times with PBS-T at 10 minutes interval. Further steps are as described in section 2.16.

### 4.2.9 Statistical analysis

For comparison of means, data was analyzed using Microsoft Excel student *t*-Test assuming unequal variances. Statistical significance was reported at either $P < 0.05$ or $P < 0.01$.

## 4.3 Results

### 4.3.1 Genotyping of plant materials utilized in the project

In order to confirm the identity of plant genetic materials used in the preceding experiments, DNA was extracted from the wild-type Col-0, *rre1*, and *pen1-1* mutants using CTAB buffer. The *rre1* mutant is a knockout of *RRE1* with a TDNA insertion at site 397 bp after ATG located in the second intron while *pen1-1* is knock down of AtPEN1 generated by ethyl methane sulfonate (EMS) mutation. The mutation introduces a stop codon early in the open reading frame leading to an incomplete translation. Wild-type Col-0 was utilized as a positive control. Amplification of *Actin*, a known house-keeping gene, revealed a fragment of expected band size in the wild-type and in all other lines indicating the successful extraction of DNA from the plant materials (Figure 4-1 C and D lower panel). The amplification of full sequence in the *rre1* was hindered due to the TDNA insertion in the sequence however, the

region between the start codon to the TDNA site was amplified (Figure 4-1 B). *AtPEN1* was amplified from *pen1-1* mutants (Figure 4-1 A). Genotyping *35S::EGFP-AtPEN1-pen1-1* and *35S::EGFP-AtPEN1-pen1-1-rre1* was based on amplification of *EGFP* in the homozygous lines (Figure 4-1 D upper panel).

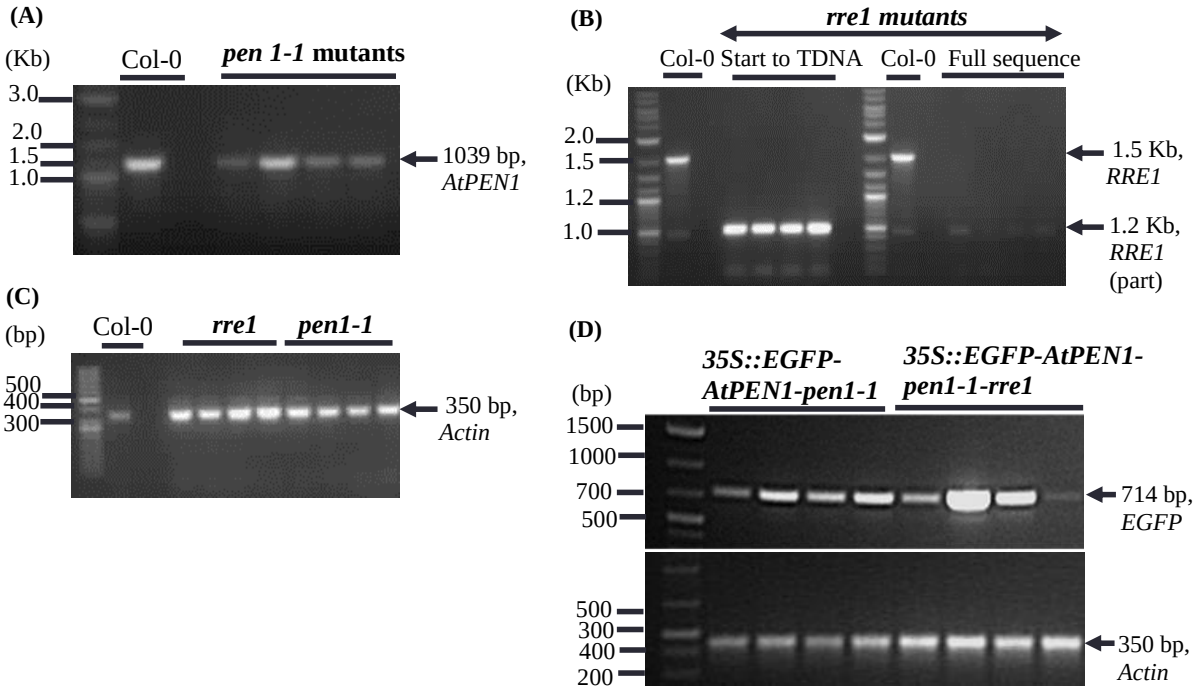


**Figure 4-1: Genotyping of *Arabidopsis* plants show expected fragments.** DNA was extracted from *pen1-1*, *rre1*, *35S::EGFP-AtPEN1-pen1-1*, *35S::EGFP-AtPEN1-pen1-1-rre1* and Col-0 using CTAB extraction buffer. (A) *pen1-1* genotyping performed by amplification of AtPEN1 using gene specific primers. (B) *rre1* genotyping performed by amplification of the region between the start of *RRE1* and start of the TDNA using primers binding the two regions. In parallel amplification was performed of the whole *RRE1* carrying a TDNA insertion. (C) *Actin* amplification for wild-type Col-0, *rre1* and *pen1-1* mutants. (D) Genotyping of *35S::EGFP-AtPEN1-pen1-1* and *35S::EGFP-AtPEN1-pen1-1-rre1* lines. *EGFP* was amplified from *35S::EGFP-AtPEN1-pen1-1* and *35S::EGFP-AtPEN1-pen1-1-rre1* lines using *EGFP* gene specific primers. Actin also amplified from the same lines to check procedural control. In all cases four plants for each background were genotyped. Arrows indicate the expected amplified fragment sizes.

### 4.3.2 Protein expression and purification

Proteins RRE1, RRE-RING domain, RRE1-Ankyrin repeat domain, RRE1-C340S, AtPEN1, 20S proteasome (α) subunit, and CSEP0443 were expressed in *Escherichia coli* for

*in vitro* investigations. The full coding sequences for *RRE1*, *RRE1-RING* and *RRE1-Ankyrin repeat*, *20S proteasome* (*α*) *subunit* and *AtPEN1* were previously amplified from Col-0 cDNA. The gene fragments were cloned into *pGEX-4TI* vector (GE Healthcare) fused to an N-terminal GST tag, by restriction enzyme digestion, except for *AtPEN1* which was cloned into a *pETG* vector in frame with an N-terminal MBP tag. RRE1-C340S was obtained by mutating the codon for cysteine 340 to serine in the wild-type *RRE1* construct using site directed mutagenesis. The coding sequence for *CSEP0443* was amplified from *pDEST22-CSEP0443* genetic construct already available in the Loake laboratory and cloned in *pET40A* vector in frame with an N-terminal MBP tag. The vectors all had resistance to ampicillin were finally transformed into expression strain BL21 (DE3) via the heat shock method. The cells were grown to the exponential phase and induced for the expression of proteins with isopropyl β-D-1-thiogalactopyranoside (IPTG). After expression the cells were lysed with appropriate lysis solution and the lysates were incubated with glutathione Sepharose resin for GST tagged proteins and amylose resin for MBP tagged proteins. Elution of the trapped proteins was undertaken with reduced glutathione for GST fused proteins and maltose for MBP recombinant proteins. Protein concentrations were quantified using the Bradford assay method and resolved in SDS PAGE. After Coomasie brilliant blue staining, proteins with expected band sizes were detected by SDS PAGE (Figure 4-2). The molecular size of GST is 26 kDa, which leads to the expected fusion proteins size of; GST-RRE1 (26 kDa + 42 kDa = 68 kDa) (Figure 4-2 A), GST-RRE1-RING (26 kDa + 5 kDa = 31 kDa) (Figure 4-2 B), GST-RRE1-Ankyrin repeat (26 kDa + 12 kDa = 38 kDa) (Figure 4-2 C), GST-RRE1-C340S (26 kDa + 42 kDa = 68 kDa) (Figure 4-2 D), GST-20S proteasome (α) subunit (26 kDa + 26 kDa = 52 kDa) (Figure 4-2 E). The molecular size of MBP is 42 kDa leading to the expected size of MBP-AtPEN1 (42 kDa + 38 kDa = 80 kDa) (Figure 4-2 F) and MBP-CSEP0443 (42 kDa + 9.6 kDa = 52 kDa) (Figure 4-2 G).

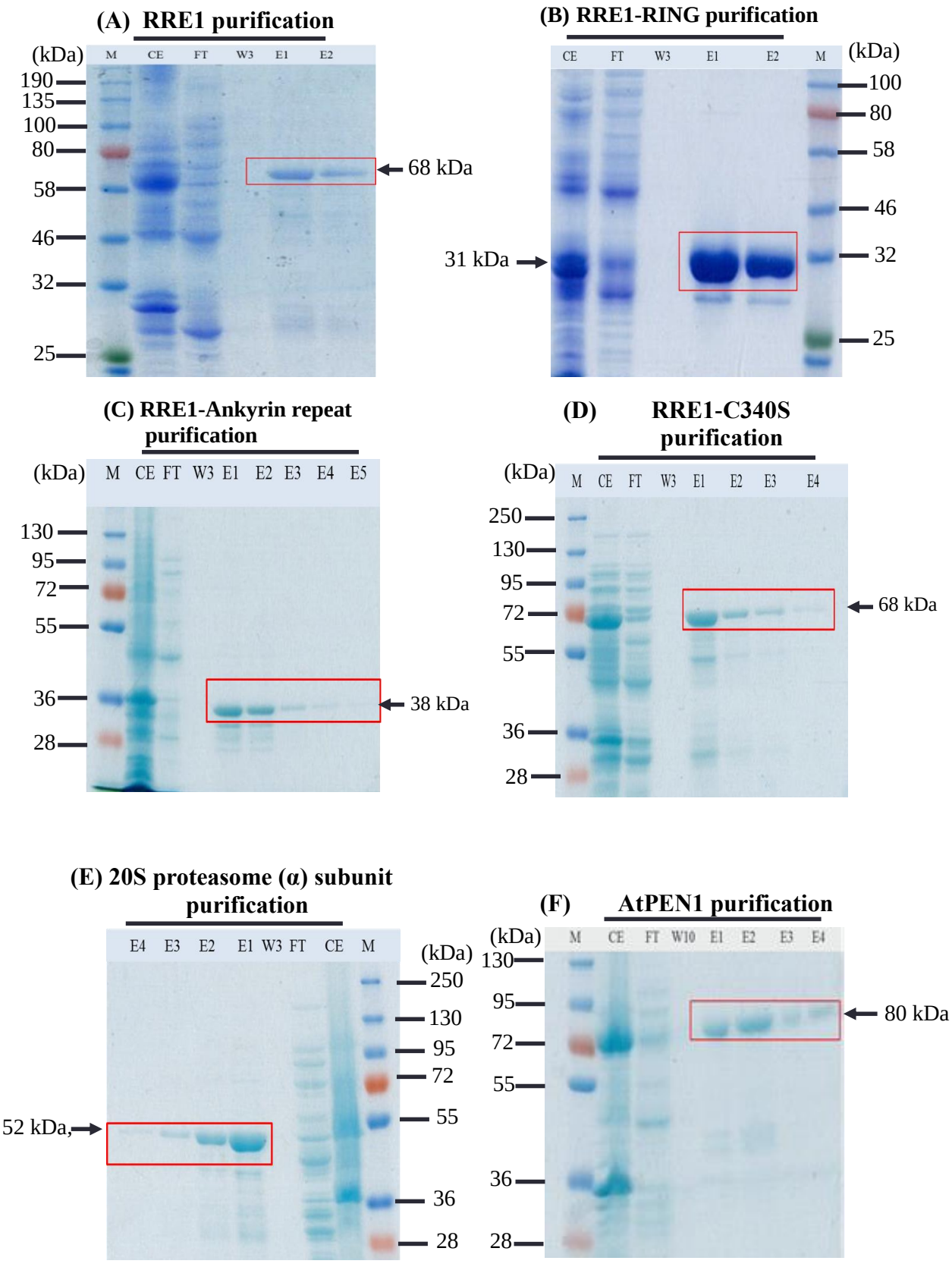
(A) RRE1 purification
(kDa)
M CE FT W3 E1 E2
190
135
100
80
58
46
32
25
68 kDa
(B) RRE1-RING purification
CE FT W3 E1 E2 M
(kDa)
100
80
58
46
32
25
31 kDa
(C) RRE1-Ankyrin repeat purification
(kDa)
M CE FT W3 E1 E2 E3 E4 E5
130
95
72
55
36
28
38 kDa
(D) RRE1-C340S purification
(kDa)
M CE FT W3 E1 E2 E3 E4
250
130
95
72
55
36
28
68 kDa
(E) 20S proteasome (α) subunit purification
E4 E3 E2 E1 W3 FT CE M
(kDa)
250
130
95
72
55
36
28
52 kDa,
(F) AtPEN1 purification
(kDa)
M CE FT W10 E1 E2 E3 E4
130
95
72
55
36
28
80 kDa

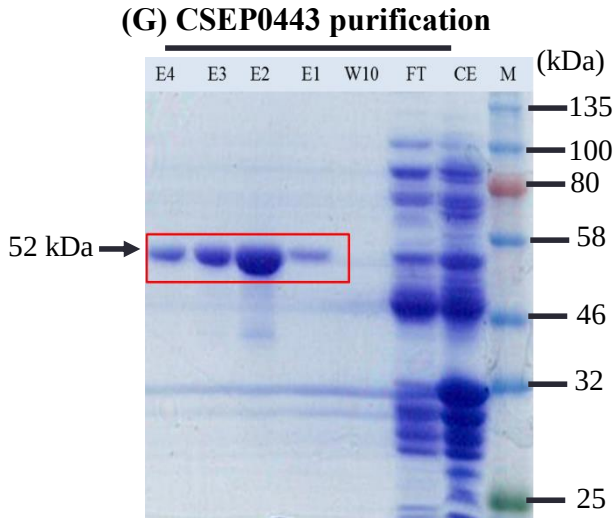


**Figure 4-2: Recombinant protein purification.** Recombinant proteins were extracted from *Escherichia* (*E. coli*) (BL21) carrying genetic constructs for expression of GST-RRE1, GST-RRE1-RING, GST-RRE1-Ankyrin repeat, GST-RRE1-C340S, GST-20S proteasome (α) subunit, MBP-AtPEN1 and MBP-CSEP0443. For GST tagged proteins extracted proteins were incubated glutathione Sepharose 4B resin and eluted with reduced glutathione solution. Extracted MBP tagged proteins were incubated with amylose resin and eluted with maltose solution. To check the sizes, the purified proteins were separated in SDS-PAGE followed by Coomassie blue staining and then destaining. (A) *In vitro* purification of GST-RRE1. (B) *In vitro* purification of GST-RRE1-RING. (C) *In vitro* purification GST-RRE1-Ankyrin repeat. (D) *In vitro* purification of RRE1-C340S. (E) *In vitro* purification of 20S proteasome (α) subunit. (F) *In vitro* purification of MBP-AtPEN1. (G) *In vitro* purification of MBP-CSEP0443. Red rectangle indicates the position of the expected protein band sizes. Protein ladder (M), cell extract (CE), flow through (FT), Elution (E)1, 2, 3, 4.

### 4.3.4 Investigating the interaction of AtPEN1 and RRE1

#### 4.3.4.1 AtPEN1 interacts with RRE1: Preference for Ankyrin repeat domain

Previous work *in vivo* revealed that AtPEN1 is important in cell surface level resistance against *Blumeria* pathogens (Collins *et al*, 2003). RRE1 was also shown to be significantly expressed during pathogen challenge in *Arabidopsis* (Yu, 2012). The yeast two-hybrid screen conducted by Yu and Loake (unpublished) revealed that the two proteins AtPEN1 and RRE1 were strongly interacting (Figure 4-3 A). The yeast two-hybrid assay further showed that the interaction was with the ankyrin repeat of RRE1 and not with the

RING domain. To confirm the interaction, I set up an *in vitro* pull-down assay. Recombinant proteins GST-RRE1 and GST-RRE1-Ankyrin were incubated with glutathione Sepharose resin. The captured GST tagged proteins were later incubated with MBP-AtPEN1 and subjected to four washes with ice cold PBS to remove unbound proteins. RRE1 and its corresponding RRE1-Ankyrin repeat domain were found to interact with AtPEN1 (Figure 4-3 B). The relative levels of interactions were quantified using ImageJ software and expressed as mean area of interaction. There was no significant difference detected in the level of interactions with AtPEN1 (Figure 4-3 C).

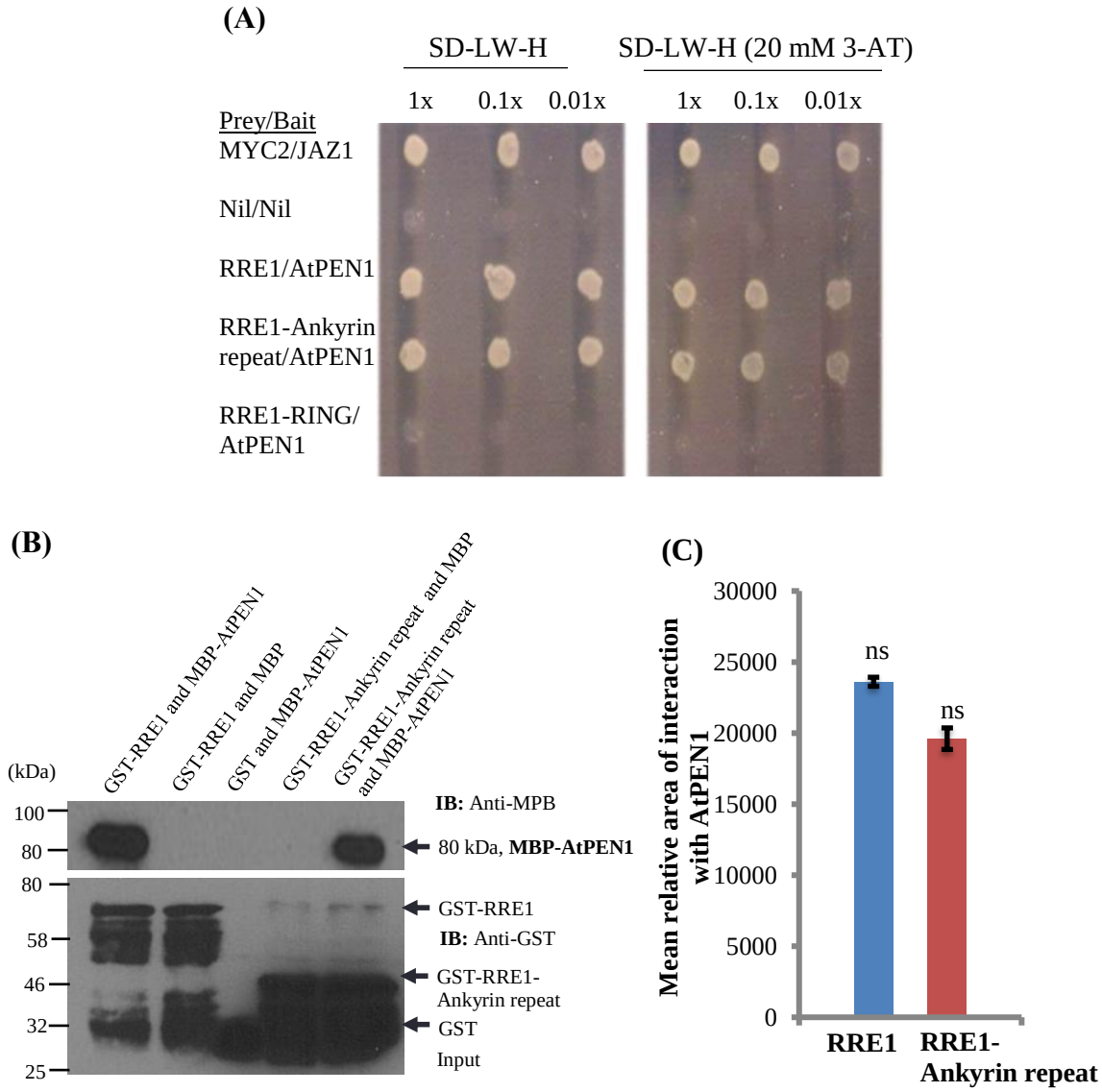


**Figure 4-3: RRE1, RRE1-Ankyrin repeat interacts with AtPEN1.** (A) Yeast-two-hybrid of RRE1 and AtPEN1. pDEST32 and pDEST22 are empty binding domain and

activation domain vectors used as negative controls. RRE1, RRE1-Ankyrin repeat, RRE1-RING and MYC2 were expressed as fusion with galactose 4 (GAL4) activation domain. AtPEN1, Jasmonate Zim domain protein 1 (JAZ1) and TOPLESS (TPL) N-250 was expressed as a fusion with GAL4 binding domain. Yeast cells were grown on selective medium without leucine, tryptophan and histidine (SD/-L-T-H) with or without 20 mM of 3-amino-1,2,4-triazole (3AT). (B) *In vitro* pull-down assay to check the interaction of RRE1 and AtPEN1. Recombinant proteins of GST-RRE1, GST-RRE1-Ankyrin and GST alone were initially incubated with glutathione Sepharose 4B resin. Then, MBP-AtPEN1 and MBP separately were added to the previously incubated GST tagged proteins and further incubated. After incubation the proteins were washed three times and resolved in SDS PAGE. Detection of interactions were performed by immuno-blotting with anti-MBP antibody. From left, Lane 1, checking the interaction of RRE1 and AtPEN1. Lane 2, checking the interaction of RRE1 and MBP. Lane 3, checking the interaction of GST and AtPEN1. Lane 4, checking the interaction of RRE1-Ankyrin repeat and MBP. Lane 5, checking the interaction of RRE1-Ankyrin repeat and AtPEN1. Loading controls were detected by immunoblotting with anti-GST antibody. (C) Relative quantification of the *in vitro* pull-down assay interactions using ImageJ software. Protein bands corresponding to the area of interaction were relatively quantified by ImageJ software and numerical values obtained expressed as mean area of interaction. The experiment was repeated three times. Error bars represent mean ± standard error. *t*-test, $P > 0.01, 0.05$. The ns indicate non-significant differences in the interactions.

#### 4.3.4.2 AtPEN1 interacts with RRE1 *in vivo*

Confirmation of the interactions of AtPEN1 and RRE1 prompted the investigation of the interplay of the two proteins *in vivo*. The full transcriptional unit (promoter-coding sequence and terminator) of *AtPEN1* expressed with the *CaMV 35S* promoter, *CaMV 35S* terminator and a C-terminal *MYC* tag, was combined with the full transcriptional unit of *RRE1*. *RRE1* was constructed with an *LHB1B1* promoter and *MAS* terminator embedded with a C-terminal *HA* tag. The combined transcription units were ligated into plant expression vectors using Golden Gate MoClo. The vectors were transformed into *Arabidopsis rre1* mutant background by *Agrobacterium* mediated transformation via floral dipping. Homozygous lines were subjected to RT-PCR to detect the transcript levels of *AtPEN1* and *RRE1*. The expressions of the two genes were confirmed (Figure 4-4 A), followed by protein extraction. The proteins were extracted in non-denaturing conditions and immuno-precipitated with anti-Myc and anti-HA antibodies, conjugated on agarose beads. Western

blot analyses were performed by incubating the membranes with anti-Myc and anti-HA antibodies. The expressions of the two proteins were detected *in vivo* (Figure 4-4 B). Lines 15||76 and 15||81 were selected for downstream experiments involving protein extractions.

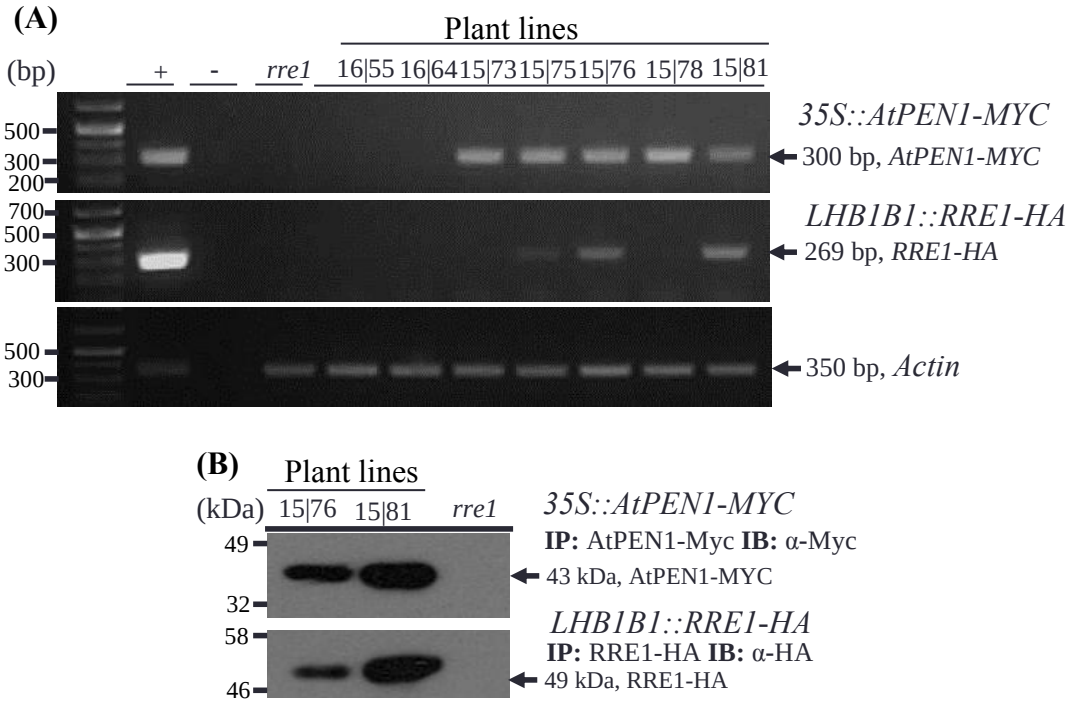


**Figure 4-4: Expression of AtPEN1 and RRE1 detected *in vivo.*** (A) RT-PCR showing the expression of *RRE1* and *AtPEN1* in different selected lines. RNA was extracted from plant lines expressing *35S::AtPEN1-MYC* and *LHB1B1::RRE1-HA*, using TRIzol reagent followed by cDNA synthesis. Expression was detected by amplification of fragments of *AtPEN1-MYC* and *RRE1-HA*. *Actin* amplification was used as a reference. (B) Detection of RRE1 and AtPEN1 proteins in the selected lines. Proteins were extracted from the selected lines in a non denaturing buffer and immunoprecipitated using anti-Myc and anti-HA antibody conjugated on agarose beads. The proteins were resolved in SDS-PAGE and detection achieved by immunoblotting with either anti-Myc or anti-HA antibody. Protein extracted from a non-transformed *rre1* mutant was used as a negative control.

After confirming the expression of the given proteins in tested lines, the proteins were extracted from the selected lines under non-denaturing conditions. Extracted proteins were incubated with anti-Myc antibody conjugated on agarose beads. After capturing of Myc tagged proteins, the proteins were washed in ice cold PBS to remove unbound proteins. The washed proteins were resolved by SDS PAGE followed by western blot analysis with anti-HA

antibody. The detection of RRE1-HA with the expected band size confirmed the interaction of RRE1 with AtPEN1 *in vivo*. A construct expressing only *AtPEN1* transcription unit was used as a negative control and no HA tagged proteins were detected with the construct (Figure 4-5).

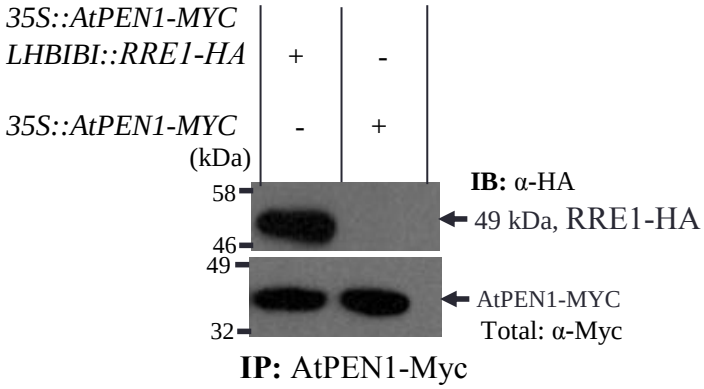


**Figure 4-5: Interaction of AtPEN1 and RRE1 *in vivo*.** Proteins were extracted in a non-denaturing buffer from plant lines expressing *35::AtPEN1-MYC* and *LHBIBI::RRE1-HA* or *35S::AtPEN1-MYC* alone. Extracted proteins were immunoprecipitated with anti-Myc antibody conjugated on agarose beads. The proteins were washed and resolved in SDS-PAGE. Detection for the interaction was performed by immunoblotting with anti-HA antibody. Proteins extracted from plants expressing *35S::AtPEN1-MYC* were used as negative control. Loading controls were detected by immunoblotting with anti-Myc antibody. Experiment repeated three times with similar results obtained.

### 4.3.5 Uncovering the substrate of RRE1

#### 4.3.5.1 RRE1 polyubiquitinates AtPEN1 *in vitro*

RRE1 was characterized and found to be an E3 ligase enzyme mediating the ubiquitination of proteins (Yu, 2012). Being an enzyme RRE1 was expected to have a possible target substrate. AtPEN1 was suspected to be the possible substrate because the two proteins have previously shown to be co-expressed during pathogen challenge and also exhibit strong interactions both *in-planta* and *in vitro*. To examine the possible ubiquitination of AtPEN1 by RRE1, recombinant proteins of both RRE1 and AtPEN1 were expressed in *E. coli* bacteria and purified with suitable tags. Ubiquitination assays were carried out in

reactions containing proteins E1 (Human), E2 (AtUBC1), Histidine-ubiquitin (His-ubiquitin), GST-RRE1 (E3), MBP-AtPEN1 and ATP with suitable buffer. The reactions were incubated at 30$^{o}$C and terminated by adding SDS loading buffer. The proteins were separated by SDS PAGE and subjected to a western blot analysis with anti-polyhistidine antibody. Polyubiquitination shown by the smear of increasing molecular mass and intensity of uniform size above the AtPEN1 monomer was detected in a reaction that had both RRE1 and AtPEN1 (Figure 4-6 lane 1). No corresponding polyubiquitination was detected in control reactions, indicating AtPEN1 as the substrate for RRE1 (Figure 4-6 lanes 2, 3, 4).

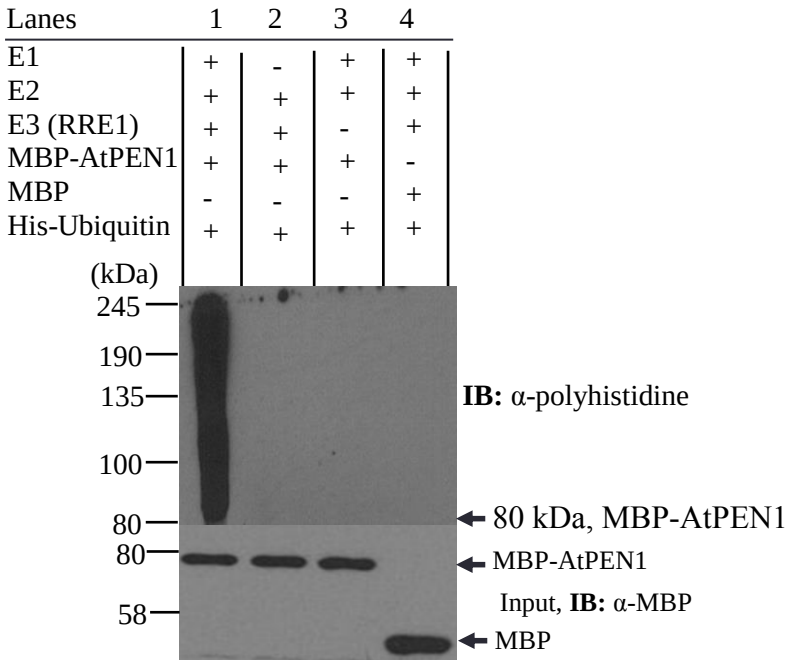


**Figure 4-6: Ubiquitination of AtPEN1.** *In vitro* ubiquitination of AtPEN1 was performed in a reaction buffer where components: E1, E2, RRE1, Histidine-Ubiquitin, ATP and either MBP-AtPEN or MBP alone as substrates were added. The proteins were incubated at 30$^{o}$C and later separated in SDS-PAGE. Detection of ubiquitination was perfomed by immunoblotting with anti-polyhistidine antibody and shown as high mass uniform smear above the MBP-AtPEN1. Lane 1, detecting the ubiquitination of AtPEN1. The absence of either E1 (lane 2) or RRE1 (lane 3) or AtPEN1 (lane 4) in reactions acted as negative control. Loading controls were dected by immunoblotting with anti-MBP antibody. Experiment repeated three times.

### 4.3.5.2 AtPEN1 polyubiquitinated *in vivo*

To investigate the polyubiquitination of AtPEN1, full transcriptional units of *AtPEN1* and *UBIQUITIN* (*UBIQ*) were generated. *AtPEN1-Myc* was expressed by the *CaMV 35S* promoter and terminator while the *UBIQ-FLAG* tagged construct was expressed by the *UBIQ* promoter and terminator. The ligated full transcriptional units were initially transiently expressed in *N. benthamiana* by *Agrobacterium* infiltration of 3 week old plants. Proteins were extracted from the infiltrated leaves in non-denaturing conditions. The proteins were immuno-precipitated with anti-Myc antibody conjugated on agarose beads and washed in ice cold PBS. Myc tagged proteins were separated by SDS PAGE and immuno-blotted with anti-flag antibody. Polyubiquitination of AtPEN1 was detected and appeared as an increasing molecular mass smear above the expected size of AtPEN1 (Figure 4-7 lane 1).

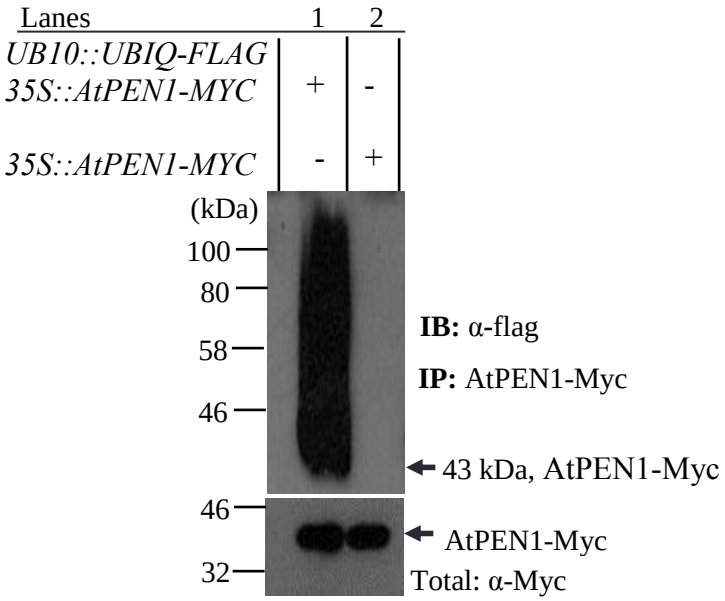


**Figure 4-7: Ubiquitination of AtPEN1 detected in *N. benthamiana*.** *Agrobacterium* carrying genetic constructs *UB10::UBIQ-FLAG 35S::AtPEN1-MYC* and *35S::AtPEN1-MYC* were infiltrated in *N. benthamiana* leaves and the plants incubated for 3 days. Proteins were extracted from the infiltrated leaves and immunoprecipitated with anti-Myc antibody conjugated on agarose beads. The proteins were washed and resolved in SDS PAGE. Detection of the ubiquitination was performed by immunoblotting with anti-flag antibody and shown by high mass smear above AtPEN1-MYC. Lane 1, checking the ubiquitination of AtPEN1. Lane 2, proteins extracted from leaves infiltrated with *35S::AtPEN1-MYC* alone were used as negative control. Loading controls were detected by immunoblotting with anti-Myc antibody. Experiment was repeated three times.

Transient expression was preceded by the stable transformation of the *Arabidopsis pen1-1* mutant background using floral dipping. Homozygous plants were screened for *AtPEN1-MYC* and *UBIQ-FLAG* expression by RT-PCR. The transcript expression in the selected lines was detected (Figure 4-8 A). Proteins were extracted from the selected lines

using non-denaturing buffer. The extracted proteins were immuno-precipitated with anti-Myc and anti-flag antibodies conjugated on agarose beads. After three washes in ice cold PBS, the proteins were resolved by SDS PAGE and analysed on a western blot using anti-Myc and anti-flag antibodies. The AtPEN1-Myc and Ubiquitin-Flag proteins were detected in the lines selected and were used for subsequent experiments (Figure 4-8 B).

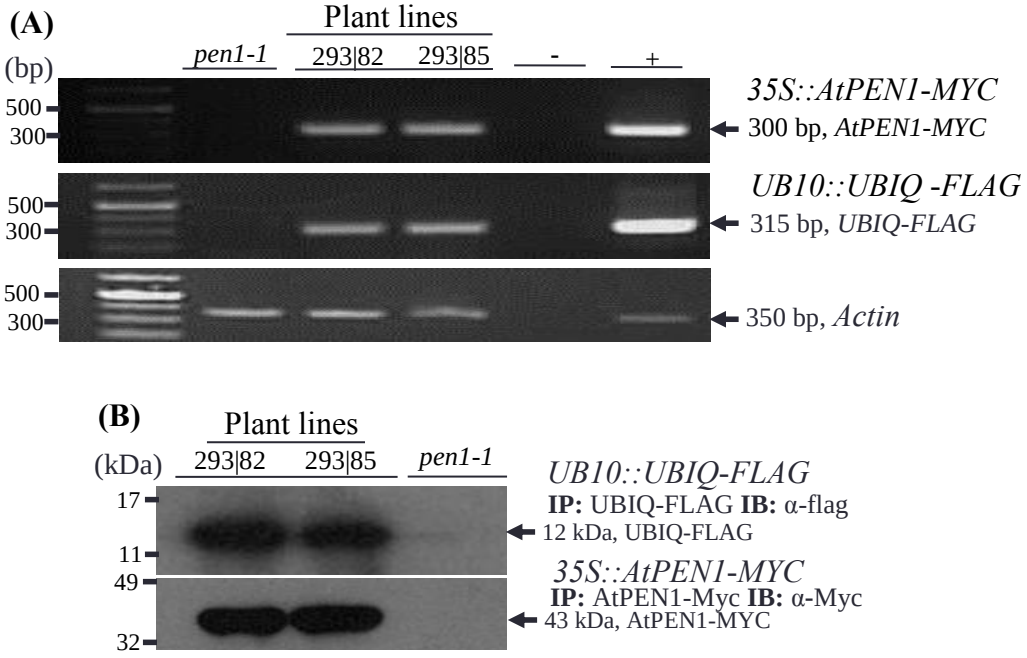


**Figure 4-8: Expression of AtPEN1 and Ubiquitin detected in *pen1-1* plants.** (A) RT-PCR showing the detection of *AtPEN1-MYC* and *UBIQ-FLAG* transcripts, *Actin* used as a reference gene. RNA was extracted using TRIzol reagent from homozygous lines expressing *UB10::UBIQ-FLAG 35S::AtPEN1-MYC* genetic construct. Extracted RNA was synthesized into cDNA and detection of the expression performed by amplification of *UBIQ-FLAG* and *AtPEN1-MYC* fragments. (B) Detection of the expression of AtPEN1-Myc and Ubiquitin-Flag in the selected lines. Proteins were extracted in non-denaturing buffer and immunoprecipitated with either anti-Myc or anti-flag antibodies conjugated on agarose beads. The proteins were washed and resolved in SDS PAGE. Detection of the proteins was performed by immunoblotting with either anti-Myc or anti-flag antibody. Proteins extracted from *pen1-1* mutant used as a negative control.

The successful expression of AtPEN1-Myc and Ubiquitin-Flag *in vivo* was followed by determining the possible ubiquitination of AtPEN1. Ubiquitination was assessed in conditions of both pathogen challenged and non-challenged lines. Plant lines were infected

with *Bgh*, and proteins were then extracted from the leaves of both infected and non-infected plants. The proteins were immuno-precipitated with an anti-Myc antibody immobilised on agarose beads. The ice cold PBS washed proteins were separated in SDS PAGE and analysed on a western blot with anti-flag antibody. Polyubiquitination of AtPEN1 shown by increasing mass uniform smear above AtPEN1 monomer was detected. Plants infected with *Bgh* displayed high level of ubiquitination (Figure 4-9 lane 1), compared to the non-infected plants (Figure 4-9 lane 3).

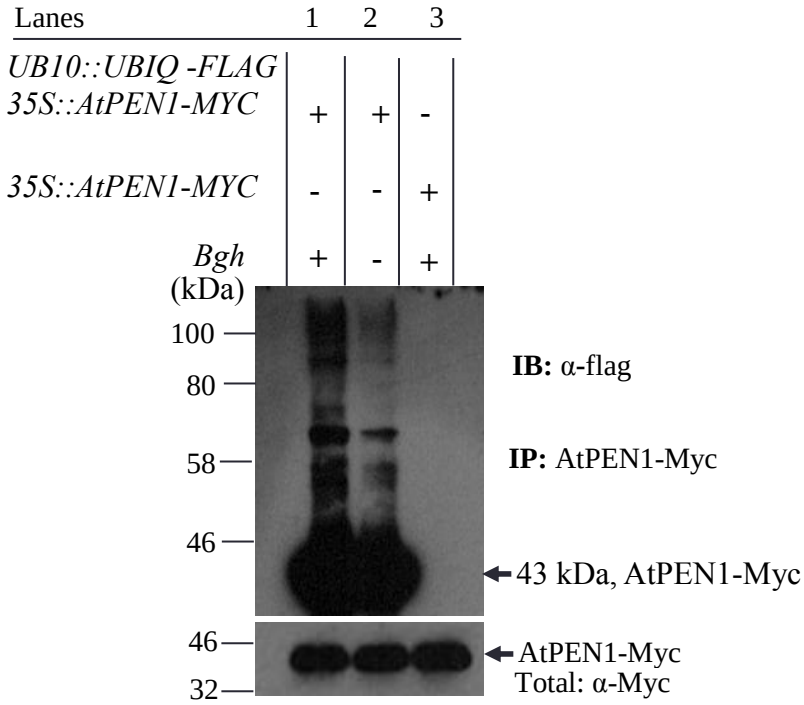


**Figure 4-9: Ubiquitination of AtPEN1 detected in *Arabidopsis*.** Plant lines double expressing *UB10::UBIQ-FLAG 35S::AtPEN1-MYC* or only *35S::AtPEN1-MYC* were either inoculated or non inoculated with *Bgh* and incubated for 3 days. Proteins were extracted from the leaf materials in non denaturing buffer and immunoprecipitated with anti-Myc antibody conjugated on agarose beads. Unbound proteins were removed by washing in PBS and then resolved in SDS PAGE. Detection of ubiquitination was then done by immunoblotting with anti-flag antibody and is shown by high mass smear above AtPEN1-MYC monomer. Lane 1, checking the ubiquitination of AtPEN1, plants were previously infected with *Bgh*. Lane 2, checking the ubiquitination of AtPEN1, plants were free from *Bgh* infection. Lane 3, proteins extracted from *35S::AtPEN1-MYC* were used as negative control. Loading controls were detected by immunoblotting with anti-Myc antibody. The experiment was repeated three times.

### 4.3.6 Ubiquitination of AtPEN1 is RRE1 dependent *in vivo*

To explore the dependency of AtPEN1 ubiquitination on RRE1, genetic constructs were designed using the Golden Gate MoClo and transformed into an *Arabidopsis rre1* mutant background. Two constructs were created one with *UBIQ-FLAG* expressed by the *UBIQ* promoter and terminator, *AtPEN1-MYC* under *CaMV 35* promoter and terminator, and *RRE1-HA* expressed by the *LHB1B1* promoter and *MAS* terminator. The second construct used as a control had only the *UBIQ-FLAG* expressed by the *UBIQ* promoter and terminator, *AtPEN1-MYC* under *CaMV 35* promoter and terminator. The generated homozygous lines that exhibited the correct segregation ratios were analysed for the expression of the *UBIQ*, *AtPEN1*, *RRE1* transcripts by RT-PCR. Transcript expression for the three genes was detected in all lines (Figure 4-10 A). Further, transcript expression of only *UBIQ* and *AtPEN1* was detected (Figure 4-10 C). Proteins were extracted from plants lines in non-denaturing buffer and immuno-precipitated with anti-flag for Ubiquitin, anti-Myc for AtPEN1 and anti-HA for RRE1, all conjugated on agarose beads. The immuno-precipitates were washed in ice cold PBS and separated by SDS PAGE. Western blot analyses were undertaken with anti-flag, anti-Myc and anti-HA antibodies. All the selected lines expressed the relevant proteins (Figure 4-10 B and D).

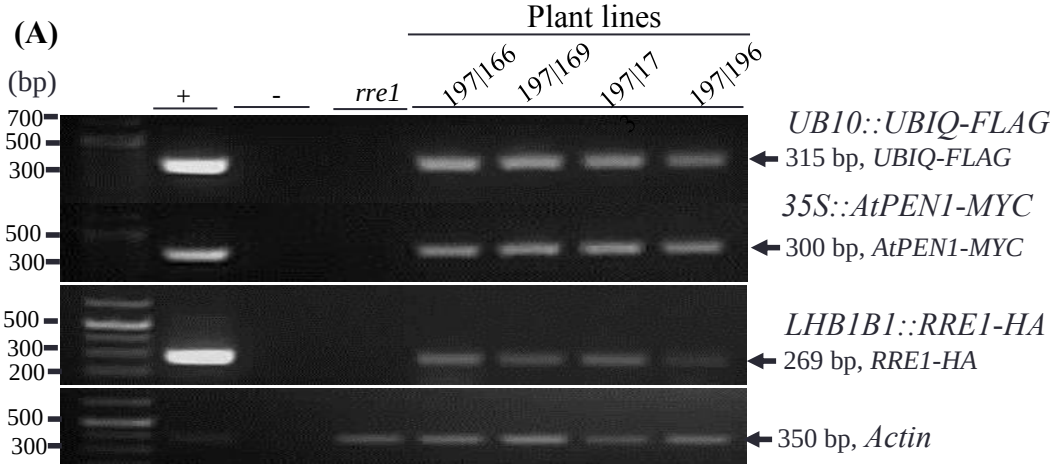

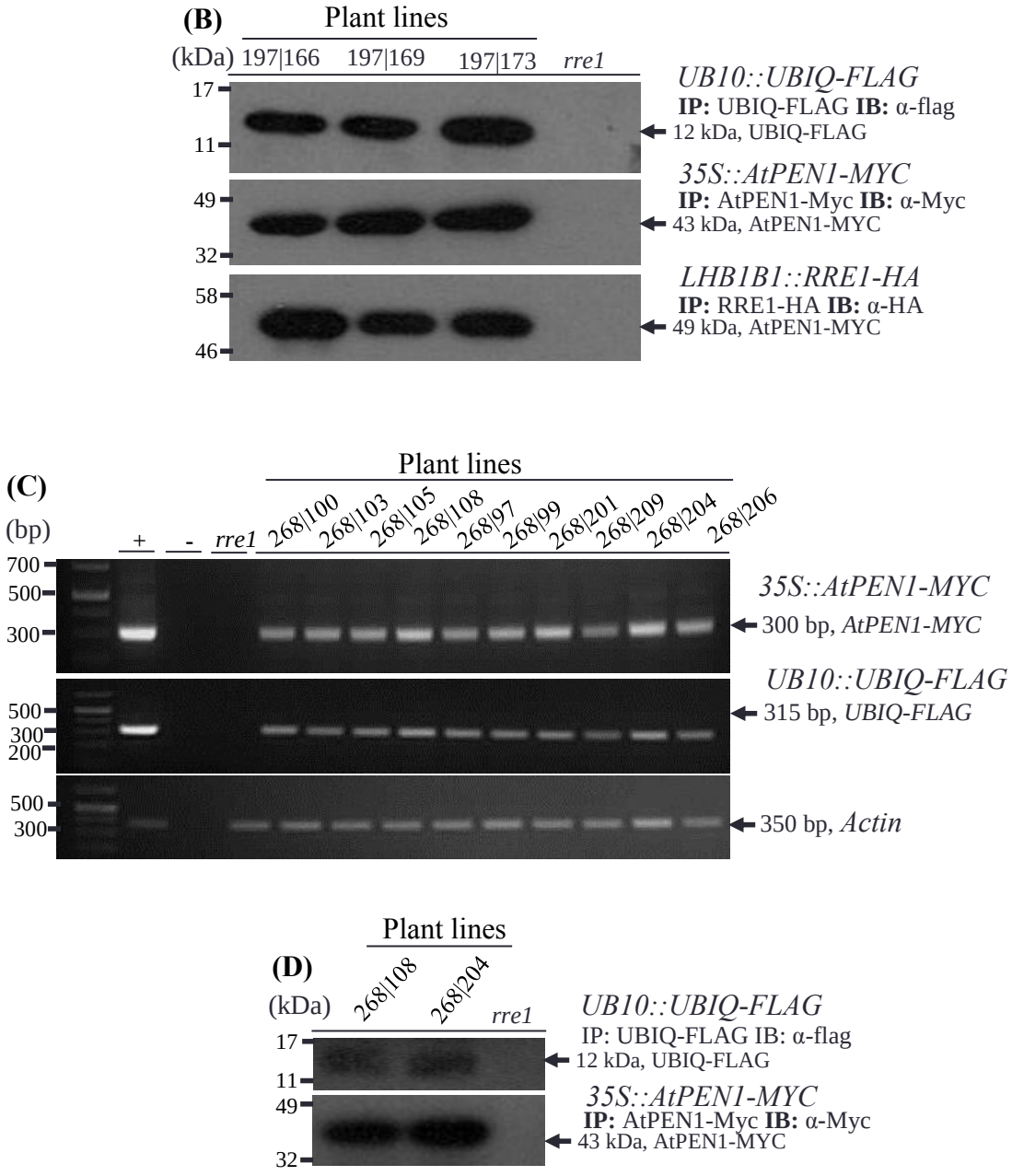


**Figure 4-11: Expression of Ubiquitin-Flag, AtPEN1-Myc and RRE1-HA.** (A) RT-PCR for the detection of *UB10::UBIQ-FLAG*, *35S::AtPEN1-MYC* and *LHBIBI::RRE1-HA* transcript in the *rre1* mutant. RNA was extracted using Trizol reagent from homozygous lines transformed with *UBIQ-FLAG*, *AtPEN1-MYC* and *RRE1-HA* and then followed with cDNA analysis. Detection of the transcript expressions were done by amplifying the *UBIQ-FLAG*, *AtPEN1-MYC* and *RRE1-HA* fragments. *Actin* used as a reference. (B) Detecting the expression of Ubiquitin-Flag, AtPEN1-Myc and RRE1-HA proteins in *rre1* mutant. Proteins were extracted from the selected lines in non denaturing buffer and immunoprecipitated with either anti-flag or anti-Myc or anti-HA antibodies conjugated on agarose beads performed by incubating overnight. The proteins were washed in PBS and separated in SDS PAGE. Detection of protein expression was performed by immunoblotting with either anti-flag or anti-Myc or anti-HA antibodies. (C) RT-PCR for detecting the expression of *UB10::UBIQ-FLAG 35S::AtPEN1-MYC* transcripts in *rre1* mutant. RNA was extracted using Trizol reagent from homozygous lines generated after

transformation with *UB10::UBIQ-FLAG 35S::AtPEN1-MYC* construct. RNA extraction was followed by cDNA synthesis and the detection of transcript expression was done by amplification of *UBIQ-FLAG* and *AtPEN1-MYC* fragments. *Actin* used as a reference. (D) Detecting the expression of Ubiquitin-Flag and AtPEN1-Myc proteins in *rre1* mutant. Proteins were extracted from the leaf materials in non denaturing buffer and immunoprecipitated by incubating with either anti-flag or anti-Myc antibody conjugated on agarose beads overnight. The unbound proteins were washed out using PBS and the remnants resolved in SDS PAGE. Protein detection was done by immunoblotting with either anti-Myc or anti-flag antibody.

After confirming the expression of the proteins in associated transgenic lines, an *in vivo* ubiquitination assay was set up. Plants were initially infected with *Bgh* and proteins extracted from both the infected and non infected leaves in non-denaturing buffer. Proteins were filtered in a micro-filter and immuno-precipitated with anti-Myc antibody. The retained proteins were washed in ice cold PBS to remove unbound proteins and resolved in SDS PAGE. Western blot analysis was undertaken by incubating with anti-flag antibody. Protein ubiquitination was shown as a uniform smear of increasing mass above AtPEN1 monomer. Plants over expressing RRE1 showed increased levels of AtPEN1 ubiquitination (Figure 4-12 lane 3), compared with plants lacking RRE1 (Figure 4-12 lane 1). Further the ubiquitination of AtPEN1 is enhanced in plants challenged with *Bgh* and less in absence of *Bgh* infection (Figure 4-12 lane 2). These findings indicate that the ubiquitination of AtPEN1 is highly dependent on RRE1 in relation to other E3 ligases present *in vivo*.

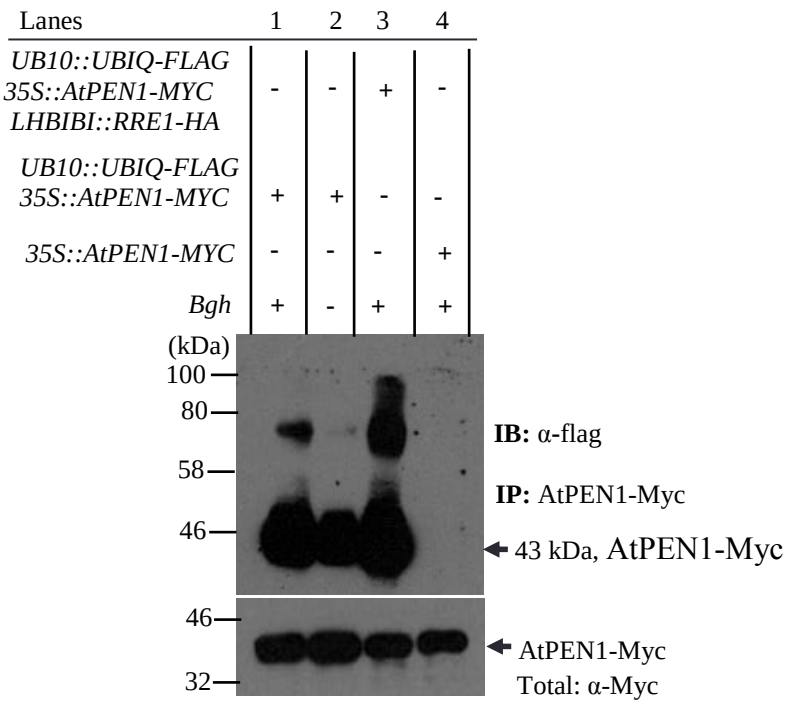


**Figure 4-12: Ubiquitination of AtPEN1 is enhanced in the presence of RRE1.** Constructs transformed into *rre1* plants were assessed for the ubiquitination of AtPEN1. Proteins were extracted from *rre1* lines expressing *UB10::UBIQ-FLAG 35S::AtPEN1-MYC LHBIBI::RRE1-HA* or *UB10::UBIQ-FLAG 35S::AtPEN1-MYC* after either infection or non infection with *Bgh* for 3 days. Extracted proteins were immunoprecipitated with anti-Myc antibody conjugated on agarose beads. The proteins were then washed in PBS and resolved in SDS PAGE. Detection of ubiquitination was performed by immunoblotting with anti-flag antibody. Ubiquitination was shown as high mass uniform smear above the AtPEN1-MYC. Lane 1, checking the ubiquitination of AtPEN1 in absence of RRE1, plants previously infected with *Bgh*. Lane 2, checking the ubiquitination of AtPEN1 in absence of RRE1, plants free from *Bgh* infection. Lane 3, checking the ubiquitination of AtPEN1 in presence of RRE1, plants previously infected with *Bgh*. Lane 4, proteins extracted from lines expressing *UB10::UBIQ-FLAG 35S::AtPEN1-MYC* were used as negative control. Loading controls were detected by immunoblotting with anti-Myc antibody. The experiment was repeated three times.

### 4.3.7 Identification of ubiquitination sites in AtPEN1

The protein sequence of AtPEN1 has 20 lysines (K), 17 of these lysines are surface exposed and 3 lysines are buried. Like all syntaxins AtPEN1 has a transmembrane domain at its C-terminal domain, none of the lysines are located within the transmembrane domain. In plant systems there is currently no information relating to the identification of ubiquitination sites in syntaxins. In mammalian systems ubiquitination sites were identified in human

syntaxin 3 and 5. The lysines identified preceded the transmembrane domain. Initially, a sequence alignment was generated of syntaxins from different plants compared to the human syntaxin 3 and 5. In plants, the lysines in the different syntaxins appear to be conserved across different species. In human syntaxins, the lysines that are close to the transmembrane domain are not perfectly conserved in plants however, they are in close proximity and lie within the same region (Figure 4-13).

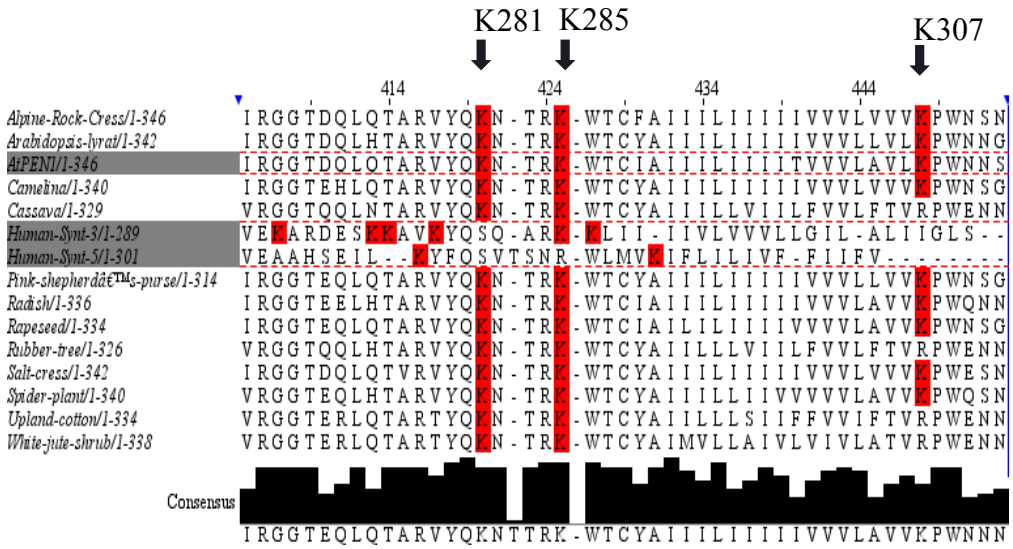


**Figure 4-13: Multiple sequence alignment of syntaxins.** AtPEN1 protein sequence was searched for at National Center for biotechnology Information (NCB1), then followed by blast search to obtain homologous protein accession numbers. The obtained accession numbers were further submitted in protein search window to obtain the protein sequences. The sequences were then submitted in T-coffee multiple sequence alignment program available at European molecular biology laboratory-European bioinformatics institute (EMBL-EBI) to generate protein alignment with settings left at default. Generated alignments were uploaded into Jalview software for further viewing. Lysines are highlighted in red. AtPEN1 and human syntaxins are in grey bars. K281, K285, and K307 corresponds to lysine positions in AtPEN1.

Based on the sequence alignment of AtPEN1 and human syntaxins, lysines (K) 281, 285 and 307 were selected as candidate sites for ubiquitination. Although K307 was not located before the transmembrane domain it was selected because it was located immediately after the transmembrane domain and was conserved across most plant species. Seven mutants of *AtPEN1-MYC* in form of *K281R*, *K285R*, *K307R*, *K281R-K285R*, *K281R-K307R*, *K285R-*

*K307R*, *K281R-K285R-K307R*, were generated using Golden Gate MoClo, where lysine was mutated to arginine. The mutated *AtPEN1* were verified by genotyping PCR and Sanger sequencing, all the desired mutations were successfully generated (Figure 4-14).

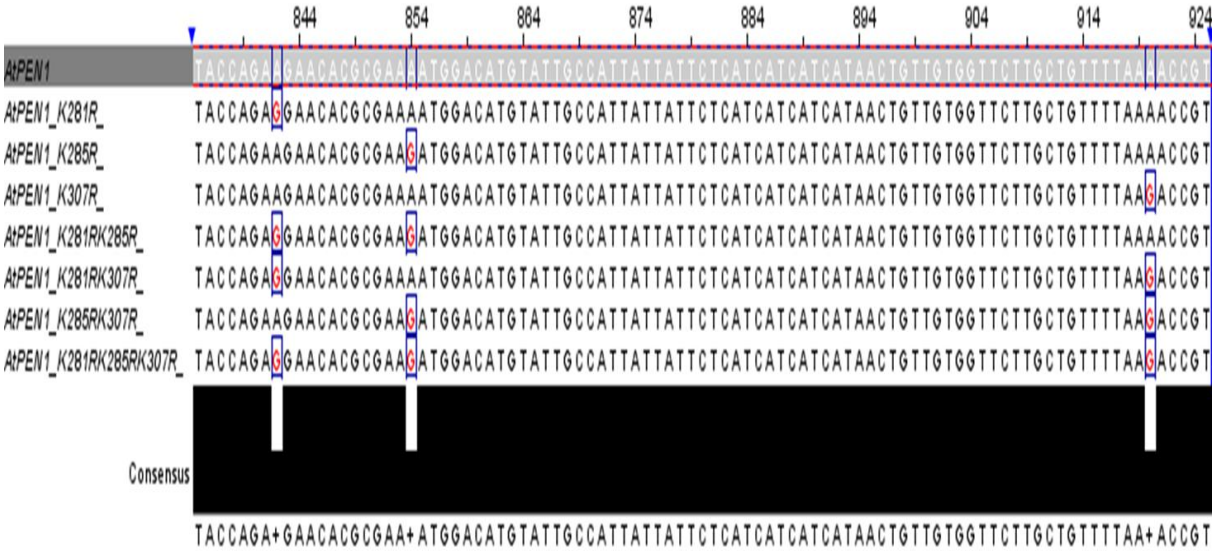


**Figure 4-14: Mutation of *AtPEN1* nucleotides for selected amino acid residues.** Nucleotide sequences for wild-type *AtPEN1* and the mutant variants were submitted into T-coffee multiple sequence alignment program available at EMBL-EBI to generate sequence alignments. Obtained alignments were uploaded into Jalview software for viewing and marking for clarity. In grey is the wild-type *AtPEN1*, the location of the mutations for K281, K285 and K307 respectively are shown in red. Sanger sequencing confirmed the correct mutation.

The mutated *AtPEN1* with a *MYC* tag was expressed by *35S CaMV* promoter and terminator combined with a *UBIQ-FLAG* under the *UBIQ* promoter and terminator using the Golden Gate MoClo. The full transcription units were subsequently ligated into the plant expression vector, confirmed by genotyping PCR, Sanger sequencing and then transformed into *Agrobacterium* GV3101 strain. To test for the ubiquitination sites, the *Agrobacterium* carrying the different constructs were grown, harvested and suspended in infiltration media. Bacteria at $O.D_{600\ nm}$ 0.2 was then infiltrated into the leaves of 3 week *N. benthamiana* plants. Proteins were extracted from the infiltrated leaves in non-denaturing conditions. The extracted proteins were filtered through Millipore filters, adjusted to the required

concentration and immuno-precipitated with anti-Myc antibody conjugated on agarose beads. Proteins were suspended in SDS loading buffer and resolved by SDS PAGE. Western blot analysis was carried out by incubating the membranes with anti-ubiquitin antibody. Ubiquitination was shown as a smear on AtPEN1 monomer. The first experiments indicated that mutation of *K281R* strongly decreased the ubiquitination of AtPEN1. However, the respective double mutations of *K281R* in form of *K281R-K285R*, *K281R-K307R*, *K285R-K307R* and triple mutation *K281R-K285R-K307R* did not strikingly change the level of AtPEN1 ubiquitination. No signal was detected with the empty vector (Figure 4-15 A). Ubiquitination levels were relatively quantified using ImageJ software and expressed as percentages (Figure 4-15 B)

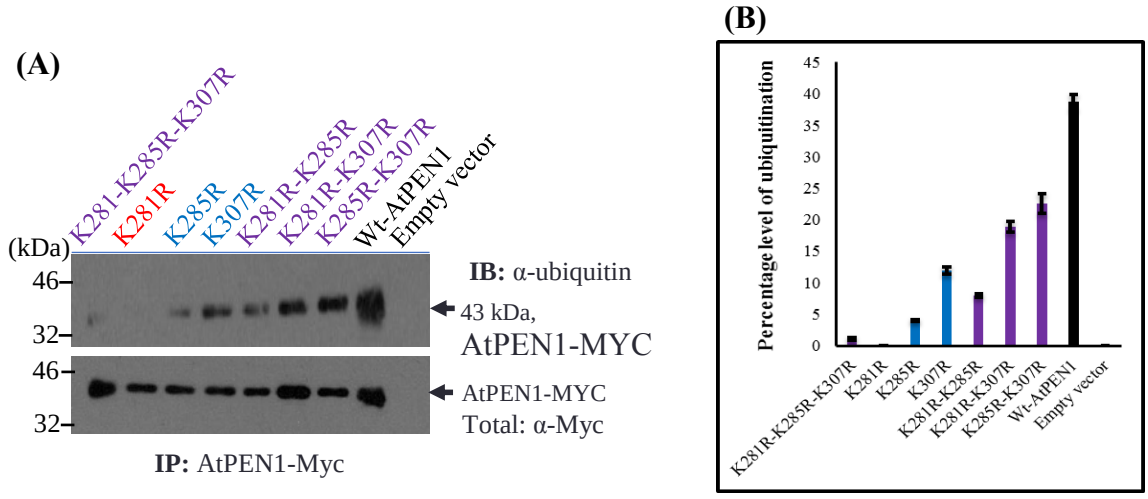


**Figure 4-15: Ubiquitination sites in AtPEN1.** (A) A western blot showing K281 as potential ubiquitination site in AtPEN1. *Agrobacterium* carrying genetic constructs of *UB10::UBIQ-FLAG* combined with either *35S::AtPEN1-MYC* or *AtPEN1* mutants in form *K281R*, *K285R*, *K307R*, *K281R-K285R*, *K281R-K307R*, *K285R-K307R*, *K281R-K285R-K307R*, were infiltrated in *N. benthamiana*. Proteins were extracted in non denaturing buffer from infiltrated leaves and immunoprecipitated with anti-Myc antibody conjugated on agarose beads. The immunoprecipitates were washed in PBS and resolved in SDS PAGE. Detection of ubiquitination was done by immunoblotting with anti-ubiquitin antibody. The absence or a decline in smear on AtPEN1-Myc indicated potential ubiquitination sites. Proteins extracted from *N. benthamiana* Agro-infiltrated with empty vector was used as negative control. Loading controls were detected by immunoblotting with anti-Myc antibody. (B) Histogram show the relative quantification of the level of ubiquitination using ImageJ software. The detected protein bands were relatively quantified using ImageJ software to generate numerical values and then

expressed as percentages. Error bars represent mean ±standard error. Experiment was repeated three times.

As the mutation of the lysines that were close to the transmembrane did not completely abolish the ubiquitination of AtPEN1, suggested that additional lysine(s) may be involved in the ubiquitination of AtPEN1. Lysine 103 suspected to be involved in AtPEN1 membrane recycling (personal communication by Hans Thordal-Christensen) and also exhibit the highest score based on prediction of ubiquitination sites with Bayesian discriminant method (Xue *et al*, 2006), was selected to be added on the list of lysines for investigation. Sequence alignment was accomplished, this lysine is located far from the transmembrane, but it is highly conserved among the syntaxins in different plant species (Figure 4-16).

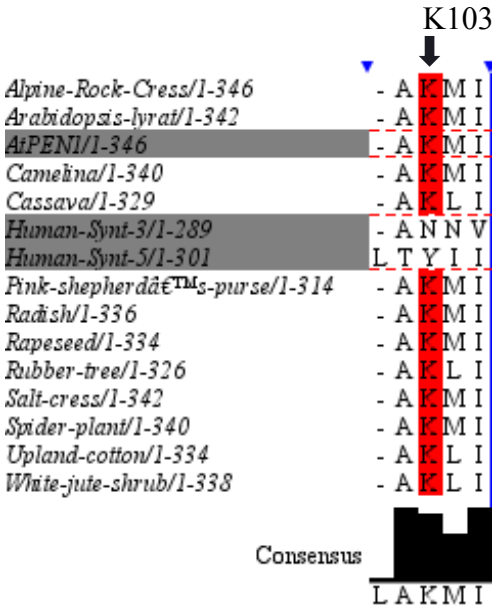


**Figure 4-16: AtPEN1-K103 is conserved among plant species.** AtPEN1 protein sequence was searched for at NCB1, then followed by blast search to obtain homologous protein accession numbers. The obtained accession numbers were further submitted in protein search window to obtain the protein sequences. The sequences were then submitted in T-coffee multiple sequence alignment program available at EMBL-EBI to generate protein alignment with settings left at default. Generated alignments were uploaded into Jalview software for further viewing. The wild-type AtPEN1 and human syntaxins are shown in grey. K103 is highlighted in red corresponding to lysine position in AtPEN1, located relatively far from the AtPEN1 transmembrane domain.

*K103* was mutated to generate *AtPEN1-K103R* by site directed mutagenesis on the wild-type construct. A tetra mutant construct of *AtPEN1-K103R-K281R-K285R-K307R* was also generated by site directed mutagenesis on the previously made triple mutant construct *AtPEN1-K281R-K285R-K307R*. The mutants were confirmed by genotyping PCR and Sanger sequencing (Figure 4-17 A and B).

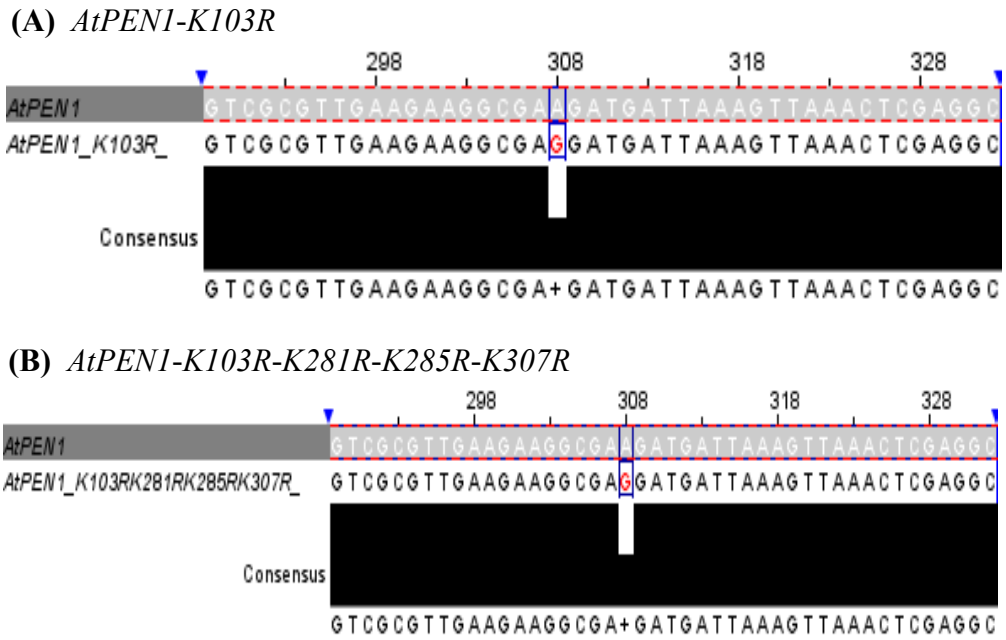


**Figure 4-17: Mutation of *AtPEN1* to *AtPEN1-K103R* sequence alignment.** Nucleotide sequences for wild-type *AtPEN1* and the mutant variants were submitted into T-coffee multiple sequence alignment program available at EMBL-EBI to generate sequence alignments. Obtained alignments were uploaded into Jalview software for viewing and markings for clarity. (A) Single mutation for *AtPEN1-K103R*, nucleotide highlighted in red. (B) Tetra mutation for *AtPEN1-K103R-K281R-K285R-K307R* highlighted in pink. Sanger sequencing confirmed the correct mutations.

The generated constructs were transformed into *Agrobacterium* using the freeze-thaw method. To check for ubiquitination, all the AtPEN1 generated mutants were infiltrated in *N. benthamiana* and the extracted proteins subjected to immuno-precipitation with anti-Myc antibody conjugated on agarose beads. The SDS PAGE resolved proteins were subjected to western blotting and analyzed with anti-ubiquitin antibody. Ubiquitination was shown as a

smear on AtPEN1 monomer. The mutation of *K103R* and *K281R* decreased the ubiquitination of AtPEN1, while the tetra mutation abolished AtPEN1 ubiquitination. As with previous results, the double mutations and single mutation of *K285R* and *K307R* did not affect the level of AtPEN1 ubiquitination (Figure 4-18 A). Levels of ubiquitination were relatively quantified using ImageJ software and expressed as percentages (Figure 4-18 B).

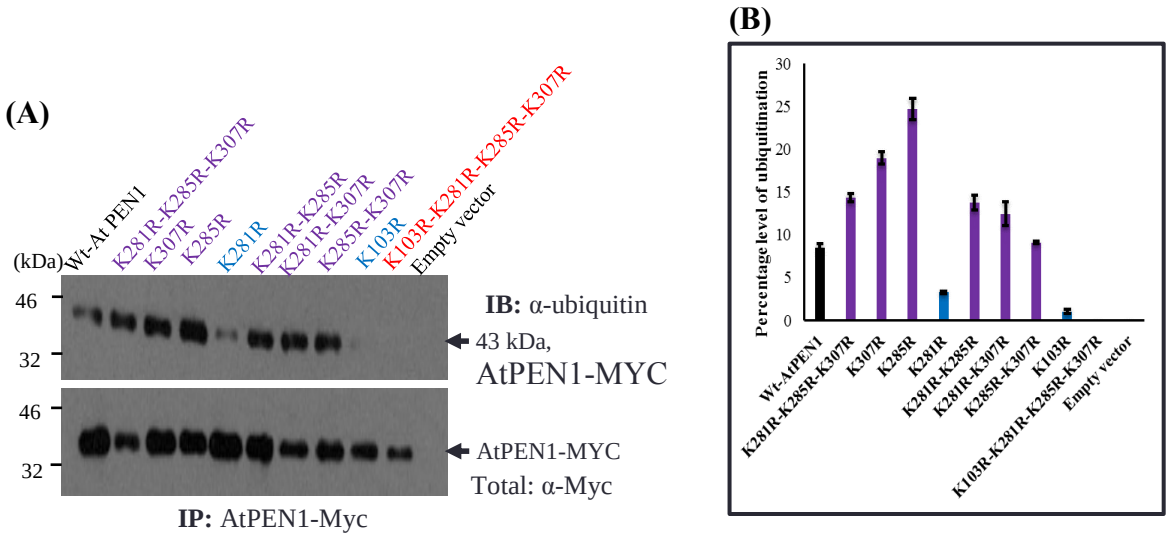


**Figure 4-18: Tetra mutation of the selected lysines abolished AtPEN1 ubiquitination.** (A) *Agrobacterium* carrying genetic construct *UB10::UBIQ-FLAG* combined with either *35S::AtPEN1-MYC* or *AtPEN1* mutants in form of *K103R*, *K281R*, *K285R*, *K307R*, *K281R-K285R*, *K281R-K307R*, *K285R-K307R*, *K281R-K285R-K307R*, *K103R-K281R-K285R-K307R* was infiltrated in *N. benthamiana* leaves. Proteins extracted in non denaturing buffer were incubated with anti-Myc antibody conjugated on agarose beads. The immunoprecipitated proteins were washed with PBS and later separated in SDS PAGE. Detection of ubiquitination was done by immunoblotting with anti-ubiquitin antibody and is shown as smear on AtPEN1-Myc. Detection of potential ubiquitination sites was based on mutated sites showing either a decline or absence of smear. Proteins extracted from *N. benthamiana* leaves infiltrated with empty vector was used as negative control. Loading controls were detected by immunoblotting with anti-Myc antibody. (B) Histogram showing the relative quantification of the level of ubiquitinations using ImageJ software. Protein bands corresponding to the area of ubiquitination was relatively quantified by ImageJ software and numerical values expressed as percentages. Error bars represent mean ± standard error. Experiment repeated three times.

The reduction in the level of AtPEN1 ubiquitination following the mutation of either *K103* or *K281* and the complete loss of ubiquitination with the tetra mutation suggested that K103 and K281 are the ubiquitination sites in AtPEN1. To confirm this position, a double

mutant of *AtPEN1-K103R-K281R* was generated by site directed mutagenesis on the previously made *AtPEN1-K281R* construct. The construct was confirmed by genotyping PCR and verified by Sanger sequencing (Figure 4-19).

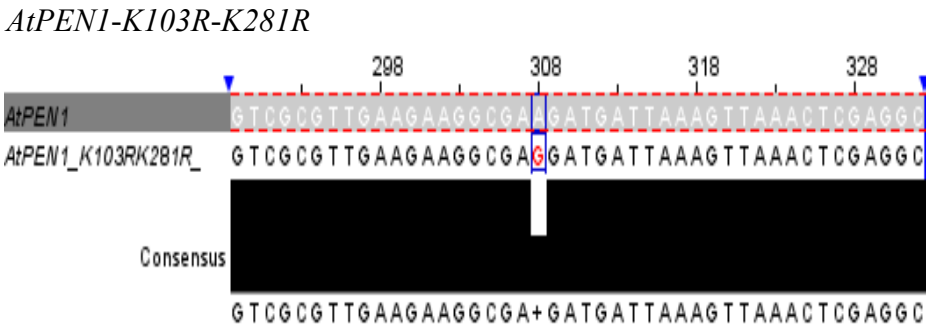


**Figure 4-19: Mutation of *K103* in *AtPEN1-K281R* sequence alignment.** Nucleotide sequences for wild-type *AtPEN1* and the mutant variant (*K103R-K281R*) were submitted into T-coffee multiple sequence alignment program available at EMBL-EBI to generate sequence alignments. Obtained alignments were uploaded into Jalview software for viewing and markings for clarity. The nucleotide site mutation is highlighted in red. Sanger sequencing confirmed the correct mutation, *K103R* mutation.

The resulting genetic construct was transformed in *Agrobacterium* and transformants were confirmed by genotyping PCR. To confirm the effect on AtPEN1 ubiquitination, wild-type *AtPEN1*, *AtPEN1-K103R*, *AtPEN1-K281R* and *AtPEN1-K103R-K281R* genetic constructs were infiltrated in *N. benthamiana*. Proteins were extracted from the infiltrated leaves and subjected to immuno-precipitation with anti-Myc antibody. The proteins were separated by SDS PAGE and western blot analysis conducted as already described. Ubiquitination was shown as a smear on AtPEN1 monomer. The single mutations decreased the level of AtPEN1 ubiquitination. In contrast, the double mutation completely abrogated AtPEN1 ubiquitination (Figure 4-20 A). The levels of ubiquitination were relatively quantified using ImageJ software and expressed as percentages (Figure 4-20 A). This result suggests that K103 and K281 are ubiquitination sites in AtPEN1.

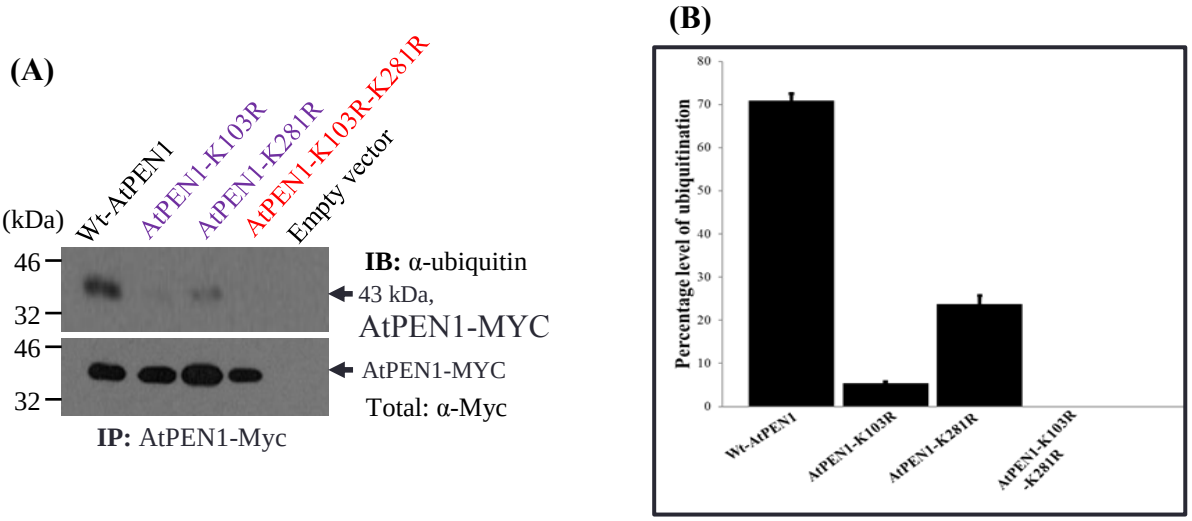


**Figure 4-20: *AtPEN1-K103R-K281R* mutation leads to complete loss of ubiquitination.** (A) *Agrobacterium* carrying genetic construct *UB10::UBIQ-FLAG* combined with either *35S::Wt-AtPEN1-MYC* or *AtPEN1* mutants in form of *K103R*, *K281R*, *K103R-281R* was infiltrated in *N. benthamiana* leaves. Proteins were extracted in non denaturing buffer and immunoprecipitated with anti-Myc antibody conjugated on agarose beads. Immunoprecipitated proteins were washed in PBS and resolved in SDS PAGE. Ubiquitination was detected by immunoblotting with anti-ubiquitin antibody and was shown by the formation of smear on AtPEN1-Myc. The loss of smear following the mutation of lysine sites indicate potential ubiquitination site. Protein extracted from *N. benthamiana* transformed with empty was used as negative control. Loading controls were detected by immunoblotting with anti-Myc antibody. (B) Histogram displays the relative quantification of the level of ubiquitination using ImageJ software. Protein bands were relatively quantified by ImageJ software and the numerical values corresponding to the area of ubiquitination expressed as percentages. Error bars represent mean ± standard error. Experiment was repeated three times.

The single combined genetic construct *UB10::UBIQ-FLAG 35S::AtPEN1-K103R-K281R-MYC* was transformed into *pen1-1* mutant background. Regenerated transgenic homozygous plants were checked for the expression of the proteins by immuno-precipitation as earlier described. Successful protein expressions were detected in the homozygous lines with non-pronounced relative differences for *AtPEN1-K103R-K28R-MYC*. For *UBIQ-FLAG* relative differential protein expression were exhibited (Figure 4-21 A). Lines displayed relatively higher protein expressions were applied in assessing the ubiquitination of AtPEN1. Immunoblotting with anti-ubiquitin antibody displayed the loss of AtPEN1 ubiquitination

where the sites K103 and K281 were mutated to arginine (Figure 4-21 B lane 5), while the wild-type exhibited polyubiquitination shown by high molecular mass smear above the monomer (Figure 4-21 B lane 4).

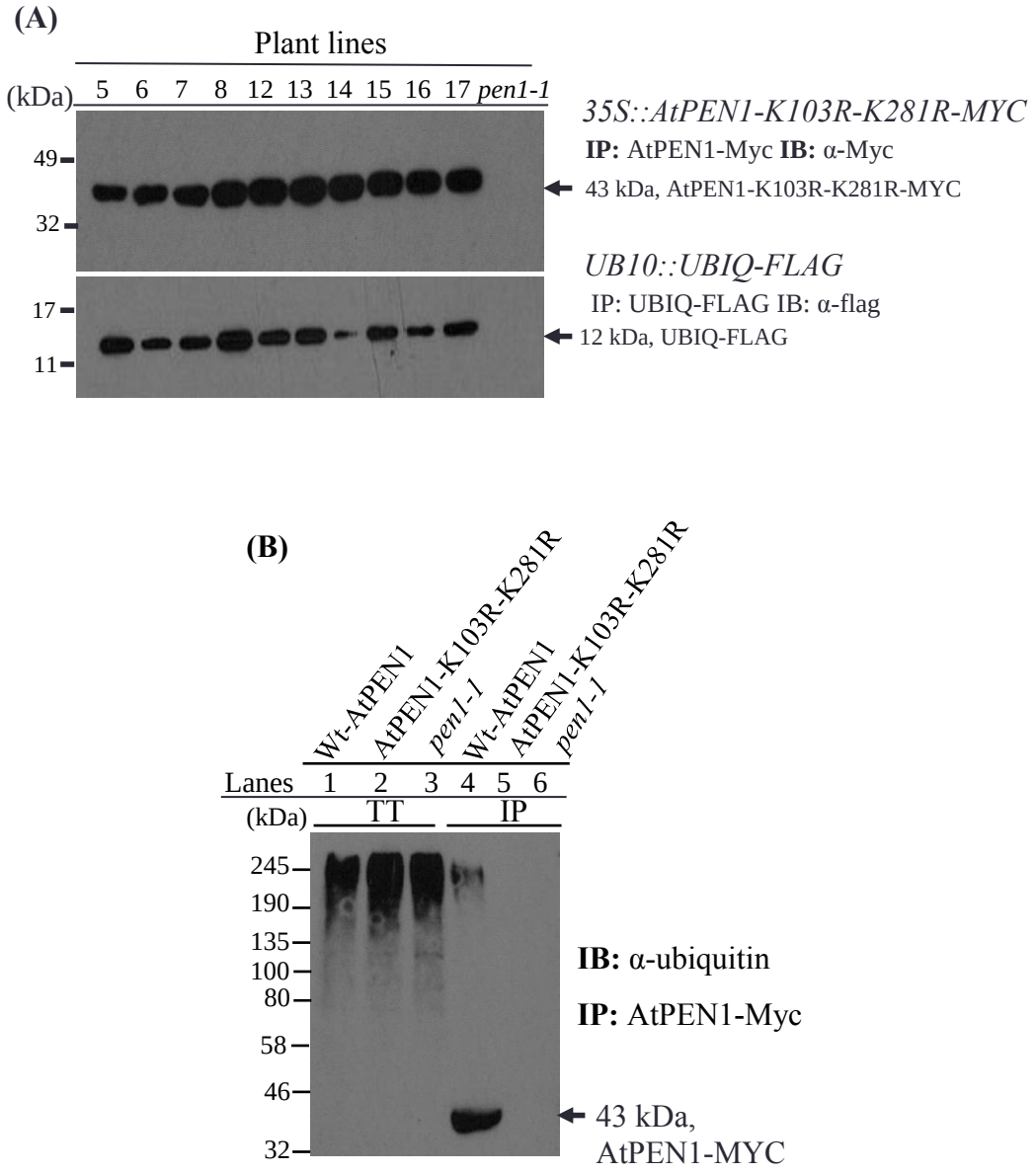


**Figure 4-21: Protein expression detection and ubiquitination assessment in AtPEN1-K103R-K281R.** (A) Detecting the expression of Ubiquitin-Flag and AtPEN1-K103R-K281R-Myc proteins in the homozygous lines. Proteins were extracted from the generated lines and immunoprecipitated with either anti-flag or anti-Myc antibody conjugated on agarose beads. Unbound proteins were washed off using PBS and retained proteins resolved in SDS PAGE. Detection of protein expression was performed by immunoblotting with either anti-flag antibody or anti-Myc antibody. Lane 1, checking ubiquitination on total protein extracted from plants expressing wild-type AtPEN1. Lane 2, checking ubiquitination on total protein extracted from plants expressing mutated AtPEN1, Lane 3, checking ubiquitination on total protein extracted from *pen1-1* mutants.

Lane 4, checking ubiquitination on protein immunoprecipitated from plants expressing wild-type AtPEN1. Lane 5, checking ubiquitination on protein immunoprecipitated from plants expressing mutated AtPEN1. Lane 6, Proteins immunoprecipitated from *pen1-1* was used as negative control. (B) Double mutation of *K103R* and *K281R* reveal loss of polyubiquitination of AtPEN1. *Arabidopsis* plants expressing *UB10::UBIQ-FLAG 35S::AtPEN1-MYC, UB10::UBIQ-FLAG 35S::AtPEN1-K103R-K281R-MYC* and *pen1-1* were initially inoculated with *Bgh* and incubated for 3 days. Proteins were extracted from the leaf tissues and immunoprecipitated with anti-Myc antibody conjugated on agarose beads. Immunoprecipitated proteins (IP) were washed in PBS and resolved in SDS PAGE in parallel with total protein (TT). Detection of ubiquitination was done by immunoblotting with anti-ubiquitin antibody. Ubiquitination was shown as high mass smear above AtPEN1-Myc monomer. Potential ubiquitination sites were shown by absence of smear. Proteins immunoprecipitated from *pen1-1* mutant was used as negative control. Experiment was repeated three times.

### 4.4 Discussion

The ubiquitination system plays a vital role not only in catabolizing aberrant proteins but also for functional modification of substrates (Chen & Sun, 2009; Cai *et al*, 2018). The E3 ligases as a component of the system ensure that the correct substrate is selected and subsequently decorated with ubiquitin (Chaugule & Walden, 2016). In plant systems the E3 ligase targets are now only beginning to emerge despite the enormous numbers of E3 ligases (Stone *et al*, 2005; Hua & Vierstra, 2011). I attempted to unveil the substrate of RRE1, initially by checking the ability to interact with its co-expressed partner AtPEN1. My results revealed a physical interaction of RRE1 and AtPEN1. The interaction occurred predominately with the RRE-Ankyrin domain. The hydrophobic nature of the two proteins supported by ankyrin repeats in RRE1 and a transmembrane domain in AtPEN1 are likely to govern the observed interactions. Moreover, the transmembrane domain is essential for the functionality of syntaxins. In mammalian systems the transmembrane domain was shown to be critical for protein-protein interactions and its deletion reduced these interactions (Lewis *et al*, 2001). To date, only limited information exists about the interaction of syntaxins with their target proteins in plants. Previous studies have revealed the interaction of

AtPEN1/Syp121 with its partners, the Vesicle associated membrane protein (VAMP) and Synaptosomal associated protein (SNAP) family proteins to form a Soluble NSF (N-ethylmaleimide-sensitive factor) attachment protein receptor (SNARE) complex important in membrane fusion in diverse trafficking pathways (Reichardt *et al*, 2011a). However, in mammalian systems the interaction of Tomosyn with syntaxin regulates SNARE mediated neuronal exocytosis (Bielopolski *et al*, 2014). My data implies that the interaction of RRE1 and AtPEN1 might enhance the ability of AtPEN1 to mediate vesicle membrane fusions.

The co-expression of RRE1 with AtPEN1 during infection and the strong interactions were suggestive of AtPEN1 as a substrate for RRE1. Indeed, my results showed AtPEN1 was a direct substrate for RRE1 (Figure 4-6, 4-7, 4-9). AtPEN1 is localised throughout the plasma membrane in absence of pathogen challenge and accumulates at the site of attempted *Bgh* penetration during pathogen infection (Collins *et al*, 2003). My results lead to the hypothesis that the ubiquitination of AtPEN1 by RRE1 drives the re-localization of AtPEN1 to the site of *Bgh* ingress to mediate the exocytosis of antimicrobial agents. In human cells Syntaxin 3 (Stx-3) is localized and functions at the apical plasma membrane of epithelial cells. The ubiquitination of Syntaxin 3 results in its removal from the basolateral membrane to achieve apical polarity and participates in the recruitment of cargo to the exosomes (Giovannone *et al*, 2017). I also suggest that the ubiquitination of AtPEN1 is mediated by RRE1 (Figure 4-12). Hence the observed decline of AtPEN1 ubiquitination in *rre1* plants. Given the large number of E3 ligases present in the *Arabidopsis* genome the RRE1 paralog, RRE2, might also to a lesser extent, mediate the ubiquitination of AtPEN1 (Smalle & Vierstra, 2004; Stone *et al*, 2005; Yu, 2012).

The unveiling of the ubiquitination site(s) within AtPEN1 is an important step to help uncover the functional relevance of AtPEN1 ubiquitination. AtPEN1 has 20 lysines (K) and 17 of them are surface exposed. In plants there is no information related to the ubiquitination

sites of syntaxin proteins despite their wide conservation across kingdoms. In humans, ubiquitination sites were identified in syntaxins 3 and 5 (Huang *et al*, 2016; Giovannone *et al*, 2017). All these sites were close to the transmembrane domain at the C-terminus of syntaxin 3 and 5. In these syntaxins the transmembrane was important for the ubiquitination, as the truncated protein lacking this sequence was insensitive to ubiquitination, despite the presence of other potential lysine target sites (Huang *et al*, 2016; Giovannone *et al*, 2017). This suggests that membrane anchorage is required for the occurrence of ubiquitination. I identified lysines 103 and 281 as the ubiquitination sites in full length AtPEN1 (Figure 4-20 A, 4-21 A). In human syntaxin 3, six lysines were revealed to be the sites for ubiquitination (Giovannone *et al*, 2017). In AtPEN1 the ubiquitination sites are relatively distant from each other. Studies in *Saccharomyces cerevisiae* have also revealed the occurrence of ubiquitination sites in different areas of the protein secondary structure, for-example in β-strand, α-helix and loop. It is anticipated that E3 ligase binds the substrate towards a preferred ubiquitination site leading to different functional modifications (Hitchcock *et al*, 2003; Peng *et al*, 2003b; Catic *et al*, 2004; Sadowski & Sarcevic, 2010). K103 was previously anticipated to be important in the recycling of AtPEN1. Hence it is logical to postulate that the binding of RRE1 towards K103 in AtPEN1 could result in recycling/activation while the binding towards K281 could lead to proteasome degradation.

# Chapter five

## 5.0 The consequences of AtPEN1 ubiquitination mediated by RRE1

### 5.1 Introduction

Ubiquitination is post translation modification of proteins involving the addition of ubiquitin to the selected target substrate (Callis, 2014). The attached ubiquitin can in turn also be ubiquitinated forming polyubiquitin chains although single ubiquitin attachment leading to mono-ubiquitination is also possible (Suryadinata *et al*, 2014). Different fates of the substrate occur depending on the nature of ubiquitin modification. Polyubiquitin linkages occurring at sites lysine (K) 48 and K63 are the most abundant (Kwon & Ciechanover, 2017). The attachment of K48 linkage is known to signal 26S proteasome degradation (Sharma *et al*, 2016; Zhou & Zeng, 2017). Conversely, K63 chain linkages are associated with protein activation, membrane trafficking, endocytosis, recently in autophagy-vacuolar degradation (Martins *et al*, 2015; Kwon & Ciechanover, 2017).

In order for any of these events to proceed, E3 ligases play the central role of ensuring the right substrate is selected. The vast number of E3 ligases in *Arabidopsis* genome (>1300) ensure specificity of substrate selection (Stone *et al*, 2006; Yee & Goring, 2009). Of these E3 ligases over 600 belong to the Really interesting new gene (RING) type, many of which are known to mediate protein ubiquitination (Stone *et al*, 2005). Unlike the Homologous to the E6-AP (E6-associated protein) carboxyl terminus (HECT) type of E3 ligases that directly transfer the ubiquitin to the selected substrate, the RING type bind the E2 and the substrate at their conserved RING domain (Stone *et al*, 2006). The transfer of the ubiquitin to the selected substrate is completed by the E2 (Callis, 2014). RRE1 is a RING type of E3 ligase and in that context, it binds AtPEN1 and later conjugates this target with ubiquitin by the action of an E2, possibly *Arabidopsis thaliana* ubiquitin conjugating enzyme 1 (AtUBC1).

I have demonstrated that Redox regulated E3 ligase 1 (RRE1) mediates the ubiquitination of *Arabidopsis thaliana* PENETRATION 1 protein (AtPEN1). In this chapter I attempt to dissect the possible fate of ubiquitinated AtPEN1 and the possible implications for plant immunity.

## 5.2 Materials and methods

### 5.2.1 Mode of ubiquitin chain linkages ligated on AtPEN1 *in vitro*

The ubiquitination assays was performed as described by Sato *et al*, (2009). To determine the mode of polyubiquitination, a 30 µl reaction was set up containing: 10 ng/µl E1, 3 ng/µl of purified E2 (AtUBC1), 3 ng/µl of purified GST-RRE1, 0.099 ng/µl AtPEN1, 1x reaction buffer, 6.7 mM adenosine triphosphate (ATP), and either 66 ng/µl Histidine 6 ubiquitin K48 only or 66 ng/µl Histidine 6 ubiquitin K63 only (Human Boston Biochem) and autoclaved double distilled water (dd$H_2O$). Further steps are as described in section 2.10. Other experiments involving, determining the ability of purified 20S proteasome subunit α7 to bind the ubiquitinated AtPEN1, assessing the ability of the impurified 26S proteasome in cell extracts to bind the polyubiquitinated AtPEN1 and assessing the ability of the 26S proteasome to degrade the polyubiquitinated AtPEN1 were carried out as described in section 2.10, with ubiquitination reactions set up as described above.

### 5.2.2 Genetic constructs for *in vivo* investigations of the mode of ubiquitination

*In vivo* experiments in *Nicotiana benthamiana* and *Arabidopsis* were made by generating genetic constructs using Golden Gate modular cloning (MoClo) (Weber *et al*, 2011; Engler *et al*, 2014). *AtPEN1*, wild-type *UBIQUITIN* (*UBIQ*) and its mutants *K48R*, *K63R*, *K48R-K63R*, were amplified from Col-0 complementary deoxyribonucleic acid (cDNA) using primers sets in (Table 4). Amplified fragments of *AtPEN1*, wild-type *UBIQ* and its mutants *K48R*, *K63R*, *K48R-K63R* were cloned in *pAGM1287*. For level 1

construction *AtPEN1* from *pAGM1287* was ligated with *MYC* tag, *CaMV 35S* promoter and *CaMV 35S* terminator in *pICH47751* vector. For level 1 construction wild-type (wt) *UBIQ* and its mutants *K48R, K63R, K48R-K63R* from *pAGM1287* were ligated with *FLAG* tag, *UBIQ10* promoter and *UBIQ5* terminator in *pICH47751*. Finally, all full transcription units of *Kanamycin* resistance (*pICSL11024*), *AtPEN1,* wild-type *UBIQ* and its mutants *K48R, K63R, K48R-K63R* and endlinker 3 (*pICH41766*) were ligated in *pAGM4723*. Vectors and modules used, enzymes used, reaction set up and reaction conditions are as described in section 2.11. *Arabidopsis* plants transformed with the above constructs were generated as described in section 2.12.

### 5.2.3 *In vivo* polyubiquitination of AtPEN1 with K48, K63 ubiquitin chain linkages

#### 5.2.3.1 Transient expression in *N. benthamiana*

The procedure was performed as described by Liu *et al*, (2016). Initial steps for growth and harvest of *Agrobacterium* carrying the constructs in section 5.2.2 were performed as described in section 2.13. The harvested pellet was washed once in infiltration media containing methyl ester sulfonates (MES) 10 mM pH 5.2, $MgCl_2$ 10 mM and acetosyringone 0.2 µM to remove residual antibiotics. The pellet was suspended in 0.5 ml infiltration media and $O.D_{600\ nm}$ adjusted to 1. The bacteria suspensions were then infiltrated in the leaves of 3 weeks old *N. benthamiana* plants and incubated for 2 days before protein extraction.

#### 5.2.3.2 Protein extraction from plants and co-immunoprecipitation assays

Proteins were extracted from 4 g of 3 weeks-old *Arabidopsis* leaves and from 2 g of Agro-infiltrated *N. benthamiana* leaves. The leaves were harvested and immediately frozen in liquid nitrogen. For ubiquitination assays in *Arabidopsis* plants were initially inoculated with *Bgh* spores and incubated for 3 days before harvesting. The leaves were then finely ground in

liquid nitrogen before further crushed in extraction buffer described in section 2.15. The rest other steps are as described in section 2.15.

For co-immunoprecipitation assays, the protein suspensions were filtered through 0.4 µM millipore filters and protein concentrations determined using the Bradford reagent (Bio-Rad). The proteins were adjusted to 350 µg using the extraction buffer. The diluted proteins were incubated appropriately with 2 µg of either anti-Myc or anti-flag antibody conjugated on agarose beads over night at 4$^{o}$C on a roller. Other steps as described in section 2.15. Finally, proteins were boiled in 1x SDS loading dye containing 10% β-Mercaptoethanol at 95$^{o}$C for 5 minutes. The rest of steps are described in section 2.15.

### 5.2.4 SDS PAGE and western blot analysis

Sodium dodecyl sulfate-Polyacrylamide gel electrophoresis (SDS PAGE) and western blot analysis were carried out as described by Sambrook *et al*, (2012). Proteins were separated in 10%, (for ubiquitination assays and detection of AtPEN1-Myc) or 15% (for detection of ubiquitin) SDS PAGE bound with a stacking gel. Other steps involved are as described in section 2.16. The membrane was initially incubated with anti-Myc antibody or anti-flag antibody for 1 hour and followed by 3 times washing with phosphate buffered saline-tween 20 (PBS-T) at 10 minutes interval. Then re-incubated with anti-mouse immunoglobin G horseradish peroxidase (IgG HRP) antibody for 1 hour followed by 3 times washing with PBS-T. List of antibodies shown in (Table 3). Preceded steps are as described in section 2.16.

### 5.2.5 Statistical analysis

For comparison of means, data was analyzed using Microsoft Excel student *t*-Test assuming unequal variances. Comparison of the differences between means were done using

one-way Analysis of variance (ANOVA) and Tukey's statistics of the Minitab 18 statistical package. Statistical significance was reported at either $P < 0.05$ or $P < 0.001$.

## 5.3 Results

### 5.3.2 Revealing the ubiquitin chain linkage during AtPEN1 ubiquitination

#### 5.3.2.1 AtPEN1 polyubiquitinated at K48 or K63 ubiquitin sites *in vitro*

The polyubiquitination of target proteins by different inter-ubiquitination chain linkages results in a number of different outcomes. K48 polyubiquitin linkage has been reported to target proteins for proteasomal degradation, while K63 polyubiquitin is associated with functional modifications. To determine the ubiquitin linkages formed on ubiquitinated AtPEN1 an *in vitro* assay involving ubiquitin mutants was utilized. As polyubiquitin linkages at K48 or K63 ubiquitin sites is by far the most widespread, polyubiquitination at these residues was investigated. The reactions were carried out with enzymes E1 (Human), E2 (AtUBC1) and E3 (RRE1), AtPEN1 as the substrate and ATP all in the same reaction buffer. Histidine tagged ubiquitin proteins where all the lysine residues were mutated to arginine except either K48 or K63 were utilized. After incubation, the reactions were stopped by adding SDS loading buffer and separated by SDS PAGE. Western blot analysis was undertaken by exposing the membrane to anti-polyhistidine antibody. Polyubiquitination is shown as uniform smear of increasing mass above the substrate. Polyubiquitin chains were detected in both reactions having either ubiquitin K48 or K63 (Figure 5-1 lanes 1 and 2), indicating that AtPEN1 polyubiquitination occur at both K48 and K63 ubiquitin sites. No polyubiquitination detected in control assays missing one of the components for the reactions (Figure 5-1 lanes 3, 4, 5 and 6).

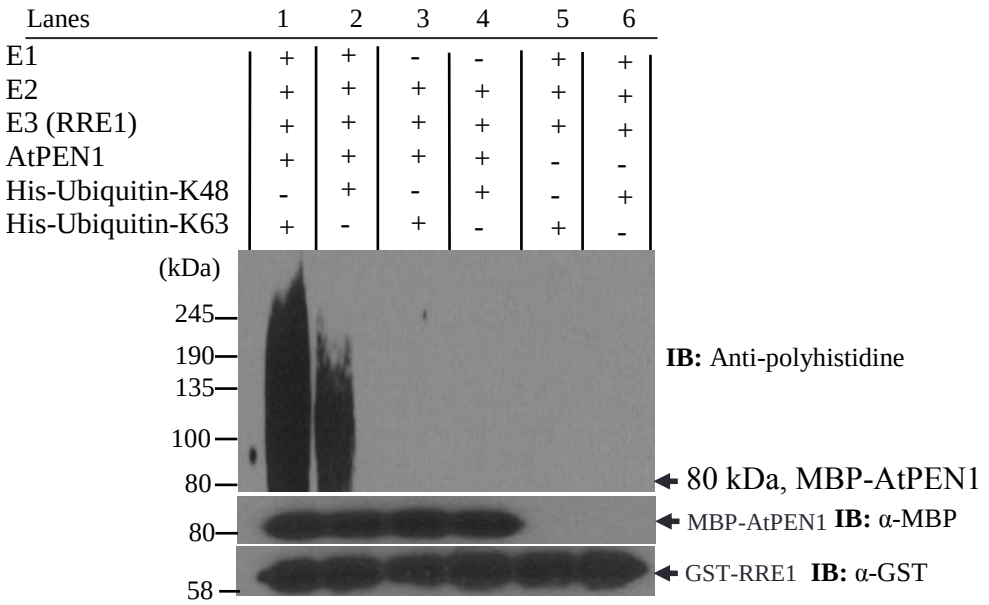


**Figure 5-1: K48 and K63 polyubiquitin chain formation on AtPEN1.** *In vitro* ubiquitination assay was carried out in a reaction containing E1, E2, RRE1 as E3, MBP-AtPEN1 as substrates, with either histidine-ubiquitin K48 only or histidine-ubiquitin K63 only. After incubation of the reactions, the proteins were resolved in SDS PAGE and ubiquitination detected by immunoblotting with anti-polyhistidine antibody. Ubiquitination was shown as high molecular mass uniform smear above MBP-AtPEN1 monomer. Lane 1, checking the polyubiquitination of AtPEN1 with K63 chain linkages. Lane 2, Checking the polyubiquitination of AtPEN1 with K48 chain linkages. Reactions lacking either E1 (lanes 3 and 4) or MBP-AtPEN1 (lanes 5 and 6) were used as negative control. Loading controls were detected by immunoblotting with either anti-GST antibody or anti-MBP antibody. Experiment was repeated three times.

### 5.3.2.2 AtPEN1 is polyubiquitinated at K48 and K63 ubiquitin sites *in vivo*

Genetic constructs were generated to investigate the formation of polyubiquitin on AtPEN1 *in vivo*. Full transcription units of *UBIQUITIN-FLAG* were generated as wild-type *UBIQ-FLAG*, *UBIQ-K48R-FLAG*, *UBIQ-K63R-FLAG* and *UBIQ-K48R-K63R-FLAG* under the *UBIQ* promoter and terminator. These constructs were fused with the full transcriptional unit of *AtPEN1-MYC* expressed under the *CaMV 35S* promoter and terminator via Golden Gate MoClo. Transcription units were finally ligated into the plant expression vector and transformed in *Agrobacterium* GV3101. The vector was transiently transformed into *N. benthamiana* by infiltrating the abaxial leaf surfaces. The expressed proteins were immuno-

precipitated with an anti-Myc antibody conjugated on agarose beads and later washed in ice cold PBS. The retained proteins were subsequently separated by SDS PAGE and analyzed by a western blot by incubating with anti-flag antibody. Loss of polyubiquitination was shown by absence of uniform smear of increasing molecular mass on AtPEN1. The analysis indicated that the polyubiquitination of AtPEN1 may only be mediated by K48 or K63 ubiquitin sites *in vivo*. The mutation of both sites to arginine resulted in the loss of polyubiquitination of AtPEN1 (Figure 5-2 lane 3). Single mutations of either K48 or K63 led to the decline in the level of polyubiquitination but did not completely abrogate polyubiquitination (Figure 5-2 lane 2 and 4). In absence of K48 and K63 mutations, the level of polyubiquitination is elevated (Figure 5-2 lane 1).

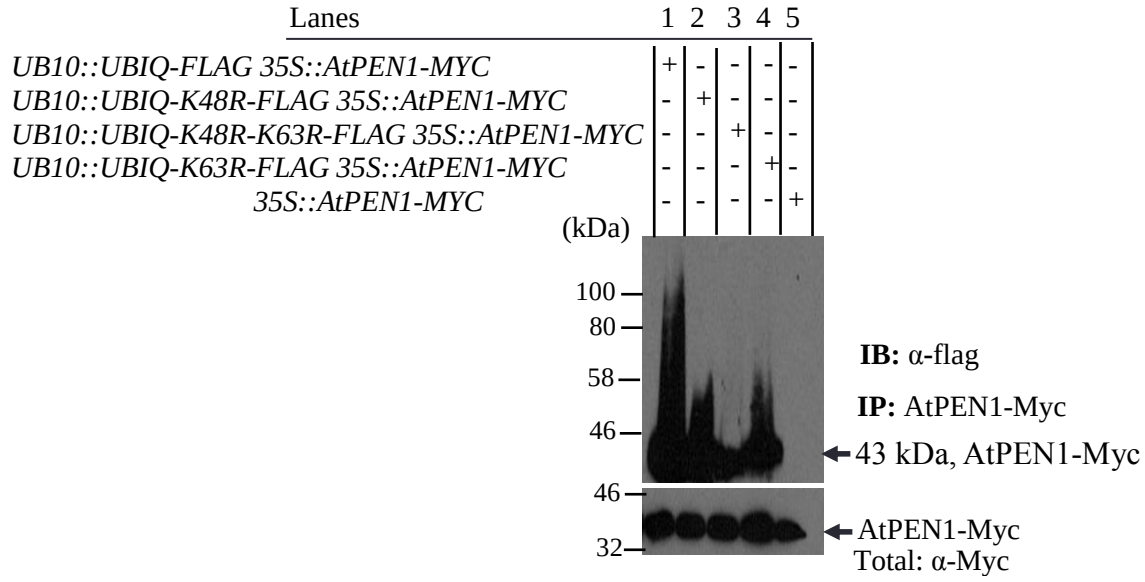


**Figure 5-2: *In vivo* polyubiquitination of AtPEN1 at either K48 or K63 ubiquitin sites.** *Agrobacterium* carrying genetic constructs: *UB10::Wt-UBIQ-FLAG*, *UB10::UBIQ-K48R-FLAG*, *UB10::UBIQ-K48R-K63R-FLAG*, *UB10::UBIQ-K63R-FLAG* fused with *35S::AtPEN1-MYC* was infiltrated in *N. benthamiana*. Proteins were later extracted from infiltrated leaves and immunoprecipitated with anti-Myc antibody conjugated on agarose beads. The proteins were washed in PBS and bound proteins resolved in SDS PAGE. Detection of ubiquitination was then done by immunoblotting with anti-flag antibody and was shown by the formation of a uniform high mass smear above the AtPEN1-Myc protein. Lane 1, checking the ubiquitination of AtPEN1 with wild-type ubiquitin. Lane 2, checking the ubiquitination of AtPEN1 with ubiquitin-K48R mutant. Lane 3, checking the ubiquitination of AtPEN1 with ubiquitin-K48R-K63R mutant. Lane

4, checking the ubiquitination of AtPEN1 with ubiquitin-K63R mutant. Lane 5, proteins extracted from leaves infiltrated with *35S::AtPEN1-MYC* was used as negative control. Loading controls were detected by immunoblotting with anti-Myc antibody. The experiment was repeated three times.

Further, the constructs were transformed in *Arabidopsis pen1-1* plants to generate stable transgenic lines. The homozygous lines were checked for the expression of the proteins by immuno-precipitation of the extracted proteins using anti-flag and anti-Myc antibodies conjugated on agarose beads. Relevant protein expression was detected for all tested lines, plants with relatively higher detectable protein levels were selected for ubiquitination assays (Figure 5-3 A). The selected lines were assessed for the ubiquitination of AtPEN1 initially by infecting the plants with *Blumeria graminis* f. sp. *hordei* (*Bgh*) and followed by protein extraction after 72 hours post inoculation. My results suggest the polyubiquitination of AtPEN1 was mediated via K48 or K63 ubiquitin sites. Mutation of both sites only led to mono-ubiquitination or/ multi-monoubiquitination of AtPEN1 (Figure 5-3 B lane 3).

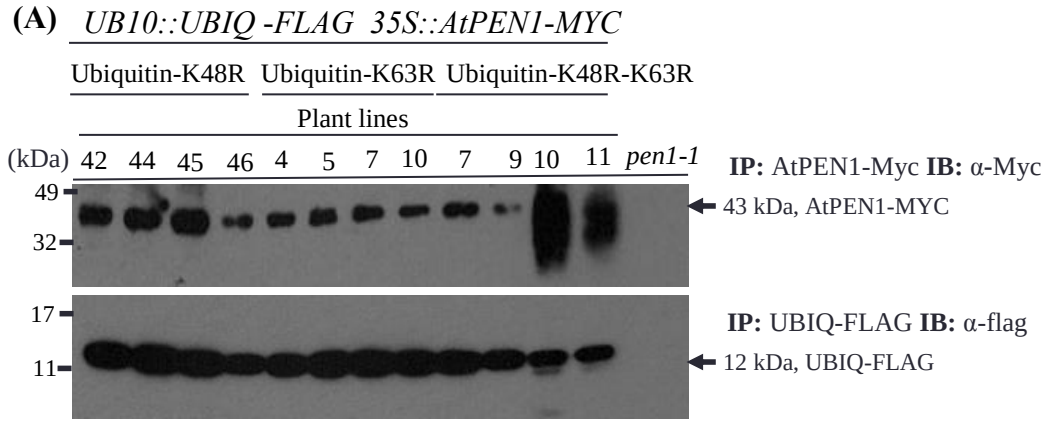

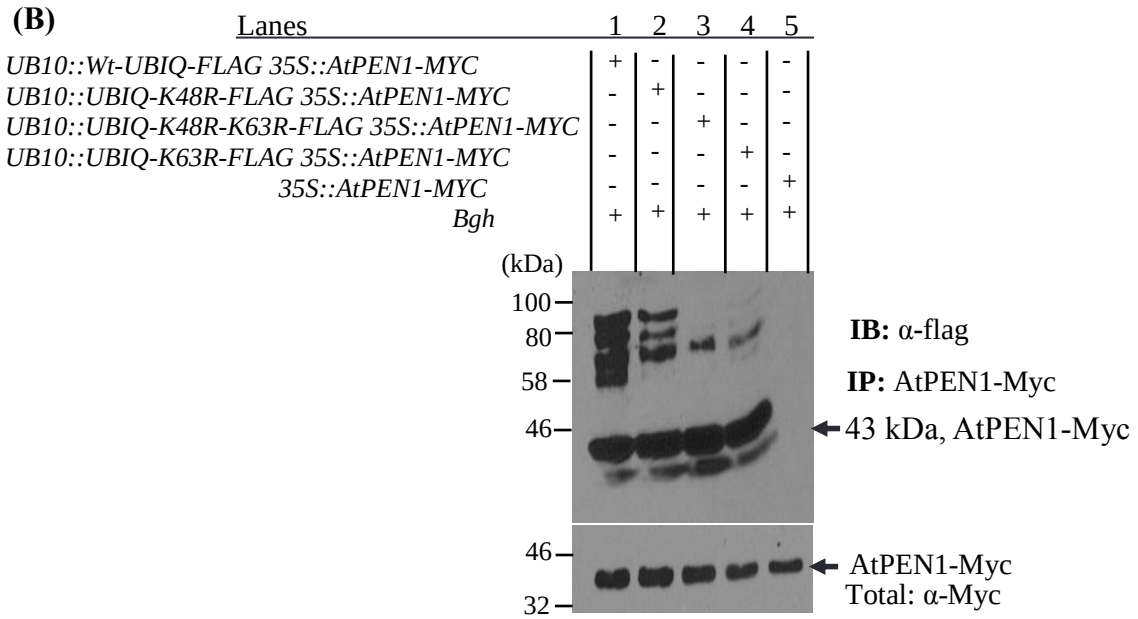


**Figure 5-3. Detection of protein expression and ubiquitination assays.** (A) Detecting the expression of AtPEN1-Myc and Ubiquitin-Flag mutants. *Arabidopsis pen1-1* mutant was transformed with genetic construct of: *UB10::Wt-UBIQ-FLAG*, *UB10::UBIQ-K48R-FLAG*, *UB10::UBIQ-K48R-K63R-FLAG*, *UB10::UBIQ-K63R-FLAG* fused with *35S::AtPEN1-MYC*. Generated homozygous lines were checked for the expression of the proteins, by extracting the proteins in non denaturing buffer. Extracted proteins were immunoprecipitated with either anti-flag antibody or anti-Myc antibody conjugated on agarose beads. Unbound proteins were washed off with PBS and the bound proteins resolved in SDS PAGE. Detection of the proteins was performed by immunoblotting with either anti-flag antibody or anti-Myc antibody. Proteins immunoprecipitated from non transformed *pen1-1* mutant was used as negative control. (B) Detecting polyubiquitination of AtPEN1 mediated at either K48 or K63 ubiquitin sites. Plant lines carrying the above genetic constructs were initially infected *Bgh* and later proteins extracted from the leaves in non denaturing buffer. Extracted proteins were immunoprecipitated with anti-Myc antibody conjugated on agarose beads and the unbound proteins washed off with PBS. Retained proteins were resolved in SDS PAGE and ubiquitination detected by immunoblotting with anti-flag antibody. The ubiquitination was shown as a high mass smear above the AtPEN1-Myc. Decline in the level of ubiquitination of AtPEN1 following the mutations of either K48 or K63 or both would indicate them as the mode of polyubiquitination. Lane 1, checking the polyubiquitination of AtPEN1 with wild-type ubiquitin. Lane 2, checking the polyubiquitination of AtPEN1 with ubiquitin-K48R mutant. Lane 3, checking the polyubiquitination of AtPEN1 with ubiquitin-K48R-K63R mutant. Lane 4, checking the polyubiquitination of AtPEN1 with ubiquitin-K63R mutant. Lane 5, proteins extracted from plant transformed with only 35S::AtPEN1-MYC was used as negative control. Loading controls were detected by immunoblotting with anti-Myc antibody. Experiment was repeated three times.

### 5.3.3 Assessing the potential of the proteasome to bind polyubiquitinated AtPEN1

#### 5.3.3.1 Proteasome subunit α7 binds to both K48 and K63 polyubiquitinated AtPEN1

Having elucidated that AtPEN1 can be modified by the addition of polyubiquitinated chains, linked to ubiquitin at either K48 or K63 or both, we explored if these modifications might recruit the proteasome to target AtPEN1 for degradation. The proteasome is a protein complex of 2.5 MDa with multiple subunits encoded by several genes (Yang *et al*, 2004; Bedford *et al*, 2010; Livneh *et al*, 2016). The α7 subunit of the 20S core particle was selected for cloning, as its over expression in *Arabidopsis* has been shown to enrich proteasome activity (Book *et al*, 2010). Therefore, the 20S proteasome subunit α7 was expressed in bacteria and purified as a glutathione S-transferase (GST) tagged protein using glutathione Sepharose 4B (GSH) resin. The ubiquitination assay was setup as described in section 5.2.1 except that MBP-AtPEN1 was initially incubated with amylose resin before use in the assay to bind the protein. The ubiquitin conjugates were later incubated with the purified 20S proteasome subunit α7. The un-bound proteins were washed off by ice cold PBS and the remained proteins were separated by SDS PAGE and finally western blot analysis performed with anti-GST antibody. The 20S proteasome subunit α7 bound non-preferentially to both ubiquitin K48 and K63 mediated polyubiquitination of AtPEN1. Control reactions with non-ubiquitinated AtPEN1 did not result in 20S proteasome subunit α7 binding. In a similar fashion GST alone were not able to bind polyubiquitinated AtPEN1 (Figure 5-4).

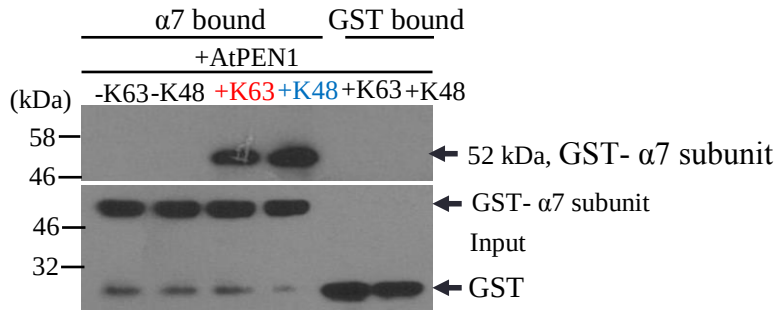


**IB:** α-GST

**Figure 5-4: Purified 20S proteasome subunit α7 binds both ubiquitin sites K48 and K63 polyubiquitinated AtPEN1 un-differentially.** Prior ubiquitination, MBP-AtPEN1 was incubated with amylose resin. The trapped MBP-AtPEN1 was then subjected to *in vitro* ubiquitination in reactions containing E1, E2, RRE1 and either histidine-ubiquitin K48 only or histidine-ubiquitin-K63 only. Purified recombinant protein of 20S proteasome α7 was then added to the ubiquitinated proteins and further incubated. The proteins were then washed to remove unbound proteins and the retained proteins resolved in SDS PAGE. Detection of 20S proteasome subunit α7 bound to modified AtPEN1 was done by immunoblotting with anti-GST antibody. The incubation of ubiquitinated AtPEN1 with GST protein alone served as negative control. Loading controls were also detected by immunoblotting with anti-GST antibody. Experiment was repeated three times.

### 5.3.3.2 The proteasome from cell lysates preferentially binds K48 polyubiquitinated AtPEN1

The ubiquitination assay was set up as in section 5.2.1 using MBP-AtPEN1 that was initially conjugated on amylose resin. The polyubiquitinated AtPEN1 was washed in washing buffer and then incubated with total protein freshly extracted from *Arabidopsis* Col-0 plants previously inoculated with *Bgh* spores. The un-bound proteins were washed off with the binding buffer lacking bovine serum albumin (BSA) and the protein conjugates incubated with leucine-leucine-valine-tyrosine- 7-amino-4-methylcoumarin (LLVY-AMC) proteasome substrate. The amount of proteasome bound to polyubiquitinated AtPEN1 was measured in terms of fluorescence released by the cleavage of LLVY-AMC substrate (Peth *et al*, 2011). The impure 26S proteasome preferentially binds to ubiquitin site K48 polyubiquitinated AtPEN1 relative to ubiquitin site K63 polyubiquitinated AtPEN1. Non polyubiquitinated AtPEN1 did not show significant proteasome binding, indicating that the 26S proteasome bound specifically to ubiquitinated AtPEN1 (Figure 5-5).

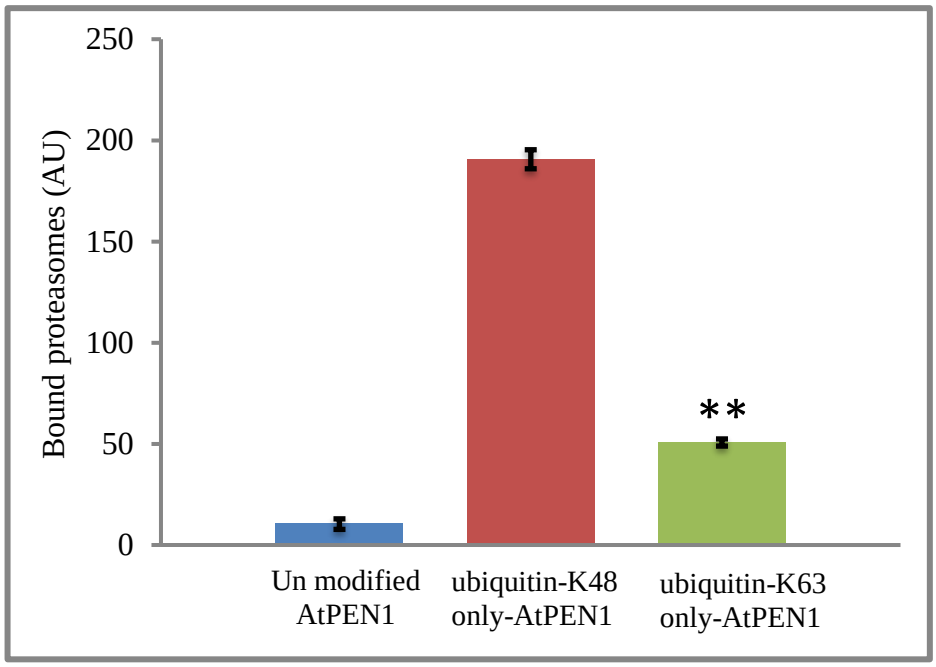


**Figure 5-5: Binding of the impure 26S proteasome to AtPEN1 polyubiquitinated with either K48 chain linkage or K63 chain linkage.** Initially MBP-AtPEN1 was incubated with amylose resin. The trapped MBP-AtPEN1 was then subjected to *in vitro* ubiquitination assay in reaction containing E1, E2, RRE1, histidine-ubiquitin K48 only or histidine-ubiquitin K63 only. The proteins were then incubated with protein extracts from *Arabidopsis* Col-0 previously infected with *Bgh*. Later, the proteins were washed to remove unbound proteins and incubated with 26S proteasome substrate (LLVY-AMC). The cleavage of the substrate released fluorescence that was detected and quantified, corresponding to the amount of 26S proteasome bound to the ubiquitinated AtPEN1. Error bars represent mean ± standard error. *n* = three biological replicates. Asterisks indicate significant difference from AtPEN1 modified with ubiquitin-K48 only, *t*- test $P < 0.01$.

### 5.3.3.3 Polyubiquitination at K48 but not K63 ubiquitin sites targets AtPEN1 for 26S proteasome degradation

To explore the effect of the observed proteasome binding to the ubiquitinated AtPEN1, AtPEN1 initially immobilised on amylose resin was subjected to an *in vitro* ubiquitination assay as described in section 5.2.1. The polyubiquitinated AtPEN1 was incubated with protein extracts from *Arabidopsis* Col-0 previously inoculated with *Bgh*. After incubation the protein samples were separated using SDS PAGE. The resolved proteins were

subjected to a western blot analysis by incubating with an anti-MPB antibody. Detected proteins were relatively quantified using ImageJ software and expressed as percentages. AtPEN1 modified with polyubiquitinated K48 chain linkage declined in abundance to (9%) while AtPEN1 modified with K63 polyubiquitins remained unchanged to (30%). The addition of the proteasome inhibitor MG132 elevated the amount of AtPEN1 modified with polyubiquitin containing K48 chain linkages to (25%). The addition of MG132 to AtPEN1 modified with K63 polyubiquitin chain did not make a pronounced change in the amount of AtPEN1 (32%) (Figure 5-6 A and B). The assay indicates that AtPEN1 is targeted for degradation to the proteasome if modified with polyubiquitin possessing K48 linkages.

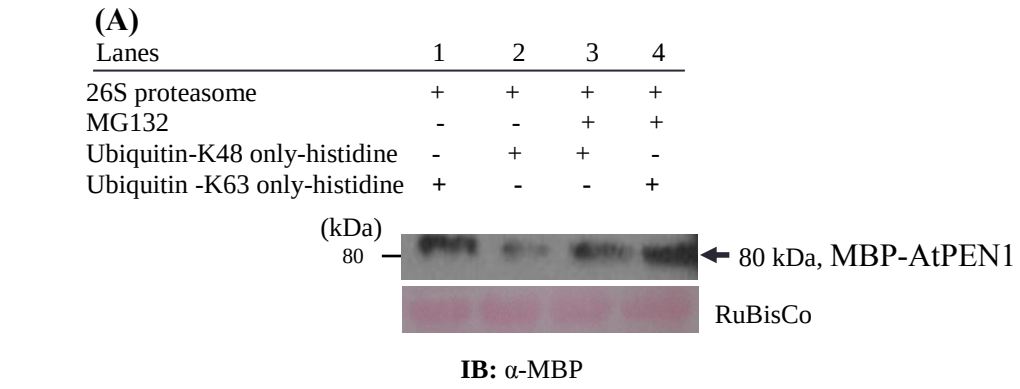


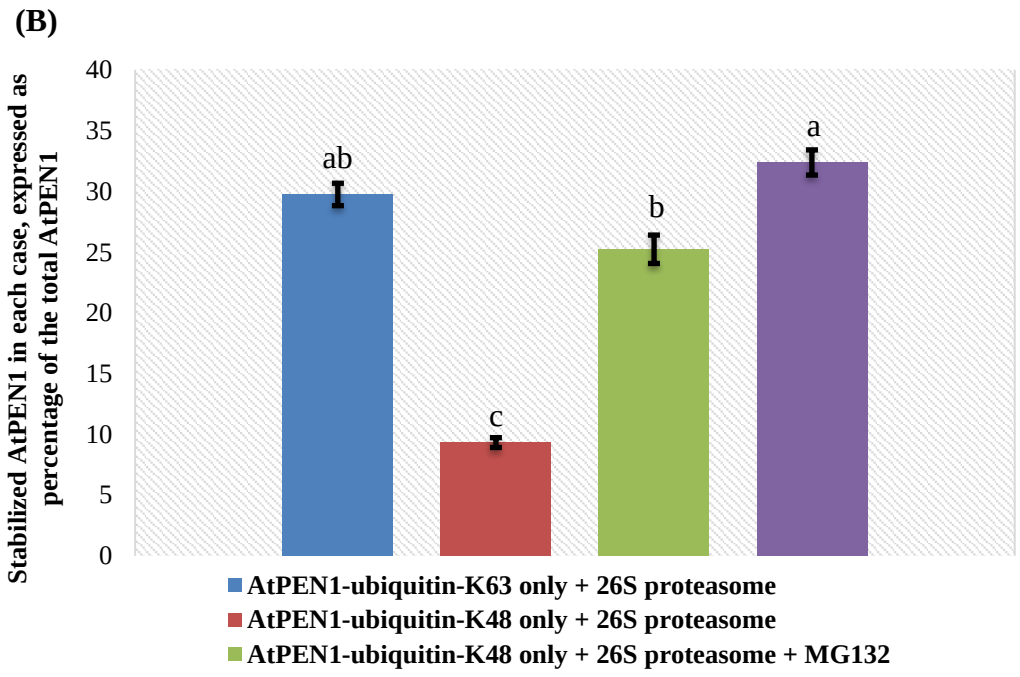

**Figure 5-6: Degradation of polyubiquitinated AtPEN1 by the 26S proteasome.** (A) MBP-AtPEN1 was initially incubated with amylose resin and the trapped MBP-AtPEN1 subjected to *in vitro* ubiquitination assay containing E1, E2, RRE1, and either histidine-ubiquitin K48 only or histidine-ubiquitin K63 only. The ubiquitinated MBP-AtPEN1 was incubated with protein extracts, extracted from *Arabidopsis* Col-0 previously infected with *Bgh*, in the presence or absence of proteasome inhibitor. The proteins were then separated in SDS PAGE and the detection in the changes of the amount of MBP-AtPEN1 was detected by immunoblotting with anti-MBP antibody. Lane 1, checking the effect of 26S proteasome on AtPEN1 modified with K63 polyubiquitins. Lane 2, checking the effect of 26S proteasome on AtPEN1 modified with K48 polyubiquitins. Lane 3, checking the effect of 26S proteasome on AtPEN1 modified with K48 polyubiquitins in presence of proteasome inhibitor. Lane 4, checking the effect of 26S proteasome on AtPEN1 modified with K63 polyubiquitins in presence of proteasome inhibitor. Ponceau staining for Ribulose-1,5-bisphosphate carboxylase (RuBisCo) protein was used as loading control. (B) Histogram displaying the percentage area of AtPEN1 stabilized after degradation. Relative area of quantification obtained using ImageJ software on the protein bands and expressed as percentages. Error bars represent means ± standard error. Experiment was repeated three times. One-way ANOVA and Tukey's comparisons for the difference of means performed by statistical package Minitab 18; Means that do not share a letter are significantly different at $P \leq 0.001$.

### 5.3.4 Ubiquitination targets AtPEN1 for 26S proteasome degradation but not for vacuolar degradation

An *in vivo* investigation was under-taken to reveal the fate of AtPEN1 following ubiquitination. The emerging evidence suggests that the addition of polyubiquitin with K63 chain linkages to the target protein may direct it for vacuolar degradation (Martins *et al*, 2015). A construct constitutively expressing *UBIQ-FLAG* by the *UBIQ* promoter and terminator and *AtPEN1-MYC* by the *35S CaMV* promoter and terminator was generated in a plant expression vector using Golden Gate MoClo. The resulted construct was transformed into the *Arabidopsis pen1-1* mutant by floral dipping. The selected homozygous plants were challenged with *Bgh* and incubated for 3 days. After 1 day of incubation the leaves were infiltrated with either concanamycin (vacuolar inhibitor) or MG132 (proteasome inhibitor). Total proteins were extracted from leaf tissues in non-denaturing buffer supplemented with either concanamycin or MG132. AtPEN1 was immuno-precipitated by incubating with anti-Myc conjugated on agarose beads overnight at 4$^{o}$C. Immuno-precipitates were washed in ice

cold PBS, suspended in SDS loading buffer and resolved in SDS PAGE. The separated proteins were analysed by western blot against ubiquitin with anti-ubiquitin antibody. Polyubiquitination was shown as a uniform smear of increasing mass on AtPEN1 monomer. In the absence of MG132 there is a decline in the quantity of polyubiquitinated AtPEN1 (Figure 5-7 lane 1), while in the presence of MG132 an increased amount of modified AtPEN1 is detected (Figure 5-7 lane 2). The stabilization of AtPEN1 in the presence of MG132 suggests that polyubiquitinated AtPEN1 is targeted by the proteasome for degradation. The presence of concanamycin did not increase the level of AtPEN1 (Figure 5-7 lane 3), suggesting that polyubiquitinated AtPEN1 is not targeted to the vacuole for degradation. The absence of concanamycin did not make any difference from the assay that included concanamycin (Figure 5-7 lane 4).

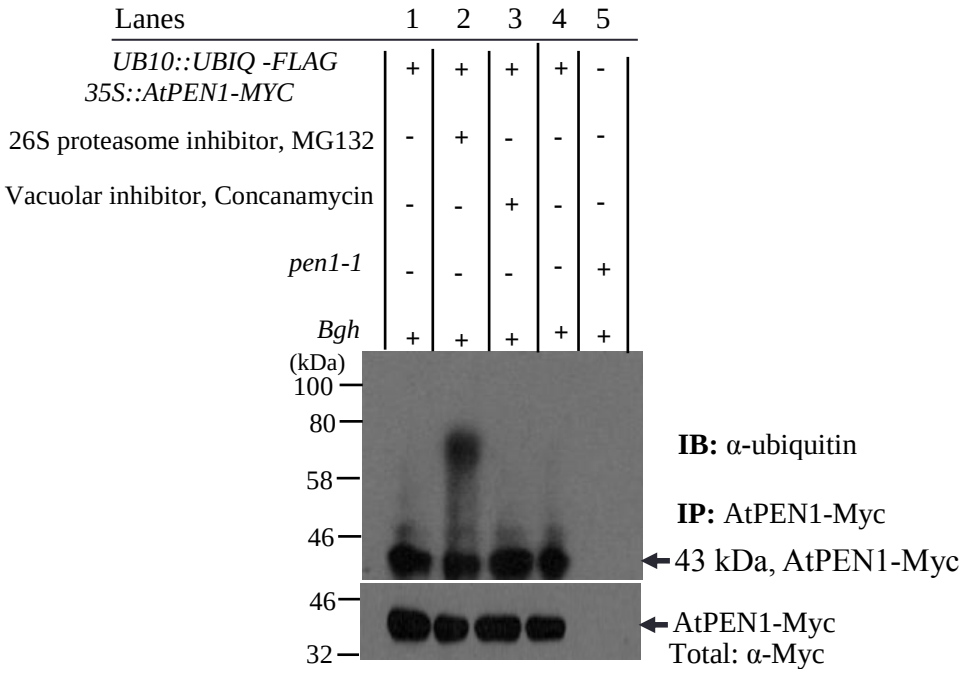


**Figure 5-7: Ubiquitinated AtPEN1 is subjected to 26S proteasome degradation not vacuolar turnover.** *Arabidopsis* plant lines expressing *UB10::UBIQ-FLAG 35S::AtPEN1-MYC* were previously infected with *Bgh* and incubated for 3 days. At 2 day post inoculation, the leaves were either non infiltrated or infiltrated with the vacuolar inhibitor or 26S proteasome inhibitor. Then, proteins were extracted in non denaturing buffer in the presence or absence of the above inhibitors and immunoprecipitated with anti-Myc antibody conjugated on agarose beads. The unbound proteins were washed in

PBS and resolved in SDS PAGE. Detecting the levels of ubiquitination was done by immunoblotting with anti-ubiquitin antibody and presented as uniform high mass smear above AtPEN1-Myc protein. Lane 1, checking the ubiquitination of AtPEN1 in absence of both inhibitors. Lane 2, checking the ubiquitination of AtPEN1 in presence of proteasome inhibitor. Lane 3, checking the ubiquitination of AtPEN1 in presence of vacuolar inhibitor. Lane 4, checking the ubiquitination of AtPEN1 in absence of vacuolar inhibitor. Lane 5, proteins immunoprecipitated from *pen1-1* was used as negative control. Loading controls were detected by immunoblotting with anti-Myc antibody. Experiment was repeated three times.

## 5.4 Discussion

The fate of a protein modified by ubiquitination is determined by the nature of the ubiquitin conjugated to the substrate (Pickart & Fushman, 2004; Sadowski & Sarcevic, 2010). While mono-ubiquitination and multi-monoubiquitination is associated with non-proteolytic functions, polyubiquitination can drive a mixture of function outcomes (Kwon & Ciechanover, 2017). Polyubiquitination at K48 and K63 ubiquitin sites are the most widely occurring in nature (Meierhofer *et al*, 2008; Tanno & Komada, 2013; Paez Valencia *et al*, 2016). K48 polyubiquitination is linked to 26S proteasome dependent protein degradation. On other hand the K63 polyubiquitination is associated predominantly with functional protein modification, although it has been shown to target the substrates to vacuolar/lysosomal dependent degradation (Kwon & Ciechanover, 2017).

Having elucidated that AtPEN1 undergoes ubiquitination I attempted to identify the type of chain linkages attached to AtPEN1. The results showed that AtPEN1 can equally be polyubiquitinated by either K48 or K63 ubiquitin chain linkages. Therefore, indicating that AtPEN1 can be marked for either proteasome proteolysis or non-proteolytic functions, including trafficking or recycling. It further reveals RRE1 as having the potential to subsequently ubiquitinate AtPEN1 by either K48 or K63 polyubiquitin linkages. Although the E3 ligases tend to act as a docking protein, with the transfer of chain linkages to the substrate completed by E2s (Kim & Huibregtse, 2009). It is likely that RRE1 is one of a small number

of novel E3 ligases that regulate the synthesis of chain linkages, given the high dependence of AtPEN1 on RRE1 for its ubiquitination. In this context, the human homologous to the E6-AP (E6-associated protein) carboxyl terminus (HECT) KIAA10 non-specifically synthesizes K29 and K48 chain linkages both implicated in proteasome proteolysis (Wang *et al*, 2006a). The human atrophin 1 interacting protein 4 (AIP4) also mediates the synthesis of K63 and K29 polyubiquitins involved in marking different fates for the given substrate (Chastagner *et al*, 2006; Scialpi *et al*, 2008). The human HECT E6AP preferentially drives the formation of K48 polyubiquitination, while the *Saccharomyces cerevisiae* (*S. cerevisiae*) Rsp5 and human itch E3 ligases catalyzes K63 polyubiquitination formation (Kim & Huibregtse, 2009; Romero-Barrios & Vert, 2018). The E6AP ligases hijacked by human papillomavirus oncogene E6 to ubiquitinate the tumour suppressor protein P53, exhibit a preference for K48 polyubiquitin linkages (Kim & Huibregtse, 2009). In an *in vivo* based assay, the mutation of either K48 or K63 ubiquitin sites resulted in the mono-ubiquitination of AtPEN1. This was expected as the first ubiquitin added to the substrate is through the C-terminal glycine on the ubiquitin and the lysine on the substrate and thus is not dependant on any lysine site in the ubiquitin (Callis, 2014).

I investigated the potential of the proteasome to bind polyubiquitinated AtPEN1 as an indication for possible degradation. The purified 20S proteasome α7 bound non-selectively to AtPEN1 linked with either K48 or K63 linkage chains with similar intensity. However, the impure proteasome in cell lysates intensively bound to ubiquitin site K48 polyubiquitinated AtPEN1 and less to ubiquitin site K63 modified AtPEN1. My results are in line with earlier studies conducted in mammalian systems. Thus the mammalian E3 ligases E6AP auto ligated with K48 polyubiquitin or Neural precursor cell expressed developmentally down-regulated protein 4 (NEDD4) auto ligated with K63 polyubiquitin were bound with purified proteasome with equal affinities (Nathan *et al*, 2013). In contrast, tissue lysates from rat muscles

preferentially bound NEDD4-K48 compared to E6AP-K63 auto-ubiquitinated proteins (Nathan *et al*, 2013). One possible explanation could be that the enzymes in cell lysates promoted the deubiquitination of K63 conjugates more rapidly that the K48 conjugates. Although deubiquitination is unlikely when incubation is conducted at 4$^{o}$C, as in our case. Earlier reports revealed the JAB1/MPN/Mov34 metalloenzyme (JAMM/MPN+) family of deubiquitinases specific for K63 polyubiquitins are active at 4$^{o}$C (Cooper *et al*, 2009). The resident proteasome deubiquitinases are also known to have preference for K63 conjugates (Jacobson *et al*, 2009; Lee *et al*, 2011). Further, in cell extracts soluble factors are known to exist that bind to K63-polyubiquitin chains and hinder the accessibility of the proteasome to the conjugated protein (Hyoung *et al*, 2007). The cytosolic ubiquitin binding domain containing proteins, especially those of the Endosomal sorting complexes required for transport (ESCRT)-0 complex, are known to bind selectively to K63 polyubiquitinated proteins *in vivo*, blocking proteasome binding (Nathan *et al*, 2013). Although the ESCRT-0 and ESCRT-1 members of the ESCRT system are not present in plants, proteins performing similar roles such as FYVE domain protein required for endosomal sorting 1 (FREE1) have been characterized (Gao *et al*, 2014).

The reduction in the abundance of K48 chain linkage modified AtPEN1 suggests that the protein is degraded by the proteasome. The level of AtPEN1-K63 polyubiquitin modification remained unchanged indicating it is not targeted by the proteasome (Figure 5-6). Although troponin I linked with either K48 or K63 conjugates was bound and degraded with pure proteasome *in vitro*, when incubated with cell lysates only K48 linked troponin I was targeted by the proteasome (Hyoung *et al*, 2007). Further suggesting that cells may contain additional factors that protect K63 ubiquitin chains from proteasomal degradation (Hyoung *et al*, 2007). It is also possible that K63 linkages may have been formed as forked chains on AtPEN1. The formation of forked chains on troponin I substrate resulted in a non-degradable

proteasome substrate. These chains are resistant to disassembly by the resident proteasomal isopeptidases accounting for the failure of the degradation process (Kim *et al*, 2009; Ohtake & Tsuchiya, 2016).

The ubiquitination of proteins by K63 polyubiquitination has been linked to vacuolar dependent turnover. Brassinosteroid insensitive 1 (BRI1), a plasma membrane localised receptor kinase for brassinosteroids, is post translationally modified by K63 polyubiquitinations. This ubiquitination promotes BRI1 internalization essential for recognition at the early endosomal or *trans*-Golgi network and lead to vacuolar degradation (Martins *et al*, 2015). The *Arabidopsis* PIN2 protein required for cellular efflux of auxin is modified by K63 linked chains leading to endosomal sorting in the vacuoles. The ubiquitination of PIN2 is important for the regulation of auxin distribution in the root meristem and environmental adaptation of root growth (Leitner *et al*, 2012a; Dubeaux & Vert, 2017). My results show that AtPEN1 modified with K63 linkages is not targeted to vacuolar degradation (Figure 5-7 lane 3 and 4), instead this may lead to a different fate. My results led to the hypothesis that the modification of AtPEN1 by K63 chain linkages promotes its translocation to the site of attempted *Bgh* ingress. The ‘‘exhausted’’ AtPEN1 can later be targeted for proteasome degradation after being decorated with K48 chain linkages. Indeed, AtPEN1 recycling to and from the membrane to the site of attempted fungal penetration has been previously described but the mechanism promoting the translocation has previously remained unclear (Nielsen & Thordal-Christensen, 2012). In similar fashion human protein kinase B (Akt) signalling plays a central role in cell proliferation and apoptosis. The cytosol localised kinase is activated for localization to the plasma membrane by K63 polyubiquitination mediated by TNF (tumour necrosis factor receptor) receptor-associated factor 6 (TRAF6) E3 ligase (Yang *et al*, 2009).

# Chapter six

## 6.0 The effect of CSEP0443 on AtPEN1-RRE1 interactions

## 6.1 Introduction

Plant penetration resistance involved in hindering the access of both host specific and non-specific pathogens is a key feature of host-microbial interactions (Chaudhari *et al*, 2014; Laur *et al*, 2018). Plant pathogens counteract plant penetration resistance by secreting an arsenal of effectors directed against specific targets (Deslandes & Rivas, 2012; Petre & Kamoun, 2014). Previous data suggest that *Arabidopsis thaliana* PENETRATION 1 (AtPEN1) and Redox regulated E3 ligase 1 (RRE1) proteins are important components of penetration resistance. The two proteins are tightly co-expressed during *Blumeria graminis* f. sp. *hordei* (*Bgh*) challenge and play a role in restricting further growth of the pathogen (Collins *et al*, 2003; Nakao *et al*, 2011; Yu, 2012; Johansson *et al*, 2014). AtPEN1 mediates resistance by facilitating fusion of vesicles that might contain anti-microbial agents with the plasma membrane (Reichardt *et al*, 2011a).

The *Bgh* mature effector protein Candidate secreted effector protein 0443 (CSEP0443) localise to cytosolic vesicles in barley epidermal haustoriated cells and co-localise with XA21 binding protein *Hordeum vulgare* 35 (XBHV35) to perihaustorial microdomain at the fungal-haustorial complex (Aguilar, 2015). XBHV35 is a barley homologue of RRE1 in *Arabidopsis* having the conserved ankyrin repeats and the C3HC4-type Really interesting new gene (RING) finger domain (Yuan *et al*, 2013). The truncated XBHV35-RING domain known to drive E3 ligase function interact with CSEP0443 (Zhang, 2012; Aguilar, 2015). In addition, full length XBHV35 interact with Required for *mlo* resistance 2 (ROR2) a barley homologue of AtPEN1 (Aguilar, 2015). Previous experiments conducted in barley linked *Bgh* virulence to the interactions of XBHV35, CSEP0443 and

ROR2 (Aguilar, 2015). Given the few studied effectors compared to the large predicted secreted effectors, the functional characterization of CSEP0443 targets in non-host plants may contribute to the knowledge of effectors.

In this chapter using the *in vitro* pull-down assays and co-immunoprecipitation techniques *in vivo* in *Arabidopsis*, I attempted to assess the ability of CSEP0443 to interact with RRE1. Further I determined the influence of CSEP0443 on the ubiquitination of AtPEN1 mediated by RRE1 deemed necessary for AtPEN1 functionality.

## 6.2 Materials and methods

### 6.2.1 *In vitro* pull-down assay for interactions of RRE1 and CSEP0443

GST-RRE1, GST-RRE1-RING, GST-RRE1-Ankyrin repeat, GST-RRE1-C340S and MBP-CSEP0443 were expressed and purified as described in section 2.8. Pre-washed glutathione Sepharose 4B beads (40 µl) (section 2.9) were incubated separately with (40 µl) of 4.3 ng/µl of GST-RRE1, GST-RRE1-RING, GST-RRE1-Ankyrin repeat, GST-RRE1-C340S, GST and incubated for $2^1/_2$ hours at 4°C on a rotary roller. Further, (40 µl) of 0.88 ng/µl MBP-CSEP0443, MBP separately was added and incubated again for $2^1/_2$ hours at 4°C. The proceeded steps are as described in section 2.9.

### 6.2.2 Investigating *in vitro* ubiquitination of CSEP0443

The ubiquitination assays were performed as described by Sato *et al*, (2009). Reaction were set up in a total 30 µl volume containing: 10 ng/µl E1, 3 ng/µl of purified E2, 3 ng/µl of purified GST-RRE1, 3 ng/µl of either MBP-CSEP0443 or MBP, 3 ng/µl of Bovine serum albumin (BSA) as a positive control, 1x reaction buffer, 6.7 mM Adenosine triphosphate (ATP), 66 ng/µl histidine tagged ubiquitin and autoclaved double distilled water ($ddH_2O$). The reagent sources and steps involved are as described in section 2.10.

### 6.2.3 *In vitro* ubiquitination of AtPEN1 in presence of CSEP0443

The ubiquitination assays were performed as described by Sato *et al*, (2009). A 30 µl reaction was set up containing: 10 ng/µl E1, 3 ng/µl of purified, 3 ng/µl of purified GST-RRE1 as E3 ligase enzyme, 0.099 ng/µl AtPEN1, 3 ng/µl of either MBP-CSEP0443 or MBP, 1x reaction buffer, 6.7 mM ATP, 66 ng/µl histidine tagged ubiquitin and autoclaved dd$H_2O$. The reagent sources and additional steps involved are as described in section 2.10.

### 6.2.4 Genetic constructs for *in vivo* investigation of CSEP0443, RRE1 and AtPEN1

Genetic constructs were generated using Golden Gate modular cloning (MoClo) and investigated in either *Nicotiana benthamiana* or *Arabidopsis* (Weber *et al*, 2011; Engler *et al*, 2014). Vectors *pAGM1287* for level 0 acceptor, *pICH47742*, *pICH47751*, *pICH47761*, for level 1 positions 2, 3, 4 and *pAGM4723* for level 2 acceptor were utilized. *pICH41744* endlinker 2, *pICH41766* endlinker 3, *pICH41780* endlinker 4 for level 2 positions 2, 3 and 4 constructions, *pICSL11024* for *Kanamycin* resistance already in position 1 level 1, modules *pICSL50007* for Flag tag, *pICSL50010* for Myc tag, *pICSL50009* for Hemagglutinin (HA) tag, *pICSL12015* for Ubiquitin (*UB*) promoter, *UB5* for ubiquitin terminator, *pICH45214* for Light-harvesting chlorophyll-protein complex ii subunit B1 (*LHB1B1*) promoter, *pICH77901* for mannopine synthase (*MAS*) terminator, *pICH41414* for Cauliflower mosaic virus (*CaMV*) *35S* terminator were utilized. The sources of the vectors and modules are described in section 2.11. The *CaMV 35S* promoter was amplified from pEarly Gateway vector (*pEG*)-*202*, Enhanced yellow fluorescent protein (*EYFP*) was amplified from *pEG-101*, *CSEP0443* was amplified from *pET-40A* while *AtPEN1* and *RRE1* were amplified from Col-0 complementary deoxyribonucleic acid (cDNA) using primers sets in (Table 4).

To investigate the interaction of CSEP0443 and RRE1, initially *RRE1* and *CSEP0443* were cloned in *pAGM1287*. The *CSEP0443* was transferred to level 1 in *pICH47742* together

with Ubiquitin promoter and terminator and a carboxyl (C) terminus *FLAG* tag generating a full transcription unit of *UB10::CSEP0443-FLAG-UB5*. *RRE1* was transferred to level 1 in *pICH47751* together with *LHB1B1* promoter and *MAS* terminator, and a C terminal *HA* tag to generate a full transcription unit of, *LHB1B1::RRE1-HA-MAS*. The two full transcription units together with the full transcription unit of *Kanamycin* resistance *pICSL11024*, and *pICH41766* endlinker 3 were finally ligated in *pAGM4723* for level 2 acceptor. All other general steps involved are as in section 2.11. Finally, the construct was transformed in *Arabidopsis rre1* mutant as described in section 2.12.

To investigate the effect of CSEP0443 on AtPEN1 polyubiquitination, *AtPEN1* was initially cloned in *pAGM1287*. Then transferred in both level 1 position 2 and 3 vectors with *CaMV 35S* promoter and *CaMV 35S* terminator and a C terminal MYC tag to generate *35S::AtPEN1-MYC-35S* full transcription unit. Finally, the two transcription units were transferred in level 2. *AtPEN1* in position two level 1 was ligated with *Kanamycin* resistance *pICSL11024* and *pICH41744* endlinker 2 into *pAGM4723* for level 2 acceptor. *AtPEN1* in level 1 position 3 was ligated with *CSEP0443* in level 1 position 2, then *Kanamycin* resistance *pICSL11024* and *pICH41766* endlinker 3 into *pAGM4723* for level 2 acceptor. All other steps are as described in section 2.11. Finally, the constructs were transiently transformed in *N. benthamiana* and later stably transformed in *Arabidopsis pen1-1* mutant as described in section 2.12.

To investigate the localization of CSEP0443, amplified *CSEP0443* (full *CSEP0433* and truncated (Δ)*CSEP0443* devoid of signal peptide), and *EYFP* fragments were ligated together or individually as *EYFP* in *pAGM1287*. The fragments were then transferred in level 1 position 2 vector with ubiquitin promoter, ubiquitin terminator and a C terminal tag to generate full transcription units of *UB10::FullCSEP0443-EYFP-FLAG-UB5*, *UB10::ΔCSEP0443-EYFP-FLAG-UB5* and *UB10::EYFP-FLAG-UB5*. Then, the

transcription units were ligated in *pAGM4723* for level 2 acceptor with *Kanamycin* resistance *pICSL11024*, and *pICH41744* endlinker 2. All other general steps involved during reaction set up are described in section 2.11. The generated constructs were initially transiently expressed in *N. benthamiana* and later transformed in *Arabidopsis* Col-0, *35S::EGFP-AtPEN1-pen1-1* and *35S::EGFP-AtPEN1-pen1-1-rre1* to generate stable plants.

### 6.2.5 Transient protein expression in *N. benthamiana*

The procedure was performed as described by Liu *et al*, (2016). Initial steps for *Agrobacterium* culture and harvest are as described in section 2.13. The pellet was washed once in infiltration media containing Methyl ester sulfonates (MES) 10 mM pH 5.2, $MgCl_2$ 10 mM and acetosyringone 0.2 µM to remove residual antibiotics. The pellet was suspended in 0.5 ml infiltration media and optical density $(O.D)_{600\ nm}$ adjusted to 1 and infiltrated in the leaves of 3 weeks-old *N. benthamiana*. The plants were further grown for 2 days before microscopic investigations and protein extractions.

### 6.2.6 RNA extraction, RT-PCR

For the ribonucleic acid (RNA) extraction, 100 mg of *Arabidopsis* leaves were collected and immediately frozen in liquid nitrogen. The leaves were finely ground in liquid nitrogen using mortar and pestle previously sterilized by autoclaving. The finely ground frozen tissues were suspended in 1 ml TRIzol® Reagent and incubated for 10 minutes at room temperature. All other steps are as described in section 2.14.

For reverse transcription polymerase chain reaction (RT-PCR), the extracted RNA was adjusted to 1.5 µg final concentration followed by cDNA synthesis. The preceded steps are described in section 2.14. Detection of *CSEP0443* expression was done using primers listed in (Table 5). PCR reactions and conditions are as in section 2.14.

### 6.2.7 Protein extraction from *N. benthamiana* and *Arabidopsis* plants

Proteins were extracted from 4 g of 3 weeks-old *Arabidopsis* leaves and from 2 g of Agro-infiltrated *N. benthamiana* leaves. For investigating the interaction of RRE1 and CSEP0443, and effect of CSEP0443 on the ubiquitination of AtPEN1, plants were previously infected with *Bgh* for 3 days. *Arabidopsis* and *N. benthamiana* leaf samples were collected and immediately frozen in liquid nitrogen. The leaves were finely ground in liquid nitrogen before further crushed in extraction buffer described by Li *et al*, (2015). Preceded steps are as described in section 2.15.

### 6.2.8 Protein co-immunoprecipitation assays

For co-immunoprecipitation assays, the protein suspensions were filtered through 0.4 µM millipore filters and protein concentrations determined using the Bradford reagent (Bio-Rad). The proteins were adjusted to 350 µg using the extraction buffer. The diluted proteins were incubated appropriately with 2 µg of anti-HA antibody, anti-Myc antibody, and anti-flag antibody conjugated on agarose beads based on the purpose of the investigation. Further steps are as described in section 2.15. Finally, the proteins were suspended in 1x sodium dodecyl sulfate (SDS) loading dye containing 10% β-Mercaptoethanol and boiled at 95$^{o}$C for 5 minutes. The proteins were then centrifuged briefly for 30 seconds in a micro-centrifuge and 20 µl of the supernatant loaded in SDS gel for western blot analysis. For the detection of EYFP-Flag, FullCSEP0443-EYFP-Flag and ΔCSEP0443-EYFP-Flag, proteins were not immunoprecipitated instead, were processed as total protein and loaded in SDS gel.

### 6.2.9 SDS PAGE and western blot analysis

Sodium dodecyl sulfate-Polyacrylamide gel electrophoresis (SDS PAGE) and western blot analysis were carried out as described by Sambrook *et al*, (2012). Proteins were separated in 10% (for ubiquitination assays and detection of proteins except CSEP0443-

Flag), or 15% (for detection of CSEP0443-Flag) SDS PAGE in 1.5 mm glass chambers bound with a stacking gel. Preceded steps are as described in section 2.16. For immunoblotting with anti-Myc antibody or anti-HA antibody or anti-flag antibody, the membranes were incubated for 1 hour and followed by 3 times washing with phosphate buffered saline tween 20 (PBS-T) at 10 minutes interval. Then re-incubated again with anti-mouse immunoglobulin G horseradish peroxidase (IgG HRP) antibody for 1 hour and washed again with PBS-T at 10 minutes interval. Dilutions of antibodies are indicated in (Table 3). For detection of EYFP-Flag, FullCSEP0443-EYFP-Flag and ΔCSEP0443-EYFP-Flag, the membranes were first stained with ponceau stain to check the loading control, then washed with PBS-T until all stain is removed and incubated with anti-green fluorescent protein (gfp) antibody-HRP conjugated and proceeded as described in section 2.16. Dilution of antibody shown in (Table 3).

### 6.2.10 Visualizing the localization of CSEP0443, AtPEN1 using confocal microscopy

The Leica SP5 and Zeiss LSM880 Airyscan confocal microscopes were employed to visualize the localization of AtPEN1 and CSEP0443 respectively. Leaf samples from *Arabidopsis* infected with *Bgh* for 1-2 days, non-infected leaves and *N. benthamiana* leaves infiltrated and non infiltrated were freshly harvested and immersed in 0.85 M sodium chloride for 10 minutes to induce plasmolysis before examination. Additional steps are described in section 2.19.

### 6.2.11 Statistical analysis

Comparison of the differences between means were done using one-way Analysis of variance (ANOVA) and Tukey's statistics of the Minitab 18 statistical package. Statistical significance was reported at either $P < 0.05$ or $P < 0.01$.

## 6.3 Results

### 6.3.1 Exploring potential CSEP0443-RRE1 interactions

#### 6.3.1.1 CSEP0443 interacts with RRE1 *in vitro*

Pathogen effectors often target key host defence proteins for inactivation to promote pathogenesis (Toruno *et al*, 2016). One mechanism for a pathogen effector to disable a key defence related protein is to physically interact with the target protein disrupting its biological activity (Petre *et al*, 2015). Therefore, I explored possible interaction of RRE1 with CSEP0443 utilizing an *in vitro* pull-down assay. RRE1 was expressed with a glutathione S-transferase (GST) tag and CSEP0443 expressed with maltose binding protein (MBP) tag. The GST-RRE1 proteins were initially incubated with glutathione Sepharose (GSH) resin. The bound GST-RRE1 was then incubated with MBP-CSEP0443. The proteins were washed in ice cold PBS to collect the un-bound proteins and boiled in SDS loading buffer. The proteins were run in SDS PAGE, subjected to western blotting and analysed by incubating with anti-MBP antibody. RRE1 was shown to interact with CSEP0443 (Figure 6-1 lane 1) indicated by the strong signal with anti-MBP antibody, while no signal was detected when MBP was exposed to RRE1 (Figure 6-1 lane 2). The absence of any signal in the control lanes confirmed that the interaction was due CSEP0443 and RRE1 (Figure 6-1 lane 2, 3, and 4).

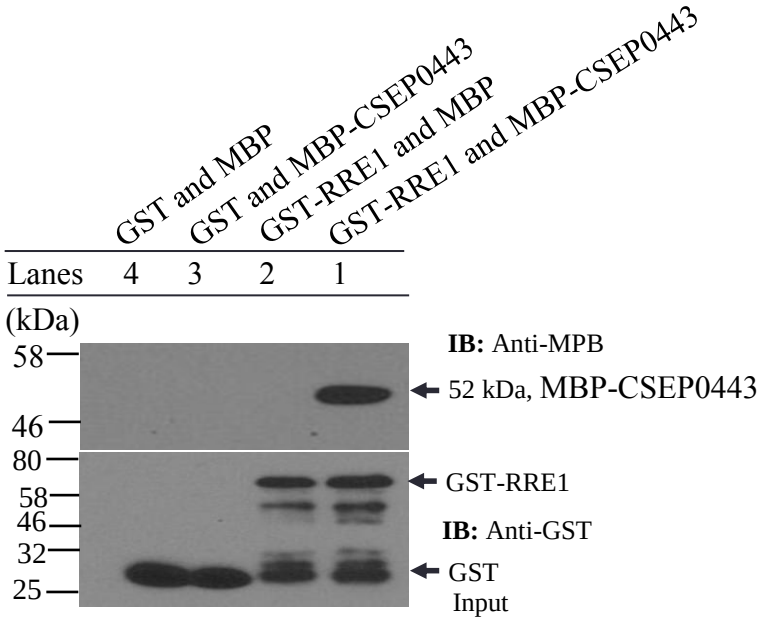

**Figure 6-1: GST-RRE1 interacts with MBP-CSEP0443 in an *in vitro* pull-down assay.** Recombinant proteins of GST-RRE1, MBP-CSEP0443, MBP and GST were purified from *Escherichia coli* using reduced glutathione for GST/GST tagged proteins and maltose for MBP/MBP tagged proteins. Purified GST/GST-RRE1 was incubated with glutathione Sepharose 4B resin and later incubated with MBP/MBP-CSEP0443 protein. After incubation, the unbound proteins were washed off and the retained proteins resolved in SDS PAGE. Detection of interaction was done by immunoblotting with anti-MBP antibody. Lane 1, checking the interaction of RRE1 and CSEP0443. Lane 2, checking the interaction of RRE1 and MBP. Lane 3, checking the interaction of GST and CSEP0443. Lane 4, checking the interaction of GST and MBP. Loading controls were detected by immunoblotting with anti-GST antibody. Experiment was repeated three times.

#### 6.3.1.2 CSEP0443 interacts with RRE1 *in vivo*

To investigate a possible *in vivo* interaction between CSEP0443 and RRE1, a genetic construct was designed having *CSEP0443* embedded with a C-terminal *FLAG* tag expressed by the *Ubiquitin* promoter and terminator. The full transcriptional unit was ligated with *RRE1* having a C- terminal *HA* tag expressed by *LHB1B1* promoter and *MAS* terminator. The full transcription units were finally cloned into a Golden Gate MoClo plant expression vector. The constructs were verified by genotyping PCR and Sanger sequencing and transformed into *Agrobacterium* GV3101 strain. Following floral dipping, the genetic constructs were transformed into *Arabidopsis rre1* plants. Homozygous lines were tested for the expression of *CSEP0443-FLAG* and *RRE1-HA* transcripts using RT-PCR. The active expression of these genes was detected in transformed lines by RT-PCR to support the selection of transgenic lines for further analysis (Figure 6-2).

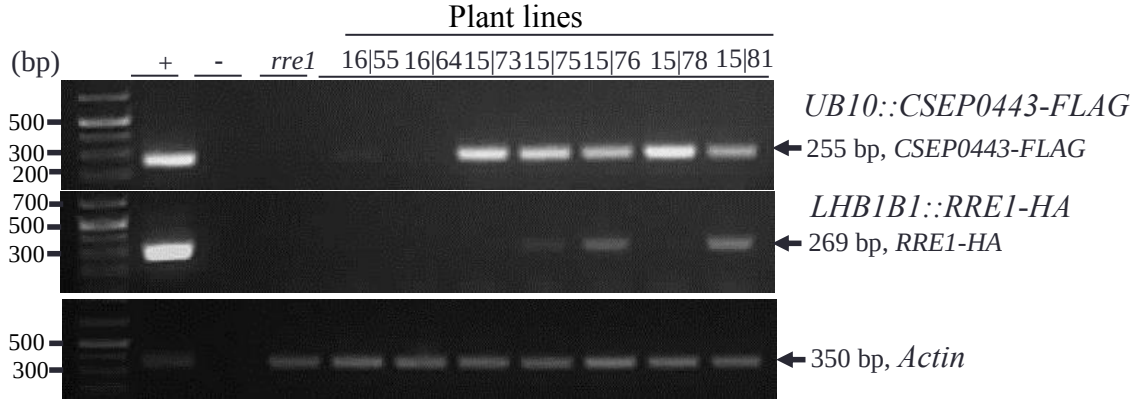


**Figure 6-2: RT-PCR detects the expression of *CSEP0443* and *RRE1* in *rre1* plants.** *Arabidopsis rre1* mutant was transformed with genetic construct of *UB10::CSEP0443-FLAG LHB1B1::RRE1-HA* and after successive selection steps homozygous lines were obtained. RNA was extracted from the lines using TRIzol reagent and synthesised into cDNA. Detection of the expression was based on the amplification of gene fragments of *CSEP0443-FLAG* and *RRE1-HA*. *Actin* amplification was used as a reference.

Plant lines showing target transcripts were then analysed for protein expressions. Proteins were extracted from leaves crushing the leafy tissues in non-denaturing buffer. The protein extracts were filtered, quantified and subjected to immunoprecipitation with either anti-flag or anti-HA antibodies immobilized on agarose resin. After incubation the proteins were washed in ice cold PBS and separated by SDS PAGE. Protein target detection was accomplished by western blot analysis with either anti-flag or anti-HA antibodies. The CSEP0443 and RRE1 proteins were detected in both lines selected (Figure 6-3).

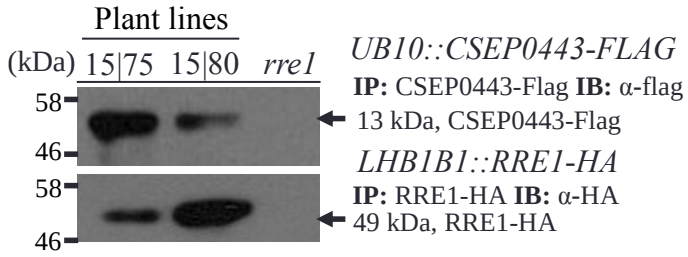


**Figure 6-3: Expression of CSEP0443-Flag and RRE1-HA proteins detected in *rre1* plants.** Proteins were extracted in non denaturing buffer from the selected homozygous lines transformed with *UB10::CSEP0443 LHB1B1::RRE1-HA*. Extracted proteins were incubated with either anti-flag antibody or anti-HA antibody conjugated on agarose beads. Unbound proteins were washed off using PBS and the retained proteins resolved

in SDS PAGE. Detection of the proteins was done by immunoblotting with either anti-flag antibody or anti-HA antibody. Proteins extracted from non transformed *rre1* mutant was used as negative control.

To check for the interaction of CSEP0443 and RRE1, proteins were extracted from the above plant lines previously challenged with *Bgh*. A line expressing CSEP0443 alone was employed as a negative control. The extracted proteins were immuno-precipitated with anti-flag antibodies conjugated on agarose beads. The proteins were further immunoblotted with either anti-HA or anti-flag antibodies. RRE1-HA was detected confirming the interaction with CSEP0443 (Figure 6-4 red lane). RRE1 was not detected in the line expressing CSEP0443 alone (Figure 6-4 black lane).

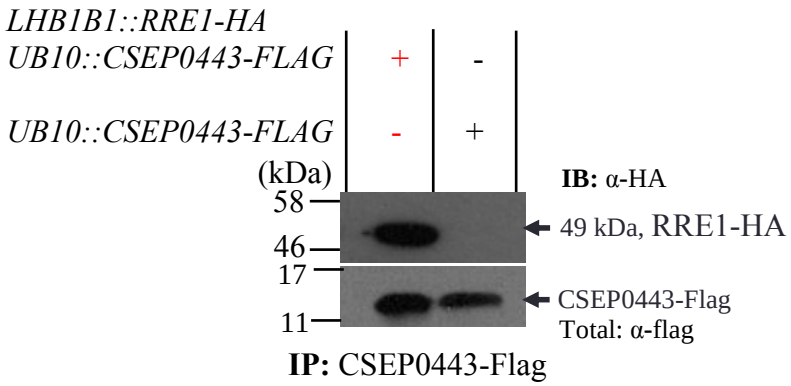


**Figure 6-4: Interaction of CSEP0443 and RRE1 detected *in vivo*.** Plant lines expressing either genetic construct *LHB1B1::RRE1 UB10::CSEP0443-FLAG* or *UB10::CSEP0443-FLAG* were initially infected with *Bgh*. Proteins were extracted from the leaf tissues in non denaturing buffer and immunoprecipitated with anti-flag antibody conjugated on agarose beads. The proteins were then washed in PBS and the bound proteins resolved in SDS PAGE. Detection of the interaction was done by immunoblotting with anti-HA antibody (red lane). Proteins extracted from plants expressing *UB10::CSEP0443-FLAG* was used as negative control (black lane). Loading controls were detected by immunoblotting with anti-HA antibody. Experiment was repeated three times.

### 6.3.1.3 CSEP0443 preferentially interacts with the RING domain of RRE1

To uncover the approximate domain of RRE1 that interacts with CSEP0443, full length RRE1, RRE1-RING and RRE1-Ankyrin repeat proteins were fused with a GST tag, expressed and purified *in vitro* from *Escherichia coli*. The GST-RRE1-RING and GST-RRE1-Ankyrin repeat proteins individually were incubated with GSH beads. The proteins were later incubated with MBP-CSEP0443. The incubated proteins were washed in ice cold PBS to remove unbound proteins. Control proteins followed the same treatment. The proteins were resolved by SDS PAGE followed by western blot analysis. The anti-MBP antibody detected the interaction of MBP-CSEP0443 and the RRE1-RING domain (Figure 6-5 lane 5). CSEP0443 interaction was also detected with RRE1-Ankyrin repeat domain but the intensity of the interaction was relatively less pronounced (lane 2) (Figure 6-5 A). The mean area of interactions were relatively quantified using ImageJ software (Figure 6-5 B).

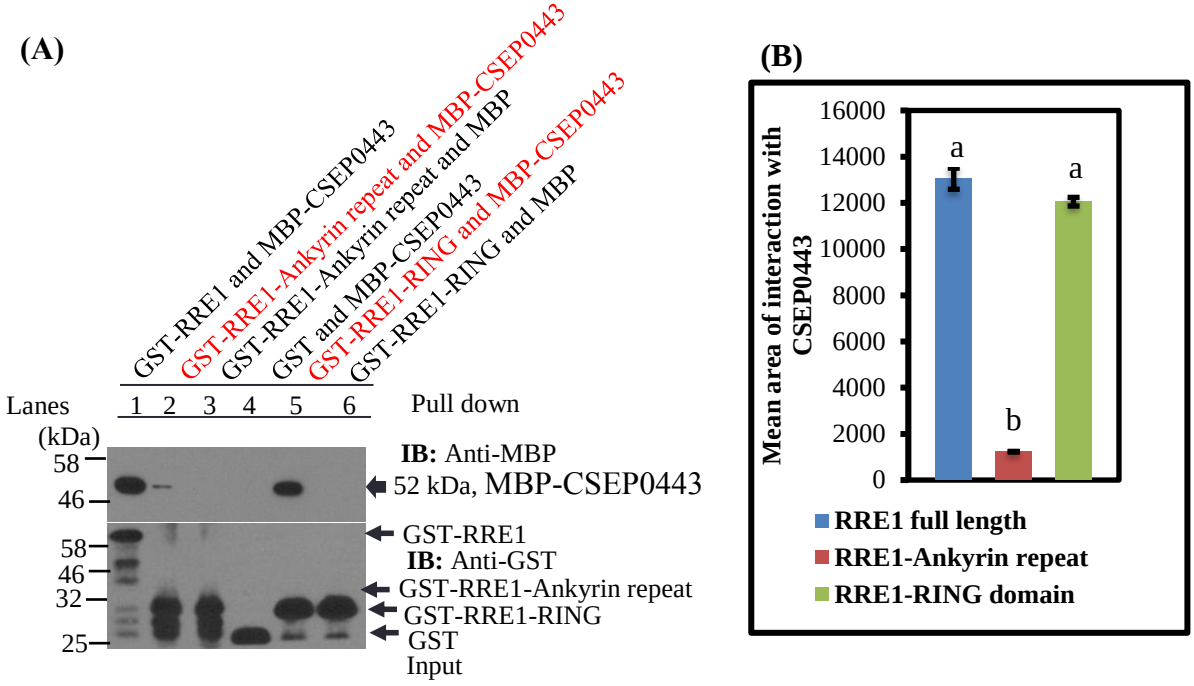


**Figure 6-5: MBP-CSEP0443 relatively exhibit high interaction with GST-RRE-RING and less with GST-RRE1-Ankyrin repeat in an *in vitro* pull down assay.** (A) Recombinant proteins of GST-RRE1, GST-RRE1-Ankyrin repeat, GST-RING, GST, MBP-CSEP0443 and MBP were expressed and extracted from *Escherichia coli*. Purified GST-RRE1, GST-RRE1-Ankyrin repeat, GST-RING, GST were initially incubated with

glutathione Sepharose 4B resin, and later MBP-CSEP0443 and MBP introduced, and further incubated. After incubation the proteins were washed in PBS and the retained proteins resolved in SDS PAGE. Detection of interactions were performed by immunoblotting with anti-MBP antibody. Lane 1, checking the interaction of RRE1 and CSEP0443. Lane 2, checking the interaction of RRE1-Ankyrin repeat and CSEP0443. Lane 3, checking the interaction of RRE1-Ankyrin repeat and MBP. Lane 4, checking the interaction of GST and CSEP0443. Lane 5, checking the interaction of RRE1-RING and CSEP0443. Lane 6, checking the interaction of RRE1-RING and MBP. Loading controls were detected by immunoblotting with anti-GST antibody. (B) Histogram displays the relative quantification of interactions using ImageJ software. Protein bands detected were relatively quantified using ImageJ software and expressed as area of interactions. Error bars represent mean ± standard error. *n* = biological replicates. One-way ANOVA and Tukey's comparisons for the difference of means performed by statistical package Minitab 18. Means that do not share a letter are significantly different at $P \leq 0.01$.

#### 6.3.1.4 The collapse of Zinc binding in RRE1 compromises the interaction with CSEP0443

RRE1 E3 ligase activity is mediated by the RING zinc finger domain. The coordination of zinc to cystine/histidine is important to maintain a cross-brace structure of the RING domain necessary for the E3 ligase activity (Chasapis *et al*, 2010). In RRE1, the mutation of C340, located in the RING domain, to serine, abolished the E3 ligase activity of RRE1 (Yu, 2012). This may be due to the perturbation of the normal arrangement of the RING domain. I investigated the level of CSEP0443 interaction with RRE1-C340S using an *in vitro* pull-down assay. Both wild-type RRE1 and RRE1-C340S, initially immobilized on GSH resin, were incubated with MBP-CSEP0443. After incubation the proteins were separated by SDS PAGE and transferred to a nitrocellulose membrane. Western blot analyses were conducted by exposing the membrane to anti-MBP antibody. The levels of interaction were relatively quantified using ImageJ software and expressed as mean area of interaction. The physical interaction of CSEP0443 with RRE1-C340S was significantly relatively reduced compared to that of wild-type RRE1(Figure 6-6 A red lane and B green bar). This

result implies a potential requirement of a functional RING domain for an interaction between CSEP0443 and RRE1.

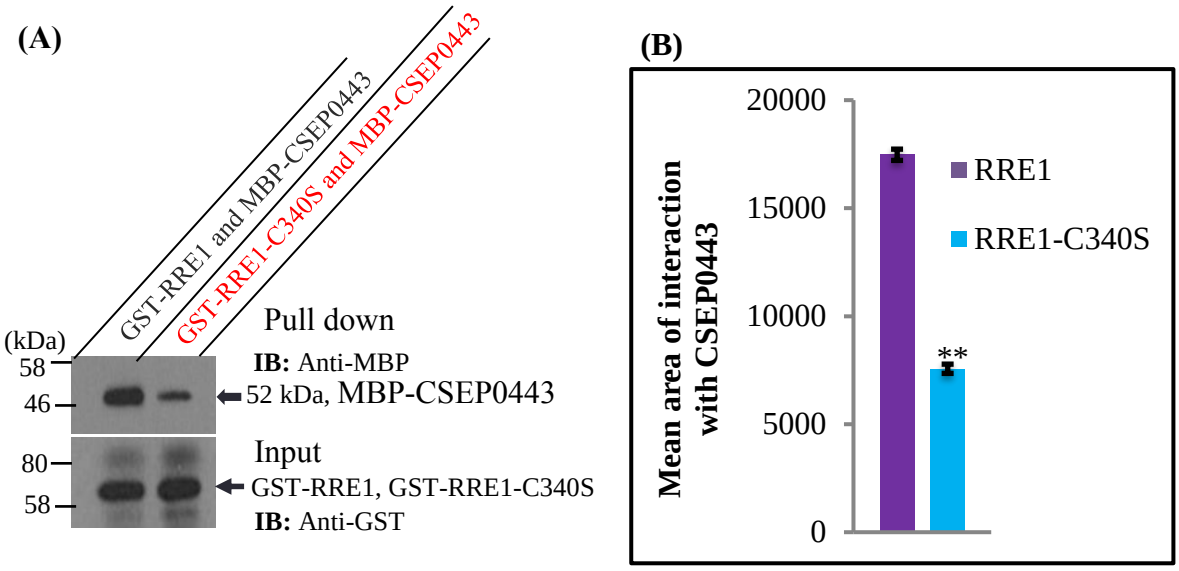


**Figure 6-6: CSEP0443 relatively show less interaction with RRE1-C340S.** (A) Recombinant proteins of GST-RRE1, GST-RRE1-C340S and MBP-CSEP0443 were expressed and purified from *Escherichia coli*. Purified GST tagged proteins were initially incubated with glutathione Sepharose 4B resin and later MBP-CSEP0443 introduced, and further incubated. After incubation, the unbound proteins were washed off using PBS and bound proteins resolved in SDS PAGE. Detection of the interaction was done by immunoblotting with anti-MBP antibody. Black lane, checking the interaction of wild-type RRE1 and CSEP0443. Red lane, checking the interaction of mutated RRE1 and CSEP0443. Loading controls were detected by immunoblotting with anti-GST antibody. (B) Histogram indicates the relative quantification of the interactions obtained by ImageJ soft aware. Protein bands were relatively quantified and were expressed as mean area of interaction. Error bars represent mean ± standard error. Experiment was repeated three times. Asterisks represent significant differences, *t*-test $P < 0.01$.

### 6.3.2 Influence of CSEP0443 on RRE1 ligase activity

#### 6.3.2.1 CSEP0443 is not a substrate of RRE1

The interaction of CSEP0443 with RRE1 prompted me to investigate the likelihood of CSEP0443 being a substrate for RRE1. Thus *in vitro* reactions were set up with E1 (Human), E2 *Arabidopsis thaliana* Ubiquitin conjugating enzyme 1 (AtUBC1) and RRE1 as E3, histidine-ubiquitin (His-ubiquitin) and ATP in a suitable buffer. In addition, CSEP0443 and MBP were included as possible substrates. BSA a known lysine exposed rich protein was

used as a positive control. After incubation the proteins were separated by SDS PAGE and subjected to western blot analysis with an anti-polyhistidine antibody. Ubiquitination was shown as a smear or ladders of ubiquitin of increasing mass above the monomer. No polyubiquitination was detected in reactions having either MBP-CSEP0443 (Figure 6-7 lane 2) or MBP (Figure 6-7 lane 3), indicating that CSEP0443 is not a substrate for RRE1. The ubiquitination of BSA (Figure 6-7 lane 1), implied that assay conditions were suitable for polyubiquitination reaction.

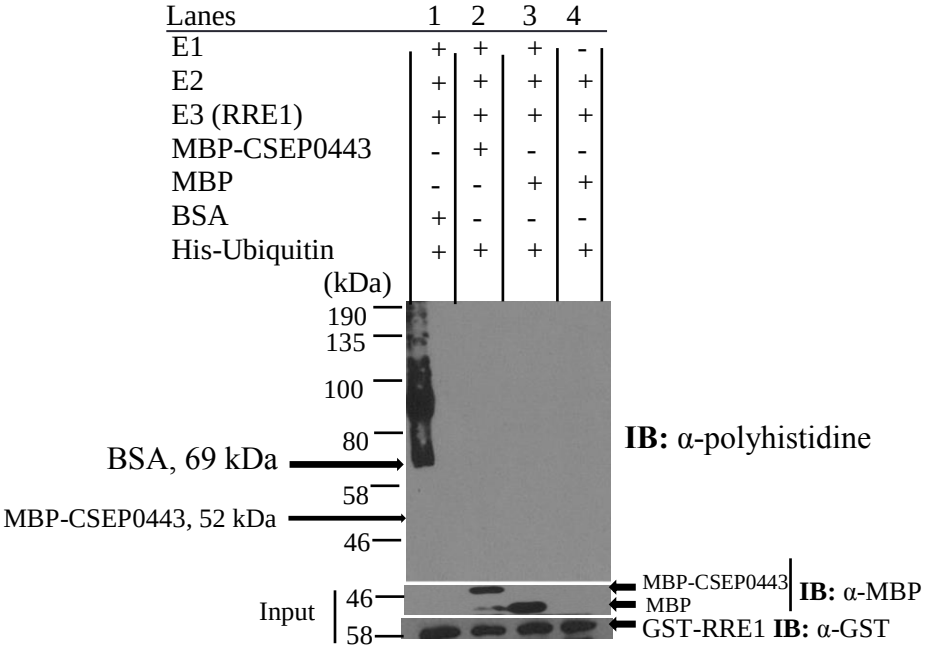


**Figure 6-7: CSEP0443 is not ubiquitinated by RRE1.** *In vitro* ubiquitination assay was set up containing E1, E2, RRE1 and histidine-ubiquitin. MBP-CSEP0443, MBP and BSA were introduced as substrates. BSA is a lysine rich exposed protein and was used as a positive control. The reaction mixtures were incubated for 2 hours and later the proteins separated in SDS PAGE. Protein ubiquitination was detected by immunoblotting with anti-polyhistidine antibody and is shown as ladders or smear of ubiquitin above the monomer. Lane 1, checking the ubiquitination of BSA (positive control). Lane 2, checking the ubiquitination of CSEP0443. Lane 3, checking the ubiquitination of MBP. Lane 4, absence of E1 in the reaction was used as negative control. Loading controls were detected by immunoblotting with anti-MBP antibody and anti-GST antibody. Experiment was repeated three times.

### 6.3.2.2 CSEP0443 inhibits RRE1-AtPEN1 polyubiquitination *in vitro*

To assess the influence of CSEP0443 on RRE1 ubiquitination activity against AtPEN1, the MBP-AtPEN1, MBP-CSEP0443 and GST-RRE1 proteins were expressed in *E. coli*, purified and eluted with both maltose and reduced glutathione. Ubiquitination assays were carried out as described above with AtPEN1 included in as a substrate. Western blot analysis was performed with anti-polyhistidine antibody. Polyubiquitination was shown as a uniform smear of increasing molecular mass above the AtPEN1 monomer. Polyubiquitination activity was detected in reactions where CSEP0443 was absent (Figure 6-8 lane 1 and 3). On the hand, a gradual loss of polyubiquitination activity against AtPEN1 was detected in reactions where CSEP0443 was present (Figure 6-8 lane 2). The presence of MBP did not affect the level of polyubiquitination (Figure 6-8 lane 3), suggesting that the observed effect is specific to CSEP0443. In the absence of E1 no ubiquitination was detected (Figure 6-8 lane 4).

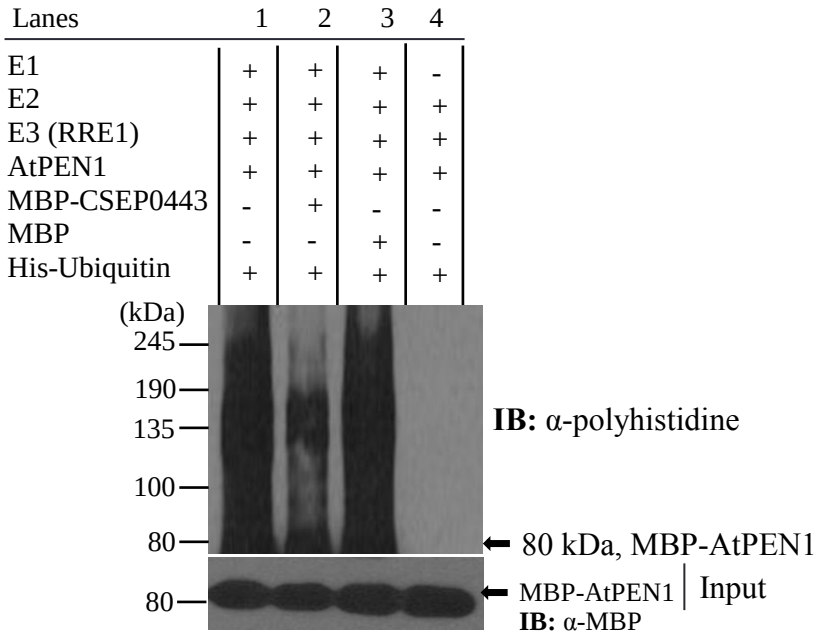


**Figure 6-8: *In vitro* ubiquitination of AtPEN1 by RRE1 in presence of CSEP0443 show reduced polyubiquitination**. *In vitro* ubiquitination assays were set up in reactions containing E1, E2, RRE1, AtPEN1, histidine-ubiquitin, MBP-CSEP0443 and MBP. After incubation for 2 hours, the proteins were separated in SDS PAGE followed by

immunoblotting with anti-polyhistidine antibody. Protein polyubiquitination was shown as high mass uniform smear on MBP-AtPEN1. Lane 1, checking the ubiquitination of AtPEN1. Lane 2, checking the ubiquitination of AtPEN1 in presence of CSEP0443. Lane 3, checking the ubiquitination of AtPEN1 in presence of MBP. Lane 4, reaction lacking E1 was used as negative control. Loading controls were detected by immunoblotting with anti-MBP antibody. The experiment was repeated three times.

#### 6.3.2.3 CSEP0443 compromise the ubiquitination of AtPEN1 *in vivo*

Genetic constructs were designed with *CSEP0443-FLAG* expressed by *Ubiquitin* promoter and terminator, combined with *AtPEN1-MYC* expressed by the *CaMV 35S* promoter and terminator. In parallel, a negative control, consisting of a full transcriptional unit of *AtPEN1-MYC* was also designed. The full transcription units were ligated into Golden Gate MoClo plant expression vectors and finally transformed into *Agrobacterium*. Cloning step verifications were performed by genotyping PCR and Sanger sequencing. To test for the effect of CSEP0443 on AtPEN1 ubiquitination, initially the vectors were Agro-infiltrated in 3 week old *N. benthamiana* plants. Proteins were extracted in non-denaturing buffer, filtered, quantified and subjected to immuno-precipitation with anti-Myc antibody conjugated on agarose beads. Ice cold PBS washed proteins were suspended in SDS loading buffer and resolved by SDS PAGE followed by western blot analysis with anti-ubiquitin antibody. The expression of CSEP0443 reduced the level of AtPEN1 ubiquitination (Figure 6-9 lane 2). In absence of CSEP0443 the level of AtPEN1 ubiquitination was increased (Figure 6-9 lane 1).

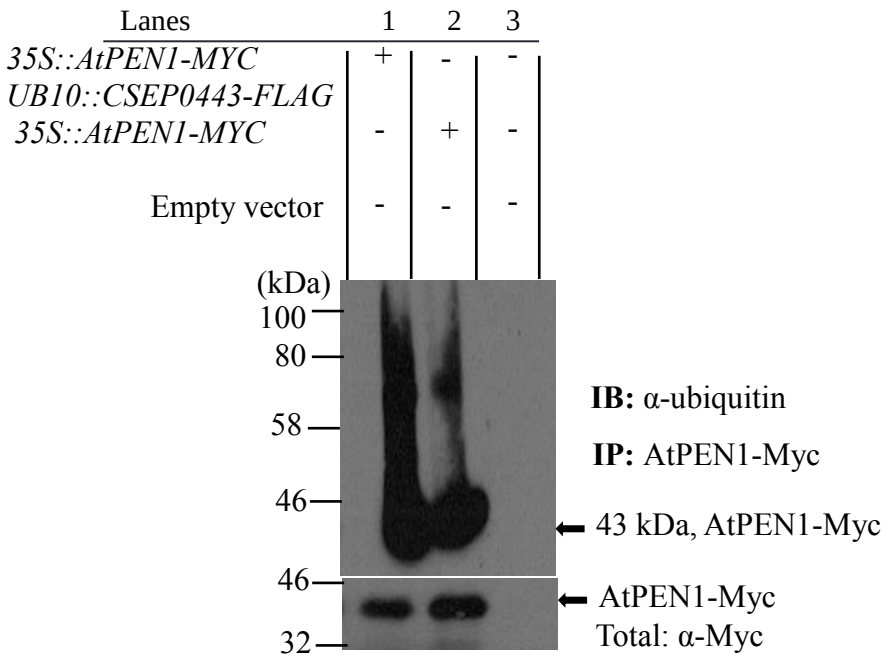


**Figure 6-9: CSEP0443 inhibits the ubiquitination of AtPEN1 *in vivo*.** *N. benthamiana* plants were infiltrated with *Agrobacterium* carrying genetic constructs *UB10::CSEP0443-FLAG 35S::AtPEN1-MYC*, *35::AtPEN1-MYC* and empty vector *pAGM4723*. Proteins were later extracted from infiltrated leaves in non denaturing buffer and immunoprecipitated with anti-Myc antibody conjugated on agarose beads. Detection of ubiquitination was done by immunoblotting with anti-ubiquitin antibody, shown as high mass uniform smear above AtPEN1-Myc monomer. Lane 1, checking the ubiquitination of AtPEN1 in absence of CSEP0443. Lane 2, checking the ubiquitination of AtPEN1 in presence of CSEP0443. Lane 3, protein extracted from plants infiltrated with empty vector was used as negative control. Loading controls were detected by immunoblotting with anti-Myc antibody. Experiment was repeated three times.

Further, the genetic constructs were transformed into *Arabidopsis pen1-1* plants to investigate if CSEP0443 could inhibit the activity of RRE1 in homozygous lines. Generated plants were checked for the expression of CSEP0443-Flag and AtPEN1-Myc. Proteins were extracted in nondenaturing buffer and immunoprecipitated with anti-flag and anti-Myc antibodies conjugated on agarose beads. The proteins were washed in ice cold PBS and retained proteins separated in SDS PAGE followed by immunoblotting with anti-flag and anti-Myc antibodies. AtPEN1-Myc and CSEP0443-Flag were detected in the selected lines (Figure 6-10 A and B). Lines 4/7, 4/10 and 4/11 displayed reduced or non-expression of

either AtPEN1 or CSEP0443 and therefore were not selected for downstream investigation (Figure 6-10).

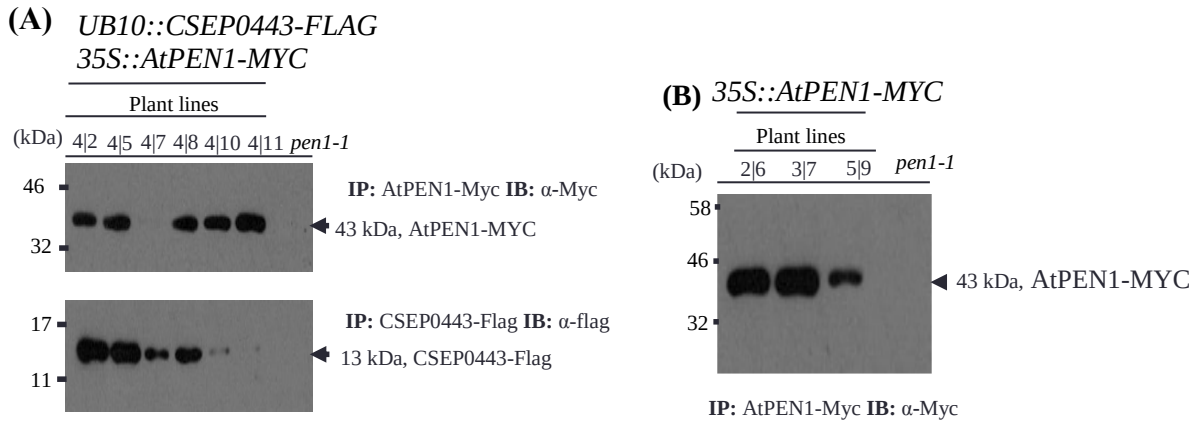


**Figure 6-10: CSEP0443-Flag and AtPEN1-Myc detected.** *Arabidopsis pen1-1* mutant was transformed with genetic constructs *UB10::CSEP0443-FLAG 35S::AtPEN1-MYC,* and *35S::AtPEN1-MYC*. Proteins were extracted from generated homozygous lines and immunoprecipitated with either anti-Myc antibody or anti-flag antibody conjugated on agarose beads. The immunoprecipitated proteins were washed with PBS and the retained proteins resolved in SDS PAGE. Detection of protein expression was done by immunoblotting with anti-Myc antibody or anti-flag antibody. Protein immunoprecipitated from non transformed *pen1-1* was used as negative control. (A) Detection of protein expression in plants transformed with *UB10::CSEP0443-FLAG 35S::AtPEN1-MYC* genetic construct. (B) Detection of protein expression in plants transformed with *35S::AtPEN1-MYC* genetic construct.

To assess the effect of CSEP0443 on the ubiquitination of AtPEN1, initially the selected plants were infected with *Bgh* and 3 days later, proteins extracted in non denaturing buffer. Proteins were then immunoprecipitated with anti-Myc antibody conjugated on agarose beads and washed in ice cold PBS buffer. Retained proteins were resolved in SDS PAGE and immunoblotted with anti-ubiquitin antibody. Ubiquitination was shown as a smear of increasing mass above the AtPEN1-Myc protein. The presence of CSEP0443 was shown to compromise the ubiquitination of AtPEN1 (Figure 6-11 lane 2). In absence of CSEP0443, the level of AtPEN1 ubiquitination was elevated (Figure 6-11 lane 1).

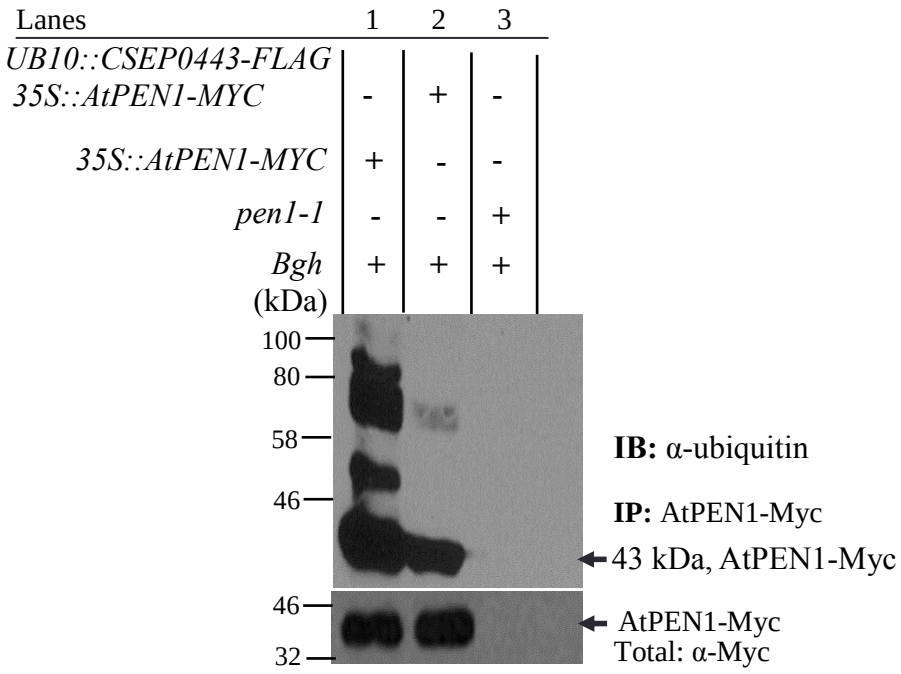


**Figure 6-11: CSEP0443 compromise AtPEN1 ubiquitination in stably transformed plants.** Plant lines expressing *UB10::CSEP0443-FLAG 35S::AtPEN1-MYC*, and *35S::AtPEN1-MYC* were previously infected with *Bgh* for 3 days. Proteins were extracted from infected leaf tissues and immunoprecipitated with anti-Myc antibody conjugated on agarose beads. Protein immunoprecipitates were washed in PBS, and bound proteins resolved in SDS PAGE. Detection of ubiquitination was done by immunoblotting with anti-ubiquitin antibody, and polyubiquitination was shown as a high mass uniform smear above AtPEN1-Myc protein. Lane 1, checking the ubiquitination of AtPEN1 in absence of CSEP0443. Lane 2, checking the ubiquitination of AtPEN1 in presence of CSEP0443. Lane 3, protein immunoprecipitated from *pen1-1* plant mutants was used as negative control. Loading controls were detected by immunoblotting with anti-Myc antibody. Experiment was repeated three times.

### 6.3.3 CSEP0443 localizes to the nucleus and intensively localize to the plasma membrane in response to *Bgh* challenge

The effector localization in the host tend to be related to the locations of potential target sites. Thus, likely to give an insight regarding their mode of action (Ahmed *et al*, 2016b). Having elucidated that CSEP0443 inhibit AtPEN1 ubiquitination, I attempted to disclose the localization of CSEP0443 in presence and absence of *Bgh*. Full length *CSEP0443* and truncated *CSEP0443* (Δ*CSEP0443*) lacking a signal peptide were fused with a C-terminal *EYFP* all in frame with a *FLAG* tag under the *Ubiquitin* promoter. In parallel

*EYFP* alone construct was also generated for comparison of the differences in the localizations. The full transcription units were ligated into Golden Gate MoClo plant expression vectors and finally the Sanger sequencing verified constructs were transformed into *Agrobacterium*. Initially the constructs were transiently transformed into *N. benthamiana* and assessed for protein expression. The expression of full and truncated CSEP0443 and EYFP were detected using anti-gfp antibody (Figure 6-12 A). Later the plants were examined for CSEP0443 localization. Both full length and truncated CSEP0443 exhibited nuclear and plasma membrane localization (Figure 6-12 C-D). No pronounced difference observed in terms of localizations for the two proteins. Free EYFP uniformly localized along the plasma membrane (Figure 6-12 B).

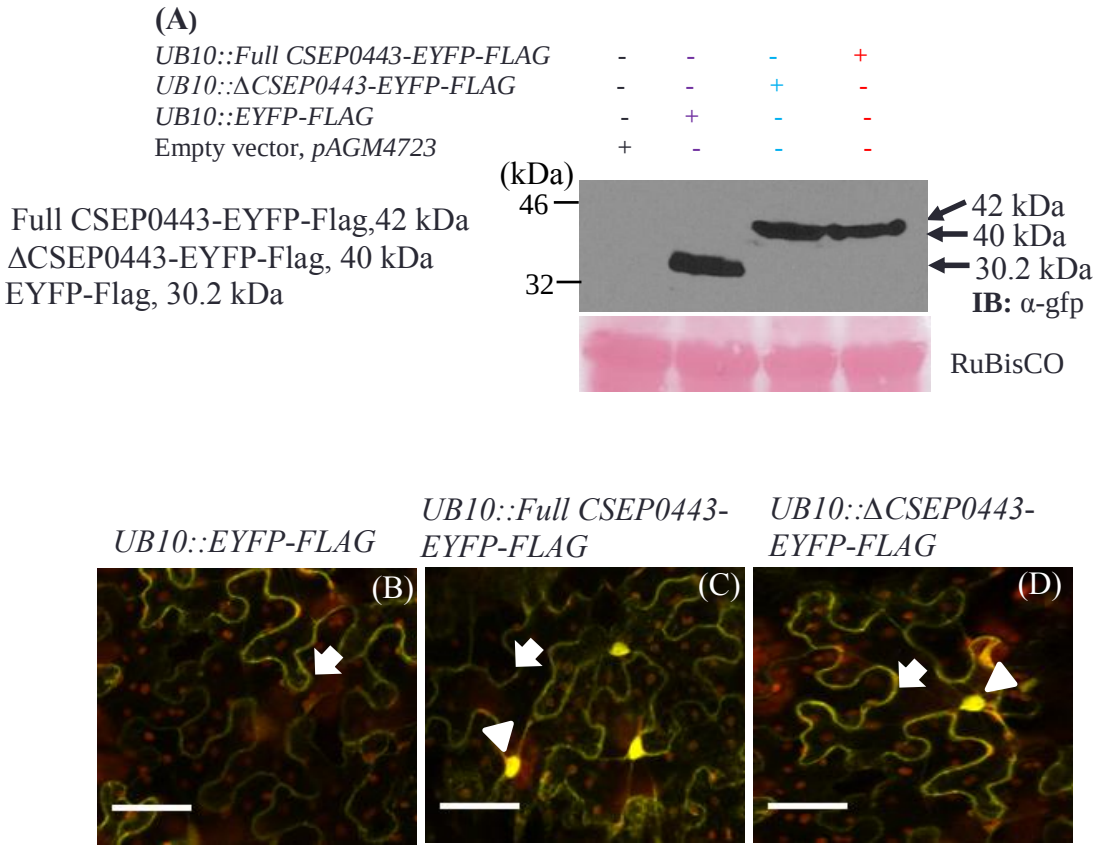


**Figure 6-12: CSEP0443 localize in the nucleus and on the plasma membrane in *N. benthamiana*.** (A) Detection of the expression of full CSEP0443, truncated (Δ) CSEP0443 (devoid of a signal peptide) and EYFP. Genetic constructs of *UB10::EYFP-FLAG*, *UB10::Full-CSEP0443-EYFP-FLAG*, and *UB10::ΔCSEP0443-EYFP-FLAG* were

generated and Agro-infiltrated in *N. benthamiana*. After incubation for 2 days, proteins were extracted in non denaturing buffer and total protein separated in SDS PAGE. Detection of protein expressions were done by immuno-blotting with anti-gfp antibody. Expression of full CSEP0443-EYFP-Flag (red lane), ΔCSEP0443-EYFP-Flag (blue lane) and EYFP-Flag (purple lane). Loading controls were detected by ponceau staining against Ribulose-1,5-bisphosphate carboxylase (RuBisCo). After detection of protein expression, infiltrated leaves were collected, incubated in sodium chloride solution for 10 minutes and observed using confocal microscopy. (B) Localization of Free EYFP. (C) Localization of full CSEP0443-EYFP-FLAG. (D) Localization of ΔCSEP0443-EYFP-FLAG. Arrow heads show nuclear localization. Arrow show plasma membrane localization. In each sub-figure, scale bar equal 259 μm.

Stable transgenic lines were then generated by transforming the constructs in *Arabidopsis* Col-0. Homozygous lines were checked for the expression of CSEP0443 by immuno-precipitation technique as described in section 6.3.2.3. CSEP0443-EYFP-Flag and EYFP-Flag expression were detected in plant lines generated. Full length CSEP0443-EYFP-Flag were more stable compared to the truncated CSEP0443-EYFP-Flag and EYFP-Flag alone (Figure 6-13 A and B). Line 15 of Full length CSEP0443-EYFP-Flag had significantly reduced levels of the protein expressions (Figure 6-13 A). Lines with stable protein expressions were selected for downstream investigation.

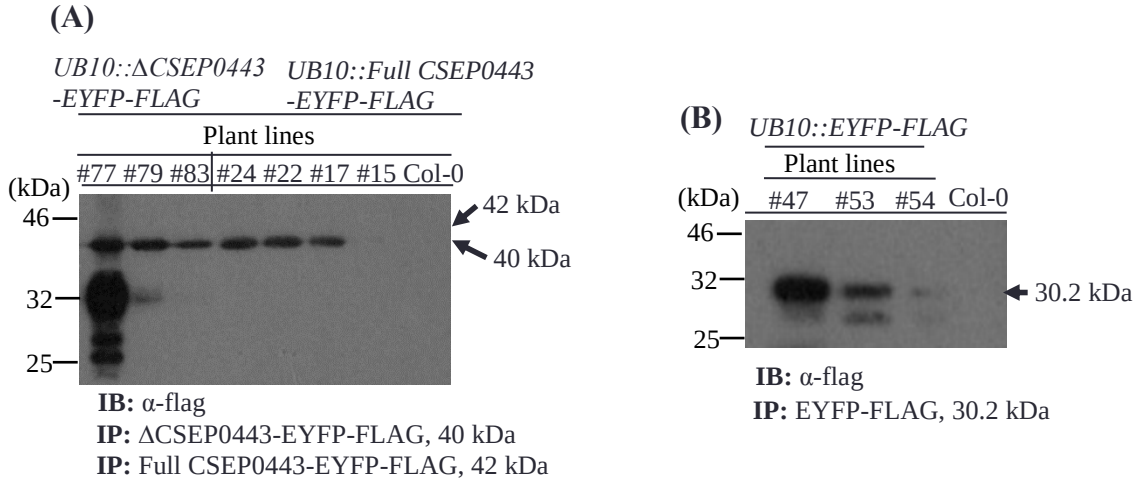


**Figure 6-13: Expression of CSEP0443-EYFP and free EYFP detected in *Arabidopsis* Col-0 plants.** The genetic constructs of: *UB10::EYFP-FLAG*, *UB10::Full CSEP0443-EYFP-FLAG*, and *UB10::ΔCSEP0443-EYFP-FLAG* were transformed in Col-0 plants. Proteins were extracted from the generated homozygous lines and immunoprecipitated with anti-flag antibody conjugated on agarose beads. Immunoprecipitated proteins were

washed in PBS and resolved in SDS PAGE. Detection of protein expression was done by immunoblotting with anti-flag antibody. Protein immunoprecipitated from non transformed Col-0 was used as negative control. (A) Detecting the expression of ΔCSEP0443-EYFP-FLAG and full CSEP0443-EYFP-FLAG proteins in selected lines. (B) Detecting the expression of free EYFP-FLAG protein in progressed lines.

To investigate the localization of CSEP0443, lines with stable protein expressions were either challenged or non-challenged with *Bgh*. Leaf samples were collected and examined. Free EYFP localized uniformly along the plasma membrane in both challenged and non-challenged plants (Figure 6-14 A and B). Both truncated and full length CSEP0443 localized in the nucleus and on the plasma membrane in non *Bgh* challenged plants (Figure 6-14 C and E). In challenged plants truncated CSEP0443 displayed targeted elevated localization on the plasma membrane (Figure 6-14 D). Full length CSEP0443 also was mobilized on the plasma membrane but with less intensity as compared to truncated CSEP0443 (Figure 6-14 E). In both proteins the expression in the nucleus were either reduced or completely un-detected in challenged conditions (Figure 6-14 D and E).

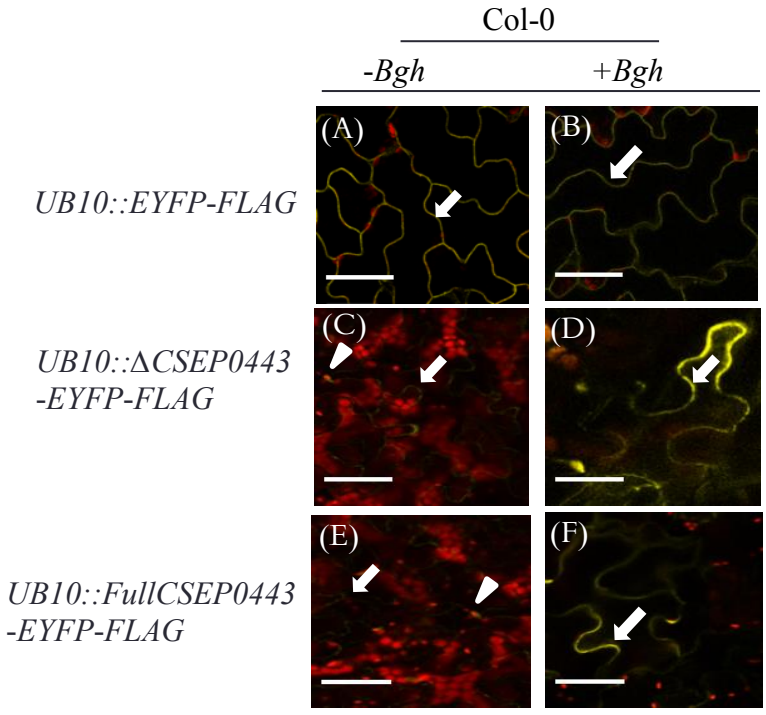

**Figure 6-14: Localization of CSEP0443 in *Arabidopsis* Col-0 lines infected and non infected with *Bgh*.** The protein localizes differentially under non-pathogen and pathogen challenge conditions. Plants lines expressing *UB10::EYFP-FLAG*, *UB10::FullCSEP0443-EYFP-FLAG*, and *UB10::ΔCSEP0443-EYFP-FLAG* were either infected or non infected with *Bgh* and incubated for 3 days. Leaf samples were collected and incubated in sodium chloride for 10 minutes before examination on confocal microscope. (A) Localization of free EYFP in absence of *Bgh* inoculation. (B) Localization of free EYFP in presence of *Bgh* inoculation. (C) Localization of ΔCSEP0443-EYFP-FLAG in absence of *Bgh* inoculation. (D) Localization of ΔCSEP0443-EYFP-FLAG in presence of *Bgh* inoculation. (E) Localization of full CSEP0443-EYFP-FLAG in absence of *Bgh* inoculation. (F) Localization of full CSEP0443-EYFP-FLAG in presence of *Bgh* inoculation. The arrows indicate plasma membrane localizations while the arrow heads display localizations in the nucleus. For each sub-figure, scale bar equal 142 µm.

### 6.3.4 Effect of CSEP0443 on the localization/recycling of AtPEN1 *in vivo*

#### 6.3.4.1 Expression of CSEP0443 in both *EGFP-AtPEN1-pen1-1* and *EGFP-AtPEN1-pen1-1-rre1* plants

Having demonstrated that CSEP0443 increasingly accumulates on the plasma membrane during *Bgh* challenge (Figure 6-14 D and F), I attempted to show the effect of CSEP0443 on AtPEN1 localization. AtPEN1 is known to localize on the plasma membrane and assemble at attempted penetration sites (Collins *et al*, 2003). Initially *CSEP0443* fused with a C-terminal *FLAG* was constructed under the *Ubiquitin* promoter and *Ubiquitin* terminator. This construct was then cloned into a plant expression vector by the Golden Gate MoClo and transformed into *Agrobacterium*. Positive transformants were verified by PCR before being utilized in the transformation of *Arabidopsis EGFP-AtPEN1-pen1-1* and *EGFP-AtPEN1-pen1-1-rre1*. Homozygous lines were checked for the expression of *CSEP0443* by RT-PCR. *CSEP0443* transcripts were detected in *EGFP-AtPEN1-pen1-1* plants (Figure 6-15).

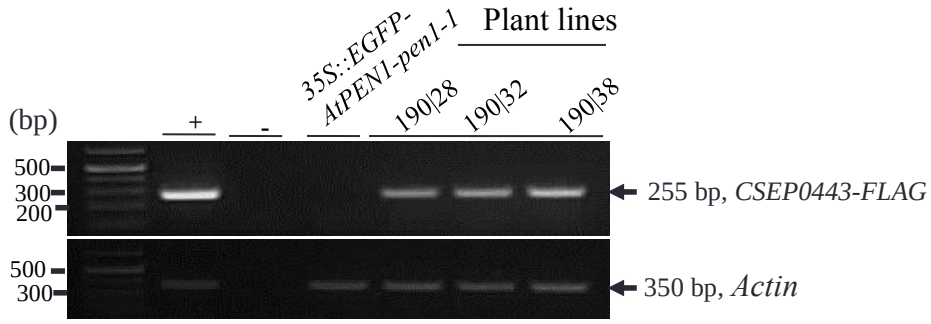


**Figure 6-15: RT-PCR detect the expression of *CSEP0443* in *EGFP-AtPEN1-pen1-1* plants.** The *Arabidopsis* line *EGFP-AtPEN1-pen1-1* was transformed with *UB10::CSEP0443-FLAG* genetic construct, after successive selections, homozygous lines were generated. RNA was extracted using TRIzol reagent from the generated lines followed by cDNA synthesis. Detection of the expression of *CSEP0443* was done by amplification *CSEP0443-FLAG* fragment. *Actin* gene amplification was used as a reference.

For the detection of CSEP0443, protein extracts were filtered through a 0.45 µM Millipore filter, quantified with a Bradford assay and immuno-precipitated with anti-flag antibody conjugated on agarose beads. The ice cold PBS washed proteins were suspended in SDS loading buffer and separated by SDS PAGE, and analysed via western blot utilising an anti-flag antibody. For *EGFP-AtPEN1-pen1-1* plants, CSEP0443 was expressed with relatively similar intensity in all lines tested (Figure 6-16 A). For *EGFP-AtPEN1-pen1-1-rre1* relative differential expression of CSEP0443 was detected (Figure 6-16 B). No protein was detected in the negative control (Figure 6-16 A and B).

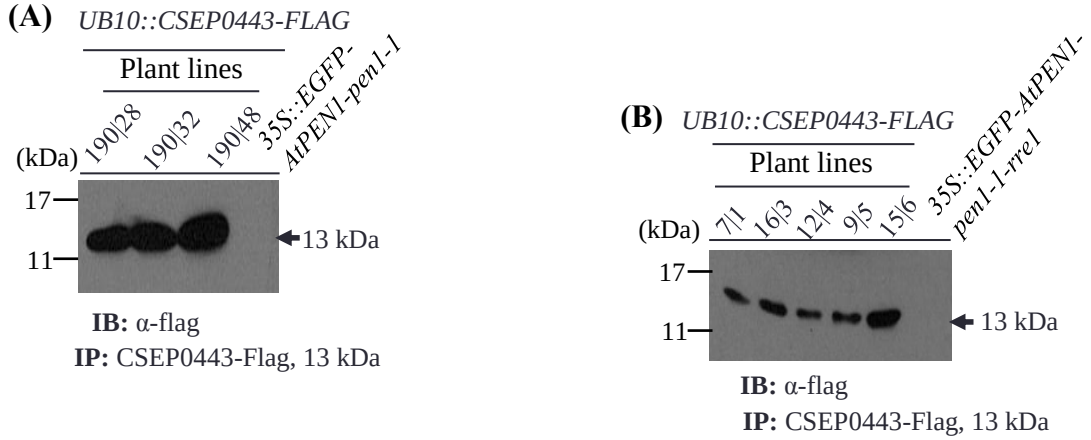

**Figure 6-16: CSEP0443 expressed in both *EGFP-AtPEN1-pen1-1* and *EGFP-AtPEN1-pen1-1-rre1* plants.** Genetic construct *UB10::ΔCSEP0443-FLAG* was transformed in *EGFP-AtPEN1-pen1-1* and *EGFP-AtPEN1-pen1-1-rre1* backgrouds, and stable homozygous plants generated after successive selections. Proteins were extracted from plant lines in non denaturing buffer and immunoprecipitated by incubating with anti-Myc antibody conjugated on agarose beads. The unbound protein were washed off using PBS and the retained proteins resolved in SDS PAGE. Detection of CSEP0443-Flag expression was performed by immunoblotting with anti-flag antibody. Proteins immunoprecipitated from non transformed *EGFP-AtPEN1-pen1-1* and *EGFP-AtPEN1-pen1-1-rre1* were used as negative control. (A) Detecting CSEP0443 expression in *EGFP-AtPEN1-pen1-1* plants. (B) Detecting CSEP0443 expression in *EGFP-AtPEN1-pen1-1-rre1* plants.

### 6.3.4.2 AtPEN1 localizes at the plasma membrane in plants constitutively expressing CSEP0443

Leaves from *35S::EGFP-AtPEN1-pen1-1* and *35S::EGFP-AtPEN1-pen1-1-rre1* plants in either the presence or absence of *CSEP0443* expression were analysed by confocal microscopy. AtPEN1 localized on the surface of the plasma membrane in the presence or absence of CSEP0443 expression (Figure 6-17 B-E). The absence of RRE1 in *35S::EGFP-AtPEN1-pen1-1-rre1* plants did not affect the localization of AtPEN1 on the plasma membrane (Figure 6-17 C and E).

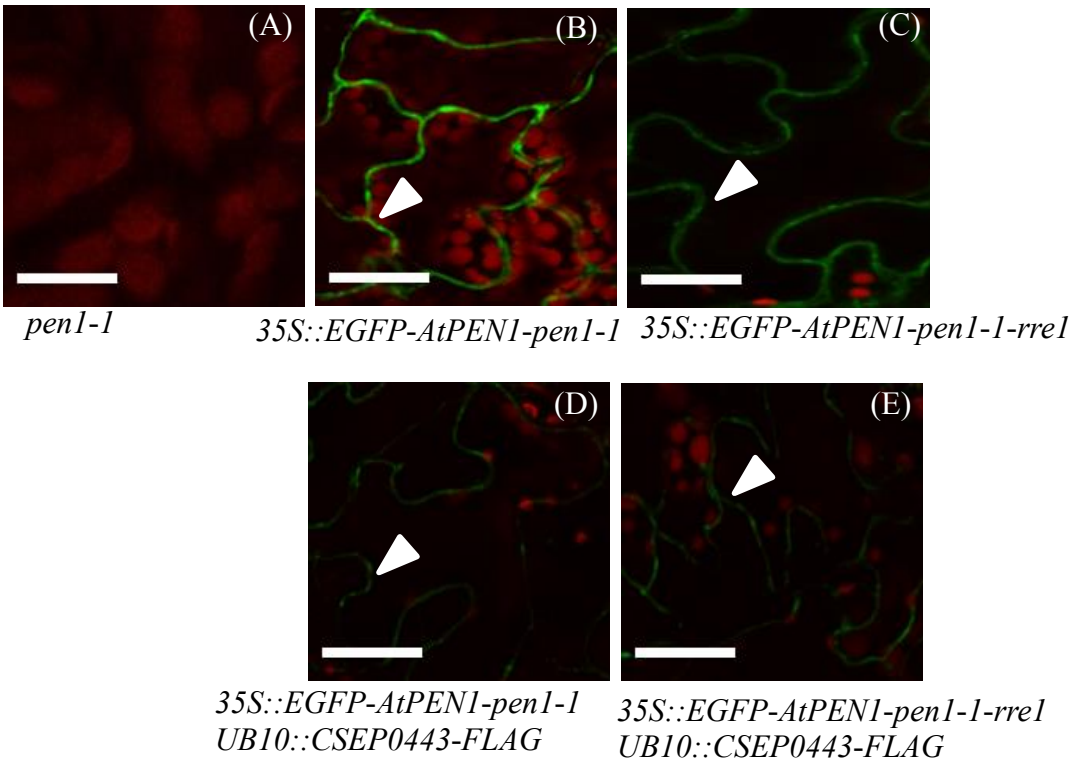


**Figure 6-17: EGFP-AtPEN1 localize on the plasma membrane under the expression of CSEP0443 in the absence of *Bgh* challenge.** Leaf samples were collected from *35S::EGFP-AtPEN1-pen1-1* and *35S::EGFP-AtPEN1-pen1-1-rre1* lines non expressing and expressing CSEP0443. Collected leaves were incubated in sodium chloride for 10 minutes and observed on a confocal microscope. Leaf samples from *pen1-1* mutant were used as negative control. (A) Detecting chlorophyl anto-flourescence in negative control line. (B) Detecting EGFP-AtPEN1 expression in lines non expressing CSEP0443 in *35S::EGFP-AtPEN1-pen1-1*. (C) Detecting EGFP-AtPEN1 expression in lines non expressing CSEP0443 in *35S::EGFP-AtPEN1-pen1-1-rre1*. (D) Detecting EGFP-AtPEN1 expression in lines expressing CSEP0443 in *35S::EGFP-AtPEN1-pen1-1*. (E) Detecting EGFP-AtPEN1 expression in lines expressing CSEP0443 in *35S::EGFP-AtPEN1-pen1-1-rre1*. EGFP-AtPEN1 shown by arrow head in all cases. Scale bars represent 210 µm.

### 6.3.4.3 Localization of AtPEN1 at the site of attempted *Bgh* penetration is compromised in plants constitutively expressing CSEP0443

Either *35S::EGFP-AtPEN1-pen1-1* or *35S::EGFP-AtPEN1-pen1-1-rre1* plant lines in the presence or absence of CSEP0443 expression were inoculated with *Bgh*. Localization of EGFP-AtPEN1 at attempted *Bgh* penetration sites, indicated by increased EGFP-AtPEN1 accumulation (Assaad *et al*, 2004), was observed in plant lines without CSEP0443 expression

(Figure 6-18 B and C). This intense localization was reduced in *rre1* plants not expressing CSEP0443(Figure 6-18 C). The localization of EGFP-AtPEN1 to attempted *Bgh* penetration sites in plants expressing CSEP0443 was reduced (Figure 6-18 D and E). The appearance and localization of EGFP-AtPEN1 in plant lines expressing CSEP0443 was similar (Figure 6-18 D and E).

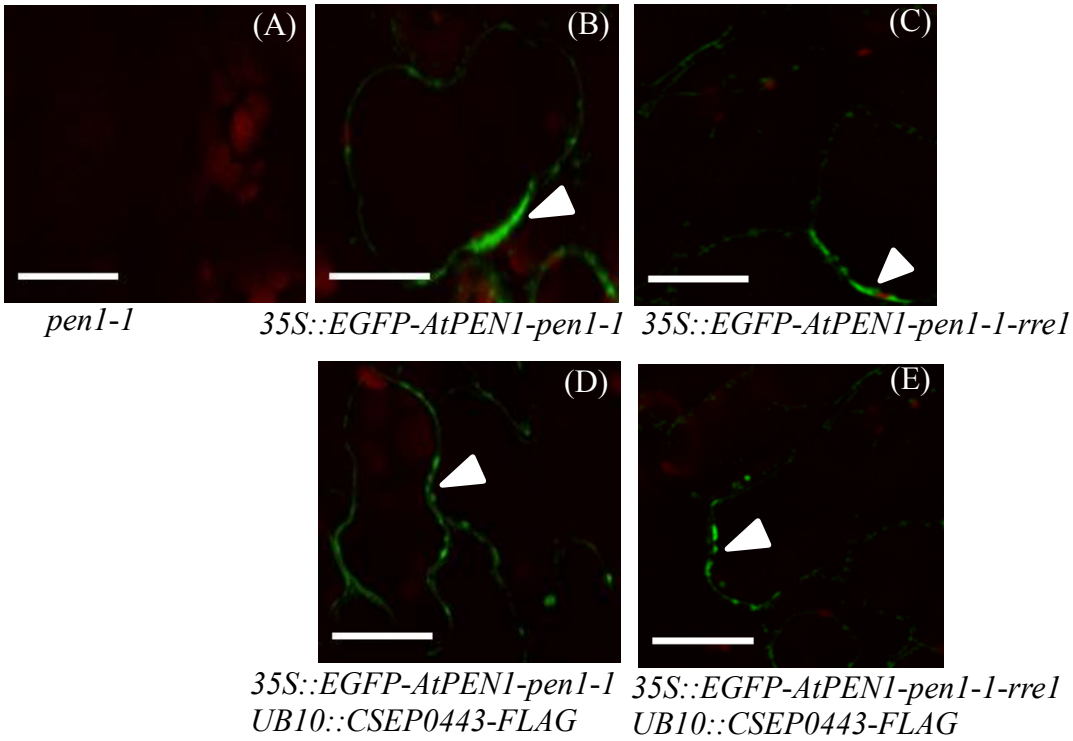


**Figure 6-18: CSEP0443 reduces AtPEN1 localization to sites of attempted *Bgh* infection.** Plant lines, *35S::EGFP-AtPEN1-pen1-1* and *35S::EGFP-AtPEN1-pen1-1-rre1* non expressing and expressing CSEP0443 were infected with *Bgh* and incubated for 3 days. Leaf samples were collected and incubated in sodium chloride solution for 10 minutes, and then examined on a confocal microscope. Leaf samples collected from *pen1-1* mutant were used as negative control. Areas of increased EGFP-AtPEN1 accumulation are presumed to be the attempted *Bgh* penetration sites. (A) Detecting chlorophyll auto-fluorescence in the negative control line. (B) Detecting EGFP-AtPEN1 localization after *Bgh* challenge in *35S::EGFP-AtPEN1-pen1-1* plants non-expressing CSEP0443. (C) Detecting EGFP-AtPEN1 localization after *Bgh* challenge in *35S::EGFP-AtPEN1-pen1-1-rre1* plants non-expressing CSEP0443. (D) Detecting EGFP-AtPEN1 localization following *Bgh* inoculation in *35S::EGFP-AtPEN1-pen1-1* expressing CSEP0443. (E) Detecting EGFP-AtPEN1 localization following *Bgh* inoculation in *35S::EGFP-AtPEN1-pen1-1-rre1* lines expressing CSEP0443. EGFP-AtPEN1 shown by arrow heads. Scale bars represent 329 µm.

### 6.3.4.4 CSEP0443 co-localize with AtPEN1 during *Bgh* challenge

Having shown that CSEP0443 compromise AtPEN1 focal accumulation during *Bgh* challenge, I investigated if CSEP0443 localize at sites where AtPEN1 is presumed to assemble. Full transcription unit of *UB10::EYFP-FLAG* and *UB10::CSEP0443-EYFP-FLAG* for both full length and truncated *CSEP0443* were transformed into *Arabidopsis 35S::EGFP-AtPEN1-pen1-1* and *35S::EGFP-AtPEN1-pen1-1-rre1* plants. Generated homozygous lines were checked for the expression of CSEP0443-EYFP-Flag and EYFP-Flag by immuno-precipitation with anti-flag antibody conjugated on agarose beads. Proteins were washed in ice cold PBS, separated in SDS PAGE followed by western blot analysis with anti-flag antibody. Expected protein size expressions of EYFP-Flag, ΔCSEP0443-EYFP-Flag and Full CSEP0443-EYFP-Flag were detected in the respective plant lines generated in *35S::EGFP-AtPEN1-pen1-1* and *35S::EGFP-AtPEN1-pen1-1-rre1* backgrounds (arrow). Some lines exhibited unstable protein expressions shown by multiple bands (Figure 6-19 A-D).

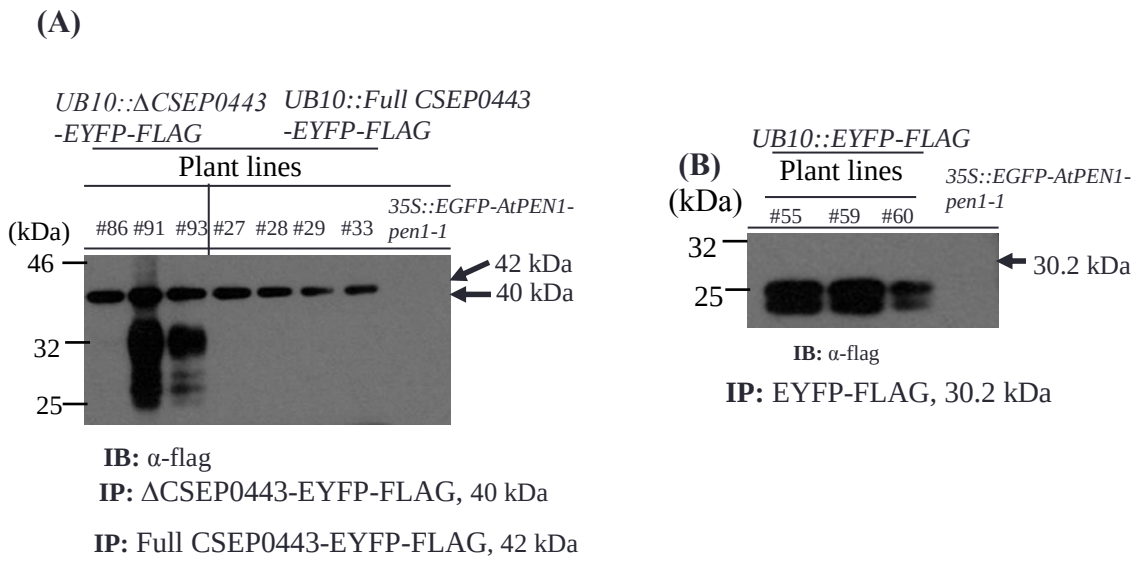

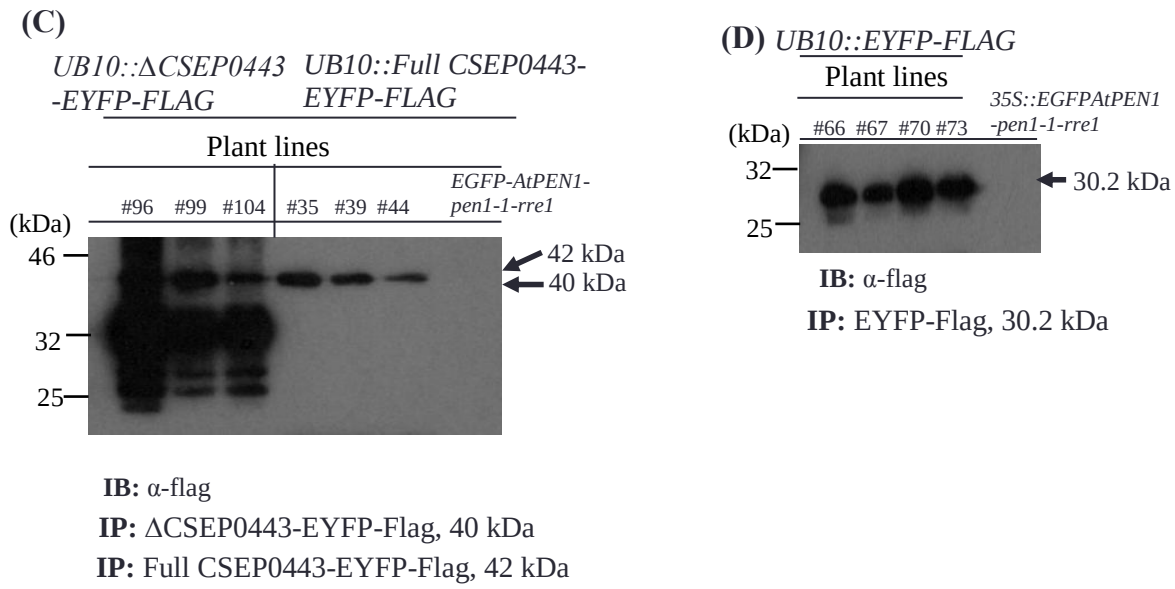


**Figure 6-19: Expression of ΔCSEP0443-EYFP-Flag, full CSEP0443-EYFP-Flag and EYFP-Flag detected in *EGFP-AtPEN1-pen1-1* and *EGFP-AtPEN1-pen1-1-rre1*.** Genetic constructs of *UB10::ΔCSEP0443-EYFP-FLAG, UB10::full-CSEP0443-EYFP-FLAG* and *UB10::EYFP-FLAG* were transformed in *35S::EGFP-AtPEN1-pen1-1* and *35S::EGFP-AtPEN1-pen1-1-rre1* backgrounds. Proteins were extracted from generated homozygous lines and immunoprecipitated by incubating with anti-flag antibody conjugated on agarose beads. Unbound proteins were removed by washing with PBS and the bound proteins resolved in SDS PAGE. Detection of CSEP0443 expression was done by immunoblotting with anti-flag antibody. Protein extracted from non transformed *35S::EGFP-AtPEN1-pen1-1* and *35S::EGFP-AtPEN1-pen1-1-rre1* were used as negative control. (A) Detecting truncated and full length CSEP0443 expression in *EGFP-AtPEN1-pen1-1* line. (B) Detecting EYFP-FLAG expression in *EGFP-AtPEN1-pen1-1* line. (C) Detecting truncated and full length CSEP0443 expression in *EGFP-AtPEN1-pen1-1-rre1* line. (D) Detecting EYFP-FLAG expression in *EGFP-AtPEN1-pen1-1-rre1*.

Lines with stable protein expressions were selected for further experimentations. The plants were challenged with *Bgh* and incubated for 3 days. Both challenged and non-challenged leaf samples were collected and examined. Under unchallenged conditions in *EGFP-AtPEN1-pen1-1* and *EGFP-AtPEN1-pen1-1-rre1* background, EYFP distributed along the plasma membrane with EGFP-AtPEN1 (Figure 6-20 A). Both full length and truncated CSEP0443 allocated in nucleus and on the plasma membrane while EGFP-AtPEN1 localized only on the plasma membrane (Figure 6-20 D and G). During pathogen challenge, in (*EYFP*)-*EGFP-AtPEN1-pen1-1* increased assembly of EGFP-AtPEN1 at specific location on the

membrane was observed (Figure 6-20 B). The site of EGFP-AtPEN1 accumulation, are regarded as the sites for attempted *Bgh* penetration (Assaad *et al*, 2004). Although mobilization of AtPEN1 in (*EYFP*)-*EGFP-AtPEN1-pen1-1-rre1* was elevated at specific area as in (*EYFP*)-*EGFP-AtPEN1-pen1-1*, was considerably reduced compared in (*EYFP*)-*EGFP-AtPEN1-pen1-1* (Figure 6-20 C). In (Δ*CSEP0443-EYFP*)-*EGFP-AtPEN1-pen1-1* the mobilization of EGFP-AtPEN1 tightly co-localized with ΔCSEP0443 and the amount of AtPEN1 was reduced (Figure 6-20 E). Moreover in (Δ*CSEP0443*)-*EGFP-AtPEN1-pen1-1-rre1* the co-localization of CSEP0443 with AtPEN1 greatly reduced AtPEN1 (Figure 6-20 F). Full length CSEP0443-EYFP also co-localized with EGFP-AtPEN1 in both cases reducing the expression levels of AtPEN1 in *EGFP-AtPEN1-pen1-1* and *EGFP-AtPEN1-pen1-1-rre1* lines (Figure 6-20 H and I). Compared to truncated CSEP0443, the expression of full CSEP0443 tightly equilibrated with the expression of AtPEN1.

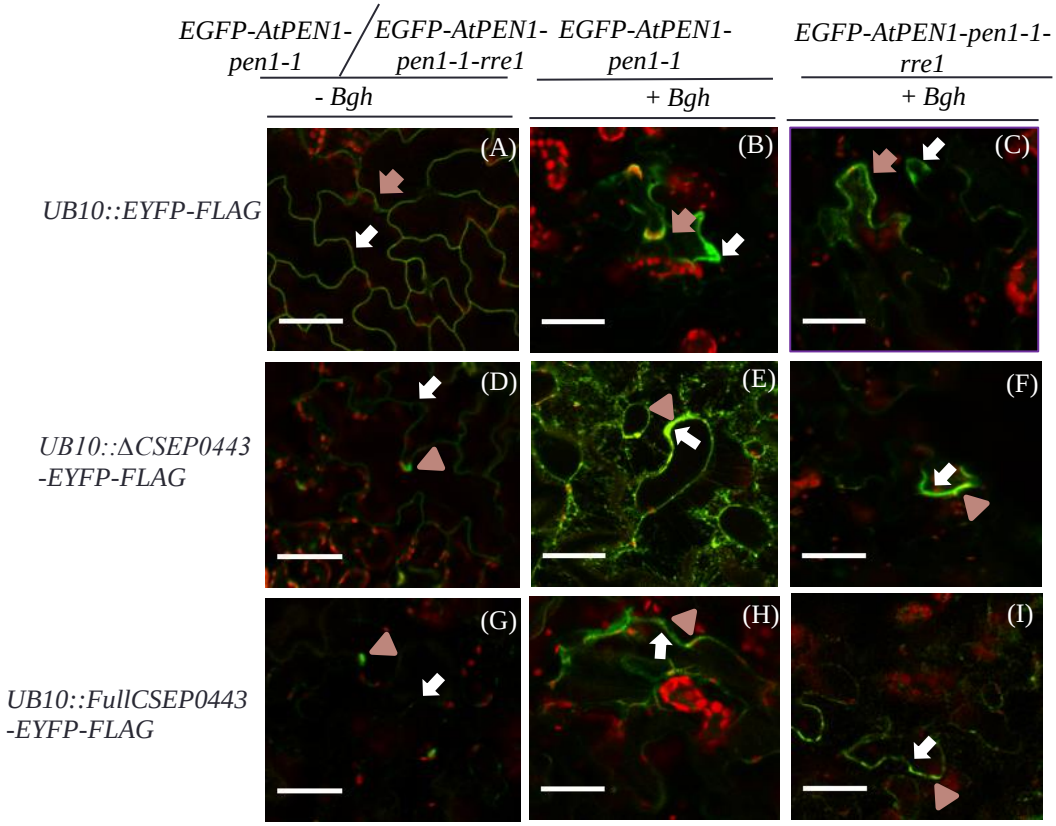


**Figure 6-20: CSEP0443 tightly colocalize with EGFP-AtPEN1 in *Bgh* infection.** The *Arabidopsis* plant lines *35S::EGFP-AtPEN1-pen1-1* and *35S::EGFP-AtPEN1-pen1-1-rre1*

expressing ΔCSEP0443-EYFP-FLAG, fullCSEP0443-EYFP-FLAG and EYFP-FLAG were either non inoculated or inoculated with *Bgh* and incubated for 3 days. Leaf samples were collected and incubated in sodium chloride solution for 10 minutes, then followed by examination on confocal microscope. Separation of EYFP and EGFP was achieved by selecting the option of un linear mixing after capturing the image. Areas of increased accumulation of EGFP-AtPEN1 are considered as sites for attempted *Bgh* penetration (Assaad *et al*, 2004). (A) Detecting the localization EGFP-AtPEN1 and EYFP in absence of *Bgh* in both *EGFP-AtPEN1-pen1-1* and *EGFP-AtPEN1-pen1-1-rre1* plants transformed with *UB10::EYFP-FLAG*. (B) Detecting the localization EGFP-AtPEN1 and EYFP after *Bgh* challenge in *EGFP-AtPEN1-pen1-1* plants transformed *UB10::EYFP-FLAG*. (C) Detecting the localization of EGFP-AtPEN1 and EYFP after *Bgh* challenge in *EGFP-AtPEN1-pen1-1-rre1* plants transformed with *UB10::EYFP-FLAG*. (D) Detecting the localization of ΔCSEP0443-EYFP and EGFP-AtPEN1 in absence of *Bgh* challenge in *EGFP-AtPEN1-pen1-1* and *EGFP-AtPEN1-pen1-1-rre1* plants transformed with *UB10::ΔCSEP0443-FLAG*. (G) Detecting the expression of Full CSEP0443-EYFP and EGFP-AtPEN1 in absence of *Bgh* challenge in *EGFP-AtPEN1-pen1-1* and *EGFP-AtPEN1-pen1-1-rre1* plants transformed with *UB10::fullCSEP0443-FLAG*. (E) Detecting the localization of ΔCSEP0443-EYFP and EGFP-AtPEN1 after *Bgh* challenge in *EGFP-AtPEN1-pen1-1* plants transformed with *UB10::ΔCSEP0443-FLAG*. (F) Detecting the localization of ΔCSEP0443-EYFP and EGFP-AtPEN1 after *Bgh* challenge in *EGFP-AtPEN1-pen1-1-rre1* plants transformed with *UB10::ΔCSEP0443-FLAG*. (H) Detecting the localization of full CSEP0443-EYFP and EGFP-AtPEN1 after *Bgh* challenge in *EGFP-AtPEN1-pen1-1* plants transformed with *UB10::fullCSEP0443-FLAG*. (I) Detecting the localization of fullCSEP0443-EYFP and EGFP-AtPEN1 after *Bgh* challenge in *EGFP-AtPEN1-pen1-1-rre1* plants transformed with *UB10::fullCSEP0443-FLAG*. Arrow heads (pink) indicate the localization of CSEP0443. Arrow (pink) display the localization of free EYFP. Arrows (white) display the localization of AtPEN1. Scale bars represent 140 μm.

## 6.4 Discussion

During recent years efforts have been undertaken to uncover the function of a multitude candidate of effectors proteins identified in the *Bgh* genome (Bindschedler *et al*, 2009, 2011; Godfrey *et al*, 2010; Spanu *et al*, 2010; Pedersen *et al*, 2012). A growing number of effectors have been shown to play a role in *Bgh* virulence following the application of Host Induced Gene Silencing (HIGS) (Zhang *et al*, 2012; Pliego *et al*, 2013; Schmidt *et al*, 2014; Ahmed *et al*, 2015a; Aguilar *et al*, 2016). However, only a few effectors have identified host protein targets (Ahmed *et al*, 2015a). My data suggests RRE1 as a potential target for CSEP0443 in *Arabidopsis* based on the physical interaction of these two proteins (Figure 6-1 lane 1, 6-3 red lane). In barley XBHV35, the homolog to RRE1, was found to interact with

CSEP0443 (Zhang, 2012; Aguilar, 2015). The revealed interaction suggested three possible outcomes:

(1) CSEP0443 target RRE1 presumably to suppress its E3 ligase activity. In rice the *Xanthomonas* outer protein P *Xanthomonas oryzae* pv. *oryzae* (XopPXoo) (Xoo3222) type III effector from *Xanthomonas oryzae* pv. *oryzae* (*X. oryzae* pv. *oryzae*) was shown to target *Oryza sativa* plant U-box 44 (OsPUB44), a rice U-box ubiquitin E3 ligase. OsPUB44 is required for the positive regulation of peptidoglycan and chitin triggered immunity. The interaction of XopPXoo and OsPUB44 abrogates the E3 ligase activity and enhances the virulence of *X. oryzae* pv. *oryzae* (Ishikawa *et al*, 2014). The effector avirulence effector Piz-t (AvrPiz-t) from the rice blast fungus *Magnaporthe oryzae* (*M. oryzae*) has been reported to suppress the ubiquitin ligase activity of the rice RING E3 ubiquitin ligase, AvrPiz-t Interacting Protein 6 (APIP6). This enzyme is required for reactive oxygen species (ROS) generation induced by both chitin and flagellin 22 (flg22). The AvrPiz-t mediated suppression of APIP6 enhances susceptibility to *M. oryzae*, indicating that AvrPiz-t functions to suppress Pathogen associated molecular patterns (PAMP) triggered immunity in rice (Park *et al*, 2012; Duplan & Rivas, 2014). (2) RRE1 could be exploited by CSEP0443 to ubiquitinate immune activators and subsequently target them for proteasome degradation. Effectors may act as or mimic ubiquitin ligases to subvert host defence mechanisms. For-example, the avirulence effector PtoB (AvrPtoB) effector from *Pseudomonas syringe* pv. *tomato* DC3000 (*Pst*DC300) suppresses programmed cell death (PCD) in plants. The effector appears to encode an E3 ligase at its C-terminus, presumably employed to target a component in the PCD pathway for proteasome degradation, thus suppressing plant immunity (Abramovitch *et al*, 2006; Maculins *et al*, 2016). (3) CSEP0443 could be ubiquitinated by RRE1 and targeted for proteasome degradation. The type III secreted effectors SopE and SptP from *Salmonella enterica* is an example of effectors ubiquitinated and degraded by the

proteasome to regulate bacteria invasion (Kubori & Galán, 2003; Kim *et al*, 2014).

My data suggests that CSEP0443 targets the E3 ligase RRE1 to inactivate its cognate activity. This is supported by the ability of CSEP0443 to interact with a functional RING domain of RRE1. The mutated RING domain, having a lost E3 ligase activity exhibited only a weak interaction with CSEP0443 (Figure 6-6 red lane). In rice mutations in the U-box E3 ligase OsPUB44$^{1–203}$ amino acid residues, leucine 86 to threonine (L86T) and histidine 94 to tryptophan (H94W) abolished its interaction with XopPXoo, an effector from the rice pathogen *X. oryzae* pv. *oryzae* (Ishikawa *et al*, 2014). In mammalian systems, the requirement of a functional RING domain in E3 ligases for protein interactions has also been demonstrated. For-example, mutations in the RING domain of Ring finger protein 2 (RNF2), a protein required for transcriptional repression of genes involved in development and cell proliferation, prevented the binding to Huntingtin interacting protein-2 (Hip-2), a ubiquitin-conjugating enzyme. Thus, suggesting, that the RING domain might be the binding determinant (Jackson *et al*, 2000; Lee *et al*, 2001).

Having demonstrated the interaction of CSEP0443 with RRE1, I attempted to understand the consequence of this interaction. Initially I investigated if CSEP0443 can be ubiquitinated by RRE1. My result indicated that CSEP0443 was not ubiquitinated by this E3 ligase (Figure 6-7 lane 2). This suggests CSEP0443 may not be targeted by RRE1 to the proteasome for degradation. I therefore subsequently explored a possible inhibitory role for CSEP0443 towards the E3 ligase activity of RRE1, preventing the ubiquitination of AtPEN1. The ubiquitination of AtPEN1 was drastically reduced in the presence of CSEP0443 (Figure 6-8 lane 2, 6-9 lane 2, 6-11 lane 2). AtPEN1 ubiquitination is presumed necessary for its accumulation at the sites of *Bgh* penetration. Hence, by hindering AtPEN1 ubiquitination, vesicle fusion at the plasma membrane and by extension papilla formation is compromised, enabling *Bgh* penetration of host cell wall. In this context, the *Hyaloperonospora*

*arabidopsidis* arginine x leucine 77 (HaRxL77) effector from the Oomycete pathogen *Hyaloperonospora arabidopsidis* (*Ha*) is known to target the plasma membrane trafficking system leading to plant susceptibility (Caillaud *et al*, 2012; Chaudhari *et al*, 2014). The Blumeria effector candidate 3 (BEC3) and Blumeria effector candidate 3 (BEC4) target thiopurine methyltransferase, a ubiquitin conjugating enzyme and an adenosine diphosphate (ADP) ribosylation factor-guanosine triphosphate hydrolases (GTPase) activating protein respectively, presumably interfering with defence associated host vesicle trafficking (Schmidt *et al*, 2014). Also, the *Pst* effector HopM1 mediates the degradation of immune related *Arabidopsis* MIN7. This protein function as an adenosine diphosphate ribosylation factor, guanine nucleotide exchange factor (ARF-GEF) protein and its suppression interferes with vesicle trafficking and callose deposition involved in surface resistance (Banfield, 2015).

The inhibition of AtPEN1 polyubiquitination by CSEP0443 prompted the investigation of the subcellular localization of CSEP0443. In unchallenged conditions CSEP0443 localized both in the nucleus and on the plasma membrane with uniform intensity (Figure 6-12 C and D, 6-14 C and E). The localization of CSEP0443 in the nucleus of epidermal cells of barley leaves was demonstrated before by (Aguilar, 2015). Interestingly in *Bgh* challenged conditions, CSEP0443 greatly accumulated on the plasma membrane. The change in the localization of CSEPs induced either by biotic stress or interactors has been previously demonstrated. The CSEP0105 and CSEP0162 exhibit nuclear and cytosolic localizations during normal state expressions. The effectors exhibit exclusive cytosolic localization when co-expressed with the heat shock proteins (Hsp)16.9 and 17.5. The Hsp16.9 and Hsp17.5 are cytosolically localized and are shown to be targeted by these effector proteins undermining their chaperon activity (Ahmed *et al*, 2015a). During *Bgh* challenge the CSEP0105 solely maintain the cytosolic localization whereas CSEP0162

translocate in the extrahaustorial matrix (Ahmed *et al*, 2015a). CSEP0081 and CSEP0254 also exhibited nuclear and cytosolic localization suggesting their possible targets to localise in these compartments (Ahmed *et al*, 2016b). The dual localization of CSEP0443 agree with the fact that the cytosol and nuclear environment are the centre for plant immuno related defence response (Wiermer *et al*, 2007; Rivas, 2012).

I then investigated the effect of CSEP0443 on the localization of AtPEN1 in the presence or absence of *Bgh* challenge. AtPEN1 localized throughout the plasma membrane in absence of *Bgh* challenge. Under *Bgh* challenge AtPEN1 was mobilized at the attempted fungal progressing sites in lines without CSEP0443 expression. These results were expected as the localization of AtPEN1 at the plasma membrane and the accumulation at the site of pathogen penetration were previously reported (Pajonk *et al*, 2008; Reichardt *et al*, 2011b; Nielsen & Thordal-Christensen, 2012). However, AtPEN1 localization at *Bgh* penetration sites was greatly reduced in *rre1* plants implying that RRE1 might play a key role in the translocation of AtPEN1. However, loss of RRE1 function did not completely abolish the localization of AtPEN1 at *Bgh* penetration sites, suggesting other factors may be involved in the process. In this context, RRE1 has a paralog RRE2, so perhaps this E3 ligase might also play a role in this process (Yu, 2012). However, when plants expressing CSEP0443 challenged with *Bgh*, the mobilization of AtPEN1 was significantly compromised (Figure 6-18 D and E). The result suggest, that the expression of CSEP0443 undermines the spatial allocation of AtPEN1 to sites of attempted *Bgh* penetration where it is required to recruit vesicles containing antifungal materials. Thus, CSEP0443 target and thereby inhibit RRE1 function reducing AtPEN1 ubiquitination and associated vesicle trafficking, promoting *Bgh* pathogenesis.

# Chapter seven

## 7.0 General discussion

### 7.1 Role of CSEP0443 in *Bgh* virulence

The *Blumeria graminis* f. sp. *hordei* (*Bgh*) genome encodes over 700 candidate effectors predicted to be important in the pathogenicity of the fungus (Kusch *et al*, 2014; Frantzeskakis *et al*, 2018). *In silico* predictions relate a relatively high number of the effectors to microbial nucleases (Pedersen *et al*, 2012). To date only a limited number of effectors have been investigated to uncover their potential target and their contribution to the virulence of *Bgh* (Aguilar *et al*, 2016). *Bgh* Effector candidate 1/ Candidate secreted effector protein 0443 (*Bgh*Efc1/CSEP0443) is one the effectors explicitly expressed in high magnitude during the early stages of infection. The protein is presumed to be required for penetration and for the formation of haustoria, the feeding structure of the fungus. The expression levels of *CSEP0443* are maximum at 4 days post inoculation after which they progressively decline (Godfrey *et al*, 2010). In the infection cycle of *Bgh* at 1 - 4 days the fungus has established maximal haustoria formation and colony formation ensues (Nottensteiner *et al*, 2018).

Using Barley stripe mosaic virus-Virus induced gene silencing (BSMV-VIGS*)* mediated Host induced gene silencing (HIGS), I attempted to unveil the contribution of CSEP0443 to *Bgh* virulence on barley, the host plant. My results indicated successful knock-down of *CSEP0443* (Figure 3-3 A and 3-4). Further the virulence of *Bgh* was reduced in plants inoculated with *BSMV-VIGS* vectors (Figure 3-5 A and B). The results suggest that CSEP0443 might play a vital role in the enhancement of *Bgh* virulence. HIGS has become a powerful tool to study not only conventional effectors but also their unconventional counterparts lacking signal peptides. For-example, the application of HIGS has demonstrated that ROP-interactive peptide 1 (ROPIP1) increases the virulence of *Bgh.* ROPIP1 is encoded

on the active non-long terminal repeat retroelement early growth response 1 (Eg-R1) of *Bgh* where it interacts with barley ROP Guanosine triphosphate hydrolases (GTPase) *Hordeum vulgare* RacB (HvRACB) involved in accommodation of fungal haustoria during *Bgh* infection (Nottensteiner *et al*, 2018).

I then investigated the possible effect of CSEP0443 in a non-host system. Non-host resistance is normally adequate to arrest non-adapted pathogens often relying on constitutive and induced defence components (Stam *et al*, 2014; Lee *et al*, 2017). The constitutive expression of CSEP0443 did not cause any aberrant growth in *Arabidopsis* (Figure 3-7). This implies CSEP0443 does not provoke *Resistance* gene (*R*)-mediated resistance. In other studies, the HopZ1a effector from *Pseudomonas syringe pv. tabaci* was constitutively expressed in *Arabidopsis* without altering the plant phenotype. The effector is an acetyltransferase and acetylates both soybean and *Arabidopsis* Jasmonate zim domain (JAZ) transcription repressors leading to their degradation to facilitate infection. Transgenic *Arabidopsis* plants expressing HopZ1a are also able to suppress stomatal defence by activating jasmonic acid (JA) signalling. JA induce the opening of the stomata aperture to facilitate pathogen entry (Ma *et al*, 2015; Toruno *et al*, 2016).

*Arabidopsis* plants expressing CSEP0443 when inoculated with *Bgh* displayed increased penetration rates. These plants had reduced callose deposition, elevated reactive oxygen species (ROS) production, elevated electrolyte leakage and limited cell death. My results implied that CSEP0443 compromised the penetration resistance components to promote *Bgh* virulence. However, further growth was arrested by the cells undergoing self-execution. The stable expression in *Arabidopsis* of Blumeria effector candidate 2 (BEC2)/CSEP0214 an orthologue of *Golovinomyces orontii* effector 2 (GoE2) from *Golovinomyces orontii*, enhanced susceptibility to the non-adapted pathogen *Erysiphe pisi*, the pea powdery mildew (Lipka *et al*, 2005; Schlicht & Kombrink, 2013). BEC2/GoE2 is

expressed early during infection 6 hour post inoculation (hpi) corresponding to the time of appressorium formation (Schmidt *et al*, 2014).

### 7.2 RRE1 mediated ubiquitination regulates the activity of AtPEN1

*Arabidopsis thaliana* PENETRATION 1 (AtPEN1) is a surface membrane localized protein that localizes at attempted *Bgh* penetration sites (Assaad *et al*, 2004; Bohlenius *et al*, 2010). The protein forms a Soluble NSF (N-ethylmaleimide-sensitive factor) attachment protein receptor (SNARE) complex with synaptosomal associated protein 33 (SNAP33) and vesicle associated membrane protein 721/2 (VAMP721/2) mediating the recruitment of vesicles containing anti-microbial agents (Kwon *et al*, 2008b). The vesicles are directed to the fungal penetration sites guided by VAMP721/2 (v-SNARE) proteins incorporated into the membranes of transport vesicles. After the release of materials the SNARE complex disassociates in an adenosine triphosphate (ATP) dependant manner for recycling (Söllner *et al*, 1993; Malsam & Söllner, 2011).

AtPEN1 and Redox regulated E3 ligase 1 (RRE1) are each expressed during attempted *Bgh* infection in both host and non-host plants. AtPEN1 and its barley homologue Required for *mlo* (mildew locus O) resistance 2 (ROR2) have been demonstrated to be required for penetration resistance (Collins *et al*, 2003; Feechan *et al*, 2013; Bracuto *et al*, 2017). Both *pen1-1* and *rre1* plants have increased susceptibly to *Bgh* infection, reinforcing their importance in non-host resistance. The physical interaction and co-expressions of RRE1 and AtPEN1 was suggestive of AtPEN1 as a possible substrate for AtPEN1 (Figure 4-3 B, 4-5). My results demonstrated RRE1 ubiquitination of AtPEN1 at lysines (K) 103 and 281 upstream of the conserved transmembrane domain. The transmembrane domain is thought to increase the anchorage and stability of the protein (Huang *et al*, 2016; Giovannone *et al*, 2017). Human syntaxin-3 is a SNARE involved in membrane fusion at the apical plasma

membrane of polarized epithelial cells. This syntaxin has also recently been shown to be ubiquitinated at lysines adjacent to the transmembrane domain (Giovannone *et al*, 2017).

Also, my findings suggest that AtPEN1 polyubiquitination is established by K48 or K63 linkages either alone or in combination. I hypothesised that the K63 polyubiquitination of AtPEN1 was required to mark this protein for accumulation at fungal penetration sites (Figure 7-1). In this context, the ubiquitination of human syntaxin-3 leads to its retrieval from the basolateral plasma membrane for either endosomal or multivesicular bodies (MVB) pathways and final exosomes delivery (Giovannone *et al*, 2017). Alternatively, K63 polyubiquitination of AtPEN1 might enable the dissociation of AtPEN1 from the SNARE complex, with free AtPEN1 able to mediate the recruitment of additional vesicles to target sites. My data implies that K48 polyubiquitination of AtPEN1 was associated with 26S proteasome degradation. I hypothesized that K48 polyubiquitination was required to clear ‘‘exhausted’’ AtPEN1 by targeting it for proteasome degradation. The dual ubiquitination of AtPEN1 for distinct functional fates by RRE1 suggests this E3 ligase is a member of only a small group of enzymes which exhibit similar dual activities. In addition, AtPEN1 also becomes one of few plant substrates modified in this fashion. In rice, *Oryza sativa* IDEAL PLANT ARCHITECTURE1 (OsIPA1) transcription factors are required for plant development. Modification of OsIPA1 with polyubiquitin containing K48 linkages by the *Oryza sativa* IPA1 INTERACTING PROTEIN1 (OsIPI1) ligase, promoted proteasome degradation in the panicles. On the other hand, modification with polyubiquitin containing K63 chain linkages regulated tiller number (Wang *et al*, 2017; Romero-Barrios & Vert, 2018). In mammalian systems, TNF (tumour necrosis factor) receptor-associated factor 3 (TRAF3) is an E3 ligase that is required for Toll/interleukin-1 receptor (Tir)-domain-containing adaptor inducing interferon β (TRIF)-dependent type I interferon signaling, but may also negatively regulate mitogen activated protein kinases (MAPK)-dependent

proinflammatory responses. TRAF3 undergoes polyubiquitination with both K48 and K63 linkage downstream of the Toll-like receptor (TLR) adaptor protein myeloid differentiation primary response 88 (Myd88) and TRIF mediated TLR signals (Tseng *et al*, 2010; Malynn & Ma, 2011).

The polyubiquitination of AtPEN1 in *rre1* plants was significantly reduced while over expression of *RRE1* increased the ubiquitination of AtPEN1. Also decreased accumulation of AtPEN1 at *Bgh* infection sites was observed in *rre1* plants, indicating that RRE1 mediated polyubiquitination of AtPEN1 might be required for AtPEN1 localization at *Bgh* infection sites. These findings reveal a dependency of AtPEN1 on RRE1 for its ubiquitination. Further, AtPEN1 polyubiquitination increased in plants challenged with *Bgh*, implying that polyubiquitination was required to drive the localization of AtPEN1 to sites of attempted *Bgh* penetration. The *Arabidopsis* KEEP ON GOING (KEG) is an E3 ligase localised on the *trans*-Golgi network/early endosomes. The enzyme is involved in the regulation of post Golgi vesicle trafficking, including targeting membrane associated proteins to vacuoles for degradation. Mutations within KEG abolish the secretion of Pathogenesis related protein 1 (PR1) and Clan type peptidase 14 (C14) proteins integral to plant immunity (Gu & Innes, 2011).

### 7.3 CSEP0443 inhibits RRE1 mediated ubiquitination of AtPEN1 to enhance *Bgh* virulence

A multitude of candidate effectors have been identified from the *Bgh* genome in a number of screens from barley leaves infected with the fungus (Godfrey *et al*, 2010; Pedersen *et al*, 2012; Schmidt *et al*, 2014). The challenge still remains to identify the potential target of each effector and elucidate how exactly they might manipulate their targets (Selin *et al*, 2016). CSEP0443 was previously shown to interact with XA21 binding protein *Hordeum*

*vulgare* 35 (XBHV35) a homologue of RRE1 in barley. I also demonstrated the interaction of CSEP0443 with *Arabidopsis* RRE1. The interactions were more pronounced with the Really interesting new gene (RING) domain of RRE1, suggesting that CSEP0443 might be targeting E3 ligase activity. Despite CSEP0443 having 5 lysines, the protein was not ubiquitinated by RRE1, implying that it may not be a substrate for RRE1. RRE1 mediated ubiquitination of AtPEN1 was compromised in the presence of CSEP0443. The absence of AtPEN1 ubiquitination suggests AtPEN1 will not be marked for recycling, becoming randomly localized, rather than accumulation at sites of attempted *Bgh* infection. The reduced accumulation of AtPEN1 at *Bgh* penetration sites would reduce the recruitment of vesicles containing antifungal materials to the developing papilla. Therefore, *Bgh* cell wall penetration will be expected to increase, promoting virulence. Interestingly, the rice blast fungus (*M. oryzae*) secretes the avirulence effector Piz-t (avrPiz-t) effector into the host cytosol compromising PAMP triggered immunity (PT1) mediated resistance. This effector targets and inhibits the activity of the RING E3 ligase AvrPiz-t interacting protein 6 (APIP6) to promote virulence of the fungus (Park *et al*, 2012; Zhou & Zeng, 2017).

I demonstrated both a decline and an irregular accumulation of AtPEN1 at *Bgh* infection sites in plants constitutively expressing CSEP0443. In absence of *Bgh* infection CSEP0443 localised in the nucleus in agreement with a previous report (Aguilar, 2015). However, during *Bgh* infection CSEP0443 localisation at the plasma membrane was detected. I posit that CSEP0443, which co-localises with RRE1-AtPEN1, antagonises the ubiquitination of AtPEN1, promoting *Bgh* virulence (Figure 7-1).

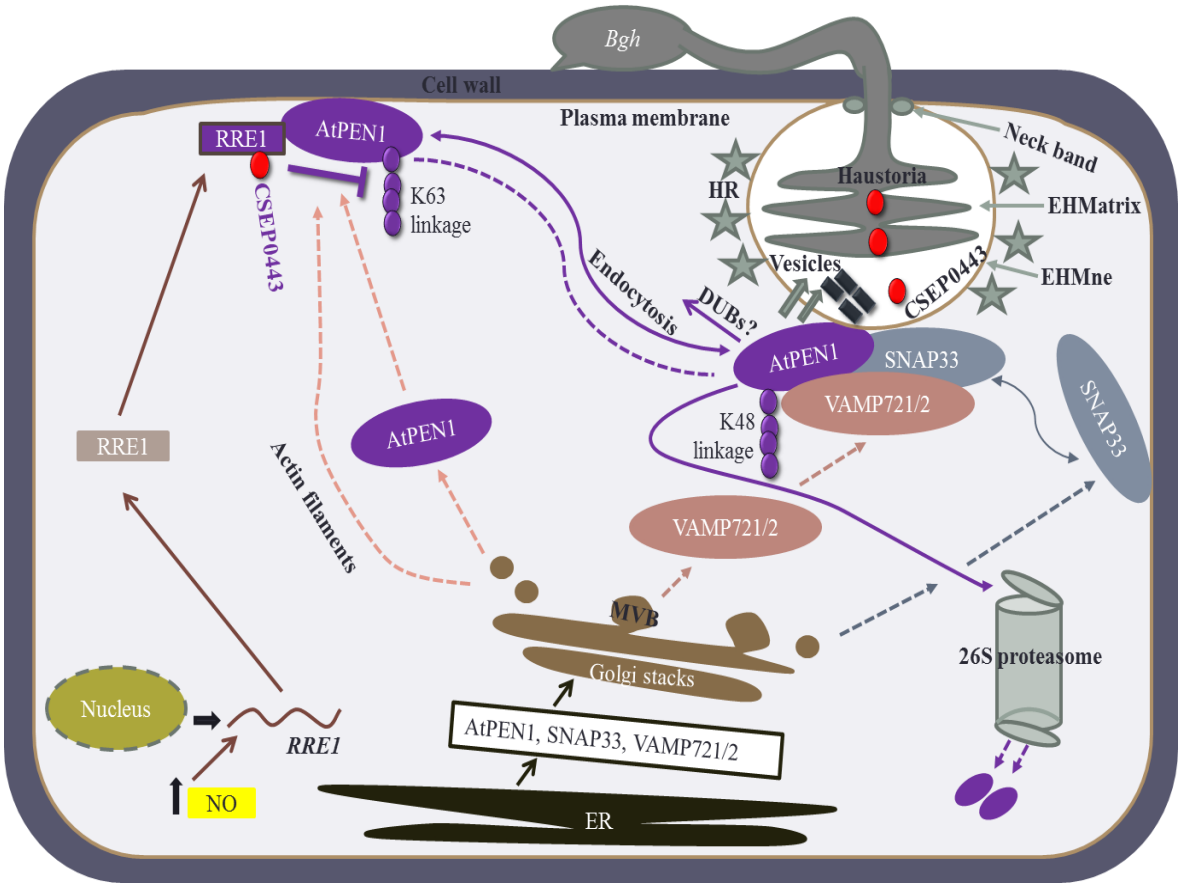


**Figure 7-1: A model for the interactions of CSEP0443, RRE1 and AtPEN1 in plant immunity.** Infections with powdery mildews are associated with increased NO production (Schlicht & Kombrink, 2013). NO is believed to both transcriptionally and post translationally regulate RRE1 (Yu, 2012). Both RRE1 and AtPEN1 are expressed during *Bgh* infections (Assaad *et al*, 2004; Toufighi *et al*, 2005; Yu, 2012). AtPEN1 and SNAP33 localise at the plasma membrane possibly driven in MVB which likely travel along actin filaments (Underwood & Somerville, 2008; Nielsen *et al*, 2012; Nielsen & Thordal-Christensen, 2012). **During attempted *Bgh* ingress, RRE1 mediates polyubiquitination of AtPEN1 with K63 linkages. This modification may mark AtPEN1 for delivery to the site of attack (sections 5.3.2.1, 5.3.2.2, 5.3.3.3 and 5.3.4).** AtPEN1 combines with SNAP33 to form the t-SNARE. The VAMP721/2 (v-SNARE) guide the vesicles containing the antimicrobial agents to the t-SNARE where they form the cis-SNARE. AtPEN1 enables the fusion of the vesicles with the plasma membrane to release their contents attenuating *Bgh* infection (Collins *et al*, 2003; Kwon *et al*, 2008b). **Further "exhausted" AtPEN1 is targeted to the proteasome for degradation by K48 polyubiquitin modification, maintaining the supply of functional AtPEN1 at the plasma membrane (sections 5.3.2.1, 5.3.2.2 and 5.3.4).** To counteract this defence strategy, *Bgh* delivers CSEP0443 into the host cell (Godfrey *et al*, 2010). **This effector suppresses the E3 ligase activity of RRE1 compromising polyubiquitination of AtPEN1. Decreased polyubiquitination of AtPEN1 promotes *Bgh* virulence. The host responds by inducing cell death in the attacked cells. (sections 3.3.2.5, 3.3.2.6, 6.3.2.2 and 6.3.2.3).** In the image key findings emanating

from my work are shown in purple. In the text, the descriptions of my findings are shown in bold.

### 7.4 Conclusions

In summary my data suggests:

RRE1 interacts with AtPEN1. *In vitro* and *in vivo* investigations conducted suggested that the two proteins interact.

AtPEN1 is a substrate for RRE1. I demonstrated that the detected interactions led to RRE1 ubiquitinating AtPEN1. The ubiquitination is shown both in the *in vitro* assays, and *in vivo* in *Nicotiana benthamiana* and *Arabidopsis*. AtPEN1 becomes the second syntaxin in plants shown to be modified by ubiquitination.

RRE1 mediates AtPEN1 polyubiquitination with K48 and K63 ubiquitin chain linkages. AtPEN1 modified with K63 ubiquitin chain linkages was shown as not targeted to vacuolar degradation. I hypothesized that, this modification leads to AtPEN1 trafficking/activation from the membrane to sites of attempted *Bgh* penetration. AtPEN1 modified with K48 ubiquitin chains linkages was shown to be a target for 26S proteasome degradation. I hypothesized that this is required to turn over the ‘‘exhausted’’ AtPEN1. The dual modification makes AtPEN1 as one of the novel substrates shown to ubiquitinated in this way.

AtPEN1 ubiquitinated at lysine 103 and lysine 281. The two sites are located before a conserved transmembrane domain. To date in plant systems, AtPEN1 becomes the first syntaxin having ubiquitination sites disclosed.

Expression of CSEP0443 in both barley and *Arabidopsis* promotes *Bgh* virulence. *CSEP0443* was previously shown as the most experienced expressed sequence tags during infection of barley. In this study the expression of CSEP0443 in the host and non host

systems was shown to promote the virulence of *Bgh* adding to few effectors whose potential roles are disclosed.

CSEP0433 interacts with RRE1 compromising its E3 ligase activity. *In vitro* and *in vivo* investigations demonstrated RRE1 as a potential target of CSEP0443 during *Bgh* virulence. By CSEP0443 disabling the E3 ligase function RRE1 leads to reduced AtPEN1 activation for relocalization to *Bgh* ingress sites presumed induced by ubiquitination. This work contributes to the knowledge of the few effectors with potential target(s) and mechanism of function disclosed.

### 7.5 Future prospects

As outline above**,** this project has revealed important novel events in relation to post-translation modifications and plant immunity. However, our knowledge could be enriched further by:

Identifying the sites of CSEP0443-RRE1 interaction revealing the specificity in the mechanism of action of CSEP0443. By demonstrating the structure of the two proteins using protein crystallography techniques the binding sites could be disclosed.

‘‘Exhausted’’ AtPEN1 is suggested to be targeted to the 26S proteasome for degradation but the mechanism underpinning the clearance of VAMP721/2 and SNAP33 remains elusive. This could be investigated for ubiquitination possibly leading to proteasome turnover or vacuolar degradation.

Investigate the possible E4 ubiquitin ligase likely to be acting with RRE1 to increase the polyubiquitin chains. Literature search in both mammalian and plant system, and cloning steps likely could reveal the possible E4 ligases(s).

Visualise RRE1-CSEP0443 co-localisations *in vivo* during *Bgh* infection. Cloning of

the *RRE1* and *CSEP0443* with fluorescent genetic reporters and examined confocal microscopy could reveal the possible co-localizations.

Investigate the behaviour of ubiquitination insensitive AtPEN1-K103R-K281R during *Bgh* infection in relation to localisation and *Bgh* virulence. This can be achieved by visualization with a confocal microscope and pathogenicity assays with stains and bright field microscopy.

Determining the specificity of CSEP0443 to RRE1, given the presence of other effectors in the same family. CSEP0443 is one of the group of effectors known belong in microbial ribonucleases family. Checking other effector from the same family for the possible interactions with RRE1, could reveal specificity of the interactions.

Uncover the secretory pathway of CSEP0443 in the host. Transformation of *Bgh* with *CSEP0443* carrying fluorescent report genes could enable the understanding of secretory pathway for CSEP0443.

Uncover the *R*-gene in *Arabidopsis* that recognise CSEP0443. Gene expression analysis in *Arabidopsis* could reveal the possible *R* gene involved in supressing CSEP0443. *R* gene could then be expressed in barley and the effect determined.

Confirm the localization of CSEP0443 in the nucleus and on the plasma membrane. 4′,6-diamidino-2-phenylindole (DAPI) and Propidium iodide staining followed by microscopy examinations could support the localization data of CSEP0443 in the nucleus and on the membrane respectively.

## 8.0 References


Abramovitch RB, Janjusevic R, Stebbins CE & Martin GB (2006) Type III effector AvrPtoB requires intrinsic E3 ubiquitin ligase activity to suppress plant cell death and immunity. *Proc. Natl. Acad. Sci.* **103:** 2851–2856

Agilent-technologies (2015) QuikChange ® II XL Site-Directed Mutagenesis Kit

Aguilar GB (2015) On the mechanism of action of selected effector candidates from the barley powdery mildew fungus. *PhD thesis*

Aguilar GB, Pedersen C & Thordal-Christensen H (2016) Identification of eight effector candidate genes involved in early aggressiveness of the barley powdery mildew fungus. *Br. Soc. Plant Pathol.***:** 953–958

Ahmed AA, McLellan H, Anguilar GB, Hein I, Thordal-Christensen H & Birch JP (2016a) Engineering barriers to infection by undermining pathogen effector function or by gaining effector recognition. In *Plant Pathogen Resistance Biotechnology* pp 21–50.

Ahmed AA, Pedersen C, Schultz-larsen T, Kwaaitaal M, Jørgen H, Jørgensen L & Thordal-christensen H (2015a) The barley powdery mildew candidate secreted effector protein CSEP0105 inhibits the chaperone activity of a small heat shock protein. *Plant Phsiology* **168:** 321–333

Ahmed AA, Pedersen C & Thordal-christensen H (2016b) The barley powdery mildew effector candidates CSEP0081 and CSEP0254 promote fungal infection success. *PLoS One* **11:** e0157586

Akutsu M, Dikic I & Bremm A (2016) Ubiquitin chain diversity at a glance. *J. Cell Sci.* **129:** 875–880

Alderton WK, Cooper CE & Knowles RG (2001) Nitric oxide synthases: structure, function and inhibition. *Biochem. J.* **357:** 593–615

Ale-agha N, Boyle H, Braun U, Butin H, Jage H, Kummer V & Shin H (2008) Taxonomy , host range and distribution of some powdery mildew fungi (Erysiphales). *Schlechtendalia* **7:** 39–54

Andersen P, Kragelund BB, Olsen AN, Larsen FH, Chua NH, Poulsen FM & Skriver K (2004) Structure and biochemical function of a prototypical Arabidopsis U-box domain. *J. Biol. Chem.* **279:** 40053–40061

Anderson JP, Gleason CA, Foley RC, Thrall PH, Burdon JB & Singh KB (2010) Plants versus pathogens: an evolutionary arms race. *Funct. plant Biol.* **37:** 499–512

Aravind L & Koonin E V. (2000) The U box is a modified RING finger - a common domain in ubiquitination. *Curr. Biol.* **10:** 132–134

Assaad FF, Qiu J, Youngs H, Ehrhardt D, Zimmerli L, Kalde M, Wanner G, Peck SC, Edwards H, Ramonell K, Somerville CR & Thordal-christensen H (2004) The PEN1 syntaxin defines a novel cellular compartment assembly of papillae. *Am. Soc. cell Biol.* **15:** 5118–5129

Bachmair A, Novatchkova M, Potuschak T & Eisenhaber F (2001) Ubiquitylation in plants: a post-genomic look at a post-translational modification. *Trends Plant Sci.* **6:** 463–470

Banerjee S, Banerjee A, Gill SS, Gupta OP, Dahuja A & Godwin ID (2017) RNA interference: A novel source of resistance to combat plant parasitic nematodes. *Front. Plant Sci.* **8:** 1–8

Banfield MJ (2015) Perturbation of host ubiquitin systems by plant pathogen/pest effector proteins. *Cell. Microbiol.* **17:** 18–25

Barberon M, Zelazny E, Robert S, Conéjéro G, Curie C, Friml J & Vert G (2011) Monoubiquitin-dependent endocytosis of the transporter controls iron uptake in plants. *Proc. Natl. Acad. Sci. U. S. A.* **108:** e450–e458

Bates PW & Vierstra RD (1999) UPL1 and 2, two 405 kDa ubiquitin-protein ligases from *Arabidopsis thaliana* related to the HECT-domain protein family. *Plant J.* **20:** 183–195

Bedford L, Paine S, Sheppard PW, Mayer RJ & Roelofs J (2010) Assembly, structure, and function of the 26S proteasome. *Trends Cell Biol.* **20:** 391–401

Bednarek P & Osbourn A (2009) Plant-microbe interactions: Chemical diversity in plant defense. *Science* **324:** 746–748

Behrends C & Harper JW (2011) Constructing and decoding unconventional ubiquitin chains. *Nat. Struct. Mol. Biol.* **18:** 520–528

Ben-Saadon R, Zaaroor D, Ziv T & Ciechanover A (2006) The polycomb protein Ring1B penerates self atypical mixed ubiquitin chains required for its *in vitro* histone H2A ligase activity. *Mol. Cell* **24:** 701–711

Berrocal-Lobo M, Stone S, Yang X, Antico J, Callis J, Ramonell KM & Somerville S (2010) ATL9, a RING zinc finger protein with E3 ubiquitin ligase activity implicated in chitin- and NADPH oxidase-mediated defense responses. *PLoS One* **5:** e14426

Bhat RA, Miklis M, Schmelzer E, Schulze-Lefert P & Panstruga R (2005) Recruitment and interaction dynamics of plant penetration resistance components in a plasma membrane microdomain. *Proc. Natl. Acad. Sci. U. S. A.* **102:** 3135–3140

Bielopolski N, Lam AD, Bar-On D, Sauer M, Stuenkel EL & Ashery U (2014) Differential interaction of tomosyn with syntaxin and SNAP25 depends on domains in the WD40 β-propeller core and determines its inhibitory activity. *J. Biol. Chem.* **289:** 17087–17099

Bindschedler LV, Panstruga R & Spanu PD (2016) Mildew-omics: How global analyses aid the understanding of life and evolution of powdery mildews. *Front. Plant Sci.* **7:** doi: 10.3389

Bindschedler LV, Burgis TA, Mills DJS, Ho JTC, Cramer R & Spanu PD (2009) In planta proteomics and proteogenomics of the biotrophic barley fungal pathogen *Blumeria graminis* f . sp. *hordei*. *Mol. Cell. proteomics* **8:** 2368–2381

Bindschedler LV, Mcguffin LJ, Burgis TA, Spanu PD & Cramer R (2011) Proteogenomics and in silico structural and functional annotation of the barley powdery mildew *Blumeria graminis* f . sp. *hordei*. *Methods* **54:** 432–441

Bock JB, Matern HT, Peden AA & Scheller RH (2001) A genomic perspective on membrane compartment organization. *Nature* **409:** 839–841

Bohlenius H, Morch SM, Godfrey D, Nielsen ME & Thordal-Christensen H (2010) The multivesicular body-localized GTPase ARFA1b/1c is important for callose deposition and ROR2 syntaxin-dependent preinvasive basal defense in barley. *Plant Cell Online*

**22:** 3831–3844

Bolwell GP & Daudi A (2009) Reactive oxygen species in plant-pathogen interactions. *Signal. Commun. plants***:** 113–133

Book AJ, Gladman NP, Lee SS, Scalf M, Smith LM & Vierstra RD (2010) Affinity purification of the Arabidopsis 26 S proteasome reveals a diverse array of plant proteolytic complexes. *J. Biol. Chem.* **285:** 25554–25569

Bracuto V, Appiano M, Zheng Z, Wolters A-MA, Yan Z, Ricciardi L, Visser RGF, Pavan S & Bai Y (2017) Functional characterization of a syntaxin involved in tomato (*Solanum lycopersicum*) resistance against powdery mildew. *Front. Plant Sci.* **8:** 1–10

Buonaurio R (2008) Infection and plant defense responses during plant-bacterial interaction. *Plant-microbe Interact.* **661:** 169–197

Byun MY, Cui LH, Oh TK, Jung Y-J, Lee A, Park KY, Kang BG & Kim WT (2017) Homologous U-box E3 ubiquitin ligases OsPUB2 and OsPUB3 are involved in the positive regulation of low temperature stress response in rice (*Oryza sativa* L.). *Front. Plant Sci.* **8:** doi: 10.3389

Cai J, Culley MK, Zhao Y & Zhao J (2018) The role of ubiquitination and deubiquitination in the regulation of cell junctions. *Protein Cell* **9:** 754–769

Caillaud MC, Piquerez SJM, Fabro G, Steinbrenner J, Ishaque N, Beynon J & Jones JDG (2012) Subcellular localization of the Hpa RxLR effector repertoire identifies a tonoplast-associated protein HaRxL17 that confers enhanced plant susceptibility. *Plant J.* **69:** 252–265

Callis J (2014) The ubiquitination machinery of the ubiquitin system. *Arab. B.* **12:** 1543–8120

Campos PS, Quartin V, Ramalho JC & Nunes MA (2003) Electrolyte leakage and lipid degradation account for cold sensitivity in leaves of Coffea sp. plants. *J. Plant Physiol.* **160:** 283–292

Cardona-López X, Cuyas L, Marín E, Rajulu C, Irigoyen ML, Gil E, Puga MI, Bligny R, Nussaume L, Geldner N, Paz-Ares J & Rubio V (2015) ESCRT-III-associated protein ALIX mediates high-affinity phosphate transporter trafficking to maintain phosphate homeostasis in Arabidopsis. *Plant Cell* **27:** 2560–2581

Carvalho SD, Saraiva R, Maia TM, Abreu I a. & Duque P (2012) XBAT35, a novel arabidopsis RING E3 ligase exhibiting dual targeting of its splice isoforms, is involved in ethylene-mediated regulation of apical hook curvature. *Mol. Plant* **5:** 1295–1309

Carver TLW, Kunoh H, Thomas BJ & Nicholson RL (1999) Release and visualization of the extracellular matrix of conidia of *Blumeria graminis*. *Mycol. Res.* **103:** 547–560

Catanzariti A-M, Dodds PN, Lawrence GJ, Ayliffe MA & Ellis JG (2006) Haustorially expressed secreted proteins from flax rust are highly enriched for avirulence elicitors. *Plant Cell* **18:** 243–256

Catic A, Collins C, Church GM & Ploegh HL (2004) Preferred *in vivo* ubiquitination sites. *Bioinformatics* **20:** 3302–3307

Chang A, Chau VW, Landas JA & Pang Y (2017) Preparation of calcium competent *Escherichia coli* and heat-shock transformation. *JEMI methods* **1:** 22–25

Chasapis CT, Loutsidou AK, Orkoula MG & Spyroulias GA (2010) Zinc binding properties of engineered ring finger domain of arkadia e3 ubiquitin ligase. *Bioinorg. Chem. Appl.***:** 1–7

Chastagner P, Israël A & Brou C (2006) Itch/AIP4 mediates Deltex degradation through the formation of K29-linked polyubiquitin chains. *EMBO Rep.* **7:** 1147–1153

Chaudhari P, Ahmed B, Joly DL & Germain H (2014) Effector biology during biotrophic invasion of plant cells. *Virulence* **5:** 703–709

Chaugule VK & Walden H (2016) Specificity and disease in the ubiquitin system. *Biochem. Soc. Trans.* **44:** 212–227

Chen L & Hellmann H (2013) Plant E3 ligases: Flexible enzymes in a sessile world. *Mol. Plant* **6:** 1388–1404

Chen X & Kim J (2009) Callose synthesis in higher plants. *Plant Signal. Behav.* **4:** 489–492

Chen ZJ & Sun LJ (2009) Nonproteolytic functions of ubiquitin in cell signaling. *Mol. Cell* **33:** 275–286

Cheng Y (2009) Towards an atomic model of the 26S proteasome. *Curr. opnion Struct. Biol.* **19:** 203–208

Chinchilla D, Bauer Z, Regenass M, Boller T & Felix G (2006) The Arabidopsis receptor kinase FLS2 binds flg22 and determines the specificity of flagellin perception. *Plant Cell* **18:** 465–476

Coll NS, Epple P & Dangl JL (2011) Programmed cell death in the plant immune system. *Cell Death Differ.* **18:** 1247–1256

Collins N, Thordal-Christensen H, Lipka V, Bau S, Kombrink E, Qiu J-L, Huckelhoven R, Stein M, Freialdenhoven A, Somerville SC & Schulze-Lefert P (2003) SNARE-protein-mediated disease resistance at the plant cell wall. *Nature* **312:** 310–312

Cooper EM, Cutcliffe C, Kristiansen TZ, Pandey A, Pickart CM & Cohen RE (2009) K63-specific deubiquitination by two JAMM/MPN+ complexes: BRISC-associated Brcc36 and proteasomal Poh1. *EMBO J.* **28:** 621–631

Corcoran A & Cotter TG (2013) Redox regulation of protein kinases. *FEBS J.* **280:** 1944–1965

Couturier J, Chibani K, Jacquot J-P & Rouhier N (2013) Cysteine-based redox regulation and signaling in plants. *Front. Plant Sci.* **4:** 105

Criqui MC, Criqui MC, Engler JDA, Engler JDA, Camasses A, Camasses A, Capron A, Capron A, Parmentier Y, Parmentier Y, Genschik P & Genschik P (2002) Molecular characterization of plant ubiquitin- conjugating enzymes belonging to the UbcP4/E2-C/UBCx/ UbcH10 gene family 1. *plant Physiol.* **130:** 1230–1240

Dean R, Van Kan JAL, Pretorius ZA, Hammond-Kosack KE, Di Pietro A, Spanu PD, Rudd JJ, Dickman M, Kahmann R, Ellis J & Foster GD (2012) The Top 10 fungal pathogens in molecular plant pathology. *Mol. Plant Pathol.* **13:** 414–430

Demidchik V, Straltsova D, Medvedev SS, Pozhvanov GA, Sokolik A & Yurin V (2014) Stress-induced electrolyte leakage: the role of K+-permeable channels and involvement in programmed cell death and metabolic adjustment. *J. Exp. Bot.* **65:** 1259–1270

Deng F, Guo T, Lefebvre M, Scaglione S, Antico CJ, Jing T, Yang X, Shan W & Ramonell KM (2017) Expression and regulation of ATL9, an E3 ubiquitin ligase involved in plant defense. *PLoS One* **12:** 1–18

Deng L, Wang C, Spencer E, Yang L, Braun A, You J, Slaughter C, Pickart C & Chen ZJ (2000) Activation of the Iκb kinase complex by TRAF6 requires a dimeric ubiquitin-conjugating enzyme complex and a unique polyubiquitin chain. *Cell* **103:** 351–361

Deshaies RJ & Joazeiro CAP (2009) RING domain E3 ubiquitin ligases. *Annu. Rev. Biochem.* **78:** 399–434

Deslandes L & Rivas S (2012) Catch me if you can: Bacterial effectors and plant targets. *Trends Plant Sci.* **17:** 644–655

Dodds PN & Rathjen JP (2010) Plant immunity: towards an integrated view of plant-pathogen interactions. *Nat. Rev. Genet.* **11:** 539–548

Downes BP, Stupar RM, Gingerich DJ & Vierstra RD (2003) The HECT ubiquitin-protein ligase (UPL) family in Arabidopsis: UPL3 has a specific role in trichome development. *Plant J.* **35:** 729–742

Dubeaux G & Vert G (2017) Zooming into plant ubiquitin-mediated endocytosis. *Curr. Opin. Plant Biol.* **40:** 56–62

Duplan V & Rivas S (2014) E3 ubiquitin-ligases and their target proteins during the regulation of plant innate immunity. *Front. Plant Sci.* **5:** 1–6

Edwards HH (2002) Development of primary germ tubes by conidia of *Blumeria graminis* f.sp. *hordei* on leaf epidermal cells of *Hordeum vulgare*. *Can. J. Bot.* **80:** 1121–1125

Eletr ZM, Huang DT, Duda DM, Schulman BA & Kuhlman B (2005) E2 conjugating enzymes must disengage from their E1 enzymes before E3-dependent ubiquitin and ubiquitin-like transfer. *Nat. Struct. Mol. Biol.* **12:** 933–934

Elia AEH, Boardman AP, Wang DC, Huttlin EL, Everley RA, Dephoure N, Zhou C, Koren I, Gygi SP & Elledge SJ (2016) Quantitative proteomic atlas of ubiquitination and acetylation in the DNA damage response. *Mol. Cell* **59:** 867–881

Engler C, Youles M, Gruetzner R, Ehnert TM, Werner S, Jones JDG, Patron NJ & Marillonnet S (2014) A Golden Gate modular cloning toolbox for plants. *ACS Synth. Biol.* **3:** 839–843

Erpapazoglou Z, Walker O & Haguenauer-Tsapis R (2014) Versatile roles of K63-linked ubiquitin chains in trafficking. *Cells* **3:** 1027–1088

Fawke S, Doumane M & Schornack S (2015) Oomycete interactions with plants: Infection strategies and resistance principles. *Microbiol. Mol. Biol. Rev.* **79:** 263–280

Feechan A, Jermakow AM, Ivancevic A, Godfrey D, Pak H, Panstruga R & Dry IB (2013) Host cell entry of powdery mildew is correlated with endosomal transport of antagonistically acting VvPEN1 and VvMLO to the papilla. *Mol. Plant-Microbe Interact.* **26:** 1138–1150

Feechan A, Kwon E, Yun BW, Wang Y, Pallas JA & Loake GJ (2005) A central role for S-nitrosothiols in plant disease resistance. *PNAS* **102:** 1–6

Fei C, Li Z, Li C, Chen Y, Chen Z, He X, Mao L, Wang X, Zeng R & Li L (2013) Smurf1-Mediated lys29-linked nonproteolytic polyubiquitination of Axin negatively regulates

Wnt/ -Catenin signaling. *Mol. Cell. Biol.* **33:** 4095–4105

Flores R, Di Serio F, Navarro B, Duran-Vila N & Owens RA (2011) Viroids and viroid diseases of plants. In studies in viral ecology: *Microbial and Botanical Host Systems* pp 307–342.

Frantzeskakis L, Kracher B, Kusch S, Yoshikawa-maekawa M, Bauer S, Pedersen C, Spanu PD, Maekawa T, Schulze-lefert P & Panstruga R (2018) Signatures of host specialization and a recent transposable element burst in the dynamic one-speed genome of the fungal barley powdery mildew pathogen. *BMC Genomics* **19:** 381

Froger A & Hall JE (2007) Transformation of plasmid DNA into *E. coli* using the heat shock method. *J. Vis. Exp.***:** 2007

Furniss JJ & Spoel SH (2015) Cullin-RING ubiquitin ligases in salicylic acid-mediated plant immune signaling. *Front. Plant Sci.* **6:** 1–10

Gao C, Luo M, Zhao Q, Yang R, Cui Y, Zeng Y, Xia J & Jiang L (2014) A unique plant ESCRT component, FREE1, regulates multivesicular body protein sorting and plant growth. *Curr. Biol.* **24:** 2556–2563

García-Cano E, Zaltsman A & Citovsky V (2014) Assaying proteasomal degradation in a cell-free system in plants. *J. Vis. Exp.***:** 1–6

Garnier M, Foissac X, Gaurivaud P, Laigret F, Renaudin J, Saillard C & Bové JM (2001) Mycoplasmas plants insect vectors: A matrimonial triangle. *Comptes Rendus l'Academie des Sci. - Ser. III* **324:** 923–928

Gingerich DJ, Gagne JM, Salter DW, Hellmann H, Estelle M, Ma L & Vierstra RD (2005) Cullins 3a and 3b assemble with members of the broad complex/tramtrack/ bric-a-brac (BTB) protein family to form essential ubiquitin-protein ligases (E3s) in Arabidopsis. *J. Biol. Chem.* **280:** 18810–18821

Giovannone AJ, Reales E, Bhattaram P, Fraile-Ramos A & Weimbs T (2017) Monoubiquitination of syntaxin 3 leads to retrieval from the basolateral plasma membrane and facilitates cargo recruitment to exosomes. *Mol. Biol. Cell* **28:** 2843–2853

Gladieux P, Byrnes EJ, Aguileta G, Fisher M, Billmyre RB, Heitman J & Giraud T (2017) Epidemiology and evolution of fungal pathogens in plants and animals. In *Genetics and Evolution of Infectious Diseases: Second Edition* pp 71–98.

Glawe DA (2008) The powdery mildews: a review of the world's most familiar (yet poorly known) plant pathogens. *Annu. Rev. Phytopathol.* **46:** 27–51

Glickman MH & Ciechanover A (2002) The ubiquitin-proteasome proteolytic pathway: destruction for the sake of construction. *Physiol. Rev.* **82:** 373–428

Godfrey D, Böhlenius H, Pedersen C, Zhang Z, Emmersen J & Thordal-Christensen H (2010) Powdery mildew fungal effector candidates share N-terminal Y/F/WxC-motif. *BMC Genomics* **11:** 317

González-Fernández R, Prats E & Jorrín-Novo J V. (2010) Proteomics of plant pathogenic fungi. *J. Biomed. Biotechnol.* **2010:** 36 pages

Gu Y & Innes RW (2011) The KEEP ON GOING protein of Arabidopsis recruits the ENHANCED DISEASE RESISTANCE1 protein to *trans*-Golgi network/early endosome vesicles. *Plant Physiol.* **155:** 1827–1838

Guo F-Q (2003) Identification of a plant nitric oxide synthase gene involved in hormonal signaling. *Science (80-. ).* **302:** 100–103

Guo Q, Liu Q, Smith N., Liang G & Wang M-B (2016) RNA silencing in plants: mechanisms, technologies and applications in horticultural crops. *Curr. Genomics* **17:** 476–489

Guo Y (2009) Study of the structure and function relationship of oncoprotein Gankyrin. *PhD thesis*

Haas AL & Rose IA (1982) The mechanism of ubiquitin activating enzyme. A kinetic and equilibrium analysis. *J. Biol. Chem.* **257:** 10329–10337

Hacker H & Karin M (2006) Regulation and function of IKK and IKK-related kinases. *Sci. STKE***:** re13

Hatfield PM, Gosink MM, Carpenter TB & Vierstra RD (1997) The ubiquitin activating gene (E1) family in Arabidopsis. *Plant J.* **11:** 213–226

Hayden MS & Ghosh S (2008) Shared principles in NF-κB signaling. *Cell* **132:** 344–362

Hegde AN (2004) Ubiquitin-proteasome-mediated local protein degradation and synaptic plasticity. *Prog. Neurobiol.* **73:** 311–357

Hegde AN (2010) The ubiquitin-proteasome pathway and synaptic plasticity. *Learn. Mem.* **17:** 314–327

Hetal P, Shruti S & Pratibha D (2015) Viruses and viroids: Insights of pathogenicity. *Int. Res. J. Biol. Sci.* **4:** 2278–3202

Hitchcock AL, Auld K, Gygi SP & Silver PA (2003) A subset of membrane-associated proteins is ubiquitinated in response to mutations in the endoplasmic reticulum degradation machinery. *Proc. Natl. Acad. Sci. U. S. A.* **100:** 12735–40

Hogenhout SA, Van der Hoorn RAL, Terauchi R & Kamoun S (2009) Emerging concepts in effector biology of plant-associated organisms. *Mol. Plant. Microbe. Interact.* **22:** 115–122

Holzberg S, Brosio P, Gross C & Pogue GP (2002) Barley strip mosaic virus-induced gene silencing in a monocot plant. *Plant J.* **30:** 315–327

Hoppe T (2005) Multiubiquitylation by E4 enzymes: 'One size' doesn't fit all. *Trends Biochem. Sci.* **30:** 183–187

Hothorn M, Belkhadir Y, Dreux M, Dabi T, Joseph P, Wilson IA & Chory J (2012) Structural basis of steroid hormone perception by the receptor kinase BRI1. *Nature* **474:** 467–471

Hotton SK & Callis J (2008) Regulation of Cullin RING ligases. *Annu. Rev. Plant Biol.* **59:** 467–489

Hua Z & Vierstra RD (2011) The Cullin-RING ubiquitin-protein ligases. *Annu. Rev. Plant Biol.* **62:** 299–334

Huang H, Jeon M shin, Liao L, Yang C, Elly C, Yates JR & Liu YC (2010) K33-linked polyubiquitination of T cell receptor-zeta regulates proteolysis-independent T cell signaling. *Immunity* **33:** 60–70

Huang S, Tang D & Wang Y (2016) Monoubiquitination of syntaxin 5 regulates Golgi membrane dynamics during the cell cycle. *Dev. Cell* **38:** 73–85

Huang Y, Minaker S, Roth C, Huang S, Hieter P, Lipka V, Wiermer M & Li X (2014) An E4 ligase facilitates polyubiquitination of plant immune receptor resistance proteins in Arabidopsis. *Plant Cell* **26:** 485–496

Hückelhoven R (2005) Powdery mildew susceptibility and biotrophic infection strategies. *FEMS Microbiol. Lett.* **245:** 9–17

Huckelhoven R, Fodor J, Preis C & Kogel K (1999) Hypersensitive cell death and papilla formation in barley attacked by the powdery mildew fungus are associated with hydrogen peroxide but not with salicylic acid accumulation. *Plant Physiol.* **119:** 1251–1260

Hückelhoven R & Panstruga R (2011) Cell biology of the plant-powdery mildew interaction. *Curr. Opin. Plant Biol.* **14:** 738–746

Humphry M, Kemmerling B, Koh S, Stein M, Göbel U & Stüber K (2010) A regulon conserved in monocot and dicot plants defines a functional module in antifungal plant immunity. *Proc. Natl. Acad. Sci. U. S. A.* **107:** 21896–21901

Hyoung TK, Kwang PK, Lledias F, Kisselev AF, Scaglione KM, Skowyra D, Gygi SP & Goldberg AL (2007) Certain pairs of ubiquitin-conjugating enzymes (E2s) and ubiquitin-protein ligases (E3s) synthesize nondegradable forked ubiquitin chains containing all possible isopeptide linkages. *J. Biol. Chem.* **282:** 17375–17386

Invitrogen (2003) Gateway ® technology a user guide. In pp 1–74.

Ishikawa K, Yamaguchi K, Sakamoto K, Yoshimura S, Inoue K, Tsuge S, Kojima C & Kawasaki T (2014) Bacterial effector modulation of host E3 ligase activity suppresses PAMP-triggered immunity in rice. *Nat. Commun.* **5:** 1–11

Jackson PK, Eldridge AG, Freed E, Furstenthal L, Hsu JY, Kaiser BK & Reimann JDR (2000) The lore of the RINGs: Substrate recognition and catalysis by ubiquitin ligases. *Trends Cell Biol.* **10:** 429–439

Jacobson AD, Zhang NY, Xu P, Han KJ, Noone S, Peng J & Liu CW (2009) The lysine 48 and lysine 63 ubiquitin conjugates are processed differently by the 26 S proteasome. *J. Biol. Chem.* **284:** 35485–35494

Jahn R & Scheller RH (2006) SNAREs-engines for membrane fusion. *Nat. Rev. Mol. Cell Biol.* **7:** 631–643

Jeandroz S, Wipf D, Stuehr DJ, Lamattina L, Melkonian M, Tian Z, Zhu Y, Carpenter EJ, Wong GK & Wendehenne D (2016) Occurrence, structure, and evolution of nitric oxide synthase – like proteins in the plant kingdom. *Sci. Signal.* **9:** 1–9

Johansson ON, Fantozzi E, Fahlberg P, Nilsson AK, Buhot N, Tör M & Andersson MX (2014) Role of the penetration-resistance genes PEN1, PEN2 and PEN3 in the hypersensitive response and race-specific resistance in *Arabidopsis thaliana*. *Plant J.* **79:** 466–76

Johnson A & Vert G (2016) Unraveling K63 polyubiquitination networks by sensor-based proteomics. *Plant Physiol.* **171:** 1808–1820

Jones JDG & Dangl JL (2006) The plant immune system. *Nature* **444:** 323–329

Jones JT, Haegeman A, Danchin EGJ, Gaur HS, Helder J, Jones MGK, Kikuchi T, Manzanilla-López R, Palomares-Rius JE, Wesemael WML & Perry RN (2013) Top 10

plant-parasitic nematodes in molecular plant pathology. *Mol. Plant Pathol.* **14:** 946–961

Jonge de R, Bolton MD & Thomma BPHJ (2011) How filamentous pathogens co-opt plants: The ins and outs of fungal effectors. *Curr. Opin. Plant Biol.* **14:** 400–406

Judelson HS & Blanco FA (2005) The spores of Phytophthora: Weapons of the plant destroyer. *Nat. Rev.* **3:** 47–58

Kabbage M & Dickman MB (2008) The BAG proteins: A ubiquitous family of chaperone regulators. *Cell. Mol. Life Sci.* **65:** 1390–1402

Kadota Y, Shirasu K & Zipfel C (2015) Regulation of the NADPH oxidase RBOHD during plant immunity. *Plant Cell Physiol.* **56:** 1472–1480

Kaku H, Nishizawa Y, Ishii-Minami N, Akimoto-Tomiyama C, Dohmae N, Takio K, Minami E & Shibuya N (2006) Plant cells recognize chitin fragments for defense signaling through a plasma membrane receptor. *Proc. Natl. Acad. Sci. U. S. A.* **103:** 11086–11091

Kamoun S (2006) A catalogue of the effector secretome of plant pathogenic oomycetes. *Annu. Rev. Phytopathol.* **44:** 41–60

Kamoun S (2007) Groovy times: filamentous pathogen effectors revealed. *Curr. Opin. Plant Biol.* **10:** 358–365

Kannan VR & Bastas KK (2016) Sustainable approaches to controlling plant pathogenic bacteria

Karin M & Gallagher E (2009) TNFR signaling: Ubiquitin-conjugated TRAFfic signals control stop-and-go for MAPK signaling complexes. *Immunol. Rev.* **228:** 225–240

Kasai K, Takano J, Miwa K, Toyoda A & Fujiwara T (2011) High boron-induced ubiquitination regulates vacuolar sorting of the BOR1 borate transporter in *Arabidopsis thaliana*. *J. Biol. Chem.* **286:** 6175–6183

Kim D-Y, Scalf M, Smith LM & Vierstra RD (2013) Advanced proteomic analyses yield a deep catalog of ubiquitylation targets in Arabidopsis. *Plant Cell* **25:** 1523–40

Kim HC & Huibregtse JM (2009) Polyubiquitination by HECT E3s and the determinants of Chain type specificity. *Mol. Cell. Biol.* **29:** 3307–3318

Kim HT, Kim KP, Uchiki T, Gygi SP & Goldberg AL (2009) S5a promotes protein degradation by blocking synthesis of nondegradable forked ubiquitin chains. *EMBO J.* **28:** 1867–1877

Kim M, Otsubo R, Morikawa H, Nishide A, Takagi K, Sasakawa C & Mizushima T (2014) Bacterial effectors and their functions in the ubiquitin-proteasome system: Insight from the modes of substrate recognition. *Cells* **3:** 848–864

Kim T, Cho M, Sangsawang K & Bhoo SH (2016) Fine mutational analysis of 2B8 and 3H7 tag epitopes with corresponding specific monoclonal antibodies. *Mol. Cells* **39:** 460–467

Kneeshaw S, Keyani R, Delorme-Hinoux V, Imrie L, Loake GJ, Le Bihan T, Reichheld J-P & Spoel SH (2017) Nucleoredoxin guards against oxidative stress by protecting antioxidant enzymes. *Proc. Natl. Acad. Sci.* **114:** 8414–8419

Knip M, Constantin ME & Thordal-christensen H (2014) Trans-kingdom cross-talk: Small RNAs on the move. *PLoS Genet.* **10:** e1004602

Kobae Y, Sekino T, Yoshioka H, Nakagawa T, Martinoia E & Maeshima M (2006) Loss of

AtPDR8, a plasma membrane ABC transporter of *Arabidopsis thaliana*, causes hypersensitive cell death upon pathogen infection. *Plant Cell Physiol.* **47:** 309–318

Koch E & Slusarenko A (1990) Arabidopsis is susceptible to infection by a downy mildew fungus. *Plant Cell Online* **2:** 437–445

Koegl M, Hoppe T, Schlenker S, Ulrich HD, Mayer TU & Jentsch S (1999) A novel ubiquitination factor, E4, is involved in multiubiquitin chain assembly. *Cell* **96:** 635–644

Kosarev P, Mayer KFX & Hardtke CS (2002) Evaluation and classification of RING-finger domains encoded by the Arabidopsis genome. *Genome Biol.* **3:** 1–12

Kraft E, Stone S, Ma L, Su N & Gao Y (2005a) Genome analysis and functional characterization of the E2 and RING-type E3 ligase ubiquitination enzymes of Arabidopsis. *Plant Anal.* **139:** 1597–1611

Kraft E, Stone SL, Ma L, Su N, Gao Y, Lau O-S, Deng X-W & Callis J (2005b) Genome analysis and functional characterization of the E2 and RING-type E3 ligase ubiquitination enzymes of Arabidopsis. *Plant Physiol.* **139:** 1597–1611

Kubori T & Galán JE (2003) Temporal regulation of Salmonella virulence effector function by proteasome-dependent protein degradation. *Cell* **115:** 333–342

Kusch S, Ahmadinejad N, Panstruga R & Kuhn H (2014) In silico analysis of the core signaling proteome from the barley powdery mildew pathogen (*Blumeria graminis* f. sp. *hordei*) In silico analysis of the core signaling proteome from the barley powdery mildew pathogen (*Blumeria graminis* f. sp. *hordei*). *Genomics* **15:** 843

Kwon C, Bednarek P & Schulze-Lefert P (2008a) Secretory pathways in plant immune responses. *Plant Physiol.* **147:** 1575–1583

Kwon C, Neu C, Pajonk S, Yun HS, Lipka U, Humphry M, Bau S, Straus M, Kwaaitaal M, Rampelt H, Kasmi F El, Jürgens G, Parker J, Panstruga R, Lipka V & Schulze-Lefert P (2008b) Co-option of a default secretory pathway for plant immune responses. *Nature* **451:** 835–840

Kwon YT & Ciechanover A (2017) The ubiquitin code in the ubiquitin-proteasome system and autophagy. *Trends Biochem. Sci.* **42:** 873–886

Lan W, Ma W & Miao Y (2018) Role of HECT ubiquitin protein ligases in *Arabidopsis thaliana*. *J. plant Sci. Phytopathol.* **2:** 20–30

Lange OF, Lakomek N-A, Farès C, Schröder GF, Walter KFA, Becker S, Meiler J, Grubmüller H, Griesinger C & de Groot BL (2008) Recognition dynamics up to microseconds revealed from an RDC-derived ubiquitin ensemble in solution. *Science* **320:** 1471–1475

Lau OS & Deng XW (2009) Effect of Arabidopsis COP10 ubiquitin E2 enhancement activity across E2 families and functional conservation among its canonical homologues. *Biochem. J.* **418:** 683–690

Laur J, Ramakrishnan GB, Labbé C, Lefebvre F, Spanu PD & Bélanger RR (2018) Effectors involved in fungal–fungal interaction lead to a rare phenomenon of hyperbiotrophy in the tritrophic system biocontrol agent–powdery mildew–plant. *New Phytol.* **217:** 713–725

Lechner E, Achard P, Vansiri A, Potuschak T & Genschik P (2006) F-box proteins

everywhere. *Curr. Opin. Plant Biol.* **9:** 631–638

Lee B, Lee MJ, Park S, Oh D, Elsasser S, Chen P, Gartner C, Dimova N, Hanna J, Gygi SP, Wilson SM, King RW & Finley D (2011) Enhancement of proteasome activity by a small-molecule inhibitor of Usp14. *Nature* **467:** 179–184

Lee H-A, Lee H-Y, Seo E, Lee J, Kim S-B, Oh S, Choi E, Choi E, Lee SE & Choi D (2017) Current understandings on plant nonhost resistance. *Mol. Plant-Microbe Interact.* **30:** 5–15

Lee J-H, Terzaghi W, Gusmaroli G, Charron J-BF, Yoon H-J, Chen H, He YJ, Xiong Y & Deng XW (2008) Characterization of Arabidopsis and rice DWD proteins and their roles as substrate receptors for CUL4-RING E3 ubiquitin ligases. *Plant Cell Online* **20:** 152–167

Lee SJ, Choi JY, Sung YM, Park H, Rhim H & Kang S (2001) E3 ligase activity of RING finger proteins that interact with Hip-2, a human ubiquitin-conjugating enzyme. *FEBS Lett.* **503:** 61–64

Lee WS, Rudd JJ & Kanyuka K (2015) Virus induced gene silencing (VIGS) for functional analysis of wheat genes involved in *Zymoseptoria tritici* susceptibility and resistance. *Fungal Genet. Biol.* **79:** 84–88

Leitner J, Petrasek J, Tomanov K, Retzer K, Parezova M, Korbei B, Bachmair A, Zazimalova E & Luschnig C (2012a) Lysine 63-linked ubiquitylation of PIN2 auxin carrier protein governs hormonally controlled adaptation of Arabidopsis root growth. *Proc. Natl. Acad. Sci.* **109:** 8322–8327

Leitner J, Retzer K, Korbei B & Luschnig C (2012b) Dynamics in PIN2 auxin carrier ubiquitylation in gravity-responding Arabidopsis roots. *Plant Signal. Behav.* **7:** 1271–1273

Lewis JL, Dong M, Earles CA & Chapman ER (2001) The transmembrane domain of syntaxin 1A is critical for cytoplasmic domain protein-protein interactions. *J. Biol. Chem.* **276:** 15458–15465

Li C-H, Chiang C-P, Yang J-Y, Ma C-J, Chen Y-C & Yen HE (2014) RING-type ubiquitin ligase McCPN1 catalyzes UBC8-dependent protein ubiquitination and interacts with Argonaute 4 in halophyte ice plant. *Plant Physiol. Biochem.* **80:** 1–9

Li J, Mahajan A & Tsai M-D (2006) Ankyrin repeat: a unique motif mediating protein-protein interactions. *Biochemistry* **45:** 15168–15178

Li W, Bengtson MH, Ulbrich A, Matsuda A, Reddy VA, Orth A, Chanda SK, Batalov S & Joazeiro CAP (2008) Genome-wide and functional annotation of human E3 ubiquitin ligases identifies MULAN, a mitochondrial E3 that regulates the organelle's dynamics and signaling. *PLoS One* **3:** e1487

Li YH, Windham MT & Trigiano RN (2005) Spore germination, infection structure formation, and colony development of *Erysiphe pulchra* on dogwood leaves and glass slides. *Plant Dis.* **89:** 1301–1304

Li ZG, Chen HW, Li QT, Tao JJ, Bian XH, Ma B, Zhang WK, Chen SY & Zhang JS (2015) Three SAUR proteins SAUR76, SAUR77 and SAUR78 promote plant growth in Arabidopsis. *Sci. Rep.* **5:** 1–19

Ling T, Bellin D, Vandelle E & Imanifard Z (2017) Host-mediated S-nitrosylation disarms

the bacterial effector HopAI1 to re-establish immunity. **29:** 2871–2881

Lipka V, Dittgen J, Bednarek P, Bhat R, Wiermer M, Stein M, Landtag J, Brandt W, Rosahl S, Scheel D, Llorente F, Molina A, Parker J, Somerville S & Schulze-Lefert P (2005) Pre- and postinvasion defenses both contribute to nonhost resistance in Arabidopsis. *Science (80).* **310:** 1180–1183

Liu C, Pedersen C, Schultz-Larsen T, Aguilar GB, Madriz-Ordeñana K, Hovmøller MS & Thordal-Christensen H (2016) The stripe rust fungal effector PEC6 suppresses pattern-triggered immunity in a host species-independent manner and interacts with adenosine kinases. *New Phytol.* **213:** 1556

Livneh I, Cohen-Kaplan V, Cohen-Rosenzweig C, Avni N & Ciechanover A (2016) The life cycle of the 26S proteasome: From birth, through regulation and function, and onto its death. *Cell Res.* **26:** 869–885

Lorenz S (2018) Structural mechanisms of HECT-type ubiquitin ligases. *Biol. Chem.* **399:** 127–145

Lu D, Lin W, Gao X, Wu S, Cheng C, Avila J, Heese A, Devarenne TP, He P & Shan L (2011) Direct ubiquitination of pattern recognition receptor FLS2 attenuates plant innate immunity. *Science (80).* **332:** 1439–1442

Luc A & Somerville SC (1996) Genetic characterization of five powdery mildew in *Arabidosis thaliana*. *Plant J.* **9:** 341–356

Lyzenga WJ & Stone SL (2012) Abiotic stress tolerance mediated by protein ubiquitination. *J. Exp. Bot.* **63:** 599–616

Ma K, Jiang S, Hawara E, Lee D, Pan S, Gitta C, Song J & Ma W (2015) Two serine residues in *Pseudomonas syringae* effector HopZ1a are required for acetyltransferase activity and association with the host co-factor. *New phtologist* **208:** 1157–1168

Macho AP & Zipfel C (2014) Plant PRRs and the activation of innate immune signaling. *Mol. Cell* **54:** 263–272

Maculins T, Fiskin E, Bhogaraju S & Dikic I (2016) Bacteria-host relationship: Ubiquitin ligases as weapons of invasion. *Cell Res.* **26:** 499–510

Majumdar R, Rajasekaran K & Cary JW (2017) RNA interference ( RNAi ) as a potential tool for control of mycotoxin contamination in crop plants : Concepts and considerations. *Front. Plant Sci.* **8:** 200

Malik SI, Hussain A, Yun BW, Spoel SH & Loake GJ (2011) GSNOR-mediated de-nitrosylation in the plant defence response. *plant Sci.* **181:** 540–4

Malsam J & Söllner TH (2011) Organization of SNAREs within the Golgi stack. *Cold Spring Harb. Perspect. Biol.* **3:** 1–17

Malynn B a & Ma A (2011) Ubiquitin makes its mark on immune regulation. *Immunity* **33:** 843–852

Mansfield J, Genin S, Magori S, Citovsky V, Sriariyanum M, Ronald P, Dow M, Verdier V, Beer S V, Machado MA, Toth I, Salmond G & Foster GD (2012) Top 10 plant pathogenic bacteria in molecular plant pathology. *Mol. Plant Pathol.* **13:** 614–629

Marín I (2010) Diversification and specialization of plant RBR ubiquitin ligases. *PLoS One* **5:** e11579

Marín I (2013) Evolution of plant HECT ubiquitin ligases. *PLoS One* **8:** e68536

Marques AJ, Palanimurugan R, Matias AC, Ramos PC & Dohmen RJ (2009) Catalytic mechanism and assembly of the proteasome catalytic mechanism and assembly of the proteasome. *Genomics* **109:** 1509–1536

Martínez-Ruiz A & Lamas S (2007) Signalling by NO-induced protein S-nitrosylation and S-glutathionylation: Convergences and divergences. *Cardiovasc. Res.* **75:** 220–228

Martins S, Dohmann EMN, Cayrel A, Johnson A, Fischer W, Pojer F, Satiat-Jeunemaître B, Jaillais Y, Chory J, Geldner N & Vert G (2015) Internalization and vacuolar targeting of the brassinosteroid hormone receptor BRI1 are regulated by ubiquitination. *Nat. Commun.* **6:** 6151

Matsuzawa A, Tseng PH, Vallabhapurapu S, Luo J-L, Zhang W, Wang H, Vignali DA., Gallagher E & Karin M (2008) Essentual cytoplasmi translocation of cytokin receptor-assembled signaling complex. *Science (80-. ).* **321:** 663–668

Mauch F, Mauch-Mani B & Boller T (1988) Antifungal hydrolases in pea tissue. *Plant Physiol.* **88:** 936–942

Mbega E & Nzogela Y (2012) Strategies used by plant parasitic nematodes to conquer the host. *J. Anim. Plant Sci.* **14:** 1848–1854

McKeon EJ, Li lian DS & Chin L-S (2015) Parkin-mediated K63-polyubiquitination targets ubiquitin C- terminal hydrolase L1 for degradation by the autophagy- lysosome system. *Mol. Cell* **72:** 1811–1824

Meierhofer D, Wang X, Huang L & Kaiser P (2008) Quantitative analysis of global ubiquitination in HeLa cells by mass spectrometry. *J. Proteome Res.* **7:** 4566–4576

Miao Y & Zentgraf U (2010) A HECT E3 ubiquitin ligase negatively regulates Arabidopsis leaf senescence through degradation of the transcription factor WRKY53. *Plant J.* **63:** 179–188

Micali CO, Neumann U, Grunewald D, Panstruga R & O'Connell R (2011) Biogenesis of a specialized plant-fungal interface during host cell internalization of *Golovinomyces orontii* haustoria. *Cell. Microbiol.* **13:** 210–226

Miya A, Albert P, Shinya T, Desaki Y, Ichimura K, Shirasu K, Narusaka Y, Kawakami N, Kaku H & Shibuya N (2007) CERK1, a lysM receptor kinase, is essential for chitin elicitor signaling in Arabidopsis. *Proc. Natl. Acad. Sci. U. S. A.* **104:** 19613–19618

Mladek C, Guger K & Hauser MT (2003) Identification and characterization of the ARIADNE gene family in Arabidopsis. A group of putative E3 ligases. *Plant Physiol.* **131:** 27–40

Møller IM, Jensen PE & Hansson A (2007) Oxidative modifications to cellular components in plants. *Annu. Rev. Plant Biol.* **58:** 459–81

Mosavi LK, Cammett TJ, Desrosiers DC & Peng Z-Y (2004) The ankyrin repeat as molecular architecture for protein recognition. *Protein Sci.* **13:** 1435–1448

Mudgil Y, Shiu S-H, Stone SL, Salt JN & Goring DR (2004) A large complement of the predicted Arabidopsis ARM repeat proteins are members of the U-Box E3 ubiquitin ligase family. *Plant Physiol.* **134:** 59–66

Nakao M, Nakamura R, Kita K, Inukai R & Ishikawa A (2011) Non-host resistance to

penetration and hyphal growth of *Magnaporthe oryzae* in Arabidopsis. *Sci. Rep.* **1:** 1–9

Nathan JA, Tae Kim H, Ting L, Gygi SP & Goldberg AL (2013) Why do cellular proteins linked to K63-polyubiquitin chains not associate with proteasomes? *EMBO J.* **32:** 552–565

Nawrath C (1999) Salicylic acid induction deficient mutants of Arabidopsis express PR-2 and PR-5 and accumulate high levels of camalexin after pathogen inoculation. *Plant Cell* **11:** 1393–1404

Nguyen TN & Goodrich JA (2006) Protein-protein interaction assays: eliminating false positive interactions. *Nat. Methods* **3:** 135–139

Nie P, Li X, Wang S, Guo J, Zhao H & Niu D (2017) Induced systemic resistance against *Botrytis cinerea* by *Bacillus cereus* AR156 through a JA/ET- and NPR1-dependent signaling pathway and activates PAMP-triggered immunity in Arabidopsis. *Front. Plant Sci.* **8:** 1–12

Nielsen M & Thordal-Christensen H (2012) Recycling of Arabidopsis plasma membrane PEN1 syntaxin. *Plant Signal. Behav.* **7:12:** 1541–1543

Nielsen ME, Feechan A, Böhlenius H, Ueda T & Thordal-Christensen H (2012) Arabidopsis ARF-GTP exchange factor, GNOM, mediates transport required for innate immunity and focal accumulation of syntaxin PEN1. *Proc. Natl. Acad. Sci. U. S. A.* **109:** 11443–8

Nielsen ME & Thordal-Christensen H (2013) Transcytosis shuts the door for an unwanted guest. *Trends Plant Sci.* **18:** 1–6

Nishikawa H, Ooka S, Sato K, Arima K, Okamoto J, Klevit RE, Fukuda M & Ohta T (2004) Mass spectrometric and mutational analyses reveal Lys-6-linked polyubiquitin chains catalyzed by BRCA1-BARD1 ubiquitin ligase. *J. Biol. Chem.* **279:** 3916–3924

Nodzon L a, Xu W-H, Wang Y, Pi L-Y, Chakrabarty PK & Song W-Y (2004) The ubiquitin ligase XBAT32 regulates lateral root development in Arabidopsis. *Plant J.* **40:** 996–1006

Noel EA, Kang M, Adamec J, Van Etten JL & Oyler GA (2014) Chlorovirus Skp1-binding ankyrin repeat protein interplay and mimicry of cellular ubiquitin ligase machinery. *J. Virol.* **88:** 13798–13810

Nottensteiner M, Zechmann B, McCollum C & Huckelhoven R (2018) A barley powdery mildew fungus non-autonomous retrotransposon encodes a peptide that supports penetration success on barley. *J. Exp. Bot.* **69:** 3745–3758

Nowara D, Gay A, Lacomme C, Shaw J, Ridout C, Douchkov D, Hensel G, Kumlehn J & Schweizer P (2010) HIGS: host-induced gene silencing in the obligate biotrophic fungal pathogen *Blumeria graminis*. *Plant Cell* **22:** 3130–3141

Ohi MD, Kooi CW Vander, Rosenberg JA, Chazin WJ & Gould KL (2003) Structural insights into the U-box, a domain associated with multi-ubiquitination. *Nat. Struct. Biol.* **10:** 250–255

Ohtake F & Tsuchiya H (2016) The emerging complexity of ubiquitin architecture. *J. Biochem.* **161:** 125–133

Van Ooijen G, Lukasik E, Van Den Burg HA, Vossen JH, Cornelissen BJC & Takken FLW (2010) The small heat shock protein 20 RSI2 interacts with and is required for stability

and function of tomato resistance protein I-2. *Plant J.* **63:** 563–572

Ordureau A, Sarraf SA, Duda DM, Heo JM, Jedrychowski MP, Sviderskiy VO, Olszewski JL, Koerber JT, Xie T, Beausoleil SA, Wells JA, Gygi SP, Schulman BA & Harper JW (2014) Quantitative proteomics reveal a feedforward mechanism for mitochondrial PARKIN translocation and ubiquitin chain synthesis. *Mol. Cell* **56:** 360–375

Paez Valencia J, Goodman K & Otegui MS (2016) Endocytosis and endosomal trafficking in plants. *Annu. Rev. Plant Biol.* **67:** 309–335

Pajonk S, Kwon C, Clemens N, Panstruga R & Schulze-Lefert P (2008) Activity determinants and functional specialization of Arabidopsis PEN1 syntaxin in innate immunity. *J. Biol. Chem.* **283:** 26974–26984

Panstruga R & Dodds PN (2009a) Terrific protein traffic: the mystery of effector protein delivery by filamentous plant pathogens. *Science* **324:** 748–750

París R, Iglesias MJ, Terrile MC & Casalongué C a (2013) Functions of S-nitrosylation in plant hormone networks. *Front. Plant Sci.* **4:** 294

Park C-H, Chen S, Shirsekar G, Zhou B, Khang CH, Songkumarn P, Afzal AJ, Ning Y, Wang R, Bellizzi M, Valent B & Wang G-L (2012) The *Magnaporthe oryzae* effector AvrPiz-t targets the RING E3 ubiquitin ligase APIP6 to suppress pathogen-associated molecular pattern-triggered immunity in rice. *Plant Cell* **24:** 4748–4762

Parra RG, Espada R, Verstraete N & Ferreiro DU (2015) Structural and energetic characterization of the ankyrin repeat protein family. *PLoS Comput. Biol.* **11:** 1–20

Pedersen C, Themaat VVE, McGuffin LJ, Abbott JC, Burgis TA, Barton G, Bindschedler L V, Lu X, Maekawa T, Weßling R, Cramer R, Thordal-Christensen H, Panstruga R & Spanu PD (2012) Structure and evolution of barley powdery mildew effector candidates. *BMC Genomics* **13:** 694

Peng J, Schwartz D, Elias JE, Thoreen CC, Cheng D, Marsischky G, Roelofs J, Finley D & Gygi SP (2003a) A proteomics approach to understanding protein ubiquitination. *Nat. Biotechnol.* **21:** 921–926

Pennington HG, Gheorghe DM, Damerum A, Pliego C, Spanu PD, Cramer R & Bindschedler L V (2016) Interactions between the powdery mildew effector BEC1054 and barley proteins identify candidate host targets. *J. Proteome Res.* **15:** 826–839

Peth A, Uchiki T & Goldberg LA (2011) ATP-dependent steps in the binding of ubiquitin conjugates to the 26S proteasome that commit to degradation. *Mol. Cell* **40:** 671–681

Petre B & Kamoun S (2014) How do filamentous pathogens deliver effector proteins into plant cells? *PLoS Biol.* **12:** e1001801

Petre B, Saunders DGO, Sklenar J, Lorrain C, Win J, Duplessis S & Kamoun S (2015) Candidate effector proteins of the rust pathogen *Melampsora larici-populina* target diverse plant cell compartments. *Mol. Plant-Microbe Interact.* **28:** 689–700

Pickart CM & Fushman D (2004) Polyubiquitin chains: Polymeric protein signals. *Curr. Opin. Chem. Biol.* **8:** 610–616

Pitzschke A, Schikora A & Hirt H (2009) MAPK cascade signalling networks in plant defence. *Curr. Opin. Plant Biol.* **12:** 421–426

Pliego C, Nowara D, Bonciani G, Gheorghe DM, Xu R, Surana P, Whigham E, Nettleton D,

Bogdanove AJ, Wise RP, Schweizer P, Bindschedler L V & Spanu PD (2013) Host-induced gene silencing in barley powdery mildew reveals a class of ribonuclease-like effectors. *Mol. Plant. Microbe. Interact.* **26:** 633–42

Pollack JD, Williams M V. & McElhaney RN (1997) The comparative metabolism of the mollicutes (Mycoplasmas): The utility for taxonomic classification and the relationship of putative gene annotation and phylogeny to enzymatic function in the smallest free-living cells. *Crit. Rev. Microbiol.* **23:** 269–354

Prasad ME, Schofield A, Lyzenga W, Liu H & Stone SL (2010) Arabidopsis RING E3 ligase XBAT32 regulates lateral root production through its role in ethylene biosynthesis. *Plant Physiol.* **153:** 1587–1596

Prasad ME & Stone SL (2010) Further analysis of XBAT32, an Arabidopsis RING E3 ligase, involved in ethylene biosynthesis. *Plant Physiol.* **153:** 1587–1596

Rahman SFSA, Singh E, Pieterse CMJ & Schenk PM (2018) Emerging microbial biocontrol strategies for plant pathogens. *Plant Sci.* **267:** 102–111

Randles J & Ogle H (1997) Viruses and viroids as agents of plant disease. *Plant Pathog. Plant Dis.***:** 104–126

Razin S (2006) The genus Mycoplasma and related genera (class Mollicutes)

Reichardt I, Slane D, El Kasmi F, Knöll C, Fuchs R, Mayer U, Lipka V & Jürgens G (2011a) Mechanisms of functional specificity among plasma-membrane syntaxins in Arabidopsis. *Traffic* **12:** 1269–1280

Ridout CJ, Skamnioti P, Porritt O, Sacristan S, Jones JDG & Brown JKM (2006) Multiple avirulence paralogues in cereal powdery mildew fungi may contribute to parasite fitness and defeat of plant resistance. *Plant Cell* **18:** 2402–2414

Rivas S (2012) Nuclear dynamics during plant innate immunity. *Plant Physiol.* **158:** 87–94

Rockel P, Strube F, Rockel A, Wildt J & Kaiser WM (2002) Regulation of nitric oxide (NO) production by plant nitrate reductase in vivo and in vitro. *J. Exp. Bot.* **53:** 103–10

Romero-Barrios N & Vert G (2018) Proteasome-independent functions of lysine-63 polyubiquitination in plants. *New Phytol.* **217:** 995–1011

Ron M, Saez MA, Williams LE, Fletcher JC & McCormick S (2010) Proper regulation of a sperm specific cis-nat-siRNA is essential for double fertilization in Arabidopsis. *Genes Dev.* **24:** 1010–1021

Ronald PC & Beutler B (2010) Plant and animal sensors of conserved microbial signatures. *Science* **330:** 1061–1064

Sadowski M & Sarcevic B (2010) Mechanisms of mono- and poly-ubiquitination: Ubiquitination specificity depends on compatibility between the E2 catalytic core and amino acid residues proximal to the lysine. *Cell Div.* **5:** 19

Sadowski M, Suryadinata R, Tan AR, Roesley SNA & Sarcevic B (2012) Protein monoubiquitination and polyubiquitination generate structural diversity to control distinct biological processes. *IUBMB Life* **64:** 136–142

Sambrook J, Fritsch E & Maniatis T (2012) Molecular cloning. Fourth edition

Sanjuán R & Domingo-Calap P (2016) Mechanisms of viral mutation. *Cell. Mol. Life Sci.* **73:**

4433–4448

Sanz L, Albertos P, Mateos I, Sánchez-Vicente I, Lechón T, Fernández-Marcos M & Lorenzo O (2015) Nitric oxide (NO) and phytohormones crosstalk during early plant development. *J. Exp. Bot.* **66:** 2857–2868

Satija YK, Bhardwaj A & Das S (2013) A portrayal of E3 ubiquitin ligases and deubiquitylases in cancer. *Int. J. Cancer* **133:** 2759–2768

Sato T, Maekawa S, Yasuda S, Sonoda Y, Katoh E, Ichikawa T, Nakazawa M, Seki M, Shinozaki K, Matsui M, Goto DB, Ikeda A & Yamaguchi J (2009) CNI1/ATL31, a RING-type ubiquitin ligase that functions in the carbon/nitrogen response for growth phase transition in Arabidopsis seedlings. *Plant J.* **60:** 852–864

Saunders DGO, Win J, Cano LM, Szabo LJ, Kamoun S & Raffaele S (2012) Using hierarchical clustering of secreted protein families to classify and rank candidate effectors of rust fungi. *PLoS One* **7:**

Savary S, Ficke A, Aubertot JN & Hollier C (2012) Crop losses due to diseases and their implications for global food production losses and food security. *Food Secur.* **4:** 519–537

Schlicht M & Kombrink E (2013) The role of nitric oxide in the interaction of *Arabidopsis thaliana* with the biotrophic fungi, *Golovinomyces orontii* and *Erysiphe pisi*. *Front. Plant Sci.* **4:** 1–12

Schmidt SM, Kuhn H, Micali C, Liller C, Kwaaitaal M & Panstruga R (2014) Interaction of a *Blumeria graminis* f. sp. *hordei* effector candidate with a barley ARF-GAP suggests that host vesicle trafficking is a fungal pathogenicity target. *Mol. Plant Pathol.* **15:** 535–549

Schmitt D & Sipes B (2018) Plant-parasitic nematodes and their management: A review. *J. Biol. Agric. Healthc.* **8:** 2224–3208

Scialpi F, Malatesta M, Peschiaroli A, Rossi M, Melino G & Bernassola F (2008) Itch self-polyubiquitylation occurs through lysine-63 linkages. *Biochem. Pharmacol.* **76:** 1515–1521

Selin C, de Kievit TR, Belmonte MF & Fernando WGD (2016) Elucidating the role of effectors in plant-fungal interactions: Progress and challenges. *Front. Microbiol.* **7:** 1–21

Serio F Di, Li S, Pallas V & Randles J (2012) Virus taxonomy: Ninth report of the international committee on taxonomy of viruses taxonomic structure of the family physicochemical and physical properties. In pp 1221–1234.

Sharma B, Joshi D, Yadav PK, Gupta AK & Bhatt TK (2016) Role of ubiquitin-mediated degradation system in plant biology. *Front. Plant Sci.* **7:** 1–8

She J, Han Z, Kim T-W, Wang J, Cheng W, Chang J, Shi S, Wang J, Yang M, Wang Z-Y & Chai J (2011) Structural insight into brassinosteroid perception by BRI1. *Nature* **474:** 472–476

Shen Q-H, Saijo Y, Mauch S, Biskup C, Bieri S, Keller B, Seki H, Ulker B, Somssich IE & Schulze-Lefert P (2007) Nuclear activity of MLA immune receptors links isolate-specific and basal disease-resistance responses. *Science* **315:** 1098–1103

Singh R & Phulera S (2015) Plant parasitic nematodes: The hidden enemies of farmers. In *Environmental issues for socio-ecological development* pp 68–81.

Smalle J & Vierstra RD (2004) The ubiquitin 26S proteasome proteolytic pathway. *Annu. Rev. Plant Biol.* **55:** 555–590

Söllner T, Bennett MK, Whiteheart SW, Scheller RH & Rothman JE (1993) A protein assembly-disassembly pathway *in vitro* that may correspond to sequential steps of synaptic vesicle docking, activation, and fusion. *Cell* **75:** 409–418

Song T, Ma Z, Shen D, Li Q, Li W, Su L, Ye T, Zhang M, Wang Y & Dou D (2015) An Oomycete CRN effector reprograms expression of plant HSP genes by targeting their promoters. *PLoS Pathog.* **11:** 1–30

Spanu PD (2017) Cereal immunity against powdery mildews targets RNase-like proteins associated with Haustoria (RALPH) effectors evolved from a common ancestral gene. *New phtologist* **213:** 969–971

Spanu PD, Butcher SA, Gurr SJ, Lebrun M, Ridout CJ, Schulze-lefert P, Talbot NJ, Ahmadinejad N, Ametz C, Barton GR, Benjdia M, Bidzinski P, Bindschedler L V, Both M, Brewer MT, Cadle-davidson L, Cadle-davidson MM, Collemare J, Cramer R, Frenkel O, et al (2010) Genome expansion and gene loss in powdery mildew fungi reveal tradeoffs in extreme parasitism. *Science (80-. ).* **330:** 1543–1546

Spanu PD & Panstruga R (2012) Powdery mildew genomes in the crosshairs. *New phtologist* **195:** 20–22

Spanu PD & Panstruga R (2017) Editorial: Biotrophic plant-microbe interactions. *Front. Plant Sci.* **8:** 192

Spoel SH & Loake GJ (2011) Redox-based protein modifications: The missing link in plant immune signalling. *Curr. Opin. Plant Biol.* **14:** 358–364

Spratt DE, Walden H & Shaw GS (2014) RBR E3 ubiquitin ligases: new structures, new insights, new questions. *Biochem. J.* **458:** 421–437

Stam R, Mantelin S, McLellan H & Thilliez G (2014) The role of effectors in nonhost resistance to filamentous plant pathogens. *Front. Plant Sci.* **5:** 1–6

Stein M, Dittgen J, Sánchez-Rodríguez C, Hou B-H, Molina A, Schulze-Lefert P, Lipka V & Somerville S (2006) Arabidopsis PEN3/PDR8, an ATP binding cassette transporter, contributes to nonhost resistance to inappropriate pathogens that enter by direct penetration. *Plant Cell* **18:** 731–746

Stewart MD, Ritterhoff T, Klevit RE & Brzovic PS (2016) E2 enzymes: More than just middle men. *Cell Res.* **26:** 423–440

Stone S, Hauksdóttir H, Troy A, Herschleb J, Kraft E & Callis J (2005) Functional analysis of the RING-type ubiquitin ligase family of Arabidopsis. *Genome Anal.* **137:** 13–30

Stone SL (2014a) The role of ubiquitin and the 26S proteasome in plant abiotic stress signaling. *Front. Plant Sci.* **5:** 1–10

Stone SL, Williams LA, Farmer LM, Vierstra RD & Callis J (2006) KEEP ON GOING, a RING E3 ligase essential for Arabidopsis growth and development, is involved in abscisic acid signaling. *Plant Cell* **18:** 3415–3428

Suryadinata R, Roesley SNA, Yang G & Šarčević B (2014) Mechanisms of generating polyubiquitin chains of different topology. *Cells* **3:** 674–689

Taj G, Agarwal P, Grant M & Kumar A (2010) MAPK machinery in plants. Recognition and

response to different stresses through multiple signal transduction pathways. *Plant Signal. Behav.* **5:** 1370–1378

Takamatsu S (2013) Molecular phylogeny reveals phenotypic evolution of powdery mildews (Erysiphales, Ascomycota). *J. Gen. Plant Pathol.* **79:** 218–226

Tanno H & Komada M (2013) The ubiquitin code and its decoding machinery in the endocytic pathway. *J. Biochem.* **153:** 497–504

Terpe K (2003) Overview of tag protein fusions: from molecular and biochemical fundamentals to commercial systems. *Appl. Microbiol. Biotechnol.* **60:** 523–533

Thomma BPHJ, Nürnberger T & Joosten MHAJ (2011) Of PAMPs and effectors: The blurred PTI-ETI dichotomy. *Plant Cell* **23:** 4–15

Thordal-Christensen H, Birch PRJ, Spanu PD & Panstruga R (2018) Why did filamentous plant pathogens evolve the potential to secrete hundreds of effectors to enable disease? *Mol. Plant Pathol.* **19:** 781–785

Tian M & Xie Q (2013) Non-26S proteasome proteolytic role of ubiquitin in plant endocytosis and endosomal trafficking. *J. Integr. Plant Biol.* **55:** 54–63

Toruno YT, Stergiopoulos L & Coaker G (2016) Plant-pathogen effectors: Cellular probes interfering with plant defenses in spatial and temporal manners. *Annu. Rev. Phytopathol.* **54:** 419–441

Toufighi K, Brady SM, Austin R, Ly E & Provart NJ (2005) The botany array resource: e-Northerns, expression angling, and promoter analyses. *Plant J.* **43:** 153–163

Tripathi D (2017) Bacterial pathogens in plants. *J. Bacteriol. Mycol. Open Access* **4:** 1–2

Trujillo M (2018) News from the PUB: Plant U-box type E3 ubiquitin ligases. *J. Exp. Bot.* **69:** 371–384

Tseng P, Matsuzawa A, Zhang W, Mino T, Dario AA & Karin M (2010) Different modes of TRAF3 ubiquitination selectively activate type I interferon and proinflammatory cytokine expression. *Nat. Immunol.* **11:** 70–75

Underwood W & Somerville SC (2008) Focal accumulation of defences at sites of fungal pathogen attack. *J. Exp. Bot.* **59:** 3501–3508

Vanacker H, Carver TLW & Foyer CH (2000) Early $H_2O_2$ accumulation in mesophyll cells leads to induction of Glutathione during the hyper-sensitive response in the barley-powdery mildew interaction. *Plant Physiol.* **123:** 1289–1300

Vellai T & Vida G (1999) The origin of eukaryotes: The difference between prokaryotic and eukaryotic cells. *Proc. R. Soc. B Biol. Sci.* **266:** 1571–1577

Vijay-Kumar S, Bugg CE & Cook WJ (1987) Structure of ubiquitin refined at 1.8 Å resolution. *J. Mol. Biol.* **194:** 531–544

Vijay-Kumar S, Bugg CE, Wilkinson KD & Cook WJ (1985) Three-dimensional structure of ubiquitin at 2.8 A resolution. *Proc. Natl. Acad. Sci. U. S. A.* **82:** 3582–3585

Voigt CA (2014) Callose-mediated resistance to pathogenic intruders in plant defense-related papillae. *Front. Plant Sci.* **5:** 1–6

Wang J, Chen X, Li J, Jiao Y, Meng X, Yu H, Lu Z, Wang Y, Xiong G & Liu G (2017) Tissue-specific ubiquitination by IPA1 INTERACTING PROTEIN1 modulates IPA1

protein levels to regulate plant architecture in rice. *Plant Cell* **29:** 697–707

Wang K (2006) Agrobacterium protocols

Wang M, Cheng D, Peng J & Pickart CM (2006a) Molecular determinants of polyubiquitin linkage selection by an HECT ubiquitin ligase. *EMBO J.* **25:** 1710–1719

Wang W, Vinocur B, Shoseyov O & Altman A (2004) Role of plant heat-shock proteins and molecular chaperones in the abiotic stress response. *Trends Plant Sci.* **9:** 1360–1385

Wang Y-S, Pi L-Y, Chen X, Chakrabarty PK, Jiang J, De Leon AL, Liu G-Z, Li L, Benny U, Oard J, Ronald PC & Song W-Y (2006b) Rice XA21 binding protein 3 is a ubiquitin ligase required for full Xa21-mediated disease resistance. *Plant Cell Online* **18:** 3635–3646

Wang YQ, Feechan A, Yun BW, Shafiei R, Hofmann A, Taylor P, Xue P, Yang FQ, Xie ZS, Pallas JA, Chu CC & Loake GJ (2009) S-nitrosylation of AtSABP3 antagonizes the expression of plant immunity. *J. Biol. Chem.* **284:** 2131–2137

Weber E, Engler C, Gruetzner R, Werner S & Marillonnet S (2011) A modular cloning system for standardized assembly of multigene constructs. *PLoS One* **6:** e16765

Weissman AM (2001) Themes and variations on ubiquitylation. *Nat. Rev. Mol. Cell Biol.* **2:** 169–178

Wenzel DM, Stoll KE & Klevit RE (2011) E2s: Structurally economical and functionally replete. *J. Biochem.* **433:** 31–42

Wiermer M, Palma K, Zhang Y & Li X (2007) Should I stay or should I go? Nucleocytoplasmic trafficking in plant innate immunity. *Cell. Microbiol.* **9:** 1880–1890

Wilkinson JQ & Crawford NM (1991) Identification of the Arabidopsis CHL3 gene as the nitrate reductase structural gene NIA2. *Plant Cell* **3:** 461–71

Wright AJ, Thomas BJ & Carver TL (2002) Early adhesion of *Blumeria graminis* to plant and artificial surfaces demonstrated by centrifugation. *Physiol. Mol. Plant Pathol.* **61:** 217–226

Wu PY, Hanlon M, Eddins M, Tsui C, Rogers RS, Jensen JP, Matunis MJ, Weissman AM, Wolberger CP & Pickart CM (2003) A conserved catalytic residue in the ubiquitin-conjugating enzyme family. *EMBO J.* **22:** 5241–5250

Wu X & Karin M (2015) Emerging roles of lys63-linked polyubiquitylation in immune responses. *Immunol. Rev.* **266:** 161–174

Xavier JC, Patil KR & Rocha I (2014) Systems biology perspectives on minimal and simpler cells. *Microbiol. Mol. Biol. Rev.* **78:** 487–509

Xue Y, Li A, Wang L, Feng H & Yao X (2006) PPSP: Prediction of PK-specific phosphorylation site with Bayesian decision theory. *BMC Bioinformatics* **7:** 1–11

Xu P, Duong DM, Seyfried NT, Cheng D, Xie Y, Rush J, Hochstrasser M, Finley D & Peng J (2009) Quantitative proteomics reveals the function of unconventional ubiquitin chains in proteasomal degradation. *Cell* **137:** 133–145

Yamaoka N, Matsumoto I & Nishiguchi M (2006) The role of primary germ tubes (PGT) in the life cycle of *Blumeria graminis*: The stopping of PGT elongation is necessary for the triggering of appressorial germ tube (AGT) emergence. *Physiol. Mol. Plant Pathol.* **69:**

153–159

Yanagawa Y, Sullivan JA, Komatsu S, Gusmaroli G, Suzuki G, Yin J, Ishibashi T, Saijo Y, Rubio V, Kimura S, Wang J & Deng XW (2004) Arabidopsis COP10 forms a complex with DDB1 and DET1 *in vivo* and enhances the activity of ubiquitin conjugating enzymes. *Genes Dev.* **18:** 2172–2181

Yang P, Fu H, Walker J, Papa CM, Smalle J, Ju YM & Vierstra RD (2004) Purification of the Arabidopsis 26S proteasome: Biochemical and molecular analyses revealed the presence of multiple isoforms. *J. Biol. Chem.* **279:** 6401–6413

Yang W-L, Wang J, Chan C-H, Lee S-W, Campos A., Lamothe B, Hur L, Grabiner BC, Lin X, Darnay BG & Lin H-K (2009) The E3 Ligase TRAF6 Regulates Akt ubiquitination and activation. *Science (80-. ).* **325:** 1134–1138

Yee D & Goring DR (2009) The diversity of plant U-box E3 ubiquitin ligases: From upstream activators to downstream target substrates. *J. Exp. Bot.* **60:** 1109–1121

Yin C & Hulbert S (2015) Host induced gene silencing ( HIGS ), a promising strategy for developing disease resistant crops. *Gene Technol.* **4:** 3

Yin C, Jurgenson JE & Hulbert SH (2011) Development of a host-induced RNAi system in the wheat stripe rust fungus *Puccinia striiformis* f. sp. *tritici*. *Am. Phytopathol. Soc.* **24:** 554–561

You Q, Zhai K, Yang D, Yang W, Wu J, Liu J, Pan W, Wang J, Zhu X, Jian Y, Liu J, Zhang Y, Deng Y, Li Q, Lou Y, Xie Q & He Z (2016) An E3 ubiquitin ligase-BAG protein module controls plant innate immunity and broad-spectrum disease resistance. *Cell Host Microbe* **20:** 758–769

Younis A, Siddique MI, Kim C & Lim K (2014) RNA interference (RNAi) induced gene silencing: A promising approach of Hi-Tech plant breeding. *Int. J. Biol. Sci.* **10:** 1150–1158

Yu M (2012) Identification and characterisation of the E3 ligase, RAP1, in Arabidopsis. *PhD thesis*

Yu M, Lamattina L, Spoel SH & Loake GJ (2014) Nitric oxide function in plant biology: A redox cue in deconvolution. *New Phytol.* **202:** 1142–1156

Yu M, Yun BW, Spoel SH & Loake GJ (2012) A sleigh ride through the SNO: Regulation of plant immune function by protein S-nitrosylation. *Curr. Opin. Plant Biol.* **15:** 424–430

Yuan C, Li C, Yan L, Jackson AO, Liu Z, Han C, Yu J & Li D (2011) A high throughput barley stripe mosaic virus vector for virus induced gene silencing in monocots and dicots. *PLoS One* **6:**

Yuan WC, Lee YR, Lin SY, Chang LY, Tan YP, Hung CC, Kuo JC, Liu CH, Lin MY, Xu M, Chen ZJ & Chen RH (2014) K33-linked polyubiquitination of Coronin 7 by Cul3-KLHL20 ubiquitin E3 ligase regulates protein trafficking. *Mol. Cell* **54:** 586–600

Yuan X, Zhang S, Liu S, Yu M, Su H, Shu H & Li X (2013) Global analysis of ankyrin repeat domain C3HC4-type RING finger gene family in plants. *PLoS One* **8:** 1–11

Yun B-W, Feechan A, Yin M, Saidi NBB, Le Bihan T, Yu M, Moore JW, Kang J-G, Kwon E, Spoel SH, Pallas J a & Loake GJ (2011) S-nitrosylation of NADPH oxidase regulates cell death in plant immunity. *Nature* **478:** 264–8

Yun B, Skelly MJ, Yin M, Yu M, Mun B, Lee S, Hussain A, Spoel SH & Loake GJ (2016) Nitric oxide and S-nitrosoglutathione function additively during plant immunity. *New Phytol.* **211:** 516–526

Yun BW, Spoel SH & Loake GJ (2012) Synthesis of and signalling by small, redox active molecules in the plant immune response. *Biochim. Biophys. Acta - Gen. Subj.* **1820:** 770–776

Zelazny E & Vert G (2015) Regulation of iron uptake by IRT1: Endocytosis pulls the trigger. *Mol. Plant* **8:** 977–979

Zhang J, Shao F, Li Y, Cui H, Chen L, Li H, Zou Y, Long C, Lan L, Chai J, Chen S, Tang X & Zhou JM (2007a) A *Pseudomonas syringae* effector inactivates MAPKs to suppress PAMP-induced immunity in plants. *Cell Host Microbe* **1:** 175–185

Zhang M, Windheim M, Roe SM, Peggie M, Cohen P, Prodromou C & Pearl LH (2005a) Chaperoned ubiquitylation - Crystal structures of the CHIP U box E3 ubiquitin ligase and a CHIP-Ubc13-Uev1a complex. *Mol. Cell* **20:** 525–538

Zhang W (2012) Identification of plant and fungal genes important for barley powdery mildew biotrophy. *PhD thesis***:** 122

Zhang WJ, Pedersen C, Kwaaitaal M, Gregersen PL, Mørch SM, Hanisch S, Kristensen A, Fuglsang AT, Collinge DB & Thordal-Christensen H (2012) Interaction of barley powdery mildew effector candidate CSEP0055 with the defence protein PR17c. *Mol. Plant Pathol.* **13:** 1110–1119

Zhang X, Henriques R, Lin SS, Niu QW & Chua NH (2006) Agrobacterium-mediated transformation of *Arabidopsis thaliana* using the floral dip method. *Nat. Protoc.* **1:** 641–646

Zhang Z, Feechan A, Pedersen C, Newman M-A, Qiu J, Olesen KL & Thordal-Christensen H (2007b) A SNARE-protein has opposing functions in penetration resistance and defence signalling pathways. *Plant J.* **49:** 302–12

Zhang Z, Henderson C, Perfect E, Carver TLW, Thomas BJ, Skamnioti P & Gurr SJ (2005b) Of genes and genomes, needles and haystacks: *Blumeria graminis* and functionality. *Mol. Plant Pathol.* **6:** 561–575

Zhang Z, Lenk A, Andersson MX, Gjetting T, Pedersen C, Nielsen ME, Newman MA, Hou BH, Somerville SC & Thordal-Christensen H (2008) A lesion-mimic syntaxin double mutant in Arabidopsis reveals novel complexity of pathogen defense signaling. *Mol. Plant* **1:** 510–527

Zhou B & Zeng L (2017) Conventional and unconventional ubiquitination in plant immunity. *Mol. Plant Pathol.* **18:** 1313–1330

Zipfel C & Felix G (2005) Plants and animals: A different taste for microbes? *Curr. Opin. Plant Biol.* **8:** 353–360